DEPARTMENT OF THE INTERIOR

U.S. GEOLOGICAL SURVEY

Geology and Mineral Resources of the White Mountains National Recreation Area, East-central Alaska

Edited by

Florence R. Weber[1], Richard B. McCammon[2],
C. Dean Rinehart[3], Thomas D. Light[4], and Karen L. Wheeler[1]

Open-File Report 88-284

[1]USGS Fairbanks, AK; [2]USGS Reston, VA;
[3]USGS Menlo Park, CA; [4]USGS Anchorage, AK

TABLE OF CONTENTS

LIST OF PLATES
(plates in pocket)

LIST OF FIGURES

LIST OF TABLES

ABSTRACT

This assessment of the potential for undiscovered mineral resources for part of the White Mountains National Recreation Area (WMNRA), Alaska, has been prepared for the U.S. Bureau of Land Management in time to meet the 1988 deadline for land-use decisions for this area. Geologic, geochemical, and geophysical data have been compiled at both 1:63,360 and 1:250,000 scales, and all available published information on mineral deposits and occurrences has been used in assessing the potential mineral resources of the area.

The White Mountains National Recreation Area is a part of the Yukon-Tanana Upland, primarily a terrane of quartzitic, pelitic, and calcic metasedimentary rocks with some metamorphosed mafic and felsic igneous rocks that have been intruded by Mesozoic and Cenozoic granitic rocks and minor amounts of intermediate and mafic rocks. The disruptive structures in the area are major thrust faults and strike-slip fault splays of the Tintina fault zone.

We have made subjective probablistic estimates for the existence and the number of undiscovered deposits within the part of the WMNRA that we evaluated. For most of the deposit types, the probability that one or more undiscovered deposits exists is low, based on the lack of evidence of mineralization in the rocks exposed at the surface. However, placer gold has been recovered from Nome Creek and its tributaries within the WMNRA since the turn of the century, and the cumulative production to date is estimated to be 29,000 oz. Based on the currently available data, we estimate that there is a probability of 0.5 for the occurrence of placer gold and polymetallic vein deposits, a probability of 0.1 for Sn-greisen, Th/REE veins, lode Au, and sedimentary exhalative Pb-Zn deposits. There is also a probability of 0.05 for a tungsten-skarn deposit. In addition, given the existence of one deposit, we estimate a 0.5 probability of 2 and a 0.10 probability for 3 or more placer gold deposits, and a 0.10 probability for 2 or more lode gold or polymetallic vein deposits. We have also estimated the mean undiscovered mineral resource endowment in the study area for Au, Ag, Pb, Sn, Th, W, Zn, rare-earth oxides, and high-calcium limestone.

At the present time, we do not expect significant undiscovered resources of chromium, asbestos, nickel, or diamonds. The recent report of the occurrence of platinum in gold samples in the nearby Tolovana mining district makes platinum worthy of further consideration as a potential metallic resource.

I. INTRODUCTION

This report has been prepared in response to a congressional mandate that directs the U.S. Geological Survey with the assistance of the State of Alaska Geological Survey to prepare a mineral resource assessment for the White Mountains National Recreation Area (WMNRA) in time for the Bureau of Land Management to meet the 1988 deadline for land-use decisions for this area.

In order to accomplish this objective, an accelerated program of field mapping, geochemical and geophysical surveying, and mineral resource investigations were undertaken during 1986 and 1987. The results of our investigations are presented in this report. The following information is provided:

(1) detailed geologic maps at 1:63,360 scale showing bedrock and surficial geology, with accompanying text describing the major rock units, structure, and stratigraphy

(2) gravimetic and aeromagnetic maps at 1:63,360 scale, with accompanying text that provides an interpretation of the data

(3) a series of geochemical maps at 1:250,000 and 1:63,360 scale that depict the distribution of geochemical elements based on rock, stream sediment, and pan-concentrate samples, with accompanying text that provides an interpretation of the data

(4) mineral resource map at 1:63,360 scale showing outline of areas judged favorable for the occurrence of undiscovered deposits, and locations of significant mineral occurrences and known gold placer deposits

(5) probabilistic estimates of the existence, number, and contained metal in undiscovered deposits of types expected to be found in the WMNRA should future exploration take place

This assessment covers the area in the WMNRA shown in figure I-1. It includes all of the WMNRA that lies within the Livengood quadrangle, and the northern- and southernmost part of the WMNRA in the Circle quadrangle. The assessment for the area in the WMNRA, not included here, was carried out by the State of Alaska, Division of Geological and Geophysical Surveys, and is contained in a separate report.

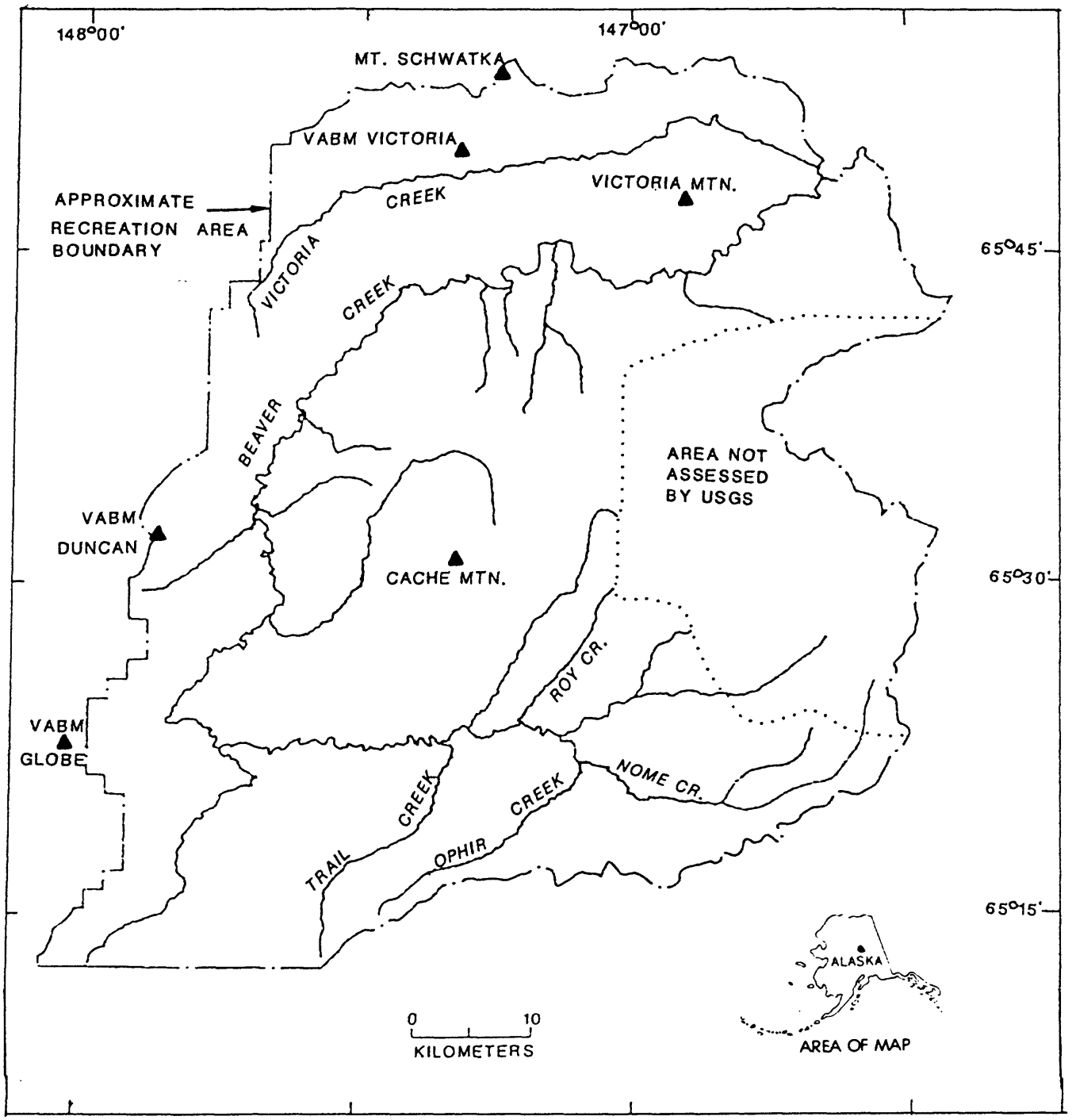

Figure I-1. Index map showing the part of the White Mountains National Recreation Area covered by this report.

II. GEOLOGIC FRAMEWORK

by F.R. Weber, K.L. Wheeler, J.H. Dover, C.D. Rinehart,
R.B. Blodgett, J.W. Cady, S.M. Karl,
R.B. McCammon, and R. Miyaoka

Acknowledgements

The White Mountains area and the adjoining parts of the Yukon-Tanana upland have been the subject of geological investigations since the turn of the century when Alfred H. Brooks, and a few other pioneer U.S. Geological Survey geologists, first passed through the country. Until the 1930's, the primary mode of access was by pack horse trains. Notable traverses through the White Mountains were made by L.M. Prindle in 1904 and 1909, R.W. Stone in 1905, Eliot Blackwelder in 1915, and J.B. Mertie, Jr. in 1921 and 1922. Their work culminated in the classic compilation of the geology of the Yukon-Tanana Upland by J.B. Mertie, Jr. in U.S. Geological Survey Bulletin 872. Geologic mapping continued in the Livengood and Circle quadrangles. The Livengood and Circle 1:250,000 geologic maps were published as Open-File Reports in 1971 (Chapman and others) and 1983 (Foster and others) respectively. The following people, directly or indirectly have contributed to our present geologic understanding of the White Mountains area:

Geologists
E. Blackwelder
A.H. Brooks
P.J. Burton
R.M. Chapman
R.E. Church
M. Churkin, Jr.
M.C. Durfee
R.B. Forbes
H.L. Foster
R.L. Foster
D.J. Grybeck
F.L. Hess
B.L. Johnson
S.M. Karl
T.E.C. Keith
J. Laird
W.D. Menzie
J.B. Mertie, Jr.
L.M. Prindle
R.W. Stone
B. Taber
J.H. Trexler, Jr.
J.D. Warner
F.R. Weber

Paleontologists
C. Carter
J.M. Berdan
J.T. Dutro, Jr.
J.W. Huddle
E. Kirk
W.A. Oliver
J.E. Repetski
A.J. Rowell
M.E. Taylor
E.O. Ulrich
J.A. Wolfe

Geophysicists
D.F. Barnes
J.W. Cady

Radiometric Dating
Z. Al-Shaieb
J. Blum
N.B. Shew
D.L. Turner
F.H. Wilson

Geochemists
J.D. Hoffman
C.M. McDougal
R.M. O'Leary
D.A. Risoli
R.B. Tripp

Data assembled during the mapping of the Livengood quadrangle (R.M. Chapman and others, 1971) and the Circle quadrangle (H.L. Foster and others, 1983)

have been incorporated into the geologic map of the WMNRA. The following people have participated in the fieldwork and report compilation for this project:

Geologists	Paleontologists	Geophysicists
J.H. Dover	J.M. Berdan	J.W. Cady
R.B. McCammon	R.B. Blodgett	C.L. Long
R. Miyaoka	R.J. Elias	R.L. Morin
C.D. Rinehart	A.G. Harris	
F.R. Weber	A.R. Ormiston	Geochemists
K.L. Wheeler	D.M. Rohr	E.A. Bailey
		J.R. Clark
		G.K. Lee
		T.D. Light
		R.M. O'Leary
		S.C. Rose
		J.L. Ryder
		S.M. Smaglik
		T. Sparks
		S.J. Sutley
		R.B. Tripp
		W.R. Willson

The authors wish to thank the Alaska Division of Geological and Geophysical Surveys for their cooperation in making preliminary copies of maps, descriptions, and other data from the adjoining part of the WMNRA available for consultation and for certain technical help in the preparation of this report.

Introduction

The White Mountains National Recreation Area (WMNRA) is located in the northwest part of the Yukon-Tanana Upland, a wedge-shaped area of considerable relief bounded by the Yukon and Tanana Rivers in east-central Alaska. The area covered by the WMNRA is approximately 1,562 sq mi (4,046 sq km). An area covering three-fourths or about 1,172 sq mi (3,033 sq km) of the WMNRA (fig. I-1), is the subject of this report.

The study area exhibits a variety of topographic features. It includes most of the upper drainage area of Beaver Creek which, from its headwaters near Mt. Prindle, flows through the area entering from the east, heading north and out into the Yukon Flats at the northeastern corner of the study area. The major tributaries of Beaver Creek within the WMNRA include Nome Creek, Bear Creek, Wickersham Creek, Fossil Creek, Willow Creek, and Victoria Creek. The total Beaver Creek drainage system from its source in the Mt. Prindle area to its mouth on the Yukon River is over 300 miles (480 km) long.

Unconsolidated alluvial gravels resting on surfaces as much as 100 ft (30 m) above the present stream level along the section of Beaver Creek in the northern part of the WMNRA reflect the regional tectonic history of the area. The northern half of the Yukon-Tanana Upland, which includes the WMNRA,

has a complicated structural history involving movement on the Tintina fault system.

The White Mountains, a relatively narrow band of rugged, bedded volcanic rocks and limestones, forms the core of the WMNRA. The name is taken from the light-colored Tolovana Limestone which, under bright sun conditions, contrasts with the darker Fossil Creek Volcanics. The highest point is 4,163 ft (1,269 m) at VABM Fossil in the northern part of the range. In many places the limestone beds stand nearly vertical in the axes of narrow synclines and erode to form spectacular crags and spires. Such a place, north of Windy Gap, was named "The High Jags" by R.W. Stone who passed by with a pack train in 1905. A natural arch, "Windy Arch", can be seen in a limestone spur on the southeast side of Windy Gap, and to the southeast of the arch, across Fossil Creek, is a low limestone outcrop with a large north-south crack called "Split Rock" by E. Blackwelder, another early explorer, in 1915.

Two large granitoid bodies, and one smaller alkaline intrusive body, intrude the rocks of the WMNRA. The northernmost, Victoria Mountain, 4,588 ft (1,398 m), stands high above the east end of the ridge between Beaver and Victoria Creeks as a large rounded mass. The relief in the vicinity of Beaver Creek is 3,700 ft (1,100 m). South and east of the White Mountains, Cache Mountain pluton, 4,772 ft (1,500 m), intrudes the surrounding metasedimentary rocks. Several tops exceeding 5,000 ft (1,524 m) can be found on the crest of a ridge that extends to the northeast from Cache Mountain. The smaller alkaline intrusive, named the Roy Creek pluton, is exposed on the ridge on the east side of Roy Creek.

The other prominent landmark in the WMNRA is Mt. Schwatka, named after the intrepid explorer, Lt. Frederick Schwatka, USA, who made a military reconnaissance along the Yukon River in 1883. This flat-topped mountain, at 4,177 ft (1,273 m), towers over the Yukon Flats to the north. Mt. Schwatka is underlain mainly by volcanic rocks.

In the following sections of this part of the report, a more complete description of the geology is provided.

Glacial Geology

Although the upland areas in the WMNRA are neither exceptionally high or very extensive, evidence of Pleistocene glaciation can be seen in the vicinity of Cache Mountain, Victoria Mountain, and to a lesser extent on the north side of the White Mountains. All streams originating on Cache Mountain have the typical U-shaped profile in their upper reaches of a glacially eroded valley. In such small mountain masses the evidence is rather circumstantial--based on valley form, location of fragmental morainal and outwash deposits, etc.--but, the evidence here suggests that three out of the four major glacial episodes seen in the Yukon-Tanana Upland could have modified the topography of Cache Mountain and the ridge extending northeast toward Rocky Mountain (Lime Peak). These were:

Age	Yukon-Tanana Upland (Weber, 1986)	Mt. Prindle area (Weber and Hamilton, 1984)
Early(?) Wisconsin	Eagle glacial episode	American Creek glacial episode
Middle(?) Pleistocene	Mount Harper glacial episode	Little Champion glacial episode
Early(?) Pleistocene	Charley River glacial episode	Prindle glacial episode

The Late Wisconsin and Holocene events recorded elsewhere in the Yukon-Tanana Upland are missing from Cache Mountain. Only the outer limits of the most extensive glaciation are shown on the geologic map, plate II-A. During the period of maximum glaciation (the Charley River glacial episode) about 65 percent of the mountainous area in the vicinity of Cache Mountain was covered with perennial ice and snow. A small ice cap may have covered the top of Cache Mountain itself.

Glaciation on Victoria Mountain was less extensive; this mountain is not quite as high as Cache Mountain, is more isolated from other high terrain, and therefore is less suitable to the retention of snow and ice. It is not clear how many glacial episodes were present on Mount Victoria but probably both the Charley River and a few very small glaciers of the Mt. Harper episode formed.

At least one small glacier formed at the head of Lost Horizon Creek and across several divides to the east in the heart of the northern part of the White Mountains. From the topographic characteristics, it was probably as young as the Mt. Harper episode.

During the Pleistocene excessive discharge of water from melting glaciers in the mountains cut into an old surface to form a prominent terrace on Beaver Creek. Terraces of similar origin can be seen on Nome Creek, Bear Creek and its tributaries, O'Brien Creek, Fossil Creek, Willow Creek, and to a small extent on lower Victoria Creek. At the same time large amounts of outwash gravel were dumped into these drainages. Placer gold was concentrated in some of these gravels in the Nome Creek area.

Subsequently these outwash gravels of the old floodplains (Qsg) were covered by reworked silt and organic deposits. The topography is flat; the ground is poorly drained, and frozen. Ice-wedge polygons are visible in many places.

Geologic Map Unit Descriptions

Under the terrane concept described by Churkin and others (1982) and Jones and others (1984), parts of the White Mountains National Recreation Area (WMNRA) were divided into the following units. The geologic names and symbols used in

this WMNRA report are included for comparison:

Churkin and others, 1982	Jones and others, 1984
Kandik terrane	Manley terrane
Wilber Creek unit (KJw)	Wilber Creek unit (KJw)
Vrain unit (MzPzv, etc)	Vrain unit (MzPzv, etc)
Globe unit (Pzg)	
Livengood terrane	Livengood terrane
Cascaden Ridge unit (Dc)	Cascaden Ridge unit (Dc)
Mafic-ultramafic unit (ϵpϵum, Pzpϵm, etc)	Mafic-ultramafic unit (ϵpϵum, Pzpϵm, etc)
Amy Creek unit (Pzpϵd, etc)	Amy Creek unit (Pzpϵd, etc)
Livengood Dome Chert (Olc)	Livengood Dome Chert (Olc)
White Mountains terrane	White Mountains terrane
Schwatka limestone and volcanic unit (Dsl, Dsv)	Schwatka limestone and volcanic unit (Dsl, Dsv)
	Globe unit (Pzg)
Tolovana Limestone (DSt)	Tolovana Limestone (DSt)
Fossil Creek Volcanics (Ofv, Ofs)	Fossil Creek Volcanics (Ofv, Ofs)
Beaver terrane	Wickersham terrane
Wickersham unit (ϵpϵga, pϵg, etc)	Wickersham unit (ϵpϵga, pϵg)
Yukon crystalline terrane	Yukon-Tanana terrane
Fairbanks schist unit (pϵf)	Fairbanks schist unit (pϵf)

However, to avoid conflict with previous terrane identifications, which may or may not be viable according to our interpretion, we are using geographic terms to identify the areas and units shown on the geologic map, plate II-A. This does not void the possibility that the geographic areas may have some geologic significance. The WMNRA has been separated into three areas (Schwatka, Livengood, and White Mountains), and the units for each are listed below according to the "Definition of map units" chart which appears on the geologic map:

The unconsolidated deposits are common to each of the three areas:

Qa	Alluvium, active channels
Qsg	Alluvium, silt to gravel, generally inactive channels
Qaf	Alluvial fan deposits

Ql	Loess
Qlc	Loess and colluvium
Qlcr	Loess and colluvium, over shallow bedrock

The Schwatka area is that part of the WMNRA generally north of Victoria Creek:

Dsl	Schwatka unit, limestone
Dsv	Schwatka unit, volcanic rocks
€p€ga	Wickersham unit, maroon and green argillite, and grit
€p€gl	Wickersham unit, dark arenaceous limestone
€p€gc	Wickersham unit, grit quartzite, phyllite, slate, and chert

The Livengood area is that part of the WMNRA generally between Victoria and Beaver Creeks:

Ts	Conglomerate
Kg	Victoria Mountain pluton, quartz syenite, quartz monzonite
KJw	Wilber Creek unit, polymictic conglomerate, graywacke, and shale
MzPzvs	Vrain unit, quartzite, siltite, phyllite
MzPzv	Vrain unit, slate
MzPzvc	Vrain unit, chert pebble conglomerate
Dc?	Cascaden Ridge(?) unit, conglomerate
Olc	Livengood Dome Chert, chert, rare greenstone
Pzp€d	Amy Creek unit, dolomite
Pzp€c	Amy Creek unit, chert
Pzp€m	Mafic igneous rocks, rare sediments
€p€um	Mafic and ultramafic igneous rocks
€p€umg	Greenstone
€p€ums	Serpentinite
€p€ga	Wickersham unit, maroon and green argillite, grit, limestone, chert, rare diabase

The White Mountains area is that part of the WMNRA roughly south and east of Beaver Creek:

Ts	Conglomerate, shale
Tg	Cache Mountain pluton, granite
Ks	Roy Creek pluton, syenite
KJw	Wilber Creek unit, polymictic conglomerate, graywacke, and shale
MzPzvs	Vrain unit, quartzite, siltite, phyllite
MzPzv	Vrain unit, slate
MzPzvc	Vrain unit, chert pebble conglomerate
MzPzvt	Vrain unit, tuff
MzPzs	Calcareous shale, shaly limestone
MzPzc	Beaver Bend unit, conglomerate, graywacke, slate
Pzg	Globe unit, vitreous quartzite, phyllite, slate,

	gabbro, diabase sills
DSt	Tolovana Limestone, limestone
Ofv	Fossil Creek Volcanics, alkali basalt, agglomerate and volcaniclastic conglomerate
Ofs	Fossil Creek Volcanics, shale, chert, limestone, gabbro
€p€ga	Wickersham unit, grit, graywacke grit, maroon, green and gray argillite and phyllite, quartzite, siltite
p€g	Wickersham unit, grit (bimodal quartzite), quartzite, slate phyllite
p€gg	Wickersham unit, pale greenish-gray quartzite, grit, phyllite, slate, and a trace of marble
p€f	Fairbanks schist unit, quartzite, muscovite schist, trace of feldspar, tiny garnets, and a trace of grit

The data used in interpreting the stratigraphy and structure, and in compiling the geologic map have been collected over many years beginning in 1902. Figure II-1 is a map showing the stations (both old and new) from which geologic information has been obtained. Old traverses have been recompiled on modern maps from the original notes. Frequently no maps were available to the early workers so a topographer was assigned to each party who surveyed and sketched the terrain on a daily basis. These early maps are surprisingly accurate and it is possible to reproduce the station locations on modern topographic maps with considerable confidence. A 1:250,000 scale geologic map of the whole Livengood quadrangle was published in 1971 by Chapman and others.

During 1986 and 1987 field seasons many new observations were made to enhance the mile-to-the-inch geologic interpretation. Specialists were called in to examine details of structure, sedimentology, paleontology, geophysics, geochemistry and particularly, the economic geology.

In the following section each geologic unit is described as it occurs in the three areas of the WMNRA. An attempt was made to place these units in probable order by increasing geologic age. Each description includes an introductory paragraph of description of the unit (as shown on the geologic map, pl. II-A), its location, extent, the nature of its boundaries, interpretation of its depositional environment, mode of emplacement or metamorphism, and in some cases a suggestion of correlative units. A detailed description of each unit follows the introductory statement.

QUATERNARY SURFICIAL DEPOSITS

Quaternary surficial deposits mantle approximately 70 percent of the southwestern part of the White Mountains National Recreation Area (WMNRA), making identification of the bedrock stratigraphy and structure in this area uncertain; however, bedrock is better exposed in the higher mountains of the northern area, and the surficial deposits are confined to lower slopes and stream bottoms.

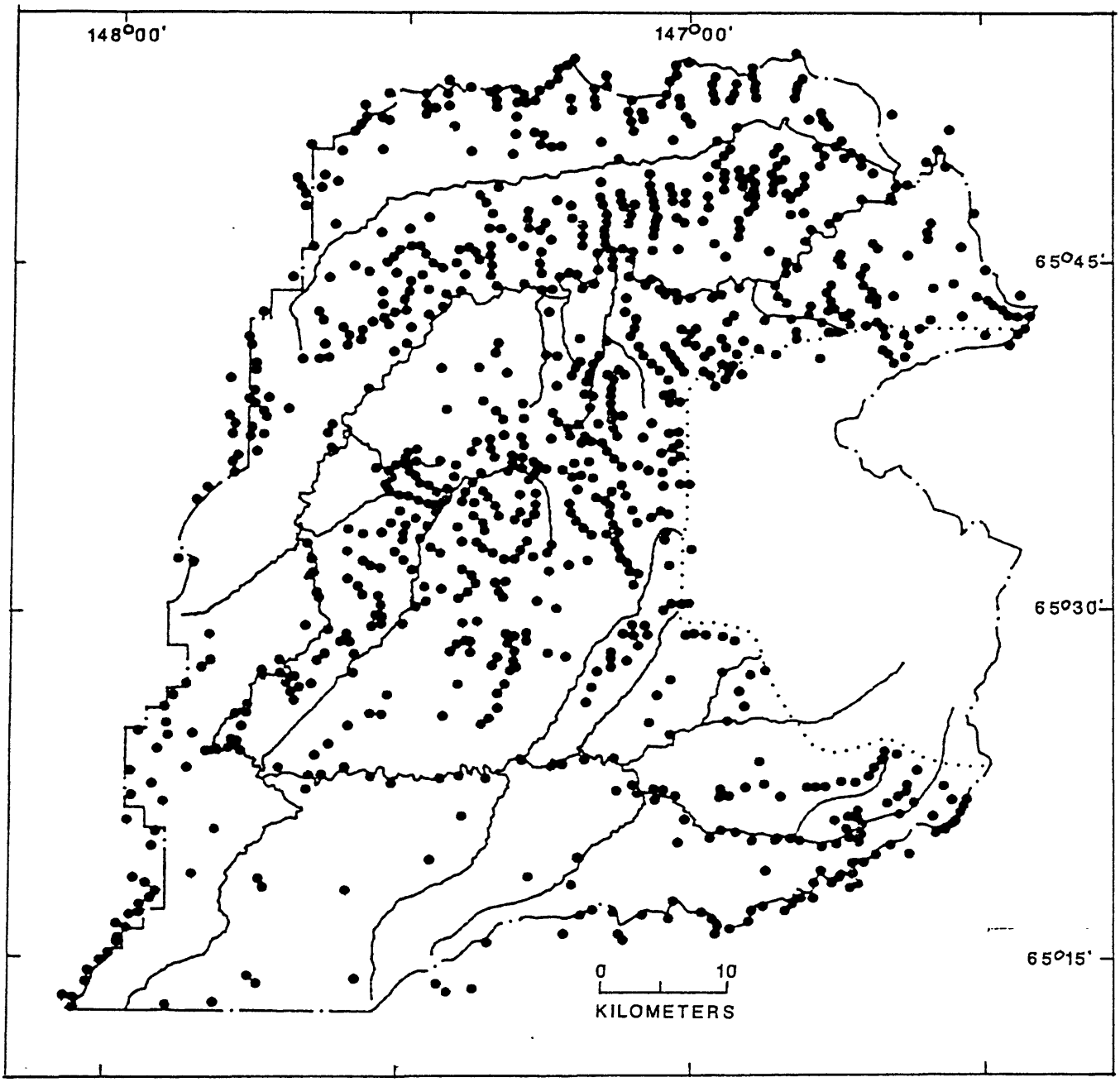

Figure II-1. Map showing stations (both old and new) from which the geologic information described in this report has been obtained.

For the purposes of this report, the Quaternary surficial deposits have been divided into six units: 1) Qa, alluvium of active stream channels, 2) Qsg, silt to gravel-size alluvium of the higher less-active parts of the floodplain or some smaller stream valleys, 3) Qaf, large alluvial fan deposits, 4) Ql, loess, 5) Qlc, a mixture of loess and colluvium, and 6) Qlcr, loess and colluvium overlying bedrock of indeterminate type at a shallow depth. Qa is Holocene and Qsg, Qaf, Ql, Qlc, and Qlcr are both Holocene and Pleistocene in age.

Qa ALLUVIUM OF ACTIVE STREAM CHANNELS--Silt, sand, and granule- to boulder-sized alluvium, with minor amounts of organic debris, gray, yellowish gray to brown. Underlies active stream beds or floodplain, is well-stratified with fining-upward cycles and well-sorted, and is generally unfrozen, except possibly in silty channels. Silty alluvium under some small streams is frozen, and the streams exhibit a beaded pattern where intersecting ice lenses have thawed in the stream bed. Alluvium locally may include reworked glacial outwash deposits from Mt. Prindle, Cache Mountain, the White Mountains, and Victoria Mountain. Thicknesses may range from one foot (0.3 m) to about 50 ft (15 m). In certain sections, parts of the valley of Beaver Creek commonly form a wide, flat, open floodplain with meandering streams and a complex of shallow, high-water channels which in places are covered with a thin layer of silt, supporting youthful vegetation. Thicker silt on the banks bordering the active channels support a dense growth of large spruce. A short section of Ophir Creek and a large part of upper Nome Creek include placer-mine tailings that have been worked by pick and shovel, mechanized surface, or dredging methods. Thickness of the tailings is commonly less than 30 ft (9 m).

Qsg ALLUVIUM, SILT TO GRAVEL, GENERALLY INACTIVE CHANNELS--Silt, sand, and granule- to pebble-size alluvium, locally includes glacial outwash deposits with large boulders, well-sorted and stratified. Characterized by abandoned stream channels 2 to 15 ft (0.6 to 4.5 m) higher than the active channels of Qa, elsewhere flat to hummocky with numerous bogs. Includes many small alluvial fans deposited by minor side streams and intermixed with the Qsg sediments. Most of the coarse alluvium is concealed by a cover of undifferentiated silt, reworked by alluvial and solifluctional processes from originally deposited silt to lower slopes and valley bottoms. Locally rich in organic layers, masses, and disseminated organic debris; commonly frozen and contains abundant ground ice as horizontal and vertical sheets, wedges, and irregular masses. Supports vegetation composed of small- to medium-stunted spruce, some willow, grass, moss, sedges, and shrubs. The thickness of the entire unit is probably quite variable and may be as much as 100 ft (30 m).

Qaf ALLUVIAL FAN DEPOSITS--Sand, gravel, and boulders. Alluvial fans, only the largest of which have been differentiated on the map, are formed of gray to brown, coarse-grained, rounded-to angular-detritus

with considerable variation in clast size. They are poorly to well-sorted, stratified, and generally composed of locally derived clasts deposited under high-energy conditions below a major decrease in slope. May be covered by reworked silt and small vegetation.

Ql LOESS--Massive, well-sorted, homogeneous, eolian silt, buff to light-gray where dry, and brown where wet, stratified, locally mottled by iron-oxide staining. Derived primarily from the floodplain of the Tanana River and glacial outwash plains of the Alaska Range, and, in part, from similar deposits in the Yukon Flats to the north. Some of the loess may have been derived locally from outwash of glaciers in the Mt. Prindle and Cache Mountain areas. In glacial or early post-glacial times, probably blanketed most of this area, was eroded and now covers lower hill slopes in about 30 percent of the southern half of the WMNRA and considerably less than that in the north. It can be free of permafrost on sunny, south-facing slopes, but it may contain perennial ice on lower north-facing slopes, or where it is poorly drained. Many of the lower slopes in this area are poorly drained and probably frozen, judging from the vegetation of small trees and tundra plants. Numerous thaw ponds on flat Ql surfaces south of Beaver Creek indicate the presence of ice lenses. Loess grades upward into unit Qlc with a very poorly defined contact, is mapped where more than 3 ft (0.9 m) thick, and is of unknown thickness at its downslope limit.

Qlc LOESS AND COLLUVIUM--Composed of an unsorted mixture of loess, as described for Ql, and angular or subrounded fragments of the local bedrock. Qlc is light-gray to brown, covers as much as 40 percent of the southern part of the WMNRA, ranges from 3 or more ft (0.92 m) thick on upper slopes to an unknown downslope thickness, and is marked by drainage channels containing reworked Qlc materials which cut the loess Ql downslope in an irregular contact. Qlc is generally located on higher hill slopes, is probably partially frozen, fairly well-drained, and in places supports a thick spruce forest.

Qlcr LOESS AND COLLUVIUM OVER SHALLOW BEDROCK--The loess and colluvium is the same as described for Qlc, but has a higher proportion of bedrock fragments in the mixture and bedrock may be sparingly exposed or at excavatible depths of 10 ft (3 m) or less. In the area of Qlcr the type of bedrock has not been determined, but it is probably the same as the surrounding outcrops. Qlcr is well-drained and probably thawed on south-facing slopes.

SCHWATKA AREA

SCHWATKA LIMESTONE AND VOLCANIC ROCKS

Small amounts of the limestone and volcanic rocks of the Schwatka unit (Dsl and Dsv, respectively) occur in the Mt. Schwatka area within the extreme northern edge of the White Mountains National Recreation Area (WMNRA) and

together cover less than 1 sq mi (2.5 sq km). A thrust fault is the southern boundary of the Dsl and Dsv outcrop belt with the Wickersham unit. The volcanic rocks are altered and are undated, but appear to be interlayered with the limestone. The Dsl unit is not to be confused with the DSt of the Tolovana Limestone which is an entirely different unit in a different tectonic block or terrane. The depositional environment of the Dsl and Dsv unit was one of shallow-marine mafic lava flows with more quiescent, shorter periods of encrinoidal and limey mud deposition.

Dsl LIMESTONE--medium-bedded to massive, light- to medium-gray lime mud- to wackestone. Locally encrinoidal, bearing abundant "two-hole" crinoid ossicles, which together with conodonts indicate late Early Devonian (Emsian) and/or Early Middle Devonian (Eifelian) age. Units range to at least 328 ft (100 m) in thickness and are interbedded with unnamed volcanic greenstone unit as separate, mappable entities in Mt. Schwatka area.

Dsv VOLCANIC ROCKS--The volcanic part of the Schwatka unit consists mainly of massive greenschist-grade basalt flows, but also includes agglomerate, tuff, and fine-grained volcaniclastic rocks that grade into both greenish-gray and dark-gray epiclastic siltstone and slate, and also into coarser pyroclastic rocks that contain pebbles of both lava and volcaniclastic and/or epiclastic varieties. The agglomerate typically consists of fragments--mainly of fluidal rocks--measuring a few inches across, but locally, fragments as large as 3 feet (1 m) across were seen. Relatively thin lenses of platy, laminated and thin-bedded, impure limestone, and locally lenticular bodies of calcite-cemented conglomerate also occur in the dominantly volcanic part of the unit. Much of the volcanic rock is strongly foliated and sheared, and sub-mylonitic rocks were seen locally. Although shearing and foliation are common, both are markedly discontinuous, and in some terranes, such as that at Mt. Schwatka, the rocks are mainly massive and even uncleaved, whereas in the saddle just north of the mountain, they are highly foliated, and the conglomerate clasts are flattened, with diameter-to-thickness ratios of pebbles as much as 8. Thin sections of the flows typically show a dense mat of moderately birefringent but unresolvable material with opaque and semi-opaque material in the interstices. Chlorite generally appears to compose a significant part of the matrix, but locally, white mica, and epidote are also generously present. Coarse grains, or aggregates, of albite showing well-developed albite twinning, present in some rocks, indicate relicts of former phenocrysts of more calcic plagioclase. In at least two localities flows were found that contain fresh unaltered augite phenocrysts 0.04-0.4 in (1 mm to 1 cm) across, embedded in a profoundly altered matrix in which chlorite appears to be stable. Varieties in which coarse porphyroblasts--or porphyroblastic aggregates--of chlorite are abundantly scattered throughout the rock are generally inferred to reflect amygdaloidal lava. This inference is particularly convincing where, on weathered surfaces, the chlorite has weathered out leaving voids that seemingly restore to

the rock an original vesicular texture. The chlorite, typically a major constituent in the amygdules, is commonly intergrown with quartz, calcite, and rarely zeolite or epidote.

WICKERSHAM UNIT

The Cambrian to Precambrian Wickersham unit within the WMNRA covers at least 490 sq mi (1,270 sq km) and has such lithologic diversity that it is mapped as five separate units. All the individual Wickersham units are lithofacies and appear to have gradational contacts with one another. They are lower greenschist-grade metamorphic facies. Within the WMNRA the Wickersham unit occurs in the 1) Schwatka area, 2) Livengood area, and 3) White Mountains area.

In the Schwatka area the Wickersham unit includes 1) maroon and green argillite, and grit (Ꞓp Ꞓga), 2) dark arenaceous limestone (Ꞓp Ꞓgl), and 3) grit, quartzite, phyllite, slate, and chert (Ꞓp Ꞓgc); the last, which is probably equivalent to unit pЄg in the White Mountains area but is a slightly different lithofacies containing chert.

The Wickersham unit of the WMNRA is very similar to the Windermere Supergroup of Yukon Territory, Canada (Eisbacher, 1981), particularly to that of the Selwyn Basin.

Ꞓp Ꞓga GRIT, GRAYWACKE GRIT, MAROON, GREEN AND GRAY ARGILLITE--Grit is much like the pЄg unit described in the White Mountains area section below. Graywacke and quartz-wacke grit are light to medium olive gray, commonly conglomeratic or unsorted, feldspars locally abundant, often slightly foliated, but sedimentary features preserved. Bedding in graywacke and quartz-wacke grit is graded, locally amalgamated, fines upward to ripple laminations in silty phyllite with small-scale trough crossbedding. Argillite is laminated, maroon and light to medium green and grayish green, fissile to blocky fractured. Locally Ꞓp Ꞓga is phyllitic and slaty, laminated, medium-light to dark gray and greenish gray, and contains rare, horizontally bedded, discontinuous 2-3 ft (0.6-0.9 m) thick beds of greenish gray, micaceous, arenaceous limestone. Basalt is interlayered, but the layers are thin and too small to differentiate on the geologic map. Oldhamia, a trace fossil of probable Late Proterozoic to Cambrian age has been found in Ꞓp Ꞓga at two localities in the Circle quadrangle, one in the WMNRA (see bedrock geologic map, Smith and Pessel, in press) and the other outside of the WMNRA in the Schwatka area, Circle quadrangle (fossil locality 2, table 2, Foster and others, 1983).

Ꞓp Ꞓgl DARK ARENACEOUS LIMESTONE--Limestone is very dark gray and weathers medium to dark gray, thin-bedded and platy, dense to very finely crystalline. Less commonly this limestone unit is medium to dark gray and weathers medium gray or various shades of brown, yellow, and red, thin- to ripple-bedded and platy to shaly, dense, sparsely arenaceous with rounded to subrounded monocrystalline quartz grains

floating in a limey matrix. €p€gl is in the upper part of the Wickersham unit and is interbedded with the maroon and green argillite.

€p€gc GRIT, QUARTZITE, PHYLLITE, SLATE, AND CHERT--Grit, quartzite, and graywacke are light to medium gray, greenish gray and olive and weather light to medium gray with iron stains and flecks of oxidized pyrite, interbedded with phyllite, slate, and argillite that are medium light to dark gray and greenish gray, and medium- to thin-bedded, generally fine-grained. Oldhamia fossils not found within the WMNRA, but occur approximately 1.3 mi (2.1 km) west of the northwest corner of WMNRA or 8.5 mi (13.6 km) northeast of Noodor Dome, in greenish-gray to olive slate and argillite, and tentatively suggest a Cambrian or possibly Hadrynian (late Precambrian) age (Hofmann and Cecile, 1981, p. 288). Some gray and black chert interbedded with the sandy and argillaceous beds of this unit.

LIVENGOOD AREA

TERTIARY CONGLOMERATE AND SHALE

Possible Tertiary sedimentary rocks are known within the WMNRA in two small areas; one includes a few small outcrops at water level on Victoria Creek near the mouth of Squaw Creek northeast of Victoria Mountain, and the other exposures are in the vicinity of the divide between the North Fork of Preacher Creek and the headwaters of Moose Creek in the Circle quadrangle. The outcrops are very poor, hardly more than rubble piles of pebbles, cobbles and boulders. Both locations are in the Tintina fault zone trench and have bearing on the age of the most recent fault activity. The deposits at these two locations are discussed separately:

Ts? CONGLOMERATE--Victoria Creek--Boulders, cobbles, and pebbles in a gray or chloritic greenish graywacke matrix; clasts composed of quartzite, chert, chert pebble conglomerate, and green, medium- to fine-grained igneous rocks (possibly diorite and porphyritic andesite), subrounded to rounded, as large as 24 in (61 cm) in diameter, but mostly 2 to 4 in (5 to 10 cm), poorly-sorted; fairly well-consolidated, and breaks across the smaller pebbles but around the larger pebbles and cobbles; slickensides abundant, oriented in various directions. Thickness is unknown, but is probably 50 ft (15 m) or less. Contact with the adjoining rocks is obscured; pyritiferous Vrain unit (MzPzvs) phyllite is present nearby downstream. Age unknown, but the lithology appears more similar to Tertiary than to Mesozoic rocks.

QUARTZ SYENITE AND QUARTZ MONZONITE OF VICTORIA MOUNTAIN

Felsic plutons of Early Tertiary to Late Cretaceous age occur in the White Mountains and the Livengood areas within the WMNRA. The three major felsic plutons exposed in the USGS-mapped part of WMNRA are located on Cache Mountain, Victoria Mountain, and the ridge west of Roy Creek (Tg, Kg, and Ks,

respectively). The Cache Mountain and Roy Creek plutons are discussed in the White Mountains area of this report. Victoria Mountain pluton covers approximately 6 sq mi (16 sq km) in the northeastern part of WMNRA and intrudes the Vrain unit (MzPzv and MzPzvs).

Kg QUARTZ SYENITE AND QUARTZ MONZONITE--The Victoria Mountain pluton is a distinctive, massive, rather dark (av. color index = 15), quartz-poor porphyritic quartz syenite and quartz monzonite (fig. II-2) with dark-grayish-lavender, blocky to tabular K-feldspar phenocrysts, as much as 1 in (2.5 cm) in maximum dimension, that compose nearly half the rock, and are set in a medium-grained matrix of oligoclase/andesine, biotite, and hornblende. Plagioclase, the coarsest constituent of the matrix, is locally as much as half the size of K-feldspar phenocrysts, but is typically much smaller. A traverse across the pluton showed the rock to be mainly homogeneous with only few substantial variations in grain size, texture, or composition. Few inclusions and no dikes or veins were found. Contacts with the country rock show little local effect in either rock. The Victoria Mountain area was examined by the U.S. Bureau of Mines in a search for cobalt and other metals. The investigation, included a limited geochemical sampling study and described the results were described in an unpublished report by J.C. Barker (1983, written commun.). He states that hornfelses "are evident up to a mile away from the known contact . . . and locally . . . contain pyroxene crystals as much as one-half inch in length." He also mentions, in addition to the main phase of the pluton the occurrence of "rhyolite porphyry sills, aplitic dikes, and pegmatite dikes", and further states that "typically the phase variations increase near the . . . periphery . . .".

In thin-section the K-feldspar phenocrysts are somewhat perthitic and locally show well-developed zoning (also seen on stained slabs) as well as zonal arrangement of poikilitically enclosed minerals--small sub- to euhedral crystals of plagioclase, biotite, hornblende, and accessory minerals. Plagioclase (about An5-35) is subhedral, well twinned, and conspicuously zoned. Quartz demonstrates late crystallization by its conspicuous and exclusively interstitial occurrence. Brownish to olive-green hornblende is commonly intergrown with biotite, and like biotite, though much less abundantly, shows pleochroic halos around zircon. Remnant clinopyroxene cores in hornblende were seen locally, and in one section, eckermanite(?) was seen sparsely intergrown with hornblende. Biotite whose ratio to hornblende is about 1:1, shows the same pleochroic formula as hornblende and is generally unaltered, though minor chlorite is intergrown sparsely.

Accessory minerals include, in approximate order of decreasing abundance: sphene (fairly coarse crystals); apatite--much conspicuously zoned; zircon, abundantly associated with pleochroic

halos in biotite, and less commonly in hornblende; allanite, sparse

but also associated with pleochroic halos in biotite; and opaque minerals.

Modal analyses of 5 representative samples, plotted on figure II-2, straddle the boundary between quartz syenite and quartz monzonite (Streckeisen, 1976). Chemical analyses and norms of three of the samples (table II-1) compare fairly closely with Nockolds' (1954) average calc-alkali syenite (between his leuco and melano types), and fall within the denser part of Le Maitre's (1976) field of 102 syenites. In the classification of Shand (1951, p. 228-229) the rocks are metaluminous based on oxide values, and subaluminous based on normative minerals. Concordant K/Ar hornblende and biotite ages of 65.5 $\pm$ 1.03 Ma and 65.3 $\pm$ 0.65 Ma (table II-2) respectively, by Wilson and Shew (1981), establish the age of the pluton as close to the Cretaceous/Tertiary boundary.

WILBER CREEK UNIT

The Wilber Creek unit is a Jurassic and/or Cretaceous sequence of lithologic units mapped in approximately 110 sq mi (285 sq km) in area in the WMNRA within the Beaver Creek valley north of the White Mountains and southwest of Victoria Mountain. This northeast-southwest trending Mesozoic flysch belt extends northeast at least as far as the mouth of Sheep Creek and well beyond the WMNRA to the southwest. Magneto-telluric resistivity work (section III) suggests this Mesozoic flysch basin is at least 0.62-1.24 mi (1-2 km) deep and that the Wilber Creek unit may be underlain by the Vrain unit. Wilber Creek unit is composed primarily of polymictic conglomerate, graywacke, siltstone, and shale. Unsorted to poorly-sorted, amalgamated beds, normally- and reversely-graded, rhythmic-bedding, flaser-bedding, flame structures, load-casts, tool-marks, convolute-laminations, and shale rip-up clasts are common characteristics of the Wilber Creek unit, and of turbidite deposits, in general. The Kathul Graywacke of the Kandik basin and the Kuskokwim Group of the Kuskokwim basin are similar types of deposits and probably roughly correlate with the Wilber Creek unit.

KJw POLYMICTIC CONGLOMERATE, GRAYWACKE, SILTSTONE AND SHALE--Polymictic conglomerate is dark olive-gray to medium-dark gray, iron-stained, unsorted, with subangular to well-rounded granules to cobbles and less abundant boulders. Clasts are locally-derived from the Yukon-Tanana Upland and consist mostly of mafic igneous, greenstone, felsic volcanic, diorite, other intrusive rocks, quartzite, dark-gray limestone, sandstone, siltstone, phyllite, chert, rare grit, and slate (rip-ups). The conglomerate clasts are generally matrix-supported with a matrix of sand, silt, and clay. Beds are mostly internally-massive, large- to medium-scale graded, and amalgamated with planar bases and tops. Some large-scale troughs internally filled with smaller-scale trough-crossbedding display fining-upward cycles. Conglomerate is approximately 5 percent of the Wilber Creek unit.

Table II-1. Chemical analyses and norms representing the granite of Cache Mountain and the quartz syenite/quartz monzonite of Victoria Mountain

(Chemical analyses in weight percent using XRF methods by the analytical laboratory of the USGS in Menlo Park, CA. LOI, loss on ignition at 900°C)

	Victoria Mountain			Cache Mountain			
Lab. No.	M-176070	M-176071	M-176072	M-176073	M0176074	M-176075	M-176076
Field No.	86ARi-1A	86ARi-1C	86ARi-1E	86ARi-13A	86ARi-16	86ARi-17	86ARi-24A
SiO_2	62.4	64.2	60.0	76.6	71.7	74.1	73.7
Al_2O_3	16.5	16.2	16.4	12.6	14.7	14.0	13.8
Fe_2O_3	4.37	3.51	5.17	1.55	2.16	1.23	1.53
MgO	1.3	1.0	2.2	0.25	0.35	0.20	0.35
CaO	3.42	3.07	5.15	0.64	0.99	1.03	0.92
Na_2O	3.8	3.8	3.7	2.8	3.0	3.2	2.4
K_2O	5.18	5.42	4.14	4.61	5.49	5.05	5.64
TiO_2	0.49	0.44	0.62	0.16	0.30	0.17	0.25
P_2O_5	0.57	0.42	0.86	0.09	0.19	0.14	0.12
MnO	0.09	0.08	0.12	0.04	0.05	0.03	0.04
LOI	0.63	0.38	0.87	0.75	1.00	0.50	0.88
Total	98.75	98.52	99.23	100.09	99.93	99.65	99.63
				CIPW norms (weight percent)			
Quartz	12.46	14.88	10.69	41.46	31.48	34.35	36.46
Corundum	--	--	--	2.07	2.51	1.75	2.39
orthoclase	31.27	32.69	24.95	27.42	32.80	30.10	33.75
albite	32.85	32.81	31.93	23.85	25.67	27.31	20.56
anorthite	12.94	11.37	16.23	2.61	3.71	4.23	3.83
diopside	0.48	1.09	3.31	--	--	--	--
hypersthene	4.76	2.45	6.53	0.63	0.88	0.50	0.88
magnetite	2.95	2.87	3.14	--	0.34	--	--
hematite	--	--	--	1.56	1.59	1.24	1.55
ilmenite	0.95	0.85	1.20	0.09	0.58	0.07	0.09
rutile	--	--	--	0.12	--	0.14	0.21
apatite	1.35	0.99	2.03	0.21	0.45	0.33	0.28
Total	100.01	100.00	100.01	100.02	100.01	100.02	100.00

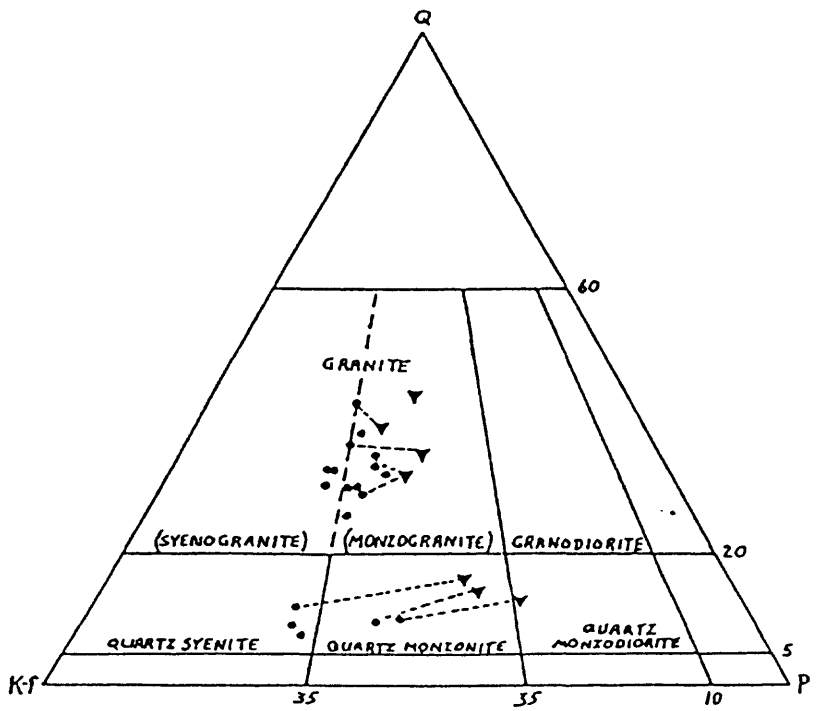

Figure II-2. Mode (dots) and norm (triangles) plots of rocks from the Cache Mountain (upper cluster) and Victoria Mountain (lower cluster) plutons. Classification of Streckeisen (1976). Dashed tie-lines connect mode and norm of same sample. Modes determined from etched and stained slabs (Norman, 1974). A minimum of 1,000 points were counted on slabs that averaged approximately 75 cm^2. Average color index: Cache Mountain 7.6; Victoria Mountain 15.

Table II-2. K-Ar data

The following mineral ages pertain to units described in text.

Location	Age (Ma)	Mineral	Lithology (Map Unit)	Analyst	Reference
Cache Mt.	58.4 ± 1.8 (minimum age)	biotite	granite (Tg)	D.L. Turner	Holm, 1973
	59.8 ± 1.8 (recalculated by Wilson)				Wilson and others, 1985
Victoria Mt.	65.5 ± 1.03	hornblende	quartz syenite/ quartz monzonite (Kg)	F.H. Wilson	Wilson and Shew, 1981
	65.5 ± 0.65	biotite		F.H. Wilson	Wilson and Shew, 1981
Roy Creek	85.4 ± 6.4 (minimum age)	biotite	aegirine-augite syenite (Ks)	Z. Al-Shaleb	Burton, 1981
	86.7 ± 3.6 (minimum age)	biotite	porphyritic biotite aegirine-augite (Ks)	Z. Al-Shaleb	Burton, 1981
	90.0 ± 2.0	biotite	lamprophyre (Ks)	F.H. Wilson	Wilson and others, 1981
West Fork	518.30 ± 15.5	hornblende	diorite (€p€um)	D.L. Turner and J. Blum	unpublished data
Amy Dome	539.48 ± 16.2	hornblende	grabbo (€p€um)	D.L. Turner and J. Blum	unpublished data
Amy Dome flank	633 ± 19	hornblende	diorite or grabbo (€p€um)	D.L. Turner	unpublished data

Graywacke is medium- to medium dark-gray to greenish-gray, iron-stained on weathered surfaces, mostly fine- to medium-grained, moderately sorted, subangular to subrounded, with some very well-rounded quartz grains. Shale rip-ups are as much as 10 in (25 cm) long. Matrix is silt and clay. Laterally continuous, graded, amalgamated, medium-scale graywacke beds are rhythmically interbedded with, and fine-upward to, siltstone and shale. Conglomeratic graywacke lenses are common, with clasts of locally derived mafic and felsic volcanics, very fine-grained sandstone, siltstone, chert, and shale rip-ups. Bases of beds are erosional, planar to slightly concave upward, and sole-marks are common. Minor small-scale scour-fills that fine-upward into ripple-laminated siltstone occur. Sandstone and conglomeratic sandstone compose approximately 20 percent of the Wilber Creek unit.

Siltstone is medium-gray to black, rusty-orange on weathered surfaces, commonly laminated with very fine-grained sandstone and shale as discontinuous lenses, flasers, and ripples, or rhythmically interbedded with sandstone. Siltstone comprises approximately 25 percent of the Wilber Creek unit.

Shale is dark-gray to black and commonly phyllitic, fissile, to blocky fracturing, with very fine-grained sandstone flasers, commonly laminated with siltstone. Some shale is rhythmically interbedded with very fine-grained, ripple-laminated thin sandstone beds that have sharp erosional bases and shaly tops. Shale is approximately 50 percent of the Wilber Creek unit.

VRAIN UNIT

In the northeastern part of the WMNRA, the Vrain unit is exposed in an area along Beaver Creek, roughly between the White Mountains and Victoria Mountain and extends to the east beyond the WMNRA past VABM Vrain in the Circle quadrangle. In the WMNRA the Vrain unit covers an area of approximately 72 sq mi (186 sq km). It is composed primarily of dark-gray slate, argillite, or phyllite, MzPzv; with some beds of a distinctive chert- and quartz-pebble meta-conglomerate, MzPzvc; and with a few interbeds of felsic tuff, MzPzvt. The argillite appears to grade westward into thinly interbedded siltstone, very fine-grained quartzite, and phyllitic slate, MzPzvs, exposed along the ridge between Willow and Sheep Creeks. Contacts between these units within the Vrain are mostly covered and are indistinct at best.

In hand specimen, clasts in the conglomerate (MzPzvc) are limited to chert, white quartz, and gray phyllite. None of the clasts appear to be locally derived from the rocks common to the White Mountains area. This suggests a further-removed depositional site for the MzPzvc than the current position in the WMNRA.

Lithogically the Vrain unit is very similar to the Devonian Lower Earn Group in the Yukon Territory of Canada as characterized by Winn and Bailes (1987). Photomicrographs in their paper (fig. 3, p. 532), of the Lower Earn Group

conglomerate and of an uncommon quartzose siltstone fragment, are very similar to the composition and texture, in thin-section, of the conglomerate (MzPzvc) and siltstone (MzPzvs) of the Vrain. They describe Devonian sedimentation along an extentional submarine fault-scarp related to stratiform lead-zinc sulfides, mudflows, and turbidites. Base and precious metals in the area of Warren and Moose Creeks (section IV) in the WMNRA, are the type common to sedimentary deposits in an extentional submarine system similar to that interpreted by Winn and Bailes, 1987, of the Lower Earn Group in the Yukon Territory of Canada.

However, the Vrain unit is also very similar in outcrop to Mesozoic flysch beds (Brabb and Churkin, 1969) in the Kandik Basin of the Charley River quadrangle; particularly, the MzPzv is similar to the upper part of the Glenn Shale or to the Biederman argillite (M. Churkin, pers. commun., 1980), and the MzPzvs is similar to the Keenan Quartzite.

The age and thickness of the Vrain unit is unknown, but magneto-telluric data suggest a similar resistive unit is underlying the White Mountains thrust sheet and may be as much as 3.7 mi (6 km) in thickness (section III).

MzPzv ARGILLITE, SLATE, SILTSTONE, AND QUARTZITE--Argillite is the dominant lithology in the vicinity of VABM Vrain, after which the unit is informally named. It is interbedded with minor quartzite and slaty argillite. Foster and others (1983) describe this unit as argillite, including siltstone, siliceous siltstone, and shale, dominantly gray, olive, or greenish-gray, and generally weathering reddish-yellow-brown or tan; commonly limonite- or manganese-stained along fractures; locally slaty; cleavage commonly well-developed and folded. Quartzite is mostly greenish-gray or gray, but some white or light-gray. Sulfides and hematite(?) are locally abundant. In the vicinity of VABM Vrain, the unit may show slight hornfelsic alteration. To the west, in the nearby WMNRA, the Vrain slate and argillite is generally dark-gray and distinctively pyritiferous. Small streams originating in this unit, and even Beaver Creek in places, are stained red from the iron-bearing water.

MzPzvc CONGLOMERATE--Conglomerate has stretched pebbles (locally mylonitic) as large as 1.2 in (3 cm) in diameter which are composed mostly of white monocrystalline quartz, gray and black argillaceous chert, and locally-abundant medium-gray phyllitic rip-up clasts. The matrix is cherty and most pebbles are clast-supported. The conglomerate is poorly sorted to unsorted, and has graded bedding in possible channels that appear to be erosional into the argillite, siltstone, quartzite sequence of the Vrain.

MzPzvs QUARTZITE, SANDSTONE, SILTSTONE, AND PHYLLITE--The rocks along the ridge between Willow and Sheep Creeks, and probably those west of Victoria Mountain, are low-grade greenschist facies, very fine- to coarse-grained, light- to medium-gray, well-sorted quartzose to subquartzose sandstone with horizontal laminae of siltstone. The internal laminations of this unit are often well-preserved ripple-

laminae, small-scale crossbedding, graded bedding, load casts, and heavy mineral laminae. The fine-grained sandstone is thinly interbedded with light-gray siltstone and silty, often phyllitic light-gray, bioturbated shale. Finely disseminated limonite and hematite(?) grains, as well as authigenic chlorite alteration occur in argillaceous laminae. The unit is overturned to the north and is internally disrupted.

CASCADEN RIDGE(?) UNIT

The unit named Dc? (Cascaden Ridge(?) unit) on the geologic map is found on the ridge between Beaver and Victoria Creeks in a band about 6 mi (9.7 km) long and as much as 1 mi (1.6 km) wide. It is composed of coarse- to fine-grained clastic rocks. These rocks found on lower hilltops or, more commonly, abutting the harder, often mafic igneous (PzpЄm) rocks. The Dc? sedimentary rocks are less resistant, and appear to lie unconformably on the PzpЄm unit; both units are probably part of a thrust sheet that has brought them north over the Cambrian-Precambrian ЄpЄga grit and argillite unit. There is another narrow band of rocks similar to Dc? in contact with the PzpЄm approximately a mile (1.6 km) northwest of Victoria Mountain. On the south, the main band of Dc? is overthrust by the Amy Creek dolomite unit (PzpЄd), is in unknown relation to another small patch of ЄpЄga, and in possible normal fault contact with the Olc.

Dc? section is made up of poorly exposed medasedimentary rocks of unknown age, but they are placed here in the Cascaden Ridge unit of Weber and others (1985) of Middle Devonian age mainly because the lithologically similar Cascaden Ridge unit, found in the vicinity of the community of Livengood, also has a basal conglomerate of very locally derived flysch-like rocks. However, the Dc? unit in the WMNRA lacks any fossils, but they are common in the Cascaden Ridge. The Dc? is distinctive and unlike any other conglomerate of the WMNRA; the locally derived immature composition of the Dc? strongly suggests that it was deposited in a fault-block basin bounded by the Amy Creek unit, the mafic unit, and possibly by the Wickersham unit.

Dc? CONGLOMERATE, GRAYWACKE, SILTSTONE, AND SLATE--Conglomerate containing abundant subrounded clasts of dolomite (some with silica boxwork), rounded clasts of varied shades of gray and mostly black chert, greenstone and other volcanic rock fragments, rare individual or intergrown calcic plagioclase grains, and rip-up clasts of siltite and argillite in a sandy matrix of the same rock fragments, particularly including a large amount of yellowish-weathering dolomite grains; clear quartz grains ("quartz eyes") ubiquitous everywhere in the matrix; dolomite clasts as much as 8 in (20 cm) in diameter; clasts are tectonically squeezed and stretched and rip-ups flattened. Graywacke, medium dark gray but yellowish-brown weathering because of abundance of dolomite clasts; same composition as sandy matrix of conglomerate described above. Slate or slaty argillite, medium-dark gray, finely layered or foliated. Crossbedding and large-scale graded bedding noted.

LIVENGOOD DOME CHERT

The Livengood Dome Chert (Olc) (Chapman and others, 1980) covers an area of 11 sq mi (29 sq km) in the Livengood portion of the WMNRA. It is composed predominantly of chert, shale, and silicified carbonate, with minor amounts of tuff and greenstone. The unit is considered Late Ordovician in age based on graptolites collected from shale layers (Chapman and others, 1980). A Mississippian fossil collection for the Livengood Chert reported by Mertie (1937) came from rocks that have since been assigned to the informal Lost Creek unit (Blodgett and others, 1988). Also the dolomitic section of Mertie's (1937) Livengood Chert now belongs to the Amy Creek unit (informal unit, Weber and others, 1985).

The depositional environment for Olc is inferred to be near a continental margin in moderate water depths, based on the presence of lithologies alternating on a meter scale, sedimentary structures in chert chip gritstone and conglomerate, and replacement textures indicating some cherts were originally carbonate rocks. The presence of graptolites indicates quiet water, either on a continentaql slope or in a restricted basin. Igneous activity contributed mainly clastic (tuff) deposits, but rare flows or sills are present.

The northern contract of Olc is the Victoria Creek fault, and Olc is overthrust from the south by mafic and ultramafic rocks. The outcrop pattern suggests the Olc is on the flanks of a large anticline with the core exposing ЄpЄga of the Wickersham unit.

Olc CHERT AND RARE GREENSTONE--Consists predominantly of gray, tan, grayish-green and some black-mottled recrystallized chert. The chert beds are as thick as 0.75-15 in (2-40 cm); most beds average 4-6 in (10-15 cm) thick. Some beds are characterized by fine laminations; replacement textures, such as irregular rounded zones of different color within beds are common; sedimentary breccia occurs in local pockets between beds with angular chert clasts of diameters generally less than 4 in (10 cm) in a chert matrix. Stylolitic partings occur in 90 percent of the chert beds. Shaly partings occur only in rare outcrops, and provide evidence for stratigraphic orientation. The chert occurs in sections greater than 0.62 mi (1 km) thick, without any other lithologies present. Due to limited exposure in tundra-covered terrain, a true thickness cannot be estimated. Isoclinal folding or tectonic repetition may have thickened the unit.

In some places in the Livengood quadrangle, but not seen in the WMNRA, chert pebble conglomerate and wacke in sections as thick as 164 ft (50 m) have scoured into the upper part of the thick chert sections in the Livengood Dome Chert. The conglomerate and wacke is overlain by alternations of beds of the following lithologies exposed in the WMNRA: black, tan, green, and red argillite, siltstone, and tuffaceous siltstone, gray chert, gray-, black-, green- and tan-mottled chert (similar to thick chert section) and

rare mafic igneous sills or flows. This suggests that the Livengood Dome Chert and the closely associated clastic rocks may be related lithofacies, and that the wacke and conglomerate could represent discrete channels cutting across the slope. The chert pebble conglomerate may be part of the Olc or a separate unit; however, the sparsity of data at this time, precludes us from making an interpretation of the conglomerate.

AMY CREEK UNIT

The Amy Creek unit is characterized by dolomite (PzpЄd) interbedded with chert (PzpЄc) and is exposed in rubble slopes in an area north of Beaver Creek and south of Victoria Creek in the WMNRA. An excellent exposure of this unit is found on the west side of Amy Creek from which it derives its name, near Livengood. This description relies heavily on that exposure as well as several other general observations along this belt of rocks 12 mi (20 km) wide and (62 km) 100 km long that extends across the entire Livengood quadrangle and into the Circle quadrangle as far as the Tintina fault zone. The Amy Creek unit covers an area of 19 sq mi (49 sq km) in the WMNRA. The southern contact is a fault in which most of Amy Creek unit is overthrust by the mafic/ultramafic complex (ЄpЄums, ЄpЄumg, and ЄpЄum). At its northern edge the Amy Creek unit is thrust northward over the mafic rocks, PzpЄm and the Dc? conglomerate. Northeast of Victoria Mountain the Amy Creek unit appears to be thrust over the Victoria Creek strand of the Tintina fault zone. Absence of recognizable megafauna, the presence of stromatolites and coated algal grains, and the style of silicification suggest correlation with late Proterozoic rocks of the Nation River area, Charley River quadrangle. Also, it is interesting to note that the Amy Creek unit characteristically occurs close (although generally in tectonic contact) to the Cambrian to Precambrian ultramafic intrusive bodies (ЄpЄum, ЄpЄumg, and ЄpЄums).

PzpЄd DOLOMITE--Dominantly medium- to thick-bedded, light-gray, yellow-gray or buff colored dolomitic mud-, wacke- and packstone. Peloids are extremely abundant in coarser grained rocks, as well as crossbedding. Laminations more common in fine muds. In other places consists of rubbly outcrops of medium-grained, light- to medium gray dolomite, with well-developed reticulate silica box-work. As much as 80 percent silicification of the dolomite has been observed. Some limestone layers within the dolomite are as much as 98 ft (30 m) thick. Small black chert nodules, lenses, and irregular masses occur rarely. Solution breccia, stromatoporoids and coated algal grains were also observed. Thickness estimates of 2,300 ft (700 m) have been made of the carbonate section at Amy Creek and it is at least that thick in the WMNRA. Minor dark gray lime mudstone is interbedded with part of section dominated by greenstone and chert.

PzpЄc CHERT--Black, rarely medium gray, with iron and manganese stains. Massive to thick-bedded, but also thinly interbedded with black carbonaceous argillite and black argillaceous chert which locally grade upward into light brown dolostone lenses with nodules (cm-

scale). Dolostone lenses with nodules grade upward into lenses of light to dull green tuff, tuffaceous siltstone and minor, very fine-grained graywacke. Locally, volcaniclastic material increases upsection in the argillite. Basaltic flows and flow breccia at least 328 ft (100 m) in thickness occur locally in the argillaceous horizons at Amy Creek which is outside the WMNRA.

MAFIC IGNEOUS ROCKS AND RARE SEDIMENTARY ROCKS

Gabbro, diabase, and diorite sills, altered greenstone, and basalt are interlayered with a small amount of laminated argillite, siliceous siltstone, quartzite, and very minor graywacke in a northeast-striking outcrop belt north of Beaver Creek and south of Victoria Creek fault. The PzpЄm unit covers approximately 14 sq mi (36 sq km) in the WMNRA. The age of these rocks has not been determined. On the north side, the PzpЄm and Dc? units are thrust over the Wickersham unit, ЄpЄga, and on the south side the PzpЄm is overthrust by the Amy Creek unit. It is possible that the PzpЄm rocks are gradational from the greenstone in the PzpЄd (Amy Creek unit) and that the two sections have undergone minor telescoping. The association of the dolomite and mafic igneous rocks in the WMNRA is similar to lithologic relations in the Tindir Group rocks of the Charley River quadrangle (Brabb and Churkin, 1969).

PzpЄm MAFIC IGNEOUS ROCKS, MINOR SEDIMENTARY ROCKS--Mafic igneous rocks dominate this unit and include: (1) gabbro and diabase sills, very fine-grained and chilled on outer margins, but more commonly medium- to coarse-grained, dark-olive green, greenish-gray to dark greenish-black, with green feldspars (plagioclase?) and black pyroxene, more resistant than surrounding rocks, locally-gradational into diorite, (2) diorite, medium- to coarse-grained, light-green to medium greenish-gray, blocky jointing, (3) greenstone, very fine-grained, medium- to dark- grayish-green and greenish-gray, dark olive-green, locally calcite amygdules, and (4) basalt, very fine- to fine-grained, with large calcite amygdules locally, medium- to dark-greenish-gray. These mafic igneous rocks are interlayered with, and in some cases show contact with, a sequence of very fine- to fine-grained sedimentary rocks composed of interbedded (1) slate, medium-dark-gray with siliceous shale and chert, (2) argillite, gray to black, tan weathering, slaty to siliceous, with some laminations of siliceous claystone, siltite, and quartzite, (3) siltstone, argillaceous, dark-gray to tan weathering, (4) very minor quartzite, light- to medium-gray, and (5) rare graywacke.

GREENSTONE AND SERPENTINITE

Mafic and ultramafic igneous rocks are exposed in the WMNRA as a northeast trending belt that ranges in width from 1.5 mi (2.4 km) to unexposed at the surface and covers an area of approximately 12 sq mi (31 km). High magnetic susceptibility, because of the presence of serpentinized peridotite and dunite, and sparsely-vegetated serpentinite mark this unit throughout the Circle and Livengood quadrangles. The age of the mafic and ultramafic belt near the town of Livengood has been determined by radiometric age dating

methods to be 518-633 Ma (table II-3). Within the WMNRA, the mafic/ultramafic rocks appear to be thrust northwest over the Livengood Dome Chert and the Amy Creek unit. The Wilber Creek unit borders the unit to the south, and it is either in thrust contact or it is unconformable on the mafic and ultramafic unit. Ground and helicopter magnetometer traverses establish that the mafic rocks occur as layers tens to hundreds of meters thick between layers of ultramafic rock. The mafic-ultramafic complex is interpreted to be a sequence of mafic and ultramafic sills, some of which may have differentiated to form cumulate layers. For the purposes of this map, the mafic/ultramafic igneous rocks of this belt are subdivided into greenstone (ЄpЄumg) and layered mafic-ultramafic complex (ЄpЄum) which includes serpentinite (ЄpЄums).

ЄpЄumg GREENSTONE--Massive, resistant, medium to dark green, yellowish green, grayish green, and greenish gray clinopyroxene-plagioclase metabasalt and diabase, with minor metatuff; weather to darker shades of yellow, yellowish brown, reddish brown, olive gray or greenish gray. Very weakly magnetic: k=0.0002 to 0.0008 SI, 0.0005 SI most common. Forms belt of hogbacks up to 0.8 mi (1.3 km) wide in eastern Livengood quadrangle, where it grades northward from aphanitic basalt to diabase near the contact with the mafic-ultramafic complex described below. The contact itself is a fault. Resistant outcrops of mylonite occur in the diabase just south of the fault. Southwest of VABM Beaver, greenstone occurs in tors south of the mafic-ultramafic complex and, together with minor gabbro, forms a ridge 1640 ft (500 m) wide within the complex. The greenstone is always associated with the mafic-ultramafic complex, although abundant greenstone occurs only sporadically along the length of the complex.

ЄpЄum and ЄpЄums LAYERED MAFIC-ULTRAMAFIC COMPLEX--Clinopyroxene gabbro, microgabbro, diorite (ЄpЄum), green or olive gray, tan to gray weathering, occur as resistant, isolated tors within swales that contain abundant sheared light to dark yellowish-green, grayish-green, greenish black and black serpentinite (ЄpЄums) which weathers to various shades of medium to dark brown, reddish brown and grayish brown, derived from clinopyroxene peridotite, dunite, and lesser clinopyroxenite. Bundtzen (1983) reports hypersthene gabbro and hornblende gabbro or diorite with minor augite among the mafic rocks, and possible cumulate textures in the serpentinite elsewhere in the Livengood quadrangle. The mafic rocks are very weakly magnetic: k=0.0002 to 0.0008 SI, 0.0005 SI being most common. The serpentinized peridotite and dunite are magnetic and cause magnetic highs: k=0.002 to 0.04 SI, with occasional readings as high as 0.2 SI. Pyroxenite is nearly nonmagnetic, with k=0.0002 SI.

WICKERSHAM UNIT

The Cambrian to Precambrian Wickersham unit within the WMNRA covers at least 490 sq mi (1,269 sq km) and has such lithologic diversity that it is mapped as five separate units. All the individual Wickersham units are lithofacies and appear to have gradational contacts with one another. They are lower

greenschist-grade metamorphic facies. Within the WMNRA the Wickersham unit occurs in the 1) Schwatka area, 2) Livengood area, and 3) White Mountains area.

In the Livengood area the Wickersham unit is mapped as maroon and green argillite, grit, dark limestone, chert, and rare diabase (ϵpϵga). The southern contact of the Wickersham unit with the Livengood Dome Chert is probably an unconformity, but has been overthrust by several different Paleozoic or Precambrian lithologic units in some areas. On the north side, the Wickersham unit is separated from the Ordovician Livengood Dome Chert (Olc) by a fault. The Wickersham unit of the WMNRA is very similar to the Windermere Supergroup of Yukon Territory, Canada (Eisbacher, 1981), particularly to that of the Selwyn Basin.

ϵpϵga GRIT, GRAYWACKE GRIT, MAROON, GREEN AND GRAY ARGILLITE AND ARENACEOUS LIMESTONE--Grit is much like the pϵg unit described in the White Mountains area section that follows. Graywacke and quartzwacke grit are light to medium olive gray, commonly conglomeratic or unsorted, feldspars locally abundant, often slightly foliated, but sedimentary features preserved. Bedding in graywacke and quartzwacke grit is graded, locally amalgamated, fines upward to ripple-laminations in silty phyllite with small-scale trough crossbedding. Argillite is laminated, maroon and light to medium green and grayish green, fissile to blocky fractured. Locally ϵpϵga is phyllitic and slaty, laminated, medium-light to dark gray and greenish gray, and contains rare, horizontally bedded, discontinuous 2-3 ft (0.6-0.9 m) thick beds of greenish-gray, micaceous, arenaceous limestone. Basaltic rocks are interlayered with ϵpϵga but are thin and too small to differentiate on the geologic map. Oldhamia, a trace fossil of probable Late Proterozoic to Cambrian age has been found in ϵpϵga at two localities in the Circle quadrangle, one in the WMNRA (see bedrock geologic map, Smith and Pessel, in press) and the other outside of the WMNRA in the Schwatka area, Circle quadrangle (fossil locality 2, table 2, Foster and others, 1983).

WHITE MOUNTAINS AREA

TERTIARY CONGLOMERATE AND SHALE

There are two small areas of exposure of possible Tertiary sediments in the White Mountains National Recreation Area. One consists of a few small outcrops at water level on Victoria Creek near the mouth of Squaw Creek northeast of Victoria Mountain and the other is in the vicinity of the divide between the North Fork of Preacher Creek and the headwaters of Moose Creek in the Circle quadrangle. The outcrops are very poor, hardly more than rubble piles of pebbles and boulders. Both locations are in the Tintina fault zone trench and have bearing on the age of the most recent fault activity. The deposits at these two locations are discussed separately:

Ts? **CONGLOMERATE, SHALE—Moose-N. Fork Preacher Creek divide--**

Boulders, cobbles, and pebbles in a fine sand to pebble matrix; clasts consist of light, dark, and greenish gray hard dense quartzite, black and gray chert and white quartz, up to 10 in (25 cm) in diameter, very well rounded and commonly with a dark manganese stain, poorly consolidated; matrix of sand includes grains of quartz, chert, feldspar, and rock fragments of quartzite, dark mafic rock, and a light bluish-green, fine-grained rock, possibly of volcanic origin. Very small amounts of gray clay shale and possible coal. In places large quartzite boulders are shattered and traces of slickensides were found. The unit crops out as rubble and may be only a few hundred feet thick, has no metamorphic features. It is cut on the south side by an east-west trace of the Tintina fault system, probably the Hot Springs fault (Weber and Foster, 1982) and is marked roughly on the north side by an east-west photo linear which may be a small subparallel Tintina fault; however, the conglomerate could lie unconformably on the Vrain tuff (mzPzvt). The Ts? is lithologically similar to Tertiary sediments lying in the Tintina Trench immediately to the north and east, identified as Oligocene or Early Miocene (J.A. Wolfe, personal comm., 1983).

FELSIC PLUTONIC ROCKS WHITE MOUNTAINS AREA

Felsic plutons of Early Tertiary to Late Cretaceous age occur in the White Mountains and the Livengood areas within the WMNRA. The three major felsic plutons exposed at the surface in the USGS-mapped part of WMNRA are located on Cache Mountain, Victoria Mountain, and the ridge west of Roy Creek (Tg, Kg, and Ks, respectively). The Victoria Creek pluton is discussed in the section on the Livengood area. Cache Mountain pluton covers approximately 10 sq mi (26 sq km), and the syenite of Roy Creek covers approximately 4 sq mi (10 sq km); both Tg and Ks intrude the Wickersham unit (pGg) in the White Mountains area.

Granite of Cache Mountain

Tg GRANITE--Distinctive massive, quartz-rich, seriate-porphyritic granite (fig. II-2) with a typically medium-grained matrix whose volume is about equal to that of the phenocrysts. Phenocrysts are sub- to euhedral nearly white K-feldspar as large as 1 in (2.5 cm) across; equant, generally somewhat rounded dark-gray quartz phenocrysts slightly smaller than the K-feldspars; and sparse but persistent broad laths of plagioclase visible in hand specimen. All three minerals show serial size relation with the matrix. Color index (biotite) averages about 7, but appears much greater megascopically because of the dark-gray quartz. Variations from the foregoing to finer, non-porphyritic varieties, appear to be common throughout the pluton, at least some occurring over horizontal distances of only a few feet, but dark and rounded phenocrysts of quartz persist even in very fine-grained varieties. A few biotite-quartz-feldspar porphyry dike rocks with an aphanitic matrix were seen in rubbly outcrops but none were found intact. In a few loose fragments, however, the porphyry clearly cuts the coarse-grained granite. A few dark-gray,

fine-grained xenoliths of country rock were seen, but are relatively uncommon. Sawed slabs, etched and stained to discriminate the feldspars and quartz, commonly reveal well-defined zoning in the K-feldspar phenocrysts, which locally display thin mantles of graphic granite. Other characteristics of the rock include sparse but seemingly ubiquitous miarolitic cavities, and the common occurrence of tourmaline, locally forming incomplete radial rosettes 0.4-1.2 in (1-3 cm) across.

In 1984, the U.S. Bureau of Mines spent one day conducting a pan-concentrate survey and a helicopter reconnaissance of the pluton in a search for tin deposits, and described the results in a brief unpublished report, (Dean Warner, 1984, written commun.). His description of the various rock types accords well with ours, although he interpreted the various textural types as separate intrusive phases of a composite pluton, evidence for which was not found by us, except for the late porphyry dikes.

In thin-section, the rock is typically xenomorphic-granular--strictly hypautomorphic-granular with a strong xenomorphic-granular tendency--K feldspar fairly commonly shows extremely fine microperthite, negative optic axial angle of about 40-50 degrees, and locally shows spectacular intergrowth with quartz, the pattern resembling myrmekite rather than the classic graphic pattern. Plagioclase, probably An 20-30 in composition, is polysynthetically twinned and typically shows moderate gradational--locally oscillatory--zoning. Biotite is mostly anhedral, reddish-brown, and contain numerous pleochroic haloes, some with tiny birefringent zircon and monazite(?) at their centers; locally these minerals show crude zonal distribution within the biotite. Biotite typically shows minor to moderate alteration to chlorite. Anhedral muscovite in trace amounts is usually present as both discrete grains or as small contiguous protrusions on, or intergrowths with, biotite.

Accessory minerals include apatite, zircon, monazite(?), tourmaline, fluorite, magnetite, and in one specimen near the southwestern contact, as much as one percent topaz in grains comparable in size to the feldspars and quartz of the matrix.

Modal analyses of 13 representative samples are plotted on figure II-2, and occupy the central part of the granite field (Streckeisen, 1976). Chemical analyses and norms of four of the samples (table II-1) compare fairly closely to Nockolds' (1984) average calc-alkali granite and fall within the denser part of Le Maitre's (1976) field of 197 granites.

A minimum K/Ar biotite age of 58.4 $\pm$ 1.8 Ma (table II-2) was determined by D.L. Turner at the Geophysical Institute, University of Alaska, Fairbanks, and reported by Bjarne Holm (1973, p. 34).

Ks SYENITE--The syenite of Roy Creek is a poorly exposed, compositionally

highly varied alkalic pluton, chiefly aegirine-augite syenite in composition, which discontinuously occupies about 4 sq mi (10.4 sq km) along upper O'Brien and Roy Creeks in the southeastern part of the map area. The most common textural and compositional type, seen both in rubbly surface exposures and in drill core, is trachytoid aegirine-augite syenite with an average color index of about 20. Variations range from leucocratic syenite with a color index of less than 5, to shonkinite containing as much as 70 percent clinopyroxene. Except where finer-grained dikes cut host rock, all compositional types appear to intergrade, including gradation to leucocratitc quartz-rich granite, the gradational nature of which was verified in drill core. Burton (1981, p. 44), however, concludes, on the basis of chemical criteria, that the syenite and granite are not comagmatic. In color the rocks range from dark gray to grayish orange with orange and brown tones predominating as a result of much limonite staining. Most rocks are massive, and average medium-grained, although the actual range in grain-size exceeds the category range 0.04-0.2 in (1-5 mm) considerably, with tabular Carlsbad-twinned K-feldspar consistently the largest, commonly 3 or 4 times the size of aegirine-augite or biotite, the next most abundant minerals. Trachytoid texture is the hallmark of the syenite although xenomorphic-granular, hypautomorphic-granular, and porphyritic textures are not uncommon. The coarsest rock is a porphyritic biotite-aegirine-augite syenite that crops out narrowly along the northwest base of hill 3603, near the southern limit of the pluton, where K-feldspar tablets measuring as much as 2 in (5 cm) compose 60-80 percent of the rock.

Microscopically the most arresting feature of most rocks is the massive unsheared, xenomorphic-granular--modified by trachytoid--texture, dominated by large Carlsbad-twinned K-feldspar typically "dusted" with cryptocrystalline argillic(?) alteration and variously perthitic with albite exsolution lamellae locally coarse enough to clearly display polysynthetic twinning. In porphyritic rocks, K-feldspar phenocrysts locally show several thin concentric zones recognized best on etched and selectively stained sawn slabs. Not uncommonly, K-feldspar shows sparse graphic intergrowth with quartz, where the latter is present in more than trace amounts. The optic angle of the K-feldspar is distinctively low, and though not precisely measured, many observations indicate a negative 2V of 30 to 50 degrees.

Aegirine-augite, the next most abundant mineral, shows optical properties typical of the aegirine/aegirine-augite group, the large optic angle and negative elongation being two of the most typical and recognizable properties when accompanied by the distinctive intense yellowish-green color. These properties reveal aegirine-augite to be present in virtually all augite-bearing rocks in the pluton, generally recognized by greenish fringes or greenish mottling of otherwise pale-green to colorless augite crystals. Biotite, brown to olive green, is generally no more than half as

abundant as pyroxene and is typically intergrown, in part, with the latter. Locally, it contains pleochroic halos from one or more of: zircon, monazite(?), allanite, and locally, sphene(?). Only locally is it slightly altered to chlorite.

Accessory minerals common to most rocks are zircon, apatite, and sphene. Quartz, in at least trace amount, was recognized in most--but not all--syenite samples, and in some, constitutes as much as 5 percent of the rock. It does not form phenocrysts, and locally, with albite/oligoclase and calcite, conspicuously fills interstices as the final minerals to crystallize. Scattered occurrences of the minerals present in accessory amounts include: calcite; opaque minerals; muscovite, both primary(?) and secondary; fluorite, locally a bright lilac color; members of the eckermanite-arfvedsonite group; tourmaline; and one occurrence of melanite(?) garnet. In addition, thin-sections commonly contain irregular areas that consist of varied yellow, brown, or green cryptocrystalline intergrowths of alteration products that may reflect partially or completely replaced feldspathoids.

Much of the adjacent country rock, although not investigated extensively, shows marked variation in response to metamorphism, from profoundly recrystallized hornfels and granofels in which original sedimentary texture and structure have been completely eradicated, to quartzite and metasiltstone in which original sedimentary texture and relict bedding are well preserved. Because the country rocks are highly siliceous, the resulting granoblastic derivatives are typically unremarkable in mineralogy except where contribution from the intruding syenite has produced a siliceous hybrid. Plagioclase, K-feldspar, muscovite, and biotite, in addition to quartz, compose the typical mineralogy of the contact metamorphic rocks. However, a small roof remnant in the east-central part of the intrusion--in the part most extensively explored for U-Th--was found to contain corundum and spinel, together totalling about 20 percent of a biotite-K-feldspar-quartz hornfels. The corundum crystals are microscopic in size and are tinged with yellow in plane light, distinctly different from the sapphire-corundum identified in a pan-concentrate from upper Roy Creek (see Chapter IV).

Because of poor exposure and great variation in both texture and composition of the alkalic rocks, no quantitative petrographic work was attempted, since it would be impossible to accurately extrapolate composition and trends to the covered but major part of the pluton. Most of the analyses of major oxides on table II-3 represent mineralized and altered syenite; only analyses 6, 7, and 8 represent relatively fresh, less-altered rock, but none of these fit well with Nockolds' (1954) or Le Maitre's (1976) alkalic rocks. This suggests that late-stage deuteric alteration, which was the process active in concentrating thorium and rare-earth elements, affected these rocks as well, although to a much lesser extent than

the others on table II-3. Nockolds' group calc-alkali syenite and trachyte, nevertheless seems to best encompass the Roy Creek syenites. These three analyses show that both oversaturated and undersaturated rocks are present, which corroborates petrographic observations.

Biotite ages of 2 syenites--aegirine-augite syenite and porphyritic aegirine-augite syenite--reported by Burton (1981, p. 50) were determined to be respectively 85.4 $\pm$ 6.4 Ma, and 86.7 $\pm$ 3.7 Ma, and were stated to be minimum ages (table II-2).

Table II-3. Chemical analyses and norms of selected samples from the Roy Creek prospect

[Chemical analyses, in weight percent, using XRF and ICP (underlined) methods by analytical laboratories of the USGS in Denver, CO ("D" nos.) and Menlo Park, CA ("M" nos.). For convenience, samples arranged in same order as those in Table V-2, except that nos. 2 and 3 are omitted owing to interference problems caused by abundant presence of REE. That problem also affects the values for nos. 5, 9, and 10, which should be considered as only semiquantitative values. LOI is loss on ignition at 900°C. CIPW norms calculated only for analyses with totals >98 percent]

	1	4	5	6	7	8	9	10
Lab No.	M-176068	M-176069	D-278549	M-176067	D-278551	D-278547	D-278545	D-278546
Field No.	86ARi-6Q	86ARi-6R	YM-2	86ARi-6P	86ARi-6-RY-4	Y-24-C(295')	Y-24-C(70')	Y-22-C(270')
SiO_2	<u>15.6</u>	<u>20.2</u>	49.6	60.0	51.5	57.0	55.5	45.0
Al_2O_3	<u>2.0</u>	<u>2.5</u>	19.5	13.8	15.5	10.9	14.9	13.2
Fe_2O_3	3.53	5.15	6.49	5.78	8.40	9.36	8.35	8.96
MgO	<0.1	0.15	0.50	1.8	3.52	2.35	<0.1	1.38
CaO	6.67	7.65	1.28	3.82	4.98	6.26	0.03	8.16
Na_2O	<0.2	<0.2	1.57	2.5	0.60	2.89	1.34	1.31
K_2O	0.07	0.06	8.42	9.51	10.5	7.29	11.2	7.24
Ti_{o2}	0.04	0.08	<0.03	0.38	0.73	1.22	0.07	0.15
P_2O_5	2.45	2.42	0.46	0.25	0.73	0.13	<0.05	0.94
MnO	0.23	0.24	0.09	0.15	0.16	0.26	<0.02	0.28
LOI	14.1	12.9	4.23	0.63	1.67	1.13	4.12	3.68
Total	44.99	51.55	92.17	98.62	98.29	98.79	95.68	90.30

CIPW norms (weight percent)

Quartz	0.80	—	0.04
orthoclase	57.52	57.16	44.41
albite	18.46	—	15.96
anorthite	—	8.95	—
leucite	—	5.86	—
nepheline	—	2.87	—
acmite	2.81	—	8.11
na-metasilicate	—	—	0.01
diopside	14.73	9.73	26.19
olivine	—	8.87	—
hypersthene	2.97	—	2.58
magnetite	1.38	3.37	—
ilmenite	0.74	1.44	2.39
apatite	0.59	1.76	0.31
Total	100.00	100.01	100.00

WILBER CREEK UNIT

The Wilber Creek unit is a Jurassic and/or Cretaceous sequence of lithologic units that covers approximately 110 sq mi (285 sq km) of the WMNRA within the Beaver Creek valley north of the White Mountains and southwest of Victoria Mountain. This northeast trending Mesozoic flysch belt extends northeast at least as far as the mouth of Sheep Creek and well outside the WMNRA to the southwest. Magneto-telluric resistivity work (section III) suggests this Mesozoic flysch basin is at least 0.62-1.24 mi (1-2 km) deep and that the Wilber Creek unit may be underlain by the Vrain unit. Wilber Creek unit is composed primarily of polymictic conglomerate, graywacke, siltstone, and shale. Unsorted to poorly sorted, amalgamated beds, normally- and reversely graded, rhythmic-bedding, flaser-bedding, flame structures, load-casts, tool-marks, convolute-laminations, and shale rip-up clasts are common characteristics of the Wilber Creek unit, and of turbidite deposits, in general. The Kathul Graywacke of the Kandik basin and the Kuskokwim Group of the Kuskokwim basin are similar types of deposits and probably roughly correlate with the Wilber Creek unit.

KJw POLYMICTIC CONGLOMERATE, GRAYWACKE, SILTSTONE AND SHALE--Polymictic conglomerate is dark olive gray to medium-dark gray, iron-stained, unsorted, with subangular to well-rounded granules to cobbles and less abundant boulders. Clasts are locally-derived from the Yukon-Tanana Upland and consist mostly of mafic igneous, greenstone, felsic volcanic, diorite, and other intrusive rocks; quartzite, dark-gray limestone, sandstone, siltstone, phyllite, chert, rare grit, and slate (rip-ups). The conglomerate clasts are generally matrix-supported with a matrix of sand, silt, and clay. Beds are mostly internally-massive, large- to medium-scale graded and amalgamated with planar bases and tops. Some large-scale troughs internally-filled with smaller-scale trough-crossbedding displaying fining-upward cycles. Conglomerate is approximately 5 percent of the Wilber Creek unit.

Graywacke is medium- to medium dark-gray to greenish-gray iron-stained on weathered surfaces, mostly fine- to medium-grained, moderately-sorted, subangular to subrounded, with some very well-rounded quartz grains. Shale rip-ups are as much as 10 in (25 cm) long. Matrix is silt and clay. Laterally-continuous, graded, amalgamated, medium-scale graywacke beds are rhythmically interbedded with, and fine upward to, siltstone and shale. Conglomeratic graywacke lenses are common, with locally derived clasts of mafic and felsic volcanics, very fine-grained sandstone, siltstone, chert, and shale rip-ups. Bases of beds are erosional, planar to slightly concave upward, and sole-marks are common. Minor small-scale scour-fills that fine upward into ripple-laminated siltstone occur. Sandstone and conglomeratic sandstone compose approximately 20 percent of the Wilber Creek unit.

Siltstone is medium-gray to black, rusty-orange on weathered surfaces, commonly laminated with very fine-grained sandstone and

shale as discontinuous lenses, flasers, and ripples, or rhythmically interbedded with sandstone. Siltstone comprises approximately 25 percent of the Wilber Creek unit.

Shale is dark-gray to black and commonly phyllitic, fissile, to blocky fracturing, with very fine-grained sandstone flasers, commonly laminated with siltstone. Some shale is rhythmically-interbedded with very fine-grained, ripple-laminated, thin sandstone beds that have sharp erosional bases and shaly tops. Shale is approximately 50 percent of the Wilber Creek unit.

VRAIN UNIT

In the northeastern part of the WMNRA, the Vrain unit is exposed in an area along Beaver Creek, between the White Mountains and Victoria Mountain and extends to the east out of the WMNRA past VABM Vrain in the Circle quadrangle. In the WMNRA the Vrain unit covers approximately 72 sq mi (186 sq km). It is composed primarily of dark-gray slate, argillite, or phyllite, MzPzv; with some beds of a distinctive chert- and quartz-pebble meta-conglomerate, MzPzvc, and a few interbeds of felsic tuff, MzPzvt. The argillite appears to grade westward into thinly-interbedded siltstone, very fine-grained quartzite, and phyllitic slate, MzPzvs, exposed along the ridge between Willow and Sheep Creek. Contacts between these units within the Vrain are mostly covered and are indistinct at best.

Conglomerate clasts identified in hand specimens (MzPzvc) are limited to chert, white quartz, and gray phyllite. None of the clasts appear to be locally derived from rocks common to the White Mountains area. This suggests a further-removed depositional site for the MzPzvc than the current position in the WMNRA.

Lithogically the Vrain unit is very similar to the Devonian Lower Earn Group of Yukon Territory, Canada as characterized by Winn and Bailes (1987). Photomicrographs in their paper (fig. 3, p. 532), of the Lower Earn Group conglomerate and of an uncommon quartzose siltstone fragment, are very similar to the composition and texture, in thin-section, of the conglomerate (MzPzvc) and siltstone (MzPzvs) of the Vrain. They describe Devonian sedimentation along an extentional submarine fault scarp related to stratiform lead-zinc sulfides, mudflows, and turbidites. Base and precious metals in the area of Warren and Moose Creeks (section IV) of the WMNRA, are the type common to sedimentary deposits in an extentional submarine system similar to that interpreted by Winn and Bailes, 1987, for the Lower Earn Group in the Yukon Territory of Canada. However, the Vrain unit is also very similar lithologically to Mesozoic flysch beds (Brabb and Churkin, 1969) in the Kandik Basin of the Charley River quadrangle; particularly, the MzPzv is similar to the upper part of the Glenn Shale or to the Biederman argillite (M. Churkin, pers. commun., 1980), and the MzPzvs is similar to the Keenan Quartzite.

The age and thickness of the Vrain unit is unknown, but magneto-telluric data suggest that a similar resistive unit underlies the White Mountains thrust sheet and may be as much as 3.7 mi (6 km) thick (section III).

MzPzv ARGILLITE, SLATE, SILTSTONE, AND QUARTZITE--Argillite is the dominant lithology in the vicinity of VABM Vrain, after which the unit is informally named. It is interbedded with minor quartzite and slaty argillite. Foster and others (1983) describe this unit as argillite, including siltstone, siliceous siltstone, and shale, dominantly gray, olive, or greenish-gray, and generally weathering reddish-yellow-brown or tan; commonly limonite- or manganese-stained along fractures; locally slaty; cleavage commonly well-developed and folded. Quartzite is mostly greenish-gray or gray, but some white or light-gray. Sulfides and hematite (?) are locally abundant. In the vicinity of VABM Vrain the unit may be slightly hornfelsic. To the west, in the nearby WMNRA, the Vrain slate and argillite is generally dark-gray and distinctively pyritiferous. Small streams originating in this unit, and even Beaver Creek in places, are stained red from the iron-bearing water.

MzPzvt FELSIC TUFF--Felsic tuff is exposed in the area southwest of VABM Vrain. Foster and others (1983) describe it as medium-light-gray, and some crystal tuff with large dark-gray, glassy quartz crystals. It is sparingly present in the WMNRA.

MzPzvc CONGLOMERATE--Conglomerate has stretched pebbles locally mylonitic, at least as large as 1.2 in (3 cm) in diameter which are composed mostly of white monocrystalline quartz, gray and black, argillaceous chert, and locally-abundant medium-gray phyllitic rip-up clasts. The matrix is cherty and most pebbles are clast-supported. The conglomerate is poorly sorted to unsorted; and has graded bedding in possible channels which appear to be erosional into the argillite, siltstone, quartzite sequence of the Vrain.

MzPzvs QUARTZITE, SANDSTONE, SILTSTONE, AND PHYLLITE--The rocks along the ridge between Willow and Sheep Creeks, and probably west of Victoria Mountain, are low-grade greenschist facies, very fine- to coarse-grained, light- to medium-gray, well-sorted quartzose to subquartzose sandstone with horizontal laminae of siltstone. The internal laminations of this unit are often well-preserved ripple-laminae, small-scale crossbedding, graded bedding, load casts and heavy mineral laminae. The fine-grained sandstone is thinly interbedded with light-gray siltstone and silty, often phyllitic light-gray, bioturbated shale. Finely disseminated limonite and hematite(?) grains, as well as authigenic chlorite alteration occur in argillaceous laminae. The unit is overturned to the north and is internally disrupted.

UNNAMED SEDIMENTARY ROCKS

This unit is identified only in one outcrop about a quarter mile (480 m) long on Beaver Creek near Windy Creek on the west side of the White Mountains. It is impossible to estimate the thickness because the unit is so pervasively folded and faulted; slickensides are common. It is separated from the Globe

unit (Pzg) on the south by a major shear and gouge zone which is visible at that end of the outcrop, and it is separated from the Wilber Creek unit (KJw) at the north by a covered interval which may hide a segment of the Beaver Creek thrust fault. One red and yellow-stained white quartz vein in the argillite contained sulfides.

Basically a shale and sandy limestone, the rock cannot be correlated with anything else seen in the WMNRA. No fossils or means of age-dating the sediments have been found as yet, however, J.T. Dutro, Jr. (Dutro, personal commun., 1987) who visited the locality suggests that the lithologies are "very typical" of those in the Triassic part of the Glenn Shale found in the Charley River quadrangle (Brabb, 1969).

MzPzs CALCAREOUS SHALE AND SANDY LIMESTONE--Shale or argillite, dark gray, non-calcareous to very calcareous, phyllitic in places, becomes very graphitic and shot with small white quartz veins toward the faulted southern end of the outcrop, white phosphatic bloom covers some of the cliff faces. Limestone, medium dark gray to dark gray, contains varying amounts of sand- or silt-sized quartz and sparite with no micritic mud (packstone), beds up to 2 in (5 cm) thick, laminated with thin shaly layers; in thin section the monocrystalline quartz grains are fractured and the fractures filled with carbonate; although once probably rounded, the quartz grains are now undergoing calcitization, sulfides are present, and possible organic material is along folia; sandy limestone makes up from 10 to 15 percent of the section; grades to medium-gray, very limey sandstone and a trace of calcareous granule conglomerate containing round black pellets which may be phosphate.

BEAVER BEND UNIT

The Beaver Bend unit (MzPzc) is a Mesozoic or Paleozoic sequence of conglomerate, graywacke, and shale that covers 3 sq mi (7.8 sq km) along the big bend of Beaver Creek in the Livengood quadrangle (pl. II-A). There are several conglomerate units within the WMNRA, but each one has distinctive lithologic characteristics that justify mapping them as separate units. The northern contact of MzPzc with the Tolovana Limestone (DSt) is covered but probably is a fault. The southern boundary with the Wickersham unit (ϴpϴga) is interpreted as a high-angle fault. Internally, the MzPzc is vertical, steeply dipping or northwest-dipping and overturned which further suggests that it is also folded and bounded by faults. Unidentifiable plant fragments are the only fossils found in the Beaver Bend unit, but lithologically the unit strongly resembles the Nation River Formation of the Charley River quadrangle, Alaska (Brabb and Churkin, 1969). The sedimentary characteristics of the Beaver Bend unit suggest that it was deposited as an inner-fan turbidite.

MzPzc CONGLOMERATE, GRAYWACKE, AND SHALE/SLATE--Polymictic conglomerate and conglomeratic graywacke are light- to medium-dark-gray, poorly sorted to unsorted, clast-supported, and well-indurated. Granules and small pebbles are abundant and are as much as 2 in (5 cm) in

diameter. Clast compositions are black to dark-gray and light-green, angular to subrounded chert, very well-rounded monocrystalline quartz with quartz overgrowths, well-rounded quartzite, mafic and felsic volcanic rock fragments, argillite, slate, siltstone, and sandstone. The contacts between clasts display pressure solution with a very minor amount of chlorite matrix. Zircon occurs as a detrital accessory mineral. Beds are as thick as 5 ft (1.5 m), graded, amalgamated, laterally-continuous with sharp, planar, erosional bases, and fining-upward cycles. Phyllitic, siliceous, dark-gray argillite rip-up clasts are common.

Graywacke is fine- to medium-grained, moderately sorted, with subangular to well-rounded grains of mostly quartz and chert, and lesser amounts of slate, polysynthetic C-twinned plagioclase, and both felsic and mafic volcanic rock fragments. Matrix is chlorite, probably recrystallized from clay. Graywacke is rhythmically interbedded with dark-gray shale (ss:sh=2:1). Thicker sandstone beds are laterally continuous with planar erosional bases and have a uniform thickness averaging 6-8 in (15-20 cm). Beds are internally filled with planar laminations deposited in a high-flow regime, commonly have sole marks, numerous fining-upward cycles, and locally display wavy bedding in sandy siltstone at the tops of some beds.

Discontinuous, thinly bedded, fine-grained graywacke is interbedded with laminated siltstone, dark-gray to black, and shale which weathers gray to olive. Shale content increases toward the northwest, which is downsection.

GLOBE UNIT

The Globe unit in the White Mountains area is bounded on the north by the Beaver Creek thrust fault and on the south by the White Mountains thrust fault. Within the WMNRA, this narrow band of folded rocks is approximately 2 mi (3 km) wide in the southwestern part and is covered by rocks that have been overthrust to the northeast just west of Mascot Creek (pl. II-A), but it emerges again to the east of Mascot Creek. The age of the Globe unit has yet to be determined since no fossils have been found, but lithologically it is most like the Keno Hill Quartzite which contains conodonts of Mississipian age (R.I. Thompson, pers. commun., 1987) in the Tombstone Mountains region of the Dawson area, Yukon Territory, Canada. In the WMNRA, the Globe unit is quartzite (frequently called vitreous because of its hardness and non-granular, glassy appearance), phyllite, and slate, intruded by gabbro, and diabase sills. The Globe unit displays sedimentary structures and lithologic compositions similar to nearshore marine deposits. The provenance for the quartz grains in the Globe unit is probably the Wickersham grit unit, pϵg. Later intrusions of the gabbro and diabase or diorite sills locally have caused hornfelsic alteration in the Globe unit.

Pzg VITREOUS QUARTZITE, PHYLLITE, SLATE, GABBRO, AND DIABASE SILLS--Light- to very light-gray, fine- to medium-grained, bimodal to moderately

sorted, dense, vitreous quartzite which weathers light or medium gray, iron stained; massive or thinly interbedded with medium- to dark-gray slate and phyllite. Thin-sections reveal an immature texture but a mature composition of well-rounded to subrounded monocrystalline quartz grains and very rare occurrences of chert grains with minor accessory minerals of zircon, augite, and hornblende. Local tectonism forms denser quartzite which has sutured grain contacts and stretched quartz grains. Cement is dominantly silica, but some limonitic clay matrix fills the interstices.

Bedding in the Globe quartzite unit is often internally-massive, as much as 3 ft (0.9 m) thick and interbedded with black, iron-stained shaly zones of up to 10 ft (3 m) thick; but, elsewhere bedding may be internally-filled with low-angle planar- to trough-crossbedding in mutually-erosive sets 1-2 ft (0.3-0.6 m) thick, that display crude fining-upward in grain size into ripple-bedded, platy siltstone with shaly tops. The erosional base of these sets commonly has been scoured down into laminated claystone.

Much of the quartzite is intruded and altered to hornfels by gabbro and diabase or diorite sills which may account for the anomolous Ag-Pb-Zn values found in this unit (section V). Gabbro and diabase or diorite is light- to medium-green, medium- to coarse-grained, equigranular, and usually altered; augite (25-30 percent), diopside, orthopyroxene, hornblende, and biotite (5-10 percent, locally). Albitized plagioclase (An 40-60) is common and frequently altered to clay psuedomorphs (Bundtzen, 1983).

TOLOVANA LIMESTONE

In the WMNRA, the Tolovana Limestone (DSt) is Silurian in age, forms the core of the White Mountains, and covers an area of approximately 36 sq mi (93 sq km). In this area, the Tolovana Limestone, a peloid- and ooid-rich platform carbonate succession more than 4000 ft (1,220 m) thick (Church and Durfee, 1961), disconformably overlies the Ordovician Fossil Creek Volcanics, Ofv and Ofs. The faunas and sedimentary features indicate extremely shallow-marine conditions on both sides of the contact that represents a very small stratigraphic hiatus (Blodgett and others, 1987). DSt is commonly preserved in synclinal axes of folds and Ofs and Ofv in the cores of anticlines. These Silurian and Ordovician units are thrust, to the north and northwest, along the White Mountains thrust fault, over the Globe unit (Pzg).

DSt LIMESTONE--In the White Mountains, where the unit is best exposed, the Tolovana Limestone consists of a thick limestone succession with a minor dolomite component. Basal beds composed of about 165 ft (50 m) of thin- to medium-bedded, alternating green and maroon lime mudstone, succeeded by yellowish-brown weathering, silty, argillaceous lime mudstone and wackestone. Conodonts from this interval indicate Llandoverian (Early Silurian) age; large poorly preserved pentameroid brachiopods common in this interval.

Conodonts in the lower Tolovana Limestone have a CAI of 5 to 5 1/2, indicating that the host rock reached at least 300-350 degrees C. Upper and greater part of unit consists of medium- to thick-bedded light-gray weathering peloid- and ooid-rich lime packstone and grainstone. Sparse megafauna known from upper part of the unit suggests Silurian age. Unit rests disconformably upon the Fossil Creek Volcanics.

Southwest of the White Mountains, a Middle Devonian limestone unit has been mapped as part of the Tolovana Limestone, and may eventually be separated pending further study. This unit is well exposed in hills near Globe Creek along Elliott Highway and sporadically to the southwest as far as the Dugan Hills. Consists of poorly bedded, highly fractured, dark-gray lime mudstone. Total thickness unknown but minimally probably exceeds several hundred meters. Rugose corals found at several localities indicate Middle Devonian age. Stratigraphic relationship with Silurian Tolovana Limestone uncertain, presumably superpositional since they both occur in the same structural block.

FOSSIL CREEK VOLCANICS

The Ordovician Fossil Creek Volcanics comprises a lower, mainly sedimentary, half (Ofs), and an upper, mainly volcanic, half (Ofv), aggregating a total thickness of about 2000 ft (600 m), and covers an area of approximately 67 sq mi (174 sq km) trending northeast in the central part of the WMNRA. Its contact with the overlying Tolovana Limestone, which is of Silurian age in the WMNRA, is interpreted as an erosional disconformity. These formations are overthrust to the northwest onto the Globe unit along the White Mountains thrust fault. The Fossil Creek Volcanics appears to unconformably overlie the Wickersham unit in the eastern part of the WMNRA, but more commonly, the southern boundary of Ofv and Ofs is concealed by the overthrust Wickersham unit, ЄpЄga. The Fossil Creek Volcanics is Ordovician in age as indicated by Early Ordovician conodonts collected near the base (table II-4, J.W. Huddle, written commun., 1972) and Late Ordovician megafossils collected from the upper few feet (Blodgett and others, 1987). Formation appears to thicken eastward, concomitantly with loss of coarse clastic rocks and dramatic reduction in volcanic component, and becomes a much-deformed, mainly pelitic section with intercalated thin beds of limestone and dolomite, and smaller content of layers--both sills and flows--of dark greenish basalt, and locally, intrusive lenses of gabbro. Depositional environment of Ofv interpreted as continental margin and (or) warm shallow-marine (shelf) environment with eruption of alkali-basalt flows, lahar and debris-flows; the underlying Ofs unit interpreted as deeper-marine environment with turbiditic influxes. This is a good example of a shallowing-upward stratigraphic section.

Ofv BASALT, AGGLOMERATE, AND VOLCANICLASTIC CONGLOMERATE--Alkali basalt, olive-green agglomerate, and volcaniclastic conglomerate. The uppermost 300 ft (100 m) consists of generally fining-upward sedimentary rocks, from massive, unsorted, boulder- to granule-conglomerate and agglomerate in lower part, to well-sorted, thin-

bedded, calcareous and feldspathic sandstone at top, disconformably overlain by the Tolovana Limestone (Wheeler and others, 1987). A few thin basalt flows intercalated near top. Clasts in upper half of Ofv include: maroon and green mafic volcanic rocks, dark-pink to maroon granite, bimodal to poorly-sorted quartzite, limestone, and phyllite. Carbonate beds in uppermost Ofv include thin- to medium-bedded, maroon and green colored lime wackestone with abundant trilobite parts (table II-4, location no. 26), interbedded within more predominant sandstone and conglomerate. At a measured locality, includes a 2.5 ft (0.76 m) thick tabulate coral biostrome composed almost solely of Chaetetipora (table II-4, location no. 25). Laterally biostrome grades into bioclastic limestone. Brachiopods in this interval indicate Ashgill (Late Ordovician) age (Blodgett and others, 1987).

Ofs SLATE, CHERT, LIMESTONE, AND GABBRO--Lower, mainly sedimentary, half, of the Fossil Creek Volcanics composed of: (1) thinly interbedded calcareous dark-gray slate to light-gray phyllite and black tuffaceous shale, (2) gray to black calcareous and siliceous siltstone, (3) medium-gray, thin-bedded, lime mudstone with partings of argillaceous platy laminae; small sets of well-preserved crossbeds noted; beds locally highly contorted, vary from 0.5 to 2 in (1.3-5.1 cm) thick; appears to represent a basinal limestone turbidite, (4) black and gray banded silty chert, and (5) minor intercalations of aquagene tuff, basalt flows, pillow lavas, and gabbroic sills.

WICKERSHAM UNIT

The Cambrian to Precambrian Wickersham unit within the WMNRA covers at least 490 sq mi (1,270 sq km) and has such lithologic diversity that it is mapped as five separate units. All the individual Wickersham units are lithofacies and appear to have gradational contacts with one another. They are lower greenschist-grade metamorphic facies. Within the WMNRA the Wickersham unit is present in the Schwatka, Livengood, and White Mountains areas.

The Wickersham unit of the White Mountains area is subdivided into three parts: 1) Cambrian to Precambrian grit (poorly sorted to bimodal quartzite), graywacke grit, maroon, green, and gray argillite and phyllite, quartzite, siltite, and thin dark limestone (Ꞓp Ꞓga), 2) Late Precambrian grit (poorly sorted to bimodal quartzite), quartzite, slate, phyllite, and argillite (p Ꞓg), and 3) Late Precambrian pale greenish quartzite, greenschist grit, phyllite, slate, and marble (p Ꞓgg).

The lower contact of the Wickersham unit with the Fairbanks schist unit in the White Mountains area is complicated by folding and possible tectonic imbrication but is interpreted as gradational in the adjoining area to the east mapped by the Alaska Division of Geological and Geophysical Surveys. The greenschist grit unit (p Ꞓgg) grades upward and laterally into the mostly grit unit (p Ꞓg), which in turn grades into the maroon and green unit (Ꞓp Ꞓga). The upper contact with the Ordovician Fossil Creek Volcanics is unconformable but commonly in thrust contact. In the White Mountains area, the Wickersham unit includes gabbroic intrusions.

The Wickersham unit of the WMNRA is very similar to the Windermere Supergroup of Yukon Territory, Canada (Eisbacher, 1981), particularly to that of the Selwyn Basin. The folded thickness of the Wickersham unit is estimated to be on the order of 10,000 ft (3,000 m). The lithology and sedimentary features of the grit unit (pЄg) display common characteristics of the channel fill and overbank deposits in inner and middle submarine fan systems. The maroon and green argillite, chert, and arenaceous limestone all display sedimentary structures that are found in outer fan turbidite deposits.

ЄpЄga GRIT, GRAYWACKE GRIT, MAROON, GREEN AND GRAY ARGILLITE AND ARENACEOUS LIMESTONE--Grit is much like the pЄg unit described below. Graywacke and quartz-wacke grit are light to medium olive gray, commonly conglomeratic or unsorted, feldspars locally abundant, often slightly foliated, but sedimentary features preserved. Bedding in graywacke and quartz-wacke grit is graded, locally amalgamated, fines-upward to ripple-laminations in silty phyllite with small-scale trough crossbedding. Argillite is laminated, maroon and light to medium green and grayish green, fissile to blocky fractured. Locally ЄpЄga is phyllitic and slaty, laminated, medium-light to dark gray and greenish gray, and contains rare, horizontally bedded, discontinuous 2-3 ft (0.6-0.9 m) thick beds of greenish gray, micaceous, arenaceous limestone. Basaltic rocks are interlayered with ЄpЄga but are thin and too small to differentiate on the geologic map. Oldhamia, a trace fossil of probable Late Proterozoic to Cambrian age has been found in ЄpЄga at two localities, both of which are in the Circle quadrangle, one in the WMNRA (see bedrock geologic map, Smith and Pessel, in press) and the other outside of the WMNRA in the Schwatka area, Circle quadrangle (Fossil locality 2, Table 2, Foster and others, 1983).

pЄg GRIT, QUARTZITE, SLATE, PHYLLITE, AND ARGILLITE--Grit and quartzite, gradational to hard sandstone and graywacke, are light to medium gray, greenish gray and olive and weather light gray with iron stain and flecks of oxidized pyrite. Arenaceous limestone occurs as a minor component. Sedimentary structures are rhythmic bedding, fining-upward, graded bedding, sole marks, large-scale amalgamated channel-fills with erosional bases, and horizonal, inclined and hummocky crossbedding. Beds are thin to thick, internally massive to trough crossbedded, with minor shale rip-ups and conglomerate at base. Grain size is fine to coarse, and conglomeratic with granules and rare small pebbles. Grains are angular to subrounded, but some are very well-rounded, suggesting multicyclicity. Quartz grains are monocrystalline, polycrystalline, glassy, frosted and clear, translucent blue-gray, white, gray or smoky (Foster and others, 1983). Feldspar grains are potassic or sodic and locally abundant in the conglomeratic sections. Argillite rip-up clasts are rare but generally present at the base of conglomeratic channel deposits. Sorting is poor to unsorted, slightly bimodal. Matrix is dominantly chlorite, recrystallized from clay. Greenish gray, and olive, thin discontinous lenses of graywacke occur in shale. Pyritic in parts, white quartz veins, pods, and irregular masses are common.

pЄgg GREENSCHIST GRIT--Quartzite, grit (poorly sorted and bimodal quartzite), siltite, phyllite, siliceous slate, thin layers of carbonate, and calcarous phyllite. Approximately same protolith as the pЄg unit but contains much more chlorite, so these rocks are predominantly light to dark greenish gray, except for the carbonates which are gray. This unit represents a slight lithofacies change from the pЄg. It is present for a short distance along Beaver Creek south of Cache Mountain but thickens rapidly eastward into the eastern part of the WMNRA until it becomes the dominant lithology at the base of the Wickersham unit. On the west side of Bear Creek it is separated from the pЄg by a fault, probably of lateral displacement similar to those seen to the east around Mt. Prindle (Smith and Pessel, in press).

FAIRBANKS SCHIST UNIT

The Fairbanks schist unit (Smith and others, 1981) is an informal new name used to designate a part of the Birch Creek Schist as described by J.B. Mertie, Jr. (Mertie, 1937). The quartzite and quartz-mica schist which compose this unit underlie the ridge forming the south boundary of the WMNRA. Regional strike is to the northeast and the unit is identified as far north as Beaver Creek in the southeastern part of the WMNRA, underlying approximately 258 sq mi (668 sq km) of the USGS mapped part of the WMNRA. All rocks are in the greenschist facies, but the metamorphic grade decreases slightly across strike toward the northwest. Quartz-muscovite schists on the south ridge, which contain pinhead garnets and a trace of biotite, change gradually to chloritic and sericitic phyllites with no garnet near Beaver Creek.

Surficial deposits heavily mantle the Fairbanks schist unit, and because of lack of outcrop, structural features are poorly defined. Thus we have not attempted to divide the schist into discrete units.

The 500 ft (150 m) thick Cleary sequence (Smith and others, 1981), a subdivision of the Fairbanks schist unit seen in the Mt. Prindle area to the northeast, is considered a possible source of gold in the Fairbanks District, but the sequence has not been identified in the White Mountains area of the WMNRA. The Cleary sequence may be present in the ridge on the south side of the WMNRA but is unrecognized because of poor outcrop. The presence under this ridge of an aeromagnetic high similar to that associated with the Cleary sequence farther east in the Circle quadrangle (section III), lends some support to this idea.

The lower contact of the Fairbanks schist unit is unknown and presumably lies outside of the map area. Its upper contact with the Wickersham unit to the north, whether depositional or tectonic, has been the subject of much investigation. Low-angle thrust and strike-slip, high-angle faults occur between the two units, but faulting at the contact is not ubiquitous throughout the area; instead, regional observations suggest the presence of a gradational sequence, of similar protolith, between the Fairbanks schist unit

and the Wickersham unit. The thickness of the Fairbanks schist unit is unknown but probably is in excess of 10,000 ft (3,000 m). The Fairbanks schist unit and the Wickersham unit are interpreted as correlative with the late Proterozoic Windermere Supergroup of Canada and represent deposition at the continental margin off the North American craton.

pЄf QUARTZITE, MUSCOVITE-CHLORITE SCHIST, AND GRIT--Quartzite, micaceous quartzite, gritty quartzite, quartz-muscovite-chlorite schist, and phyllite are the major lithologies, with lesser amounts of grit, feldspathic schist, calcareous schist and marble. Tiny pinhead garnets and rare biotite are present in minor amounts. The rocks are light to medium light gray and greenish gray, but in many places weather to rubble that is iron-stained yellowish gray to light reddish brown. The quartzite layers range in thickness from a few inches to rarely 3 ft (0.9 m). Quartzite and quartz-muscovite-chlorite schist are fine to coarse grained and equigranular. These rocks are found with various amounts of large, subangular to subrounded megacrysts of clear, white, gray, bluish-gray or black quartz, known locally as "quartz eyes", that give it a bimodal appearance in the field. If the quartz megacrysts are abundant and generally accompanied by feldspar grains the rock is known as a grit. Minor thin, dark gray impure marble is present. Unit is well foliated and commonly the foliation is parallel to the lithologic layering.

Structure

The degree of structural segmentation of the WMNRA and the complexity of its disrupted stratigraphy are clear from previously published geologic maps (Chapman and others, 1971; Foster and others, 1983) and are inherent in its subdivision into numerous tectonostratigraphic terranes by Silberling and Jones (1984) and Churkin and others (1982). The disrupting structures are mainly the thrust faults illustrated on plates II-A and II-B, and strike-slip fault splays of the Tintina fault zone.

FOLD AND THRUST BELT STRUCTURES

The map distribution of thrust faults and associated folds shown on plate II-A and their cross-section configuration interpreted on plate II-B define a broad fold and thrust belt that juxtaposes, telescopes, and internally complicates the various stratigraphic sequences previously described. Thrust faults have relatively narrow and sharply defined fault zones, are typically stratigraphically controlled, are associated with large-scale low-plunging folds, and form systems of splaying individual thrusts, each of relatively limited extent and displacement. Many details of thrust distribution and subsurface interpretation are hindered by limited surface data and poor exposure, lack of subsurface information, and stratigraphic uncertainties, but the overall fold and thrust belt interpretation is consistant with that involving comparable rock sequences in adjacent parts of east-central Alaska (Dover, in press).

Important thrust faults characterize all three of the principal stratigraphic areas of the WMNRA.

White Mountains

The most prominent of the mapped thrust faults in the White Mountains area are here named informally the White Mountains and Beaver Creek thrusts (pl. II-A and II-B). The White Mountains thrust, which may be the more important of the two because of the large stratigraphic throw involved, places the lower Paleozoic to Precambrian Fossil Creek Volcanics (Ofv and Ofs) and Wickersham unit (Ꝑp Ꝑga, pꝐg, and pꝐgg) basement over presumed upper Paleozoic rocks of the Globe (Pzg) and Vrain units (MzPzv, MzPzvc, MzPzvt, and MzPzvs). The Tolovana Limestone (DSt) occurs in the faulted cores of large synclines associated with the White Mountains thrust. Locally, where the basal contact of the Tolovana Limestone is discordant and deformed, it is mapped as a younger-on-older thrust, but this contact is best interpreted as a stratigraphic contact along which detachment occurred and sheering was concentrated during folding and thrusting.

The Beaver Creek thrust brings the Paleozoic Globe unit over strata as young as Cretaceous to Jurassic. Map relations suggest the Beaver Creek thrust is steeper and has less stratigraphic throw than the White Mountains thrust, but uncertain stratigraphic relations of the Globe and Vrain units raise questions as to the amount of tectonic transport on the Beaver Creek fault.

Stratigraphically higher thrust faults within the White Mountains stratigraphic belt change gradually southward toward the south edge of the study area from relatively minor listric imbrications involving the Fossil Creek Volcanics-Tolovana Limestone section, to those involving progressively more ductile rocks of the Wickersham unit and the Fairbanks schist unit. Most of these are tentatively interpreted to be thrust faults that formed within the axial areas of large anticlines related to the same folding and thrusting event that produced the White Mountains and Beaver Creek thrusts, but in a somewhat deeper crustal and more ductile environment. Lack of outcrop in the southern part of the study area precludes a structural interpretation. It is reasonable to assume that structures identified by Alaska Division of Geological and Geophysical Surveys in the adjoining Lime Peak-Mt. Prindle area are essentially continuous to the southwest.

Directions of overturning, fold vergence, and thrust dips all clearly indicate that thrusting within the White Mountains belt was toward the north and northwest. Precise amounts of thrust transport are unknown for most of the thrusts because of the lack of marker beds and tie points, but repetition of generally similar stratigraphic sequences suggests that the White Mountains belt is an imbricate zone that did not involve great distances of transport. The structural shortening suggested in plate II-B could be as little as a few tens' of kilometers.

Livengood Area

Structural interpretation is less clear in the Livengood belt because of greater stratigraphic uncertainties involving several key units--particularly the Amy Creek unit (PzpCd and PzpЄc) and various mafic and ultramafic units. Where exposure is adequate and mapping is sufficiently detailed, a structural style of broad folds and older-on-younger thrust faults like that of the White Mountains belt can be demonstrated. The most prominent of the thrust faults underlies the enigmatic mafic-ultramafic unit (ЄpЄum) that in most places separates the Paleozoic? and Mesozoic rocks of Beaver Creek valley from lower Paleozoic and older rocks to the north. Geophysical evidence for the origin and subsurface configuration of the highly magnetic mafic-ultramafic units is reviewed in detail by Cady, section III, of this report. The cross-section interpretation illustrated in plate II-B is that the thrust-bounded mafic-ultramafic unit projects southward with low dip under the Beaver Creek valley, and that it represents an unusually thick, serpentinized sequence of differentiated sills like those characterizing the mafic intrusive-rich unit (PzpЄm) north of Victoria Mountain. If these mafic-rich rocks represent a rock package within the Livengood Dome Chert-Wickersham unit sequence of the Livengood stratigraphic belt, or mafic-rich variations of either of those units, transport on thrusts involving these rocks may be relatively modest.

The fault distribution and pattern of imbrication of units within the Livengood stratigraphic belt indicate north to northwestward thrusting similar in scale, style, and sense and amount of tectonic transport to that of the White Mountains belt.

The late Paleozoic to Mesozoic rocks of Beaver Creek valley are shown on plate II-A to be in depositional contact on other rocks north of Beaver Creek. However, the discordance of this contact where it is best exposed, and the structural disharmony across it, suggest that the contact may be a normal fault, and most likely a listric one that merges in the subsurface with the thrust under the mafic-ultramafic unit. Complex folding within the Wilber Creek unit (KJw) and Vrain units of Beaver Creek valley are attributed to shortening within this sequence of relatively weak shaly rocks compressed between thrust plates of more resistant rocks in the Livengood and White Mountains belts.

Schwatka Area

The Schwatka stratigraphic belt, located north of the Victoria Creek fault resembles the White Mountains and Livengood belts in overall fold and thrust belt framework, but differs significantly in that vergence and thrusting were directed predominantly southward. Some details of folding are defined on plate II-A by a thick, mappable limestone marker bed (ЄpЄgl) within the Wickersham unit, but most of the complex folding and imbricate south-directed thrusting are in limestone and volcanic rocks of the Schwatka unit north of the WMNRA.

VICTORIA CREEK FAULT

The curvilinear topographic trench that marks the trace of the Victoria Creek fault across the northern part of the study area merges without break with the Tintina fault zone to the east. The keys to recognizing the Victoria Creek fault as a major strike-slip fault are (1) its curvilinear topographic expression and continuity across diverse geologic belts, and (2) the width, and intensity and character of shearing of the fault zone. Where exposed along Victoria Creek, the fault zone forms a topographic trench one to one and a half kilometers wide and contains disconnected tectonic lenses of wallrock units--some present locally and some from units now far removed by Tintina movement--within an intensely and pervasively sheared, mylonitic matrix. Tectonic lenses range from microscopic in size to blocks hundreds of meters long. Axes of crenulations and small folds are variable but are most commonly steep to vertical; slickensides are generally low-plunging. As for The Victoria Creek zone, like the main Tintina zone, marks a profound discordance in mapped surface geologic patterns. Within the study area, the most striking feature of the Victoria Creek fault zone is that it separates fold and thrust belt segments with opposing senses of structural vergence and tectonic transport. The continuity and linearity of the Victoria Creek fault zone, and its low-angle truncation of fold and thrust belt structural trends, clearly demonstrates its steep dip and post-thrusting age. There is no direct evidence from the WMNRA alone for the sense and magnitude of slip on the Victoria Creek fault zone, but its character and regional continuity mark it as the principal splay of the Tintina fault system in interior Alaska. Furthermore, when viewed in a regional context, the geologic framework of the study area is critical to the concept that the Tintina fault system of east-central Alaska has undergone about 279 mi (450 km) right-lateral movement comparable to that documented for the Canadian segment of the Tintina fault system (Gordey, 1981). This estimate is based on the correlation of stratigraphic and structural belts lying south of the Victoria Creek fault in the WMNRA with comparable belts lying north of the Tintina fault in the Dawson area of Yukon Territory. The correlation between these two areas and the implication that they were directly connected prior to Tintina strike-slip is based on several lines of evidence, including (1) the close similarity of the general sequence of thrust-bounded rock packages between the two areas, (2) striking similarities in lithologic details within each of these packages, (3) similarities in their fold and thrust belt character, sense of tectonic transport and deformational age, and (4) the alinement, after restoration to a pre-strike-slip position, of chemically and compositionally distinctive Late Cretaceous syenitic plutons in the two areas.

A detailed discussion of the evidence documenting large-scale right-separation on the Tintina-Victoria Creek fault system, and its regional stratigraphic and tectonic implications is beyond the scope of this report. However, if true, the significance of this displacement model to mineral resource evaluation is that resources known in the Dawson area could have counterparts in the WMNRA, and mineral exploration, evaluation, and development techniques used successfully there might be applicable here.

The principal lateral movement on the Victoria Creek-Tintina fault zone

occurred between the time that fold and thrust belt compressional deformation ceased and unconformable Late Cretaceous to Early Tertiary deposition across the Tintina trench began in areas to the east of the study area.

Fossil data

The fossils listed on table II-4 include numerous collections made since the turn of the century. The collections identified by Edwin Kirk (Mertie, 1937) are in need of taxonomic re-evaluation in light of the great amount of taxonomic splitting and range refinement that has subsequently occurred. The fossil locations cited in Mertie were not precisely located so, for the purposes of this report, the original field notes have been consulted and the locations of the collections plotted on the geologic map, plate II-A, as closely as can be determined. The preservation of Paleozoic fossils from the White Mountains is quite poor in general. This is especially true for collections from the Tolovana Limestone, a unit characterized by extensive recrystallization. "Crack-out" specimens of brachiopods from this unit typically are decorticated of their external shell material, commonly resulting in identifications which cannot be taken below the subfamilial level. Also hindering identification is the common presence of tectonic stretching of fossil material. Preservation is fair to moderate for collections from the uppermost sedimentary interbeds of the Fossil Creek Volcanics; faunal elements of which were illustrated in Blodgett and others (1987). The better preservation of this stratigraphically lower horizon is perhaps best explained by the fact that this fauna is hosted in a predominantly clastic-supported matrix, in contrast to the carbonate of the overlying Tolovana Limestone which displays a high degree of recrystallization.

Table II-4.--Fossil collection localities in the White Mountains National Recreation Area

GEOLOGIC MAP LOCATION NO.	FIELD NUMBER (USGS COLLN. NO.)	LOCATION	FOSSILS	IDENTIFIED BY	AGE	UNIT
1	86A Bd 58	Livengood B-2 65°22'17" 147°55'53"	undetermined dendroid tabulate corals	R.B. Blodgett 1986	Silurian or Devonian	DSt
2	21A Mt 33	Livengood B-2 65°27'08" 147°44'10"	Clorinda? sp.	E. Kirk pre 1937	Silurian	DSt
3	04A H 186	Livengood B-2 65°27'48" 147°36'32"	Favosites sp., Cladopora sp.	E. Kirk pre 1937	Silurian	DSt
4	04A P 192-195	Livengood B-2 65°27'51" 147°36'45"	Cytherella sp., Cladopora sp., Ptilodictya cf. frontosa, Favosites nr. limitaris, Stromatopora	E. Kirk pre 1937	Silurian or Devonian	DSt
5	04A P 240-346	Livengood B-2 65°28'34" + 147°35'41" +	Zaphrentis sp., Cyathophyllum sp. Favosites cf. F. favosus, Favosites sp., Conchidium? sp. Favosites cf. F. niagarensis	E. Kirk pre 1937	Silurian	DSt
6	60 MCD F-57	Livengood B-2 65°28'53" 147°35'05"	Pentamerus sp., Favosites sp.	H. Duncan, J. Berdan 1960	Probably Silurian	DSt
7	86A Bd 41	Livengood B-2 65°29'07" 147°33'05"	Ozarkodina sp. indet., Panderodus sp., indet. gastropod	A.G. Harris R.B. Blodgett 1986	Silurian-Early Devonian	DSt
8	86A Bd 42	Livengood B-2 65°29'18" 147°32'57"	undetermined dendroid tabulate corals	R.B. Blodgett 1986	Silurian or Devonian	DSt
9	86A Bd 44	Livengood B-2 65°29'30" 147°32'50"	Briartina sp., Straparollus (n. subgenus) sp. aff. S. (Serpulospira), indet. high-spired gastropod	J.M. Berdan R.B. Blodgett 1986	Probably Silurian or Devonian	DSt
10	86A Bd 8	Livengood C-2 65°30'53" 147°34'31"	lamellar stromatoporoids exposed in cross-section in dolostone	R.B. Blodgett 1986	Silurian or Devonian	DSt
11	86A Bd 6	Livengood C-2 65°30'57" 147°34'36"	Distomodus sp. or Icriodella sp., Panderodus sp.	A.G. Harris 1986	Early-Middle Silurian (Llandoverian-Wenlockian)	DSt

GEOLOGIC MAP LOCATION NO.	FIELD NUMBER (USGS COLLN. NO.)	LOCATION	FOSSILS	IDENTIFIED BY	AGE	UNIT
12	15A B 262 (152002)	Livengood C-2 65°32'06" 147°31'58"	Favosites sp.	E. Kirk pre 1937	Silurian	DSt
	15A B 262 (152001)	Livengood C-2 65°32'06" 147°31'58"	Streptelasma sp., Dinorthis sp., Liospira cf. L. progne	E. Kirk pre 1937	Middle Ordovician	Ots
	68A Ch 296 (8302-SD)	Livengood C-2 65°32'06" 147°31'58"	Halysites sp., stromatoporoid?	W.A. Oliver 1968	Silurian	DSt
			Pentamerus or Pentameroides	J.T. Dutro 1972	Silurian	DSt
	(6709-CO)		Belodina sp., Drepanodus sp. Paltodus sp., Panderodus sp.	J.W. Huddle 1969	Middle or Late Ordovician	Ots
	71A Wr 521-68		Pentameroid coquina	J.T. Dutro 1972	Silurian	DSt
	86A Bd 27		Streptelasma sp., pentameroid brachiopods, Oulodus? sp. indet., Panderodus sp., Ozarkodina sp. indet., Distomodus sp. indet. or Icriodella sp. indet., Ozarkodina hassi, Ozarkodina cf. O. oldhamensis, Walliserodus sp.	A.G. Harris R.B. Blodgett R.J. Ellis 1986	Early Silurian (early to middle Llandoverian)	DSt
13	68A Gk 431 (8300-SD)	Livengood C-2 65°32'25" 147°31'40"	Favosites sp. Halysites sp.	W.A. Oliver 1968	Silurian	DSt
			Pentamerus or Pentameroides	J.T. Dutro 1972	Silurian (Llandovery through Wenlock)	DSt
			Oulodus sp. indet. Panderodus sp.	A.G. Harris 1985	Middle Ordovician through Middle Devonian	DSt or Ots
14	60 MCD F-3	Livengood C-2 65°32'49" 147°20'40"	cf. Palaeophyllum, favositoid coral	W.A. Oliver 1961	Late Ordovician to Middle Silurian, probably Silurian	DSt
15	71A Wr 520A	Livengood C-2 65°33'02" 147°30'54"	Pentamerus sp.	J.T. Dutro 1972	Silurian	DSt

GEOLOGIC MAP LOCATION NO.	FIELD NUMBER (USGS COLLN. NO.)	LOCATION	FOSSILS	IDENTIFIED BY	AGE	UNIT
16	68A Cn 1861B (8920-SD)	Livengood C-2 65°33'50" 147°30'02"	Mesofavosites sp., Paleofavosites sp.	W.A. Oliver 1972	Ordovician to Devonian, probably Silurian	DSt
	68A Cn 1861C (8921-SD)		Catenipora? favositoid, Heliolites? sp.	W.A. Oliver 1972	Silurian	DSt
17	60 MCD F-2	Livengood C-2 65°34'20" 147°30'34"	Favosites? sp.	W.A. Oliver 1961	Silurian or Devonian	DSt
18	15A B 256 (1520B)	Livengood C-1 65°32'39" 147°28'33"	Clorinda? sp.	E. Kirk pre 1937	Silurian	DSt
19	60 MCD F-1	Livengood C-1 65°34'18" 147°29'05"	Favosites sp., Favosites? sp.	W.A. Oliver 1961	Silurian or Devonian	DSt
20	09A J 82 09A P 94	Livengood C-1 65°36'03" 147°23'13"	Conchidium? sp.	E. Kirk pre 1937	Silurian	DSt
	15A B 237 (1520A)		Conchidium? sp., crinoid columns	E. Kirk pre 1937	Silurian	DSt
21	60 REC F-4	Livengood C-1 65°37'27" 147°26'50"	Favosites sp., favositoid coral	W.A. Oliver 1961	Silurian or Devonian	DSt
			Pentamerus or Conchidium	J.T. Dutro 1961	Silurian or Devonian	
22	60 REC F-3	Livengood C-1 65°37'43" 147°26'47"	Syringopora? sp.	W.A. Oliver 1961	Silurian to Carboniferous	DSt
23	86A Bd 1	Livengood C-1 65°36'34" 147°20'00"	smooth pentameroid brachiopods, favositid corals, undetermined solitary rugose coral, Kockella sp. indet. or Oulodus sp. indet., Panderodus sp.	R.B. Blodgett A.G. Harris 1986	Silurian	DSt
	86A Bd 2		Belodina sp. indet., Protopanderodus? sp. indet.	A.G. Harris 1986	Middle-Late Ordovician	Ots
24	60 REC F-2	Livengood C-1 65°36'58" 147°17'42"	Favosites sp.	W.A. Oliver 1961	Silurian or Devonian	DSt

GEOLOGIC MAP LOCATION NO.	FIELD NUMBER (USGS COLLN. NO.)	LOCATION	FOSSILS	IDENTIFIED BY	AGE	UNIT
25	09A J 70 09A P 87	Livengood C-1 65°37'17" 147°21'46"	Streptelasma rusticum, Streptelasma sp., Columnaria (Paleophyllum) thomi, Columnaria? sp., Halysites gracilis, var., Rhombotrypa sp., Dinorthis sp., Plectambonites sericeus, var., Plectambonites sp., Rafinesquina sp., Triplecia sp., Rhynchotrema increbescens, var., Maclurea? sp., Raphistomina sp., Cyclonema sp., Dyeria? sp., Isotelus sp.	E. Kirk pre 1937	Middle Ordovician	Ofs
	09A P 87 (7092-CO)		"Chaetetipora" sp. cf. "C." ellesmerensis, Sarcinula sp.	W.A. Oliver 1972	Late Ordovician	Ofs
	15A B 230 (1519C)		Streptelasma? sp., Columnaria (Paleophyllum) thomi, Halysites sp. Calymene sp., Rhombotrypa sp., Platystrophia sp., Dalmanella sp., Dinorthis sp., Leptaena near L. unicostata, Plectambonites sericeus, var., Triplecia sp., Rhynchotrema increbescens, var., Isotelus sp.	E. Kirk pre 1937	Middle Ordovician	Ofs
	68A Cn 1751 (7093-CO)		"Chaetetipora" sp. cf. "C." ellesmerensis, Palaeofavosites sp., cerioid rugose coral	W.A. Oliver 1972	Late Ordovician	Ofs
	86A Bd 5 (86A Bd 60)		Chaetetipora sp., inarticulate brachiopods (both linguloids and tremerellids), orthoid and strophomenoid brachiopods, Platystrophia sp., Holorhynchus n. sp., Maclurites sp., Liospira sp., Trochonemella sp., Belodina sp. indet.	R.B. Blodgett D.M. Rohr A.G. Harris 1986	Late Ordovician (Ashgillian)	Ofs
26	86A Bd 4	Livengood C-1 65°37'23" 147°20'36"	Holorhynchus n. sp., Anataphrus? sp., Donella n. sp., Belodina sp. indet. of Late Ordovician morphotype	R.B. Blodgett A.R. Ormiston A.G. Harris 1986	Late Ordovician (Ashgillian)	Ofs
27	86A Bd 22	Livengood C-1 65°37'28" 147°21'40"	pentameroid brachiopods and stromatoporoids exposed in cross-section in dolostone	R.B. Blodgett 1986	Silurian	DSt
28	60 REC F-1	Livengood C-1 65°37'58" 147°19'10"	Favosites? sp., favositoid coral, coral?	E. Kirk pre 1937	Silurian or Devonian	DSt

GEOLOGIC MAP LOCATION NO.	FIELD NUMBER (USGS COLLN. NO.)	LOCATION	FOSSILS	IDENTIFIED BY	AGE	UNIT
29	15A B 215 (1519B)	Livengood C-1 65°37'36" 147°13'40"	Cyathophyllum sp., Diphyphyllum sp., crinoid columns, Trimerella sp., Conchidium sp., Atrypa? sp., Megalomphala? sp., Modiomorpha sp.	E. Kirk pre 1937	Silurian	DSt
30	86A Bd 13	Livengood C-1 65°37'45" 147°12'58"	ribbed pentameroid brachiopod, Atrypa sp., favositid coral, Ozarkodina excavata, Panderodus sp.	R.B. Blodgett A.G. Harris 1986	Middle-Late Silurian	DSt
31	15A B 211 (1519A)	Livengood C-1 65°37'30" 147°11'42"	Linguiella sp., Agnostus sp., Bathyurellus? sp., Hemigyraspis? sp., Megalaspis? sp.	E. Kirk E.O. Ulrich pre 1937	Early Ordovician	Ots
	(7359-CO)		cf. Bellefontia sp., Cleiandia sp., Geragnostus sp., ?Proeatokephalus sp., Pseudagnostus sp., asaphiod, gen. and sp. indet., olenoid, gen. and sp. indet., Schizambon sp., acrotretoid, gen. and sp. indet. linguloid, gen. and sp. indet., "Pelagiella" sp., cf. Hulshea sp.	M.E. Taylor A.J. Rowell 1972	Early Ordovician	Ots
	(7359-CO)		Acodus oneotensis, Acontiodus sp., Cordylodus sp., Cordylodus sp., Drepanodus acutus? D. dsubarcuatus, D. sp., Drepanoistodus suberectus, Oneotodus aff. O. nakanurai, Paltodus cf. bassleri, Scandodus aff. rectus, Scolopodus filosus	J.W. Huddle 1972	Early Ordovician	Ots
	(7359-CO)		Cordylodus aff. C. intermedius, Cordylodus rotundatus, Paltodus bassleri, Paltodus bassleri?, Paltodus spurius cf. Drepanodus suberectus, Scolopodus gracilis, Scolopodus cf. S. filosus	J. Repetski 1976	Early Ordovician	Ots
32	86A Do 138	Livengood D-1 65°52'56" 147°18'29"	crinoid ossicles (including the distinctive two-hole ossicles of Gasterocoma? bicauli), Panderodus sp., Polygnathus sp. of Eifelian morphotype	A.G. Harris R.B. Blodgett 1986	Early Middle Devonian (Eifelian)	Dsl
33	87A Bd 62	Livengood D-1 65°53'06" 147°14'10"	crinoid ossicles (including the distinctive two-hole ossicles of Gasterocoma? bicauli)	R.B. Blodgett 1987	late Early or early Middle Devonian (Emsian-Eifelian)	Dsl
34	87A Bd 61	Livengood D-1 65°53'33" 147°16'09"	crinoid ossicles (including the distinctive two-hole ossicles of Gasterocoma? bicauli)	R.B. Blodgett 1987	late Early or early Middle Devonian (Emsian-Eifelian)	Dsl

GEOLOGIC MAP LOCATION NO.	FIELD NUMBER (USGS COLLN. NO.)	LOCATION	FOSSILS	IDENTIFIED BY	AGE	UNIT
35	87A Bd 60	Livengood D-1 65°53'34" 147°16'18"	crinoid ossicles	R.B. Blodgett 1987	late Early or early Middle Devonian (Emsian-Eifelian)	Dsl

REFERENCES CITED

Barton, P.J., 1981, Radioactive mineral occurrences, Mt. Prindle area, Yukon-Tanana Uplands, Alaska: Fairbanks, Alaska, University of Alaska, M.S. thesis, 72 p.

Blodgett, R.B., Wheeler, K.L., Rohr, D.M., Harris, A.G., and Weber, F.R., 1987, A Late Ordovician age reappraisal for the upper Fossil Creek Volcanics, and possible significance for glacio-eustacy, p. 54-58, in Hamilton, T.D., and Galloway, J.P., eds., Geological studies in Alaska by the U.S. Geological Survey during 1986, 195 p.

Blodgett, R.B, Zhang Ning, Ormiston, A.R., and Weber, F.R., 1988, A Late Silurizn age determination for the limestone of the Lost Creek unit, Livengood C-4 quadrangle, east-central Alaska in Galloway, J.P., and Hamilton T.D., eds., Geologic studies in Alaska by the U.S. Geological Survey during 1987: U.S. geological Survey Circular 1016, in press.

Brabb, E.E., 1969, Six new Paleozoic and Mesozoic formations in east-central Alaska: U.S. Geological Survey, Bull. 1274-I, 126 p.

Brabb, E.E., and Churkin, Michael, Jr., 1969, Geologic map of the Charley River quadrangle, east-central Alaska: U.S. Geological Survey Misc. Geological Invest. I-573, 1 sh. (1:250,000).

Bundtzen, T.K., 1983, Bedrock geologic outcrop map of the Livengood B-3 quadrangle, Alaska: Alaska Division of Geological and Geophysical Surveys Report of Investigations 83-6, 1 sh. (1:40,000).

Burton, P.J., 1981, Radioactive mineral occurrences, Mt. Prindle area, Yukon-Tanana Uplands, Alaska: Fairbanks, Alaska, University of Alaska, M.S. thesis, 72 p.

Chapman, R.M., Weber, F.R., Churkin, Michael, Jr., and Carter, Claire, 1980, The Livengood Dome Chert, a new Ordovician Formation in central Alaska, and its relation to displacement on the Tintina Fault: U.S. Geol. Survey Prof. Paper 1126-F, p. F1-13.

Chapman, R.M., Weber, F.R., and Taber, Bond, 1971, Preliminary geologic map of the Livengood quadrangle, Alaska: U.S. Geological Survey Open-File Report 71-66, scale 1:250,000.

Churkin, Michael, Jr., Foster, H.L., Chapman, R.M., and Weber, F.R., 1982, Terranes and suture zones in east-central Alaska: Journal of Geophysical Research, v. 87, no. 5, p. 3718-3730.

Dover, J.H., in press, Geologic map and fold and thrust belt interpretation of the southeastern part of the Charley River quadrangle, east-central Alaska: U.S. Geological Survey Miscellaneous Investigations Map I-1942, (1:100,000).

Eisbacher, G.H., 1981, Sedimentary tectonics and glacial record in the Windermere Supergroup, Mackenzie Mountains, Northwestern Canada: Geol. Survey Canada Paper 80-27, 40 p.

Foster, H.L., Laird, Jo, Keith, Terry E.C., Cushing, G.W., and Menzie, W.D., 1983, Preliminary geologic map of the Circle quadrangle, Alaska, U.S. Geological Survey Open File Report 83-170-A, 30 p., 1 sh. (1:250,000).

Gordey, S. P., 1981, Stratigraphy, structure, and tectonic evolution of southern Pelly Mountains in the Indigo Lake area, Yukon Territory: Geological Survey of Canada Bulletin 318, 44 p., 1 sh. (1:60,000).

Hofmann, H.J., and Cecile, M.P., 1981, Occurrence of Oldhamia and other trace fossils in lower Cambrian(?) argillites, Niddery Lake map area, Selwyn

Mountains, Yukon Territory, in Current Research, Part A: Geological Survey of Canada, Paper 81-1A, p. 281-290.
Holm, Bjarne, 1973, Bedrock geology and mineralization of the Mt. Prindle area, Yukon-Tanana Upland, Alaska: Fairbanks, Alaska, University of Alaska, M.S. thesis, 55 p.
Le Maitre, R.W., 1976, The chemical variability of some igneous rock: Journal of Petrology, v. 17, p. 589-637.
Mertie, J.B., Jr., 1937, The Yukon-Tanana region, Alaska: U.S. Geological Survey Bulletin 872, 276 p.
Nockolds, S.R., 1954, Average chemical compositions of some igneous rocks: Geological Society of America Bulletin, v. 65, p. 1007-1032.
Shand, S.J., 1951, Eruptive rocks (4th ed.): New York, John Wiley, 488 p.
Silberling, N.J., and Jones, D.L., eds., 1984, Lithotectonic terrane map of the North American Cordillera: U.S. Geological Survey Open-File Report 84-523.
Smith, T.E. and Pessel, G.H., compilers, in press, Bedrock geologic map of the Lime Peak-Mt. Prindle area, east-central Alaska: Alaska Division of Geological and Geophysical Surveys, Rept. of Investigations 87-4, Pl 2-1A.
Smith, T.E., Robinson, M.S., Bundtzen, T.K., and Metz, P.A., 1981, Fairbanks mining district in 1981: New look at an old mineral province: The Alaska Miner, The Journal of the Alaska Miners Association, v. 9, no. 22, p. 8, 28.
Streckeisen, A., 1976, To each plutonic rock its proper name: Earth Science Reviews, v. 12, p. 133.
Weber, F.R., and Foster, H.L., 1982, Tertiary(?) conglomerate and Quaternary faulting in the Circle quadrangle, Alaska, in Coonrad, W.L., and Elliott, R.L., eds., The United States Geological Survey in Alaska: Accomplishments during 1980: U.S. Geological Survey Circular 844, p. 58-60.
Weber, F.R., Smith, T.E., Hall, M.H., and Forbes, R.B., 1985, Geologic guide to the Fairbanks-Livengood area, east-central Alaska: Alaska Geological Society, Anchorage, 44 p.
Wheeler, K.L., Forbes, R.B., Weber, F.R., and Rinehart, C.D., 1987, Lithostratigraphy, petrology and geochemistry of the Ordovician Fossil Creek Volcanics, White Mountains, east-central Alaska, p. 70-73, in Hamilton, T.D., and Galloway, J.P., (eds.), Geological studies in Alaska by the U.S. Geological Survey during 1986, 195 p.
Wilson, F.H., and Shew, Nora, 1981, Maps and tables showing preliminary results of potassium-argon age studies in the Circle quadrangle, Alaska, with a compilation of previous dating work: U.S. Geological Survey Open-File Report 81-889, 1 sh. (1:250,000).
Wilson, F.H., Smith, J.G., and Shew, Nora, 1985, Review of radiometric data from the Yukon crystalline terrane, Alaska and Yukon Territory: Canadian Journal of Earth Sciences, v. 22, no. 4, p. 525-537.
Winn, R.D., Jr., and Bailes, R.J., 1987, Stratiform lead-zinc sulfides, mudflows, turbidites: Devonian sedimentation along a submarine fault scarp of extensional origin, Jason deposit, Yukon Territory, Canada: Geological Society of America Bulletin, v. 98, p. 528-539.

III. GEOPHYSICAL STUDIES

by J.W. Cady, C.L. Long, and R.L. Morin

Introduction

Aeromagnetic, gravity, magnetotelluric, and audiomagnetotelluric studies were conducted in order to better understand the geologic setting and subsurface geology in the WMNRA. Such studies are especially useful for delineation of buried targets for mineral exploration, mainly granitic intrusions, regionally metamorphosed magnetic schist, and contact-metamorphic aureoles.

Aeromagnetic and Gravity Data

by J.W. Cady and R.L. Morin

Aeromagnetic data were reprocessed from digital tapes used to make 1:63,360- and 1:250,000-scale aeromagnetic maps of the Circle quadrangle and the eastern Livengood quadrangle (U.S. Geological Survey, 1974a,b). The data were gridded at an interval of 1333 ft and contoured by computer. The International Geomagnetic Reference Field (IGRF) was subtracted by the aeromagnetic contractor. An additional arbitrary magnetic datum was subtracted during reprocessing. Some isolated magnetic highs and lows shown on the contour map were previously deleted by the contractor in making the 1974 Open-file maps. These anomalies may be spurious, but they have been retained on the premise that it is better to have a few false anomalies than to discard a potentially important one. The aeromagnetic map was compiled from lines flown at a spacing of 1 mile, draped nominally 1000 ft above mean terrain. The magnetic map is useful for showing the distribution of magnetic rock units, for planning geologic traverses, and for resolving major problems in constructing a geologic map. The flight line spacing is too wide, however, to provide much assistance in locating geologic contacts at a scale of 1:63,360.

Approximately 120 gravity stations were collected for the White Mountains study by Robert L. Morin in 1986. Most of these gravity stations were obtained at geochemical sampling sites. Previously established gravity data were obtained from computer files maintained by David F. Barnes. All the data were processed by Morin and gridded and contoured by computer to produce a complete Bouguer gravity anomaly map (pl. III-B). The gravity stations are too widely spaced to help interpret the details of the geology. Gravity lows delineate large bodies of low density rocks, such as granitic plutons, the Fairbanks schist, and sedimentary units such as the flysch of Wilber Creek. Gravity highs delineate denser rocks, such as the Fossil Creek Volcanics and the mafic Rampart Group, north of the WMNRA.

Interpretation of Aeromagnetic and Gravity Data

This section refers to the aeromagnetic map (pl. III-A) and the gravity map (pl. III-B). In order to understand the regional setting of magnetic and gravity anomalies, the study area for this section is the area of plates III-A and III-B. This area encompasses the entire WMNRA, including the Mt. Prindle-

Lime Peak area reported on separately by the State of Alaska Division of Geological and Geophysical Surveys. An aeromagnetic interpretive sketch is combined with the gravity map in order to allow the aeromagnetic interpretation and the gravity data to be directly compared. The main features shown on the aeromagnetic interpretation map (pl. III-A) are the axes of magnetic highs and lows, which emphasize continuity of magnetic trends and the correlation of geologic units along magnetic strike. Rock units are labeled with the same symbols as the geologic map (pl. II-A). The symbol alone indicates a magnetic or nonmagnetic rock unit at or near the surface. Parentheses indicate an inferred buried magnetic rock unit. Square brackets indicate a nonmagnetic rock unit at or near the surface. Parentheses around brackets indicate an inferred, buried, nonmagnetic rock unit. A full explanation of plates III-A and III-B is given in table III-1. Discussion of the sources of magnetic highs proceeds from northwest to southeast.

Discussion of the nonmagnetic rock types has a topical rather than geographic order.

MAJOR SOURCES OF MAGNETIC HIGHS

Mafic and Ultramafic Rocks

SCHWATKA VOLCANIC SEQUENCE (Dsv)

A belt of low-amplitude magnetic highs coincides with the Schwatka volcanic sequence, which lies outside the WMNRA except near Mount Schwatka. West of Long. 147°30', the magnetic high is linear and coincides with the mapped belt of volcanic rocks. Farther east, complex magnetic anomalies reflect complexly folded metavolcanic rocks and adjacent nonmagnetic limestone. Although the aeromagnetic data do not have sufficient resolution to resolve details of structure, the coincidence of magnetic gradients and mapped contacts is good. Aeromagnetic highs occur over synclines containing volcanic rocks, and magnetic lows occur over limestone in the cores of anticlines.

CAMBRIAN-PRECAMBRIAN MAFIC-ULTRAMAFIC SILL COMPLEX, GREENSTONE AND SERPENTINITE (ꞒpꞒum, CpꞒumg, ꞒpꞒums)

Serpentinite, both exposed and covered, forms a belt (Ul on pl. III-b) 50 mi long within the area of plates III-A and III-B. The belt is marked by magnetic highs and topographic swales. A summary of the magnetic properties of the belt are given in the unit descriptions for the geologic map. Briefly, the serpentinite is highly magnetic and the associated mafic rocks are very weakly magnetic. Although the aeromagnetic map (pl. III-A) is useful for showing the overall configuration of the mafic-ultramafic belt within the surrounding nonmagnetic sedimentary rocks, more detailed profiles are necessary to determine the lithologic variations within the mafic-ultramafic belt and to accurately determine the dip of the belt. Cady spent about a week mapping the mafic-ultramafic belt, both to locate its outer contacts and to determine the internal structural relationships between the mafic and

Table III-1. Explanations for Aeromagnetic and Gravity Maps.

PLATE III-A AEROMAGNETIC MAP--Explanation

Contour interval 10 nanoteslas (nT). Flight lines north-south spaced 1 mile, flown 1,000 ft above mean ground surface. International Geomagnetic Reference Field removed by contractor. In addition, an arbitrary datum was removed to make the average near zero.

PLATE III-B COMPLETE BOUGUER GRAVITY ANOMALY MAP AND AEROMAGNETIC INTERPRETATION--Explanation

Complete Bouguer gravity contours--Reduction density 2.67 g/cm^3. Terrain corrections to 167 km. Hachures indicate closed gravity low. Contour interval 2 mGal

Gravity station

Axis of magnetic high. Locally combined with antiform or synform symbol

Axis of magnetic low. Locally combined with antiform or synform symbol

Ꞓpꞓum

Exposed or shallow magnetic rock type

(Ꞓpꞓum)

Inferred (covered) magnetic rock type

[Kg]

Exposed or shallow nonmagnetic rock type

([Kg])

Inferred (covered) nonmagnetic rock type

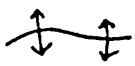

Inferred antiform

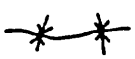

Inferred synform

Inferred strike and dip direction of planar structure

Inferred thrust fault. Teeth on upper plate

F2, U3, etc.

Magnetic features referred to in text

ultramafic rocks. He also conducted ground and helicopter magnetometer traverses across the belt to better determine the location and dip of the contacts.

Within the serpentinite belt are isolated bodies of resistant gabbro, microgabbro, and diorite that commonly form tors. When first seen in the field, these outcrops look like isolated blocks of gabbro in a serpentinite matrix. When studied closely, however, the gabbro exposures can be seen to be alined with each other and with lows on surface magnetometer profiles, thus proving that the gabbro forms steeply-dipping, sub-continuous layers. An appealing interpretation is that the mafic and ultramafic layers formed by differential gravity settling within large sills. Shearing, possibly accompanied by simultaneous serpentinization, was localized in the ultramafic rocks. The gabbro sills were folded and jointed, and may have undergone stretching to form a boudinage structure, but the overall alternating layered structure of mafic and ultramafic rock was preserved.

Resistant greenstone forms hogbacks within and along the southern margin of the mafic-ultramafic belt near the western margin of the WMNRA. To the north, the belt appears to be thrust over the Amy Creek dolomite unit or the Livengood Dome Chert. To the south, the mafic and ultramafic rocks of the belt, and associated greenstones, are unconformably overlain by the Mesozoic flysch of Wilber Creek unit. The subsurface configuration of the mafic-ultramafic complex was further investigated by means of detailed aeromagnetic studies, a semi-detailed gravity profile, and magnetotelluric and audiomagneto-telluric measurements.

The belt of magnetic highs has a central high flanked by deep lows both to the northwest and southeast. Paired, deep flanking lows are caused by sources that have shallow bottoms, such as klippen. It is unlikely, however, that a klippe of easily eroded serpentine would be continuous over such a long distance through a history of uplift and erosion. The source of the magnetic anomalies is therefore either rooted, or is part of a resistant rock unit that controls topography. The string-of-beads appearance that segments both the central high and the flanking lows is mainly an artifact of the line spacing and the gridding algorithm: highs occur on flight lines and lows occur between them.

Magnetic Modeling Confirms the Shallow-Bottom Interpretation.

Modeling the aeromagnetic data of plate III-A showed that magnetic profiles over the ultramafic belt could be satisfied best by a source with its top at the ground surface and its bottom about 1000 m (3300 ft) deep. The aeromagnetic flight lines were not well oriented, however, for modeling of northeast-trending structures. In order to better determine the attitude of the ultramafic belt, several helicopter magnetometer profiles were flown along northwest-trending flight lines, perpendicular to strike. Magnetic modeling of two of these profiles, flown along the same ground track (A-A' on pl. III-B), is shown in figures III-1, III-2, and III-3. Figure III-1 shows the magnetic field recorded at a constant barometric elevation of 853 m (2800 ft), about 75 m (250 ft) above the highest topography along the profile. The

observed magnetic anomaly can be reproduced by assuming a source body with uniform susceptibility; the dip of the body, steep near the surface, decreases with depth. The source crops out, and has a thickness of about 1000 m (3300 ft).

The profile in figure III-2 was flown along the same ground track as the first, draped approximately 100 m (330 ft) above the ground. Only the central portion is shown, and the horizontal scale is expanded to show more detail. The amplitude is 400 nT higher, and instead of one peak, there are four. A careful look at the constant elevation profile (fig. III-1) shows two points of inflection that coincide with peaks on the draped profile. Four peaks and two points of inflection in the draped profile require six magnetic layers separated by less-magnetic layers, as shown in the underlying model. This may seem like a complicated model to be derived from a single magnetic profile; but the complexity is justified by field observations, described above, that show many alternating layers of magnetic serpentinite and less-magnetic gabbro occur throughout the mafic-ultramafic belt.

The model was obtained by interactive inverse magnetic modeling (Webring, 1985). Initially, vertical contacts between layers were located at the zones of steepest gradient bounding the magnetic highs or inflection points. The elevation of the tops of the boundaries was constrained to be at the ground surface. The horizontal position of body vertices at the surface, and the horizontal and vertical positions of body vertices at depth, were allowed free movement during magnetic inversion. Magnetic susceptibility of the six magnetic bodies was allowed to change to improve the fit, but values stayed in the range 0.05 to 0.07 SI. The best-fit model shows six magnetic serpentinite layers dipping steeply (75 degrees or steeper), generally to the south. The depth extent of the layers increases from about 800 m (2600 ft) in the northwest to about 1200 m (3900 ft) in the southeast. A reasonable interpretation is that the magnetic layers may be truncated at depth by a south-dipping basal thrust or detachment fault.

The model calculated from the detailed, central portion of the draped profile shown by figure III-2 roughly satisfies the constant-elevation profile (fig. III-3). A model that would accurately fit both the constant elevation and draped profiles should have the layering shown in figure III-2 and the dip that decreases with depth shown in figure III-1.

The mafic-ultramafic belt occurs in a zone in which the Bouguer gravity anomaly increases northward towards gravity highs over the Rampart Group, north of the WMNRA. No consistent gravity high is associated with the mafic-ultramafic belt, supporting the interpretation that the belt is unrooted. Massive, resistant, weakly-magnetic to nonmagnetic greenstone forms a belt up to 4000 ft (6.4 km) wide south of, or within, the ultramafic belt along part of its length. The greenstone belt pinches out or is faulted out elsewhere. The greenstone appears to grade northward into diabase near the contact with the adjacent mafic-ultramafic complex; the latter contact is faulted. Resistant outcrops of mylonite occur in the diabase just south of the fault. The greenstone consistently occurs adjacent to or within the ultramafic belt, indicating that the two are probably related. The resistant greenstone, as

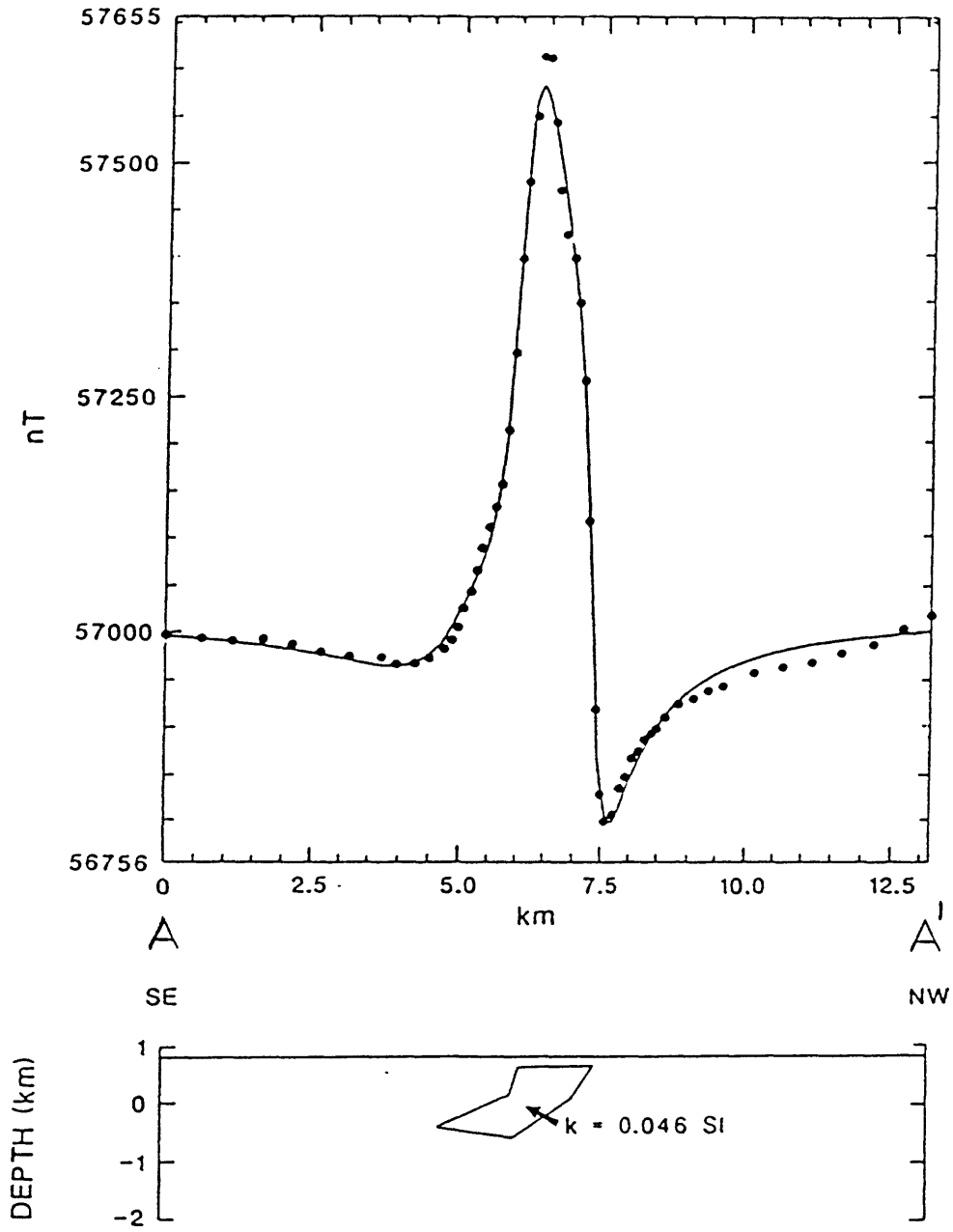

Figure III-1. Magnetometer profile, constant elevation, simple model on plate III-B.

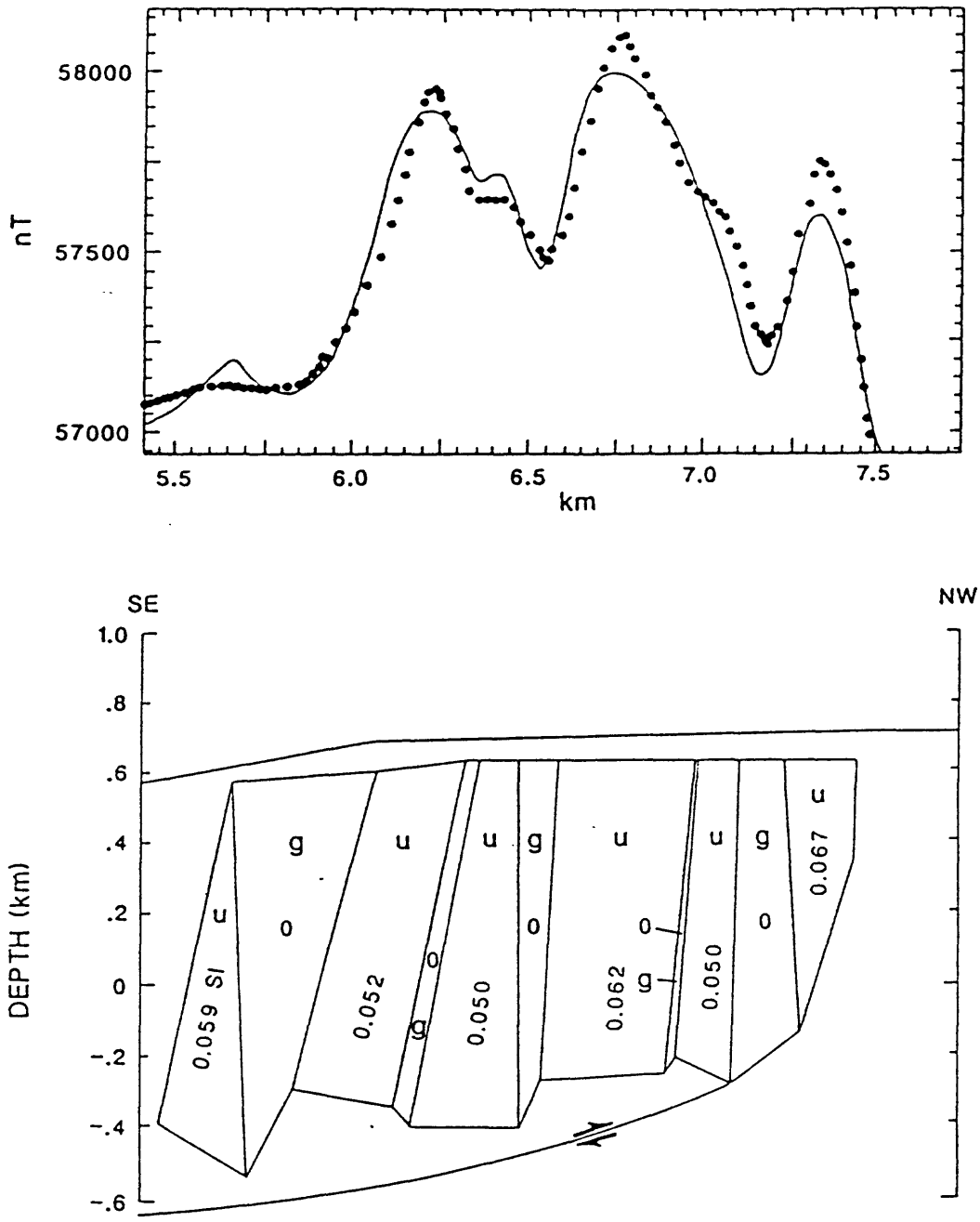

Figure III-2. Magnetometer profile, detailed, complex model.

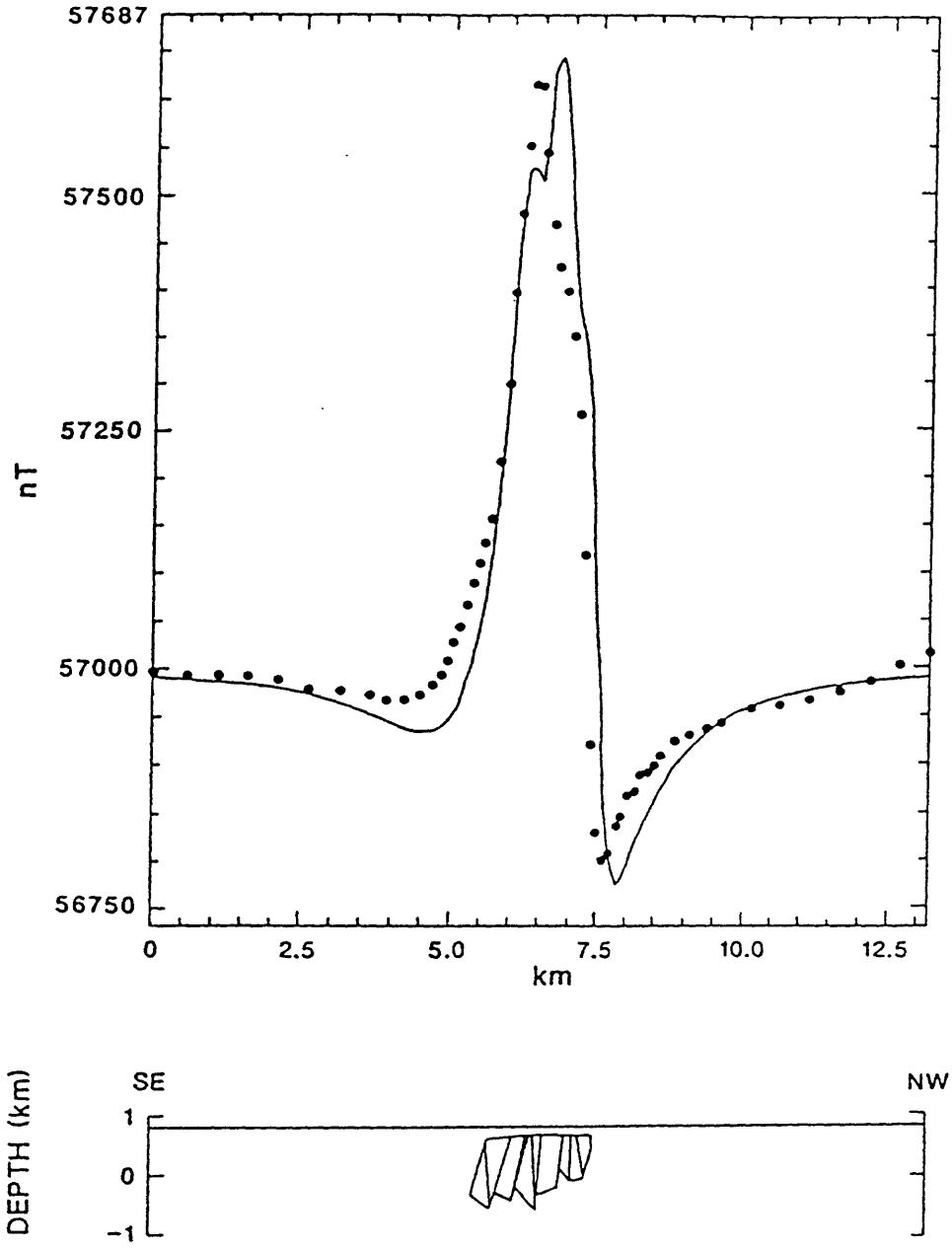

Figure III-3. Magnetometer profile, complex model.

well as the mafic layers within the mafic-ultramafic complex, probably provide the resistance to erosion that has preserved the soft serpentinite band. Northwest of the exposed ultramafic belt is a belt of aeromagnetic highs (U2, pl. III-B) caused by a buried source. It is possible that U2 is caused by buried ultramafic rocks related to the exposed ultramafic belt. However, Weber (oral commun., 1987) says that this interpretation is unlikely for stratigraphic and structural reasons, and suggests that magnetic granite like that of Victoria Mountain, or basalts of the Tindir Group, might cause high U2.

FOSSIL CREEK VOLCANICS (Ofv)

An irregular belt of magnetic highs coincides roughly with the mapped distribution of Ordovician Fossil Creek Volcanics. Magnetic lows generally accompany the associated limestone and clastic sedimentary rocks. The correlation is not perfect, however, suggesting the presence of complex structure. For example, where magnetic highs occur over nonmagnetic sedimentary rocks, magnetic volcanic rocks are inferred to lie beneath thin, nonmagnetic rocks in a thrust sheet. Two inferred thrust faults are shown on plate III-B. The mapped depiction of the Fossil Creek Volcanics could probably be improved by tracing magnetic marker beds, especially if a higher resolution aeromagnetic map were available. A relative gravity high of about 15 m Gal occurs in a 3- to 6 mi-wide (5-10 km) belt that includes the Fossil Creek Volcanics. This suggests that the volcanic rocks are part of a relatively large unit that is denser than the flysch of Wilber Creek unit to the north and the Cache Creek pluton to the south.

MAFIC METAVOLCANICS OF THE FAIRBANKS SCHIST (pGf)

The southeastern part of the map is characterized by elongate, east-northeast-trending magnetic highs that are interpreted to be caused by chlorite-bearing portions of the Fairbanks schist. Cady and Weber (1983) discussed the magnetic schists of Circle quadrangle. Magnetic schists were found along magnetic high F1 (pl. III-B) and were interpreted to lie in the south limb of a breached antiform.

Nonmagnetic rocks, possibly granite, were inferred to lie in the core of the antiform. Except for the rocks beneath magnetic high F1, magnetic rocks could not be found in outcrop; although magnetic anomaly amplitudes and gradients indicate that thick (>1 km) layers of magnetic rock, with susceptibilities of at least 0.012 SI or equivalent remanent magnetization, should crop out or occur in the shallow subsurface. Cady and Weber (1983) proposed a model in which magnetic chloritic pelitic schist, occurring in one or more layers with quartzite, has been gently folded about east-northeast-trending axes. Many of the magnetic highs are inferred to occur at the crests of antiforms that bring magnetic schist close to the surface. Quartzite presumably forms a resistant carapace covering the less resistant schist, making it difficult to observe the schist, especially along ridges where most of the geologic traverses have been made and most outcrops occur. Only where the antiforms have been breached, as along magnetic high F1, are exposures of magnetic schist abundant.

The Cleary sequence, part of the Fairbanks schist unit, is important as a likely source of placer gold, especially where it occurs close to granitic plutons (Smith and others, 1981; Robinson and others, 1982). The magnetic marker units that lie above and below the Cleary sequence (Smith and Pessel, 1987) can be roughly mapped by using the existing aeromagnetic maps, but higher resolution aeromagnetic maps would facilitate mapping of the Cleary.

MARBLE/CHLORITE MARKER OF PRECAMBRIAN GRIT (pЄg, pЄga on Plate III-B)

Local magnetic highs occur over the Precambrian grit/metagrit unit of Smith and Pessel (1987), especially in areas where the marble/chlorite marker is mapped. Presumably the chlorite portion of the marker unit is the source of the magnetic highs. The marble/chlorite marker interfingers with the Fairbanks schist, so it probably has the same protolith as the chloritic parts of the Fairbanks schist unit. Low amplitude, short wavelength magnetic highs occur in the vicinity of Rocky Mountain (Lime Peak) and Quartz Creek plutons

and the intrusive rocks (TKi on pl. III-B) that lie between. The cause of these anomalies is unknown, but the anomalies may be due to contact metamorphism of the chlorite/marble marker.

Magnetic Granitoid Plutons

SYENITE OF VICTORIA MOUNTAIN (Ks on Plate III-B)

An intense magnetic high is caused by syenite of Victoria Mountain. Magnetic modeling suggests that the south boundary of the pluton dips to the south, but this interpretation is uncertain because large errors in elevation control must have occurred when drape-flying the steep south side of the mountain. Based on the magnetic expression, the north boundary may be vertical.

Victoria Mountain lies about 1.2 mi (2 km) south of the Cambrian-Precambrian mafic-ultramafic belt described above. Serpentinite is mapped directly north of the pluton, but it does not cause a magnetic high there. The Victoria Mountain pluton is one of several late Cretaceous magnetic granitoid plutons that lie along the Tintina-Kaltag fault system. These include the Sawtooth Mountain and possibly the Tolovana Hot Springs Dome plutons in Livengood quadrangle, although the latter lies about 14 mi from the known ultramafic belt and about 20 mi (32 km) from mapped traces of the Tintina-Kaltag fault system. A broad magnetic high in the Tintina fault zone near Circle City may have a similar source (Cady and Weber, 1983). It is possible that these plutons were emplaced in zones of weakness or extension associated with the fault zone. The magnetic properties of the plutons may derive from contamination by older mafic and ultramafic rocks through which they were intruded.

SYENITE OF ROY CREEK (Ks)

A strong east-northeast-trending magnetic high with twin crests, 8 mi (13 km) east-southeast of Cache Mountain, occurs over the syenite of Roy Creek, and

extends slightly east-northeast of mapped exposures of the pluton. The syenite is host to anomalous concentrations of uranium, thorium, and rare-earth elements explored in the late 1970s and early 1980s by MAPCO. The most abundant exposures and most of the explored ground lie below the center and southwestern part of the anomaly. The more poorly exposed and less explored area beneath the northeastern crest of the elongate high would provide a likely target for further exploration. The configuration of the anomaly suggests that the pluton underlies about 10 mi^2 (25 km^2), and the steepness of the magnetic gradients indicates that the cover over the more poorly exposed northeastern part is only about 400 ft (120 m) thick.

SOURCES OF MAJOR MAGNETIC LOWS

Nonmagnetic Granitoid Plutons (Kg)

Magnetic lows occur over Mt. Prindle and Quartz Creek plutons and inferred buried plutons along strike. The Mt. Prindle and Quartz creek plutons are two of several plutons in the Circle quadrangle that correlate with magnetic lows, and wherever measured, have magnetic susceptibilities less than 0.0012 SI (Cady and Weber, 1983). This places them in the ilmenite series of Ishihara (1981). Magnetic lows coincide in many places with the Quartz Creek and Mt. Prindle granite plutons, but the magnetic lows cover a much larger area than the exposed plutons. Lows to the east and north of Mt. Prindle coincide with hypabyssal felsic igneous rocks and a small pluton that suggest the presence of a larger pluton at depth. A broad gravity low, poorly-defined by the available data, roughly coincides with the magnetic lows over the inferred pluton. It is reasonable to conclude, therefore, that the area encompassed by these lows is underlain by nonmagnetic granitic rocks.

Several high-amplitude magnetic lows, with local amplitudes of 50 to 120 nT, occur north and east of Mt. Prindle at latitude 65° 28' N., longitude 146° 29' W. One of the lows on plate II-A, 1.2 mi (2 km) northeast of Mt. Prindle. The large amplitude of these negative anomalies, isolated from positive anomalies, suggests that they may be caused by reverse remanent magnetization. Cady and Weber (1983) searched for but could not find rocks with significant reverse remanent magnetization.

Cady and Weber (1983) inferred, from continuity of gravity and magnetic lows and correlation of hypabyssal felsic intrusions with magnetic lows, that granitic plutons occur in the subsurface from east of Mt. Prindle to the vicinity of Mastodon Dome. Gold placers occur in the vicinity of Mt. Prindle, and Mastodon Dome lies in the headwaters of the Circle placer gold mining district. The two areas have another feature in common--magnetic highs that suggest the presence of chloritic Fairbanks schist, within which the gold-bearing Cleary sequence is commonly infolded. We infer that the intrusion of Cretaceous and(or) Tertiary plutons caused hydrothermal remobilization of gold from the Cleary sequence in both the Mt. Prindle and Circle mining districts (Cady and Weber, 1983; Light and others, 1987) A belt of magnetic lows (L1, pl. III-B) extends southwest from Mt. Prindle, reaching a minimum near Long. 147°25' W. A belt of magnetic highs labeled F5 lies southeast of the low. The placer gold deposits mined at Nome Creek coincide with the gradient

between the magnetic low and the magnetic high. Lesser quantities of placer gold have been found in Trail and Ophir Creeks in the area of the magnetic low. Light and others (1987) inferred that the high, F5, is caused by schist of the Cleary sequence, and the low, L1, is caused by a buried granitoid pluton. They concluded that gold was mobilized from the schist by heat and fluids associated with the intrusion of the granite. However, recent magnetotelluric and audiomagnetotelluric measurements by Carl Long (this report) have revealed low apparent resistivities (<100 ohm-meters) beneath magnetic low L1. These resistivities are too low for a granitic pluton, being more typical of unmetamorphosed sedimentary rocks. Magnetic high F5 is probably caused by schist of the Cleary sequence, but a granitic pluton beneath low L1 cannot be invoked as a cause of gold mobilization.

Magnetic high F5 has low amplitude and is discontinuous near Mt. Prindle, suggesting that the magnetic source has been deeply eroded. Hence the deep erosion of schist near Mt. Prindle may have freed the contained gold, thus giving rise to the abundant placers of Nome Creek. To the southwest, where F5 has higher amplitude and better continuity, less schist has been eroded to form placer deposits. Consequently, gold-bearing veins may still be in place along the ridge south of Trail and Ophir Creeks, at the southern border of the WMNRA.

ROCKY MOUNTAIN (LIME PEAK) PLUTON (Kg on Plate III-B)

The nonmagnetic Rocky Mountain (Lime Peak) pluton produces a weak magnetic low because of its susceptibility contrast with very weakly magnetic grit to the northwest and schist and quartzite to the southeast. A weak magnetic high along the northwest margin of the pluton may be caused by a contact aureole. The northwest contact of the pluton lies outside the magnetic low, and magnetic lows are displaced outside of the southeastern contact. That relationship implies that the pluton may be boat-shaped, with a keel that dips to the southeast.

LAMPROPHYRE (TKi ON PLATE III-B)

Nonmagnetic lamprophyre occurs in an east-northeast trending belt of magnetic lows between the Quartz Creek and Rocky Mountain (Lime Peak) plutons. The magnetic lows show that the pluton continues to the northeast about 4 mi (6 km) beyond the mapped exposures. Magnetic highs surrounding the lows may be caused by contact metamorphism of the marble/chlorite marker unit.

WEAKLY-MAGNETIC GRANITE OF CACHE MOUNTAIN PLUTON (Tg)

Cache Mountain pluton is weakly magnetic. Small magnetic highs correlate with granite exposures. The highs are flanked by a belt of magnetic lows over the nonmagnetic Precambrian grit. The intensity of the flanking lows, and the displacement of the magnetic highs 3000 ft (900 m) or more inside the pluton's contact, indicate that the pluton is shaped like a bowl, with contacts that dip inward about 45 degrees.

OTHER ROCKS WITH VARIED MAGNETIC SIGNATURES

Vrain Area Magnetic Anomaly (MzPzv)

A concentric magnetic high, truncated on the south by the Preacher Creek strand of the Tintina fault, occurs over nonmagnetic slate. Although as yet we have no evidence, the source of the magnetic high may be a contact aureole, possibly caused by the formation of pyrrhotite in slate, surrounding the top of a buried pluton. Tuff is reported from the central magnetic low (Foster and others, 1983), and if it is locally derived, the concentric magnetic high may be related to a caldera complex.

Magnetic and Gravity Lows Characteristic of Two Major Sedimentary Units (GpGa, KJw)

Two sedimentary units are typically associated with magnetic lows. The Livengood Dome Chert, which crops out between exposed and possible buried ultramafic rocks (U1 and U2, pl. III-B), causes a broad magnetic low. The magnetic low suggests that the chert section is thick. However, the gravity stations are too sparse to reveal much about the configuration of the chert. The flysch of Wilber Creek unit, which crops out between ultramafic rocks (GpGum) and the Fossil Creek Volcanics (Ofv), causes both gravity and magnetic lows. Both gravity and magnetic anomalies become more positive to the northeast, indicating a northeastward thinning of the sedimentary section.

Lithologic Units that are Geophysically Neutral

Some lithologic units are magnetically and gravimetrically neutral. Causing neither highs nor lows, they tend to occur in gradient zones. The sandstones, including the Wickersham grit and the Globe quartzite unit, cause wide areas of subdued gravity and magnetic anomalies. Relatively featureless gravity and magnetic fields are characteristic of the Fossil Creek sedimentary rocks and the Tolovana Limestone. There is a susceptibility contrast between the Fossil Creek Volcanics and the Tolovana Limestone, but the anomalies are too small to be resolved on the aeromagnetic map. Mapping of the Fossil Creek Volcanics and Tolovana Limestone could be facilitated by a higher resolution aeromagnetic map.

REFERENCES CITED

Bundtzen, T.K., 1983, Bedrock geologic map of the Livengood B-3 quadrangle, Alaska: Alaska Division of Geological and Geophysical Surveys, Report of Investigations 83-6, scale 1:40,000.

Cady, J.W., and Weber, F.R., 1983, Aeromagnetic map and intepretation of magnetic and gravity data, Circle Quadrangle, Alaska: U.S. Geological Survey Open-File Report 83-170-C, scale 1:250,000, 29 p.

Foster, H.L., Laird, Jo, Keith, T.E.C., Cushing, Grant, and Menzie, D., 1983, Preliminary geologic map of the Circle quadrangle, Alaska: U.S. Geological Survey Open-File Report 83-170-A.

Ishihara, Shunso, 1981, The granitoid series and mineralization: Economic Geology, 75th Anniversary Volume, 1981, pp. 458-454.

Light, T.D., Cady, J.W., Weber, F.R., McCammon, R.B., and Rinehart, C.D., 1987, Sources of placer gold in the southern part of the White Mountains Recreation Area, East-Central Alaska, in Hamilton, T.D., and Galloway, J.P., eds., Geological Studies in Alaska by the U.S. Geological Survey during 1986: U.S. Geological Survey Circular 998, p. 67-69.

Robinson, M.S., Smith, T.E., and Bundtzen, T.K., 1982, Cleary sequence of the Fairbanks mining district--primary stratigraphic control of lode gold/antimony mineralization (abs.): Cordilleran Section Meeting, Anaheim, Calif., Geological Society of America, Abstracts with Program, v. 14, no. 4, p. 228.

Smith, T.E., Robinson, M.S., Bundtzen, T.K., and Metz, P.A., 1981, Fairbanks mining district in 1981--New look at an old mineral province: The Alaska Miner, The Journal of the Alaska Miners Association, v. 9, no. 11, p. 8,28.

U.S. Geological Survey, 1974a, Aeromagnetic map of the Circle Quadrangle, northeastern Alaska: U.S. Geological Survey Open-File Report 74-1102, scale 1:250,000.

U.S. Geological Survey, 1974b, Aeromagnetic map of the eastern half of the Livengood quadrangle, northeastern Alaska: U.S. Geological Survey Open-File Report 74-1103, scale 1:250,000.

Webring, Michael, 1985, SAKI: A Fortran program for generalized linear inversion of gravity and magnetic profiles: U.S. Geological Survey Open-File Report 85-122, 28 p.

Resistivity-Cross Section

by C.L. Long and R. Miyaoka

INTRODUCTION

Twenty Audiomagnetotelluric (AMT) and seven Magnetotelluric (MT) soundings were made across the WMNRA in the northwestern part of the Yukon-Tanana Upland (fig. III-4a). The objective of the electromagnetic soundings was to create a resistivity section that would define electrical resistivity changes laterally and vertically and to relate those changes to lithology and structure.

AMT-MT METHODS

The AMT system used in this survey was designed and built by the U.S. Geological Survey (Hoover and others, 1976). Details of the data processing and interpretation are given by Hoover and others (1978) and Long (unpub. computer programs). Theory and applications of the AMT method to mineral exploration have been described by Strangway and others (1973), Hoover and others (1978), Long (1983), and Long (1985). The MT system used in this survey was also designed and built by the U.S. Geological Survey. The MT data for this report was processed with the AMT data for a deeper look at each of the coincidental AMT-MT sites.

AMT-MT DATA

Figure III-4b is a resistivity cross-section of the AMT-MT data collected in this study. The section is derived from inversions of the AMT-MT sounding curves using the Bostick (1977) computer algorithm. The inversion process produces a horizontally layered resistivity-depth model whose calculated effects match the data recorded at each station to an acceptable degree of fit. Resistivity models were computed for the N-S profile A-A' (fig. III-4b) and were hand contoured. Utilizing the resistivity changes laterally and vertically, an implied geologic section (fig. III-4c) was made to help resolve the subsurface geologic features that were not evident at the surface. Any mismatch of the implied geologic section (fig. III-4c) with other geologic sections may be due to the nature of the electromagnetic method, which averages large volumes of rock vertically and laterally, therefore it is hard to discriminate between individual rock units of similar resistivities.

INTERPRETATION

The AMT-MT resistivity-depth models suggest that major high and low resistivities and varying resistivity gradients are present that reflect changes in lithologies and geologic structures. Resistivities across the section (fig. III-4b) vary from a 1 ohm-m low at station 10 to a high greater than 10,000 ohm-m below stations 14-16. The implied geological contacts and structural features are shown on figure III-4c.

A vertical high resistivity gradient between stations 4 and 3, and a large separation in the apparent resistivities of the two sounding directions at

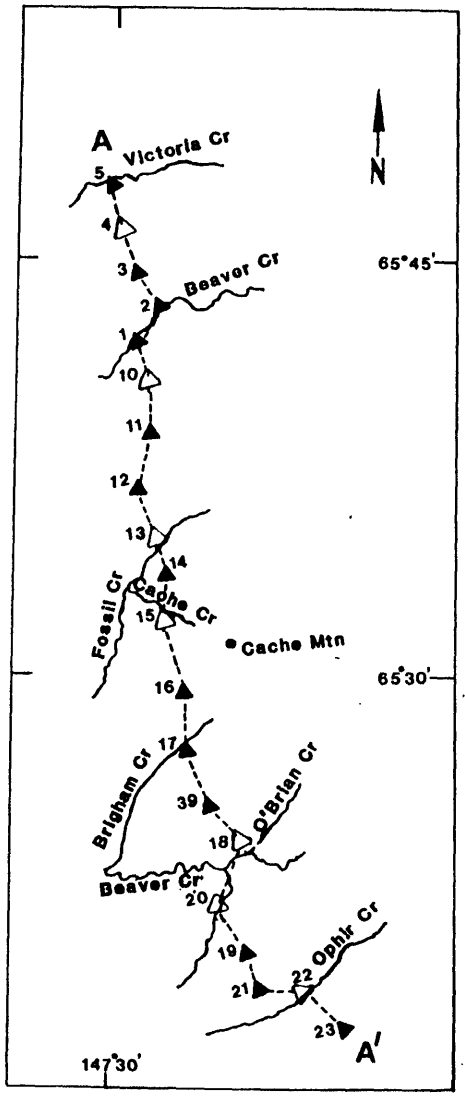

Figure III-4a

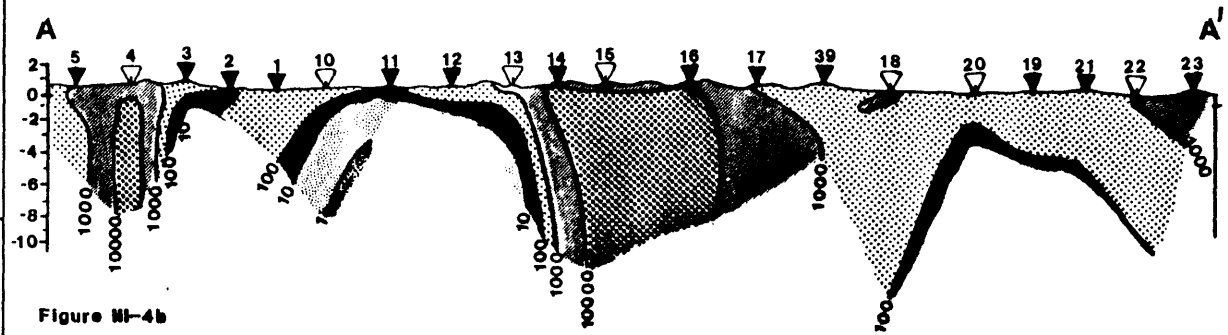

Figure III-4b

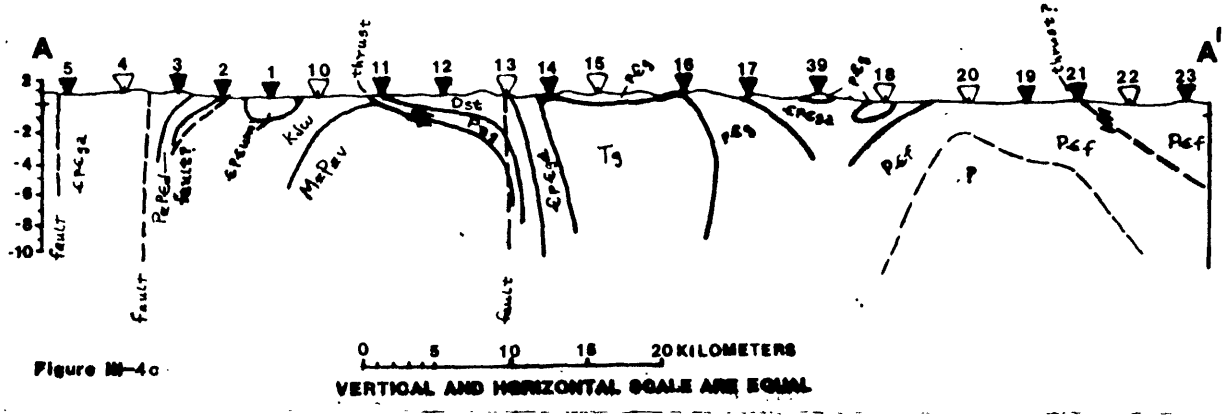

Figure III-4c

Figure III-4---Map showing station numbers and location of resistivity section A-A' shown in figure III-4a. AMT station locations are indicated by solid triangles. AMT-MT station locations are indicated by open triangles. Resistivity section along traverse A-A' shown in figure III-4b. Resistivity contours are one interval per decade in ohm-meters. Resistivity levels of each decade are shown below the section. Implied geologic section along traverse A-A' shown in figure III-4c.

station 4, indicate a major east-west trending fault there that extends to a depth greater than 3 mi (5 km). The Amy Creek unit (PzpЄd) mapped between stations 3 and 2 reflects a resistivity range of 100-250+ ohm-m. Resistivities greater than 250 ohm-m below station 1 are thought to reflect buried Cambrian or Precambrian mafic or ultramafic rocks. From stations 10 to 13 a low resistivity unit of less than 10 ohm-m at varying depths is interpreted to be the Wilbur Creek unit. The resistivity units between stations 11 and 13 dip gently to the south-southeast and suggest the angle of the mapped thrust fault at the western edge of the White Mountains. These soundings also give a rough thickness estimate of 0.87 mi (1.4 km) for the Globe unit and the Tolovana Limestone combined. Another nearly east-west fault similar to the one near station 4 is indicated at station 13 by a large separation in the two sounding directions; indications are that it extends to depths greater than 6 mi (10 km). These two faults suggest a major tectonic feature, and may represent splays of the Tintina fault zone. The 1,000-10,000 ohm-m resistivity unit between stations 13-14 suggest that the Cambrian to Precambrian Wickersham unit (ЄpЄga) has a nearly uniform resistivity.

The large resistivity high between stations 14 and 16 greater than 10,000 ohm-m reflects the very dense rocks of Tertiary granite of the Cache Mountain pluton. Although the traverse is very near the southwestern outcrop of the pluton, it is evident that the pluton extends further northward at about 0.62 mi (1 km) depth to near station 14. The grit and quartzite of the Wickersham unit has resistivities of 1,000-10,000 ohm-m and covers the Cache Mountain pluton along the traverse from stations 14 and 16, and it appears to be the resistivity unit observed between stations 16 and 17. Some smaller quartzite units are shown on figure III-4c, between stations 17 and 18. A change to more uniform resistivities between stations 18 and 20 that continues on to the south probably indicates the location of the contact between the Wickersham unit and Fairbanks schist unit. A resistivity low of less than 100 ohm-m at about 1-3 mi (2-5 km) below stations 20-21 is an unknown unit below the Fairbanks schist, possibly a remnant of an extensive Cretaceous or Jurassic flysch basin (Stanley, 1986) containing low resistivity shales similar to or part of the Wilbur Creek unit as seen near AMT station 10. At station 21 the separation of the two sounding directions indicates that a fault or lithologic contact is present.

CONCLUSIONS

The resistivity cross section indicates two fault zones that are interpreted to reflect the possible boundaries of the Tintina trench. Resistivity and depth information in the models suggest the thickness of the Tolovana Limestone and associated Fossil Creek Volcanics, and possibly the angle that they were thrust to the north-northwest. Resistivities in the northwestern Beaver Creek valley confirm the presence there of a buried piece of the Cambrian or Precambrian mafic/ultramafic rocks. High-resistivity closures (>10,000 ohm-m) indicate a width of about 10 km and a depth of greater than 10 km for the Cache Mountain pluton. The resistivity data are consistent with the mapped geologic features, but added new information giving a more detailed picture of this segment of the Earth's crust.

REFERENCES CITED

Bostick, F.X., Jr., 1977, A simple almost exact method of MT analysis, in Electrical Methods in Geothermal Exploration: Salt Lake City, University of Utah, Department of Geology and Geophysics, p. 175-177.

Hoover, D.B., Frischknecht, F.C., and Tippens, C.L., 1976, Audio-magnetotelluric soundings as a reconnaissance exploration technique in Long Valley, California: Journal of Geophysical Research, v. 81, p. 801-809.

Hoover, D.B., Long, C.L., and Senterfit, R.M., 1978, Some results from audio-magnetotelluric investigations in geothermal areas: Geophysics, v. 43, no. 7, p. 1501-1514.

Long, C.L., 1983, Audio-magnetotelluric studies in the Wallace 1 X 2 quadrangle, Montana and Idaho: U.S. Geological Survey Miscellaneous Field Studies Map MF-1354-B, 1 sheet, scale 1:250,000.

Long, C.L., 1985, Regional audiomagnetotelluric study of the Questa Caldera, New Mexico: Journal of Geophysical Research, v. 90, no. B13, p. 11270-11274.

Stanley, W.D., 1986, Magnetotelluric study of a compressed flysch system in the Healy and adjacent quadrangles, in Bartsch-Winkler, Susan, and Reed, K.M., eds., Geologic Studies in Alaska by the U.S. Geological Survey during 1985, U.S. Geological Survey Circular 978, p. 78-81.

Strangway, D.C., Swift, C.M., Jr., and Holmer, R.C., 1973, The application of audio-frequency magnetotellurics (AMT) to mineral exploration: Geophysics, v. 38, no. 6, p. 1159-1175.

IV. GEOCHEMISTRY

by T.D. Light, G.K. Lee, and R.B. Tripp

Introduction

The U.S. Geological Survey has conducted a reconnaissance geochemical study for the part of the WMNRA covered in this report. Analytical data for rock samples were reported by Sutley and others (1987a), and analytical data for stream-sediment, moss-trap and heavy-mineral-concentrate samples were reported by Sutley and others (1987b). Stream-sediment samples that had been previously collected from the Livengood and western Circle quadrangles, under the National Uranium Resource Evaluation (NURE) program, were also analyzed by semiquantitative spectrography for 31 elements (Bailey and others, 1987).

Analytical Methods

Geochemical samples were analyzed for 31 elements using a semiquantitative, direct-current arc emission spectrographic method (Grimes and Marranzino, 1968). The types of samples analyzed were: 1) rocks, 2) the minus-80 mesh fraction of stream sediments, 3) the minus-30 mesh to plus-80 mesh fraction of moss-trap sediments, 4) the minus-80 mesh fraction of moss-trap sediments, and 5) the non-magnetic heavy-mineral concentrates. The elements determined and their lower limits of analytical determination are listed in table IV-1. Spectrographic results were obtained by visual comparison of spectra derived from the sample against spectra obtained from standards made from pure oxides and carbonates. Analytical values are given in parts per million (ppm) for all elements except Fe, Mg, Ca, and Ti, which are given in percent. Standard concentrations are geometrically spaced over a given order of magnitude of concentration as, for example, 100, 50, 20, and 10 ppm. Elements whose concentrations are estimated to fall between those values are assigned the values of 70, 30, and 15, respectively. The precision of the analytical method is plus or minus one reporting interval at the 83 percent confidence level and plus or minus two reporting intervals at the 96 percent confidence level (Motooka and Grimes, 1976).

Stream-sediment samples and the minus-80 mesh fraction of the moss-trap sediment samples from the WMNRA were also analyzed for As, Bi, Cd, Sb, and Zn by atomic absorption spectrometry using a method by O'Leary and Viets (1986). The non-magnetic fractions of heavy-mineral concentrates were optically examined using a binocular microscope to determine the presence of ore-related minerals.

Geochemical Data

The raw analytical data were processed using the USGS STATPAC computer programs (VanTrump and Miesch, 1977). The univariate statistics, including the maximum, minimum, mean, standard deviation, and number of qualified values for the rocks, heavy-mineral concentrates, stream sediments, coarse (minus-30 to plus-80 mesh) moss-trap sediments, and fine (minus-80 mesh) moss-trap sediments are listed in tables IV-2 through IV-6, respectively.

TABLE IV-1.--Limits of determination for the spectrographic analysis of rocks stream sediments, and moss-trap sediments, based on a 10-mg sample

[The spectrographic limits of determination for heavy-mineral-concentrate samples are based on a 5-mg sample, and are therefore two reporting intervals higher than the limits given below]

Elements	Lower determination limit	Upper determination limit
	Percent	
Iron (Fe)	0.05	20
Magnesium (Mg)	.02	10
Calcium (Ca)	.05	20
Titanium (Ti)	.002	1
	Parts per million	
Manganese (Mn)	10	5,000
Silver (Ag)	0.5	5,000
Arsenic (As)	200	10,000
Gold (Au)	10	500
Boron (B)	10	2,000
Barium (Ba)	20	5,000
Beryllium (Be)	1	1,000
Bismuth (Bi)	10	1,000
Cadmium (Cd)	20	500
Cobalt (Co)	5	2,000
Chromium (Cr)	10	5,000
Copper (Cu)	5	20,000
Lanthanum (La)	20	1,000
Molybdenum (Mo)	5	2,000
Niobium (Nb)	20	2,000
Nickel (Ni)	5	5,000
Lead (Pb)	10	20,000
Antimony (Sb)	100	10,000
Scandium (Sc)	5	100
Tin (Sn)	10	1,000
Strontium (Sr)	100	5,000
Vanadium (V)	10	10,000
Tungsten (W)	50	10,000
Yttrium (Y)	10	2,000
Zinc (Zn)	200	10,000
Zirconium (Zr)	10	1,000
Thorium (Th)	100	2,000

Table IV-2. Rock Samples, White Mts. NRA;
Univariate Statistics of Analytical Data

Column	Minimum	Maximum	Mean	Deviation	Valid	B	L	N	G	Other
S-FE%	.050000	20.00000	3.514726	3.876274	601	0	12	5	2	0
S-MG%	.020000	10.00000	1.661786	2.074603	588	0	20	1	11	0
S-CA%	.050000	20.00000	3.054536	5.120849	399	0	138	41	42	0
S-TI%	.002000	1.000000	.311408	.300475	596	0	11	2	11	0
S-MN	10.00000	5000.000	578.4463	618.7566	605	0	10	1	4	0
S-AG	.500000	10.00000	1.436842	2.083840	38	0	45	537	0	0
S-AS	200.0000	5000.000	1266.667	1870.472	6	0	1	613	0	0
S-AU	***	***	***	***	0	0	0	620	0	0
S-B	10.00000	2000.000	56.96320	113.8288	489	0	79	52	0	0
S-BA	20.00000	5000.000	555.1240	809.9182	564	0	37	9	10	0
S-BE	1.000000	30.00000	2.829843	3.569402	191	0	228	201	0	0
S-BI	10.00000	50.00000	22.00000	16.43167	5	0	7	608	0	0
S-CD	20.00000	50.00000	30.00000	14.14214	4	0	17	599	0	0
S-CO	5.000000	100.0000	27.99460	22.48866	370	0	37	213	0	0
S-CR	10.00000	3000.000	148.3951	286.8850	405	0	90	124	1	0
S-CU	5.000000	300.0000	32.74825	37.20155	429	0	114	77	0	0
S-LA	20.00000	700.0000	53.33333	64.10408	201	0	36	381	2	0
S-MO	5.000000	50.00000	13.42857	12.62302	14	0	10	596	0	0
S-NB	20.00000	200.0000	31.76471	26.53870	68	0	78	474	0	0
S-NI	5.000000	5000.000	69.41083	270.0981	443	0	56	121	0	0
S-PB	10.00000	7000.000	60.11905	440.8379	252	0	135	233	0	0
S-SB	100.0000	100.0000	100.0000	***	3	0	1	616	0	0
S-SC	5.000000	50.00000	15.30787	10.25884	432	0	72	116	0	0
S-SN	10.00000	150.0000	23.33333	32.43336	27	0	31	562	0	0
S-SR	100.0000	5000.000	389.5061	484.2808	243	0	122	254	1	0
S-V	10.00000	700.0000	100.5427	96.79037	562	0	46	12	0	0
S-W	***	***	***	***	0	0	1	619	0	0
S-Y	10.00000	300.0000	27.73100	24.01207	487	0	51	80	2	0
S-ZN	200.0000	2000.000	424.2424	469.7275	33	0	22	565	0	0
S-ZR	10.00000	1000.000	139.0253	133.2764	554	0	17	45	4	0
S-TH	200.0000	200.0000	200.0000	***	2	0	0	616	2	0
AA-AU-P	.150000	.150000	.150000	***	1	559	0	60	0	0
AA-AS-P	10.00000	1000.000	41.59091	119.8264	88	137	0	393	2	0
AA-BI-P	1.000000	56.00000	8.352942	13.64707	17	137	0	466	0	0
AA-CD-P	.100000	33.00000	.801744	2.882526	258	137	16	209	0	0
AA-SB-P	2.000000	120.0000	9.506024	17.44984	83	137	0	400	0	0
AA-ZN-P	5.000000	1300.000	81.57016	131.8161	449	137	7	25	2	0

Table IV-3. Heavy-mineral-concentrate samples, White Mts. NRA; Univariate Statistics of Analytical Data

Column	Minimum	Maximum	Mean	Deviation	Valid	B	L	N	G	Other
S-FE%	.100000	30.00000	.808360	2.709577	317	0	22	1	0	0
S-MG%	.050000	15.00000	.290854	1.053217	281	0	59	0	0	0
S-CA%	.100000	20.00000	2.088838	3.424997	327	0	10	3	0	0
S-TI%	.100000	2.000000	1.332243	.701422	107	0	0	0	233	0
S-MN	20.00000	10000.00	261.1504	929.1060	339	0	1	0	0	0
S-AG	1.000000	2000.000	107.8365	390.7456	52	0	1	287	0	0
S-AS	500.0000	2000.000	900.0000	651.9202	5	0	1	334	0	0
S-AU	20.00000	1000.000	313.5293	368.6960	17	0	9	311	3	0
S-B	20.00000	2000.000	129.5370	192.6163	324	0	16	0	0	0
S-BA	50.00000	10000.00	1770.548	2770.763	219	0	2	0	119	0
S-BE	2.000000	500.0000	16.64865	81.32961	74	0	142	124	0	0
S-BI	20.00000	2000.000	227.9487	434.7183	39	0	19	280	2	0
S-CD	50.00000	1000.000	186.1905	229.1762	42	0	15	283	0	0
S-CO	10.00000	700.0000	37.95918	98.29228	49	0	18	273	0	0
S-CR	10.00000	3000.000	98.64285	261.1587	280	0	54	6	0	0
S-CU	10.00000	2000.000	57.63393	209.6823	112	0	96	132	0	0
S-LA	50.00000	2000.000	188.9908	268.6506	218	0	27	95	0	0
S-MO	10.00000	20.00000	16.25000	4.787135	4	0	3	333	0	0
S-NB	50.00000	500.0000	79.73569	63.82997	227	0	85	28	0	0
S-NI	10.00000	700.0000	79.56522	122.0739	46	0	2	292	0	0
S-PB	20.00000	2000.000	90.20305	194.3250	197	0	92	51	0	0
S-SB	200.0000	7000.000	1015.385	1864.066	13	0	6	321	0	0
S-SC	7.000000	150.0000	36.54266	25.13911	293	0	11	36	0	0
S-SN	20.00000	2000.000	408.3530	553.5938	170	0	28	38	104	0
S-SR	200.0000	5000.000	869.2708	717.1377	192	0	26	122	0	0
S-V	20.00000	500.0000	65.71875	51.45636	320	0	18	2	0	0
S-W	100.0000	10000.00	834.4827	1720.774	87	0	43	210	0	0
S-Y	20.00000	1000.000	204.6567	166.6339	335	0	4	1	0	0
S-ZN	500.0000	20000.00	2663.513	4001.526	74	0	8	257	1	0
S-ZR	20.00000	2000.000	1049.839	679.6733	62	0	0	0	278	0
S-TH	200.0000	2000.000	572.7273	485.1919	22	0	16	302	0	0

Table IV-4. Stream-sediment samples, White Mts. NRA;
Univariate Statistics of Analytical Data

Column	Minimum	Maximum	Mean	Deviation	Valid	B	L	N	G	Other
S-FE%	.500000	10.00000	2.520173	1.261919	461	0	0	0	0	0
S-MG%	.070000	5.000000	.739414	.540392	461	0	0	0	0	0
S-CA%	.050000	20.00000	.404286	1.261381	427	0	34	0	0	0
S-TI%	.050000	1.000000	.424013	.154871	461	0	0	0	0	0
S-MN	70.00000	5000.000	525.9607	401.6748	458	0	0	0	3	0
S-AG	.500000	1.500000	.608333	.214310	36	0	70	355	0	0
S-AS	200.0000	200.0000	200.0000	***	1	0	0	460	0	0
S-B	10.00000	200.0000	84.20824	34.47861	461	0	0	0	0	0
S-BA	100.0000	5000.000	596.6377	498.5791	461	0	0	0	0	0
S-BE	1.000000	10.00000	1.524532	1.095010	428	0	33	0	0	0
S-BI	10.00000	10.00000	10.00000	***	1	0	0	460	0	0
S-CO	5.000000	100.0000	17.47150	8.772287	456	0	5	0	0	0
S-CR	10.00000	1500.000	70.38293	82.63225	457	0	4	0	0	0
S-CU	5.000000	70.00000	14.86889	8.291631	450	0	11	0	0	0
S-LA	20.00000	300.0000	36.49484	22.92741	388	0	46	27	0	0
S-MO	5.000000	10.00000	6.761905	2.047066	21	0	24	416	0	0
S-NB	20.00000	50.00000	23.47826	7.140598	23	0	75	363	0	0
S-NI	5.000000	200.0000	30.66013	18.73401	459	0	2	0	0	0
S-PB	10.00000	200.0000	22.70686	17.05342	423	0	35	3	0	0
S-SC	5.000000	20.00000	12.01089	3.569322	459	0	2	0	0	0
S-SN	10.00000	700.0000	47.93103	128.3586	29	0	19	413	0	0
S-SR	100.0000	1000.000	130.8429	70.41675	261	0	163	37	0	0
S-V	10.00000	200.0000	101.3883	34.34200	461	0	0	0	0	0
S-Y	10.00000	100.0000	24.07408	9.965166	459	0	2	0	0	0
S-ZN	200.0000	1000.000	264.7058	202.9199	17	0	42	402	0	0
S-ZR	20.00000	500.0000	156.3991	71.86374	461	0	0	0	0	0
AA-AS-P	10.00000	110.0000	17.43517	12.81452	347	0	0	114	0	0
AA-BI-P	1.000000	14.00000	2.888889	4.284986	9	0	0	452	0	0
AA-CD-P	.100000	8.200000	.464554	.643327	426	0	15	20	0	0
AA-SB-P	2.000000	40.00000	5.146789	6.667813	109	0	0	352	0	0
AA-ZN-P	5.000000	1000.000	68.12364	79.55586	461	0	0	0	0	0

Table IV-5. Coarse (-30+80 mesh) moss-trap sediment samples, White Mts. NRA; Univariate Statistics of Analytical Data

Column	Minimum	Maximum	Mean	Deviation	Valid	B	L	N	G	Other
S-FE%	.200000	7.000000	2.562088	1.180788	364	0	0	0	0	0
S-MG%	.050000	7.000000	.783159	.787094	364	0	0	0	0	0
S-CA%	.050000	20.00000	.358508	1.290163	315	0	49	0	0	0
S-TI%	.050000	1.000000	.319918	.145200	364	0	0	0	0	0
S-MN	50.00000	5000.000	573.3242	544.5049	364	0	0	0	0	0
S-AG	.500000	1.500000	.605714	.195453	35	0	53	276	0	0
S-B	10.00000	300.0000	91.99176	40.62125	364	0	0	0	0	0
S-BA	70.00000	3000.000	591.2397	480.6636	363	0	0	0	1	0
S-BE	1.000000	15.00000	1.589939	1.496782	328	0	36	0	0	0
S-CO	5.000000	100.0000	19.08530	13.13629	340	0	4	20	0	0
S-CR	10.00000	1000.000	80.62674	103.5364	359	0	4	1	0	0
S-CU	5.000000	70.00000	15.58028	9.653965	355	0	9	0	0	0
S-LA	20.00000	200.0000	34.19087	20.21419	241	0	58	65	0	0
S-MO	5.000000	10.00000	6.400000	2.010499	20	0	28	316	0	0
S-NB	20.00000	50.00000	23.50000	9.333020	20	0	49	295	0	0
S-NI	5.000000	200.0000	31.23204	22.22539	362	0	2	0	0	0
S-PB	10.00000	1000.000	27.83488	57.27457	321	0	35	8	0	0
S-SB	700.0000	700.0000	700.0000	***	1	0	0	363	0	0
S-SC	5.000000	30.00000	11.23955	3.977380	359	0	4	1	0	0
S-SN	10.00000	300.0000	43.33333	61.86763	33	0	13	318	0	0
S-SR	100.0000	1000.000	142.1488	115.4715	121	0	182	61	0	0
S-V	20.00000	300.0000	111.1813	47.17917	364	0	0	0	0	0
S-Y	10.00000	150.0000	22.11111	10.24703	360	0	3	1	0	0
S-ZN	200.0000	700.0000	270.0000	156.7021	10	0	24	330	0	0
S-ZR	20.00000	1000.000	137.3626	87.66119	364	0	0	0	0	0

Table IV-6. Fine (-80 mesh) moss-trap sediment samples, White Mts. NRA; Univariate Statistics of Analytical Data

Column	Minimum	Maximum	Mean	Deviation	Valid	B	L	N	G	Other
S-FE%	.700000	7.000000	2.507418	1.026468	364	0	0	0	0	0
S-MG%	.150000	7.000000	.892445	.720961	364	0	0	0	0	0
S-CA%	.050000	5.000000	.423599	.585381	364	0	0	0	0	0
S-TI%	.100000	1.000000	.491484	.151745	364	0	0	0	0	0
S-MN	50.00000	5000.000	535.5496	476.7739	364	0	0	0	0	0
S-AG	.500000	20.00000	1.217949	3.106857	39	0	70	255	0	0
S-B	20.00000	300.0000	105.9890	34.06944	364	0	0	0	0	0
S-BA	100.0000	5000.000	570.0549	433.1274	364	0	0	0	0	0
S-BE	1.000000	10.00000	1.427869	1.150534	305	0	57	2	0	0
S-BI	20.00000	20.00000	20.00000	***	1	0	4	359	0	0
S-CO	5.000000	100.0000	17.96962	10.04045	362	0	0	2	0	0
S-CR	10.00000	1000.000	96.62535	82.77376	363	0	1	0	0	0
S-CU	5.000000	100.0000	14.78187	10.33861	353	0	11	0	0	0
S-LA	20.00000	300.0000	45.17572	32.92451	313	0	26	25	0	0
S-MO	5.000000	10.00000	6.222222	1.715939	9	0	13	342	0	0
S-NB	20.00000	50.00000	25.60001	11.21011	25	0	100	239	0	0
S-NI	5.000000	200.0000	31.36212	18.96313	359	0	3	2	0	0
S-PB	10.00000	150.0000	23.87573	16.13857	338	0	26	0	0	0
S-SC	5.000000	30.00000	13.02747	3.884604	364	0	0	0	0	0
S-SN	10.00000	200.0000	41.15384	46.22354	26	0	15	323	0	0
S-SR	100.0000	700.0000	134.8077	63.89816	260	0	99	5	0	0
S-V	20.00000	300.0000	108.8462	36.23900	364	0	0	0	0	0
S-Y	10.00000	200.0000	32.44505	24.18785	364	0	0	0	0	0
S-ZN	200.0000	500.0000	233.3333	88.76254	12	0	17	335	0	0
S-ZR	50.00000	1000.000	310.9365	185.8345	363	0	0	0	1	0
AA-AS-P	10.00000	120.0000	17.11806	10.64276	288	3	48	25	0	0
AA-BI-P	1.000000	3.000000	2.333333	1.154700	3	3	0	358	0	0
AA-CD-P	.100000	19.00000	.544898	1.178000	343	3	17	1	0	0
AA-SB-P	2.000000	30.00000	6.465117	6.815070	43	3	3	315	0	0
AA-ZN-P	5.000000	1200.000	73.13889	91.83374	360	3	0	1	0	0

Of the 31 elements analyzed by semiquantitative emission spectrography, 19 elements commonly associated with a wide variety of mineral deposit types were selected for graphical illustration. The elements that were selected and their respective anomaly threshold values for each sample medium are given in table IV-7. In addition to the precious metals, Ag and Au, the elements represented are B, Be, Bi, As, Ba, Cd, Cu, Fe, Mo, Pb, Sb, Sn, W, and Zn. La, Nb, and Th are also included as potential indicators of areas underlain by alkalic or granitic rocks with a potential for Th or rare-earth elements (REE). The thresholds used to define anomalous concentrations of the selected target and pathfinder elements were subjectively determined by visual inspection of histograms and by inflection points in the cumulative frequency plots. Because the significance of distributions of elements varies among the different sample media, not all 19 elements were included in the illustrations of the distributions of each sample type. For example, Fe is used only from the heavy-mineral-concentrate data because most of the iron contributed by the common mafic rock-forming minerals has been eliminated in the sample preparation process, and any Fe remaining is normally in ore-related or pathfinder minerals. Conversely, Ba and Sn were so ubiquitous in heavy-mineral-concentrate samples that they were not included in the plots for that sample medium. In the stream-sediment data, chemically determined Au and spectrographically determined As, Au, Bi, Cd, Sb, Th, and W were either not detected or had too few unqualified values to contribute to the geochemical interpretation.

Histogram plots showing the frequency distributions of analytical values for the selected target and pathfinder elements are given in Appendix IV-A for the rocks, Appendix IV-B for heavy-mineral concentrates, and Appendix IV-C for stream-sediment samples. The distributions of metals in the moss-trap sediments are consistent with the distributions determined for stream-sediment samples. Separate plots of the distributions of elements in moss-trap sediments have not been included in this report. The data for moss-trap sediments have been incorporated in the composite geochemical contour plots to be discussed later in the report.

Geochemically Anomalous Areas

The occurrence and distribution of metals in geochemical samples from the WMNRA were used to identify areas of anomalous metal concentration. Metals were grouped into associations or suites of elements thought to represent potentially mineralized areas. These suites of elements were plotted together in the accompanying illustrations (pl. IV-A through IV-K). Table IV-8 lists the individual plates, the elements plotted on each plate, and the representative sample medium.

Table IV-7. Threshold values and elements selected from geochemical data.

[Fe in percent, all other values in parts per million; NA = not analyzed; -- = threshold not determined; aa = atomic absorption analyses, all others by semiquantitative emission spectrography]

Element	Threshold		
	Rocks	Concentrates	Sediments
Ag	0.5	1.0	.5
As	200	500	---
As-aa	10	NA	50
Au	10	20	---
Au-aa	0.1	NA	---
B	300	500	200
Ba	1500	---	1500
Be	5	3	3
Bi	10	150	---
Bi-aa	10	NA	1
Cd	20	150	---
Cd-aa	1	NA	1.5
Cu	100	50	50
Fe	---	2	---
La	100	---	70
Mo	5	10	5
Nb	30	150	20
Pb	50	100	70
Sb	100	200	---
Sb-aa	5	NA	5
Sn	15	---	10
Th	200	200	---
W	200	150	---
Zn	200	500	200
Zn-aa	200	NA	200

Plates IV-A through IV-D illustrate the distribution of anomalously high concentrations of selected elements in heavy-mineral-concentrate samples from the WMNRA. Similar distributions for elements are shown on plates IV-E through IV-G for stream-sediment samples, and on plates IV-H through IV-K for rock samples. Plates IV-A and IV-H show the distribution of Ag, As, and Au in heavy-mineral-concentrate and rock samples. This assemblage illustrates areas favorable for placer Au occurrences or for precious metals associated with hydrothermal mineralization in vein or near granitic plutons. Plates IV-B, IV-E, and IV-I represent a predominantly chalcophile assemblage of Ba, Cd, Pb, and Zn (plus Ag on pl. IV-E) commonly associated with sedimentary massive sulfides or, where combined with other metals, in hydrothermal veins and porphyry systems. Ba is not shown on plate IV-B because over 50 percent of the heavy-mineral-concentrate samples had Ba concentrations above the upper level of determination.

The distributions of Cu and the higher ($\geq$ + 3) valence metals Fe, Mo, Sb, Sn, and W are shown on plates IV-C, IV-F, and IV-J for the heavy-mineral concentrates, stream sediments, and rocks, respectively. Cu was included with the assemblage because the few Cu values observed in the WMNRA appear to be more closely related with these elements than with the Pb-Zn base metal assemblage. Tungsten values for the stream sediment and rock data sets were all below the lower limit of determination so W distributions are shown only on plate IV-C. Iron is also only shown on plate IV-C because of the dilution of Fe by the common rock-forming minerals in the other sample media. Because there are insufficient data to plot an Ag, As, and Au assemblage for stream sediments, As in stream sediments is included on plate IV-F. Tin is not plotted on plate IV-C because 65 percent of the samples contained Sn concentrations above the upper limit of determination.

Plates IV-D, IV-G, and IV-K illustrate the B, Be, Bi, La, Nb, and Th assemblage. Thorium was not detected in any of the stream-sediment samples, and, therefore, is not shown on plate IV-G. Because the heavy-mineral-concentrate samples intentionally eliminate the lighter rock forming minerals, La is not shown on plate IV-D.

In order to present the anomalous high concentrations of pathfinder elements for all sample media, contour plots were generated using standardized data. The data were standardized by subtracting the mean from each value in each data set and dividing by the standard deviation. This gives a value that represents the number of standard deviations above or below the mean for each element concentration, and allows the direct comparison of data from the various sample media. In preparation for the calculation, in instances where the analytical values were qualified by N (not detected), L (detected but less than the lower limit of determination), or G (greater than the upper limit of determination), replacement values were substituted in the following manner: L's were replaced by 1 spectrographic interval value less than the lower determination limit; N's were replaced by 3 spectrographic interval values less than the lower limit of determination; and G's were replaced by 1 spectrographic interval value higher than the upper determination limit. The calculations were then performed on the "replaced" data. The data were subsequently combined to form a single composite set of standardized values.

Table IV-8. List of Geochemical plates showing the elements plotted, and the sample media.

[Plates IV-A through IV-O, scale = 1:100,000; plates IV-P and IV-Q, scale = 1:63,360]

Plate	Elements Plotted	Sample Media
IV-A	Ag, As, Au	Heavy Mineral Concentrates
IV-B	Cd, Pb, Zn	-Do.-
IV-C	Cu, Fe, Mo, Sb, W	-Do.-
IV-D	B, Be, Bi, Nb, Th	-Do.-
IV-E	Ag, Ba, Cd, Pb, Zn	Stream Sediments
IV-F	As, Cu, Mo, Sb, Sn	-Do.-
IV-G	B, Be, Bi, La, Nb	-Do.-
IV-H	Ag, As, Au	Rocks
IV-I	Ba, Cd, Pb, Zn	-Do.-
IV-J	Cu, Mo, Sb, Sn	-Do.-
IV-K	B, Be, Bi, La, Nb, Th	-Do.-
IV-L	Ag, As, Au	Standardized Composite
IV-M	Ba, Cd, Cu, Pb, Zn	-Do.-
IV-N	As, Cu, Fe, Mo, Sb, Sn, W	-Do.-
IV-O	B, Be, Bi,La, Nb, Th	-Do.-
IV-P	Sample Sites	All Media
IV-Q	Drainage Basin Geochemistry	-Do.-
IV-R	Mineralogy	Heavy Mineral Concentrates

In cases where more than one sample was collected at a location, the maximum standardized value for each element was selected to represent the concentration at the site. There were 937 discrete sample locations from all combined sample media.

In order to depict the distributions of assemblages of elements that might be indicative of various types of mineralization, the combined standardized data were grouped by adding the standardized values of the constituent elements included in each assemblage and dividing the result by the number of elements in the suite. Thus, for the assemblage consisting of Ag, As, and Au (pl. IV-L), the value at a site would be calculated as the sum of the standardized values for these 3 elements divided by 3. Similarly, for the suite composed of Ba, Cd, Cu, Pb, and Zn (pl. IV-M), the value at a location would be calculated as the sum of the standardized values of these 5 elements divided by 5.

Contour plots of the combined data were generated using the STATPAC program GENPLOT. The study area was divided into a 48 by 50 cell grid (approximately 1 sq mi per grid cell) and the data were interpolated using an algorithm employed in GENPLOT to project theoretical values into grid cells where no actual data exists. The contour plots (pl. IV-L through IV-O) were then derived from the resultant gridded data. Table IV-8 lists the elements represented in each of the contour plots.

The distribution of sample sites for all sample media are illustrated on plate IV-P. A composite of the geochemically anomalous areas was compiled on a drainage basin map at the 1:63,360 scale (pl. IV-Q). The distribution of ore-related minerals observed in the heavy-mineral-concentrate samples is shown on plate IV-R.

Areas containing anomalously high metal concentrations in geochemical samples (fig. IV-1) are as follows: 1) Nome Creek; 2) Cache Mountain; 3) Roy Creek ; 4) Victoria Mountain-Glacier Creek; 5) Windy Creek; 6) Warren Creek-Moose Creek; and 7) Willow Creek. Each of these areas is discussed below.

NOME CREEK

The Nome Creek area comprises the southeastern portion of the WMNRA . For the most part, this area lies east of Trail Creek and south of Beaver Creek, and includes the Nome Creek placer deposits. Greenschist facies metamorphic rocks of the Precambrian Fairbanks schist unit described by Robinson and others (1982) and the Wickersham unit described by Weber and others (1985) underlie the Nome Creek area. Anomalously high concentrations of Ag, As, Au, Be, Pb, Sb, and Sn were observed in samples from the Nome Creek area (pl. IV-A, IV-B, and IV-G through IV-L). In addition, Cu, Fe, and W are anomalously high in the eastern part of the area (pl. IV-C). Heavy-mineral-concentrate samples collected from the eastern portion of the Nome Creek area contained gold, cassiterite, scheelite, pyrite, and arsenopyrite (pl. IV-R). To the east of the Nome Creek area, Tripp and others (1986) have reported abundant cassiterite and scheelite and anomalously high values for Sn, W, Pb, Bi, Ag, Be, Mo, Th, U, and La in stream-sediment samples from the Mount Prindle

area. Cinnabar was also found in several samples from Trail and Ophir Creeks. The abundance of scheelite and cassiterite in the area gradually decreases from east to west.

CACHE MOUNTAIN

The Cache Mountain pluton is a Tertiary granitic intrusion dated at about 58 Ma (Holm, 1975). The mineralogical and geochemical association of lithophile elements in samples from this pluton plus the common occurrence of fluorite and tourmaline suggest that these rocks were formed from a highly evolved siliceous magma. The presence of miarolitic cavities is indicative of a fairly shallow intrusion. Our data indicate anomalously high concentrations of Sn, Sb, Pb, Zn, Cd, Ag, B, Bi, and Be in and around the Cache Mountain pluton (pl. IV-A through IV-K and IV-M through IV-O). Heavy-mineral-concentrate samples from drainages underlain by the Cache Mountain pluton contain abundant cassiterite and scheelite. Areas adjacent to the pluton contain sphalerite, pyrite, and barite. Chapman and Weber (1972) reported anomalously high concentrations of Cu, Mo, Ni, and Pb in rock samples from the area. With the exception of Ni, the association of light and transition metals suggests the presence of Sn-bearing greisen or vein mineralization.

ROY CREEK

The Roy Creek pluton has been interpreted elsewhere in this report as a strongly alkaline syenite with Th and REE concentrated in fractures. Anomalously high concentrations of As, B, Be, La, Th, and Y were observed in samples from the Roy Creek area (pl. IV-D, IV-F through IV-L, IV-N, and IV-O). Samples of a mineralized fracture zone from a drill core at the Roy Creek prospect contained more than 2000 parts per million (ppm) Th, the upper limit of determination by emission spectrography (table V-1). A concentrate sample from sediment in Roy Creek contained thorite, allanite, cassiterite, scheelite, and sapphire corundum. The corundum, which occurs as pale blue platy crystals, is more than likely derived from the pluton rather than from the mineralized fracture zones.

VICTORIA MOUNTAIN-GLACIER CREEK

The Victoria Mountain pluton is a 65 Ma quartz syenite/quartz monzonite intrusion (Wilson and Shew, 1981) between Beaver Creek and Victoria Creek in the northern part of the WMNRA. Anomalously high values of Ag, As, Au, B, Bi, Co, Cu, Fe, La, Mo, Ni, Pb, Sb, Sn, Th, W, or Zn occur in scattered localities around the periphery of the pluton (pl. IV-A through IV-O). Tripp and others (1986) reported chalcopyrite and arsenopyrite occurrences along with scattered Be anomalies in the area. The association of these elements and the abundance of scheelite and cassiterite in streams draining Victoria Mountain suggests the possibility of skarn mineralization, probably in the Amy Creek dolomite, along the borders of the Victoria Mountain pluton.

Several samples from the area east of Mount Schwatka, north of Victoria Creek, and west of Glacier Creek, exhibited anomalously high base metal concentrations. This area is underlain mainly by quartzites and greenstones

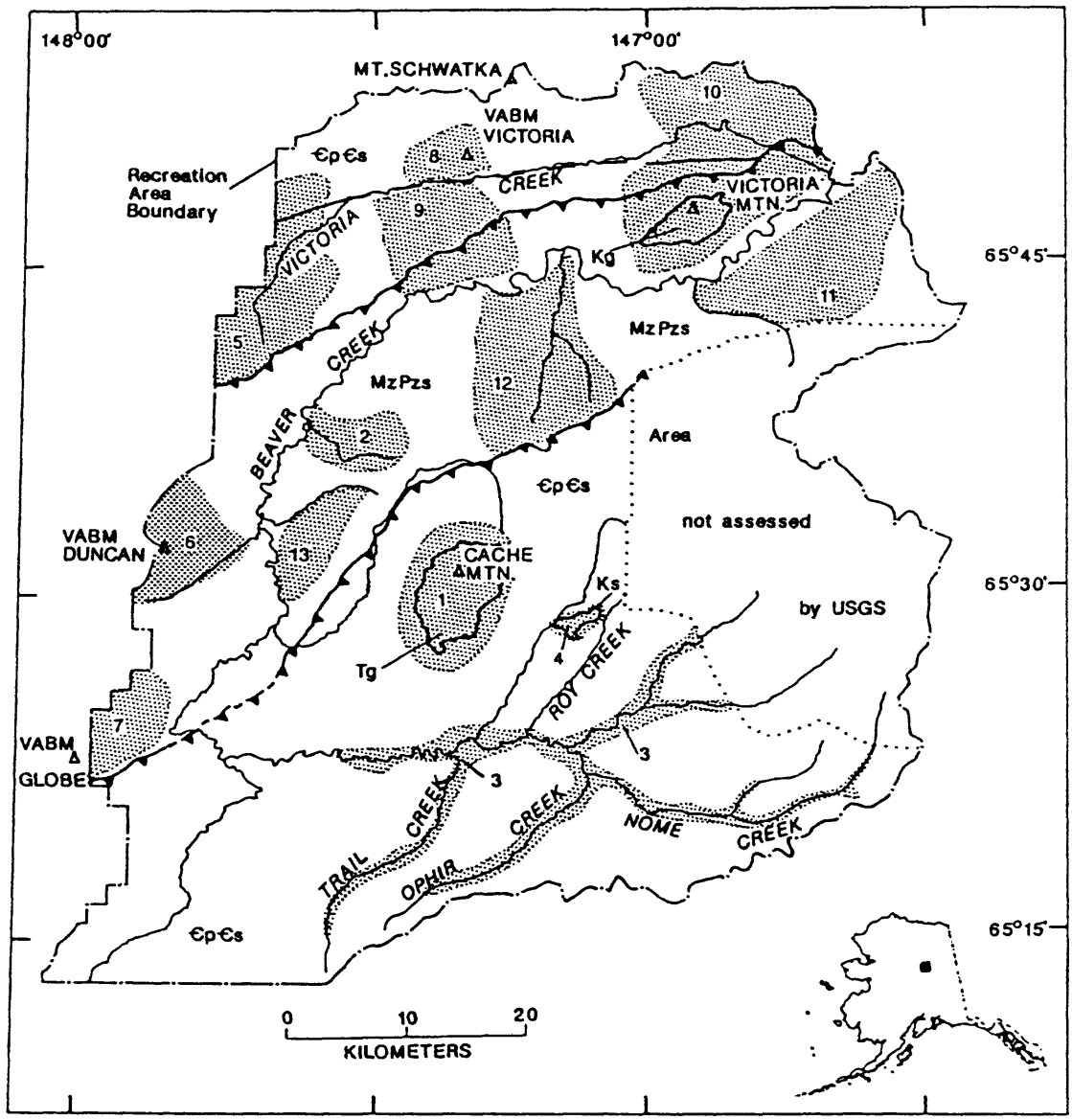

Figure IV-1. Geochemically anomalous areas in the WMNRA. [1, Cache Mtn.; 2, Lost Horizon Cr.; 3, Nome Cr.; 4, Roy Cr.; 5, Upper Victoria Cr.; 6, VABM Duncan; 7, VABM GloBe; 8, VABM Victoria; 9, Victoria Cr.-Beaver Cr. Ridge; 10, Victoria Mtn.-Glacier Cr.; 11, Warren Cr.-Moose Cr.; 12, Willow Cr.; 13, Windy Cr.]

of the Cambrian to Precambrian Wickersham grit. The occurrence of anomalously high metal concentrations in this area suggests the presence of a buried granitoid body. The geophysical data however do not support such an interpretation. It is possible that the mineralization is related to the primary dispersion of hydrothermal fluids outward from the Victoria Mountain pluton. More likely, the source of the metals is from either the greenstones or from fluids migrating along small faults related to the Tintina fault system.

WARREN CREEK-MOOSE CREEK

The Warren Creek-Moose Creek area lies along the south side of Beaver Creek in the northern part of the WMNRA and includes the Warren, Yellow, and Moose Creek drainages. Rock units underlying this area comprise the Wickersham grit, the Fossil Creek Volcanics, the Globe quartzite, and the Vrain sedimentary rocks. Anomalously high values of Ag, As, B, Ba, Bi, Cd, Cu, Fe, La, Mo, Pb, Sb, Th, and Zn were found in samples from the Warren Creek-Moose Creek area (pl. IV-A through IV-J, IV-L, and IV-N). The collective suite of minerals found in heavy-mineral concentrates from this area contains sphalerite, stibnite, arsenopyrite, pyrite, barite, and scheelite. Allanite, cyrtolite, fluorite, galena, monazite, sphalerite, tourmaline, and uranothorite were also observed in several samples from this area. This broad assemblage of elements and minerals suggests the possibility of more than one type of mineral occurrence. In particular, the concentrations of base and precious metals together with pyrite, barite, and sphalerite from the Vrain sedimentary rocks, suggest the possibility of sedimentary exhalative type deposits in reduced shales and siltstones. Anomalously high concentrations of base metals in sediments from streams draining areas of Globe quartzite, Wickersham grit, and Fossil Creek Volcanics suggest the possibility of polymetallic vein type deposits.

WINDY CREEK

Several samples from tributaries on the east side of Beaver Creek, between Windy Creek and Montana Creek, contain anomalously high concentrations of Ag, As, Cd, Cu, Fe, Mo, Nb, Sb, Pb, Th, W, and Zn (pl. IV-B, IV-D through IV-F, IV-H, through IV-J and IV-L through IV-N). The streams in this area drain Wilber Creek flysch, Globe quartzite, and Fossil Creek volcanic and sedimentary rocks. Although the source of these anomalies is unknown, they could be derived from indigenous metals in the Wilber Creek flysch or from polymetallic veins. Hydrothermal mineralization in this area, if any, may have been channeled along the two large east-west trending thrust faults. The relatively limited extent of alteration observed around the Cache Mountain pluton and the relatively low concentrations of Sn and B in the Windy Creek area suggest that the Windy Creek anomalies are not related to the mineralization associated with the Cache Mountain pluton.

WILLOW CREEK

Samples from Willow Creek and two small drainages to the west contained anomalous concentrations of Ag, As, B, Ba, Cd, Cu, Nb, Pb, Sb, and Zn (pl. IV-

A through IV-E, IV-G through IV-K, IV-M and IV-O). The Willow Creek area is underlain by the Wickersham grit, Fossil Creek volcanic and sedimentary rocks, Globe quartzite, Vrain sedimentary rocks, and Wilber Creek flysch. One hypothesis is that metal-bearing sediments, derived from the Cache Mountain area, were carried into the Willow Creek area by glaciation on the northeast side of Cache Mountain. However, this area is similar to the Windy Creek area in that the low concentrations of Sn suggest that the metals were not derived from or related to the Cache Mountain pluton. It seems more likely that the metals were locally derived from the sedimentary units, and possibly mobilized and concentrated along faults.

MISCELLANEOUS GEOCHEMICAL ANOMALIES

Several small or isolated geochemical anomalies in the WMNRA are not extensive or consistent enough to define a geochemically anomalous area, but do warrant a brief discussion.

Several samples south of VABM Victoria on the north side of Victoria Creek exhibit anomalously high concentrations of Ag, Ba, Be, Cd, La, Nb, Pb, or Zn (pl. IV-A, IV-B, IV-O, IV-E, IV-I, and IV-K). This area is underlain by the Wickersham grit. The source of metals in this area is not known, but may be related to the movement of hydrothermal fluids along the Victoria Creek fault.

Near the headwaters of Victoria Creek are scattered high values of La, Nb, Pb, W, and Zn (pl. IV-B through IV-O, IV-G, IV-K, IV-M, and IV-O). This area is underlain by Wickersham grit and maroon and green shale. Some Paleozoic to Precambrian mafic rocks probably occur beneath the Quaternary cover, and are a likely source for some of the metals.

Lost Horizon Creek drains areas of Wilber Creek flysch, Globe quartzite, Fossil Creek Volcanics, and Tolovana Limestone. Samples from Lost Horizon Creek contain high concentrations of Ag, Ba, Cd, Cu, Pb, and Zn (pl. IV-A through IV-C, IV-I, IV-J, and IV-M), which may have been derived from from mafic rocks in the Globe quartzite or Fossil Creek Volcanics. However the occurrence of cinnabar together with pyrite, barite, and sphalerite in heavy-mineral concentrates from the Lost Horizon Creek (pl. IV-R) area suggests relatively low temperature and pressure hydrothermal activity, possibly channeled along low angle thrust faults. This hypothesis is supported by additional occurrences of cinnabar along the western side of the White Mountains. Such hydrothermal activity may have remobilized and reconcentrated metals from the Paleozoic to Precambrian mafic rocks as well as introduced additional metals.

East of VABM Duncan anomalously high concentrations of Ag, Cd, Cu, Pb, Sb, and Zn were observed in samples containing barite, cassiterite, chalcopyrite, pyrite, sphalerite, and stibnite (pl. IV-A through IV-C, IV-E, IV-L through IV-N, and IV-R). The source of the metals is probably either the Wilber Creek flysch, which comprises the drainage basins for these samples, or small polymetallic veins intruding the flysch.

Samples from drainages along the flanks of the ridge between Victoria and Beaver Creek (T. 10-11 N., R. 1-2 E.) contain anomalously high concentrations of Ag, As, Ba, Cd, Pb, and Zn (pl. IV-A, IV-B, IV-E, IV-H, IV-I, IV-L, IV-M, and IV-O). This area is underlain by the Wilber Creek flysch, Paleozoic to Precambrian mafic rocks, and the Amy Creek dolomite and chert. This element assemblage is similar to that in the Lost Horizon Creek and VABM Duncan areas. It is probable that hydrothermal remobilization of locally derived metals and subsequent concentration of these metals along faults occurred in all three areas.

Along the ridge northeast of VABM Globe anomalously high concentrations of Ba, Cu, Mo, and W were found in the Globe quartzite (pl. IV-C, IV-I, and IV-J). The source of these metals is not known.

REFERENCES CITED

Armbrustmacher, T.J., 1984, Rare-earth/Thorium deposits associated with a complex of syenitic rocks near Mt. Prindle, East-Central Alaska: Geological Society America Abstracts with Programs, v. 16, no. 5, p. 266-267.

Bailey, E.A., Lee, G.K., and Light, T.D., 1987, Semiquantitative emission spectrographic analyses of stream-sediment samples collected in the Livengood and western 1/3 of the Circle 1° X 3° quadrangles, Alaska: U.S. Geological Survey Open-File Report 87-264,74 p.

Burton, P.J., 1981, Radioactive mineral occurrences, Mt. Prindle area, Yukon-Tanana Uplands, Alaska: MSc thesis, University of Alaska, Fairbanks, Alaska, 72 p.

Cady, J.W., and Weber, F.R., 1983, Aeromagnetic map and interpretation of magnetic and gravity data, Circle quadrangle, Alaska: U.S. Geological Survey Open-File Report 83-170-C, 29 p., 2 sheets, scale 1:250,000.

Chapman, R.M., and Weber, F.R., 1972, Geochemical analyses of bedrock and stream sediment samples from the Livengood quadrangle, Alaska: U.S. Geological Survey Open-File Report 72-67, 2 sheets, scale 1:250,000.

Grimes, D.J., and Marranzino. A.P., 1968, Direct-current arc and alternating-current spark emission spectrographic field methods for the semiquantitative analysis of geologic materials: U.S. Geological Survey Circular 591, 6 p.

Holm, Bjarne, 1975, Bedrock geology and mineralization of the Mount Prindle area, Yukon-Tanana Upland, Alaska: MSc thesis, University of Alaska, Fairbanks, Alaska, 55 p.

Menzie, W.D., Reed, B.L., and Keith, T.E.C., 1986, Lime Peak--An evolved granite with tin-enriched alteration, in Bartsch-Winkler, Susan, and Reed, K.M., eds., Geologic studies in Alaska by the U.S. Geological Survey during 1985: U.S. Geological Survey Circular 978, p. 25-27.

Mootoka, J.M., and Grimes, D.J., 1976, Analytical precision of one-sixth order semiquantitative spectrographic analyses: U.S. Geological Survey Circular 738, 25 p.

O'Leary, R.M., and Viets, J.G., 1986, Determination of antimony, arsenic, bismuth, cadmium, copper, lead, molybdenum, silver, and zinc in geologic materials by atomic absorption spectrometry using a hydrochloric acid-hydrogen peroxide digestion: Atomic Sectroscopy, v. 7, no. 1, p. 4-8.

Robinson, M.S., Smith, T.E., and Bundtzen, T.K., 1982, Cleary sequence of the Fairbanks mining district--Primary stratigraphic control of lode gold/antimony mineralization (abs): Geological Society of America Abstracts with Programs v. 14, no. 4, p. 228.

Smith, T.E., Robinson, M.S., Bundtzen, T.K., and Metz, P.A., 1981, Fairbanks mining district in 1981: New look at an old mineral province: The Alaska Miner, the Journal of the Alaska Miners Association, v. 9, no. 11, p. 8, 28.

Sutley, S.J., Ryder, J.T., Light, T.D., and Weber, F.R., 1987a, Analytical results and sample locality map of rock samples from the White Mountains National Recreation Area, Livengood and Circle quadrangles, east-central Alaska: U.S. Geological Survey Open-File Report 87-284, 61 p.

Sutley, S.J., O'Leary, R.M., Lee, G.K., and Light, T.D., 1987b, Analytical results and sample locality map of stream-sediment, moss-trap sediment, and heavy-mineral-concentrate samples from the White Mountains National Recreation Area, Livengood and Circle quadrangles, east-central Alaska: U.S. Geological Survey Open-File Report 87-285, 110 p.

Tripp, R.B., Crim, W.D., Hoffman, J.D., O'Leary, R.M., and Risoli, D.A., 1986, Mineralogical and geochemical maps showing the distribution of selected minerals and elements found in the minus-80-mesh stream-sediment and related minus-30-mesh heavy-mineral-concentrate samples from the Circle quadrangle, Alaska: U.S. Geological Survey Open-File Report 86-170-F,G,H, 7 p., 6 plates, scale 1:250,000.

VanTrump, G., Jr., and Miesch, A.T., 1977, The U.S. Geological Survey RASS-STATPAC system for management and reduction of geochemical data: Computers and Geosciences, v. 3, p. 475-488.

Weber, F.R., Smith, T.E., Hall, M.H., and Forbes, R.B., 1985, Geologic guide to the Fairbanks-Livengood area, east-central Alaska: Anchorage, Alaska Geological Society Guidebook, 44 p.

Wilson, F.H., and Shew, N., 1981, Map and tables showing preliminary results of potassium-argon age studies in the Circle quadrangle, Alaska, with a compilation of previous dating work: U.S. Geological Survey, Open-File Report 81-889, 1 sheet, scale 1:250,000.

Wilson, F.H., Smith, J.G., and Shew, N., 1985, Review of radiometric data from the Yukon crystalline terrane, Alaska and Yukon Territory: Canadian Journal of Earth Sciences, v. 22, no. 4, p. 525-537.

MINERAL RESOURCE ASSESSMENT

by R.B. McCammon, T.D. Light, and C.D. Rinehart

Introduction

The potential mineral resources for part of the WMNRA have been assessed using the concept of geologic deposit models. For purposes of this report, a deposit model is defined as the set of attributes common to a particular class of mineral deposit. Most of the deposit models referred to in this report can be found in U.S. Geological Survey Bulletin 1693 (Cox and Singer, 1986). The deposit models were used to identify areas within the WMNRA that exhibited features common to a particular model. The identification of each area was based on detailed geologic mapping, interpretation of the geophysical and geochemical data, and examination of the known mineral occurrences. Table V-1 is a list of mineralized rock, stream sediment and pan concentrate samples from the WNMRA. For each identified area, subjective estimates of the number of undiscovered deposits were made and these were combined with grade-tonnage data for the respective model to produce estimates of the contained metal content. The assessment methodology used in this report is described by Drew and others (1986) and is embodied in a computer program known informally as MARK3. We have used MARK3 to estimate the contained metal content in undiscovered deposits for the major types of deposits described below.

Potential Mineral Resources

POTENTIAL FOR TIN (SN) GREISEN DEPOSITS

Tin greisen deposits have been described by Reed (1986) as being comprised of veinlets, stockworks, lenses, pipes and breccias in granitoid rocks which are siliceous (>70 percent SiO2) leucogranites. Tin occurs in the mineral cassiterite which is associated with a unique alteration (greisen) assemblage, quartz-muscovite-topaz-fluorite-tourmaline, that modifies the host granitoid and, in many instances, its adjacent wall rock. Fluids rich in these minerals represent the youngest fractionated fluid phases of an almost completely consolidated granitoid body. Tin greisens occur in the uppermost cupolas and apical parts of the intrusion. Mineralization is typically fracture-controlled. Tin greisen deposits vary greatly in size, ranging from a few million tons to over 100 million tons. The average grade is on the order of 0.3 percent tin, but in some deposits, the grade is as high as 1.4 percent tin.

Table V-1. List of significant mineralized rock, stream sediment, and pan concentrate samples in the WMNRA

No.	Sample	Lat-Long	Desc	Comments
1	CA09	65-38-32 147-46-34	srptzd dunite	>5000 Cr 1000 Ni
2	5	65-37-48 147-48-05	chromitite	Foster (1969)
3	3	65-42-51 147-28-23	amp asbestos	Barker (1978)
4	LA007C	65-33-12 147-38-45	pan conc	gal,sph,pyr,stb, cin,bar
5	LA480C	65-31-39 147-38-50	pan conc	gal,sph,pyr,stb, cin,sch,bar
6	LA326R2	65-32-28 147-21-15	alt hrnfls	7000 Pb >2000 AA-Zn 100 Sn
7	MC06	65-29-09 147-04-31	alt vein	>2000 Th >1000 La >2000 Sc >2000 Y >2000 As
8	DO77B	65-40-22 147-12-10	blk slty arg	1100 AA-Zn 150 Pb
9	WR084B	65-48-04 147-04-41	dk gry cht	>2000 AA-Zn
10	LA466C	65-42-10 146-45-25	pan conc	sph,pyr,cas,sch,UTh, saph,fluor,bar

The area surrounding the Cache Mountain pluton (Tract I in pl. V) in the WMNRA is identified as being permissive for the occurrence of undiscovered tin greisen deposits. The Cache Mountain pluton exhibits the following attributes common among tin-bearing granites:

(1 silica-rich leucogranite (table II-1 and fig. II-2)
(2 peraluminous and relatively potassic composition (table II-1)
(3 presence of topaz, tourmaline, fluorite, and muscovite
(4 presence of miarolitic cavities

(5 presence of anomalous values of tin in the bedrock at 15 localities in the pluton (pl. IV-J)
(6 anomalous concentrations of W, Pb, Zn, Cd, Ag, B, Bi, and Be in and around the pluton (pl. IV-A through IV-R)
(7 abundant cassiterite recovered from pan concentrates from streams draining the exposed pluton (pl. IV-R).

The occurrence of tin at Cache Mountain was first noted by Chapman and Weber (1972). This was followed up by the U.S. Bureau of Mines (Dean Warner, 1984, written commun.) when brief reconnaissance mapping and sampling showed 1,050 ppm tin from weakly altered fine-grained granite in the southeast part of the pluton. A pan concentrate sample from Brigham Creek yielded 2,390 ppm tin. The earlier discovery of tin in the Rocky Mountain (Lime Peak) pluton, 12 miles to the northeast, had prompted the investigation at Cache Mountain. Warner's report stated that the Cache Mountain pluton is "identical to the Lime Peak pluton", even to being a "composite pluton" consisting of distinct phases that have correlative counterparts in the Lime Peak pluton. We indeed found rock types equivalent to the varieties described by Foster and others (1983) at Lime Peak. However, with the exceptions of an aplitic phase and a hypabyssal porphyritic phase, both of which were observed to cut coarser-grained varieties, gradational variation, commonly over a few feet among several textural types, was found to be the pattern most typical of relations among constituent rocks in the Cache Mountain pluton. Based on our current knowledge, without further detailed mapping, there is insufficient evidence to conclude that Cache Mountain represents a composite pluton.

Despite the evidence that establishes the Cache Mountain pluton as a tin-bearing granite, we lack the evidence for the presence of tin-greisen zones within the pluton and the certain knowledge that Cache Mountain represents more than one intrusive episode. In comparing Cache Mountain with other areas that host tin-greisen deposits, we estimate there is only a 10 percent probability that at least one undiscovered tin greisen deposit exists in tract I within the WMNRA. Using this probability and the tonnage-grade model for tin greisen deposits compiled by Menzie and Reed (1986) in the MARK3 program, we estimate there is an expected 200,000 tons of undiscovered ore-bearing rock containing 500 tons of tin. The 5th and 95th percentiles of the estimates are 0 and 520,000 tons for undiscovered ore-bearing rock, and 0 and 1,100 tons of tin, respectively.

POTENTIAL FOR URANIUM/THORIUM RARE-EARTH ELEMENT (U/TH REE) DEPOSITS

Vein deposits of this type have been described by Staatz and others (1979) as consisting of tabular bodies ranging from several feet to thousands of feet in length and from less than a foot to tens of feet in width. Although most of the veins are tabular, some are lenticular, and in others, vein material is interstitial to brecciated unmineralized country rock. In some areas where these deposits occur, only one small vein or breccia zone is known, whereas in other areas, more than 100 veins have been found. The veins are genetically related to alkalic intrusive complexes. Thorium, uranium, and rare-earth elements (REE) are the principal metals found in these veins. The dominant thorium mineral is thorite. Associated with the thorium minerals are a variety of rare-earth minerals. The relative amount of thorium oxide to total rare-earth oxides varies greatly from one district to another. Uranium minerals are also présent, but generally, they occur in lesser amounts. The size of vein deposits is small, on the order of a few tens of thousands of tons. Some districts however, contain over a hundred such veins, and contain tens of millions of tons of ore. Average ore grade in the known districts is highly variable, ranging from less than 0.1 percent to over 1.0 percent ThO_2, less than 0.1 percent to over 1.0 REO (rare-earth oxides), and, generally less than 0.1 percent U_3O_8.

Tract II in plate V is identified as being favorable for the occurrence of U/Th REE vein type deposits. This is due mainly to the occurrence within the tract of the Roy Creek prospect, an alkalic syenite-hosted U/Th REE deposit discovered as a result of the U.S. Bureau of Mines report of anomalous U concentration in the Mt. Prindle area (Barker and Clautice, 1977). In December 1978, MAPCO, Inc., announced the discovery of surface samples containing 5-7 percent eU_3O_8 from "the Mt. Prindle area". Those samples were presumably from the Roy Creek prospect (called "Y block" by MAPCO), 18 miles west of Mt. Prindle. The prospect is exposed on a ridge that separates the upper reaches of Roy and O'Brien Creeks where the host plutonic body is exposed discontinuously over an area of about 4 square miles (Map location 6 in pl. V).

Our knowledge about the prospect has come mainly from samples collected by us during the past two summers, from samples collected by others at an earlier date which were made available to us, and from previously published and unpublished work. The information from others consists of: (1) hand samples and thin-sections, with map locations and field notes, collected and prepared by W.D. Menzie of the USGS as the result of a brief visit in 1979; (2) results of mineralogic studies on some of Menzie's samples by M.H. Staatz of the USGS; (3) unpublished information obtained during a visit to the property in 1981 by T.J. Armbrustmacher of the USGS; (4) an abstract by Armbrustmacher (1984); and (5) a Master's thesis (1981) at the University of Alaska by P.J. Burton, who was formerly employed by MAPCO.

The host plutonic body, described elsewhere herein as the syenite of Roy Creek, has been explored extensively by surface scraping and trenching, excavation of exploration pits, and diamond drilling. Exploration and drilling was most active in 1979. Based upon our examination of core stacked

in boxes out-of-doors on private property along the Steese Highway near Belle Creek, we estimate that a total of 11,000 feet (3,700 M) of drilling occurred during MAPCO's evaluation of the prospect. The data obtained in that examination are only general in nature, owing to both the faded and otherwise illegible numbers on many boxes, and to the unavailability of a map of the property showing locations and identities of drill holes. Several hundred feet of additional, skeletonized core, originally selected and prepared by MAPCO and subsequently given to the U.S. Bureau of Mines for archiving, was made available to us for examination and sampling. MAPCO also conducted extensive geophysical and geochemical surveys as part of their exploration program, but results of these surveys were not available. When we visited the property in 1986, only a few drilling sites and mainly covered exploration pits and trenches could be found. The only significant radioactive anomaly we detected using a gamma-ray spectrometer, coincides with a largely covered pit identified by MAPCO as the "P" pit (pl. II), which was also probably the discovery site. A gamma-ray spectrometer examination box-by-box of the large quantity of showed no significant radioactive anomalies. This could mean either that most of the drilling had encountered no anomalous radioactive zones, or that any radioactive rock encountered had been removed. The skeletonized core, however, showed anomalous radioactivity in two places.

Our assessment of the potential for vein-type U/TH REE deposits in Tract II within the WMNRA is derived from the following two main considerations. First, the host rock is a complex, varied, and generally strongly alkaline syenite of a type similar to syenites associated with known U/Th REE deposits (Staatz, 1974, written commun., 1981). Its pattern of exposure, abundance of wall-rock inclusions and roof pendants, and the abrupt variations in its composition and texture expressed in the rubbly exposures indicate that the pluton is apically truncated. Because U/Th and REE are concentrated in late-stage fluids of a crystallizing alkaline magma, cupolas in the magma chamber, irregularities in its roof, and fractures in brittle wall and roof rock are favored loci for the deposition of minerals rich in these elements. The presence of miarolitic cavities in the syenite, and of vugs in the veins, indicate that both the magma and the veins were emplaced at shallow depth. Second, the U/Th REE metals occur mainly in veins (Burton, 1981; Menzie, written commun., 1979; Armbrustmacher, written commun., 1984).

Although we lack data on the dimensions and distribution of the veins, the analyses we have for 10 samples (tables II-3 and V-2) indicate that some veins contain high values of both thorium and cerium-group REE. Samples 1, 4, and 6 are grab samples from a bag (10-20 lbs) labeled "P" pit, found alongside the core stored along the Steese Highway. The rock in that bag was more highly radioactive--than any other rocks examined, except samples 2 and 3 whose levels of radioactivity were comparable. The latter, and sample 5, were obtained from W.D. Menzie, who obtained them from MAPCO. Unfortunately we have been unsuccessful in finding a map showing their coordinates. In addition to coordinates, sample 2 also bears the word "discovery" and therefore may also represent the vein explored in the "P" pit. Samples 5 and 6 are less radioactive than samples 1-4, and, expectably, are poorer in U/Th and REE. Sample 7 is a relatively unmineralized syenite. Samples 8, 9, and 10 are from drill core, the latter two of which represent the only radioactive

zones in the skeletonized core. The four highest-grade samples, 1 and 4, and probably 2, are from the vein explored by "P" pit, but 3, a very high-grade sample, and 5, poorer in grade but still within the high five, are from two different sites, and thus possibly represent different veins or different sites along the same vein. Samples 9 and 10, from radioactive zones in drill holes, are an order of magnitude lower in REE than samples 1-5, but both thorium and uranium values are significantly elevated. These samples could represent two veins, or one vein sampled at two different sites. U/Th REE minerals identified from the Roy Creek prospect are shown in table V-2.

No suitable analogs for the Roy Creek prospect can be found among reported U/Th REE deposits and occurrences in Alaska. In the compilation by Nokleberg and others (1987, in press), eight U/Th prospects are recorded but none are comparable in all three major requisites: (1) host rock, (2) manner of ore mineral occurrence and distribution, (3) elements present and their relative abundances. Perhaps best known, the Bokan Mountain U/Th deposit (MacKevett, 1963) is mainly a uranium deposit, hosted by a peralkaline granite, and containing very low levels of REE. Niobium is a conspicuous element in the ore there, but is absent at Roy Creek. The nearest Canadian deposits described are about 225 miles to the east in the Tombstone Mountains near Dawson, Yukon Territory. The host rock in these deposits is a weakly zoned granitoid body that grades outward from a core of granite through quartz monzonite and monzonite to syenite. The ore consists chiefly of primary and secondary uranium minerals accompanied by other metallic sulfides. No associated concentrations of thorium and REE are reported. Burton (1981) favors the possibility of an original genetic connection between the Tombstone batholith and the Roy Creek syenite, which have subsequently been separated by large-scale dislocation along the Tintina fault (Olade and Goodfellow, 1978; Anderson, 1987). Carbonatites are known to contain radioactive and rare-earth elements and are associated with strongly alkaline intrusive rocks, all of which are features of the Roy Creek prospect. The essential intimate association with abundant carbonates, however, is in striking contrast with rocks at Roy Creek, which commonly show minor late calcite in both vein material and host rocks.

The known occurrences of thorium and rare-earth metals that most closely resemble those of the Roy Creek deposit are the thorium vein deposits described by Staatz and others (1979). In his summary descriptions of seven districts in the United States, all of the features known in the Roy Creek deposit can be found, though no one district is directly comparable. The potential resources within Tract II then must be evaluated within the context of these districts. Grade-tonnage models were compiled for the seven thorium vein districts based on the data in Staatz and others (1979). Because of the lack of data on uranium, only thorium and rare-earth elements were included in the models. These data are shown in table V-4. It is estimated there is a 10 percent probability for an undiscovered thorium vein district in tract II. Using this probability and the grade-tonnage model for the seven thorium vein districts in the MARK3 program, there are an estimated 500,000 tons of undiscovered thorium-bearing ore that contains 7,000 tons of ThO_2 and 6,000 tons of Rare-Earth Oxides (REO). The latter figure is especially significant in light of the recent advances in superconducting materials which are

Table V-2. Rare earth, uranium, and thorium analyses, in weight percent, of selected samples from the Roy Creek prospect

[Chemical analyses by analytical laboratory of the U.S. Geological Survey, Lakewood, CO. Methods used were ICP and optical spectrography. Analyses reported in ppm, converted to weight percent oxide by us. Numbers in parentheses mainly field numbers, except that 8, 9, and 10 are MAPCO drill-hole numbers, including depth to sample; YM-1, YM-2, and YM-5 are numbers assigned by us to MAPCO coordinate identifiers which are, respectively, 15+ 80S, 00 80E, "discovery"; 13+ 60S, 2+ 00E; 65+ 00S, 01+ 50E]

	1 (86ARi-6Q)	2 (YM-1)	3 (YM-5)	4 (86ARi-6R)	5 (YM-2)	6 (86ARi-6RY-4)	7 (86ARi-6RY-4)	8 (Y-24-C(295))	9 (Y-24-C(70))	10 (Y-22-C(270))
La_2O_3	8.13	7.98	6.92	6.19	0.85	0.026	0.015	0.010	0.015	0.042
Ce_2O_3	15.11	15.22	12.88	10.88	1.64	0.025	0.027	0.023	0.019	0.085
Nd_2O_3	5.73	5.48	4.31	4.21	0.54	0.015	0.014	0.013	0.007	0.039
Sm_2O_3	0.95	nd	nd	0.72	nd	<0.023	nd	nd	nd	nd
Eu_2O_3	0.19	0.19	0.13	0.14	0.02	<0.004	0.001	0.001	0.0001	0.001
	30.11	28.87	24.24	22.14	3.05	0.066	0.057	0.047	0.0411	0.167
Ho_2O_3	0.08	0.08	0.05	0.06	0.01	<0.01	<0.01	<0.01	0.001	0.001
Yb_2O_3	0.10	0.09	0.06	0.07	0.01	<0.01	0.001	0.001	0.001	0.001
Y_2O_3	1.89	1.78	1.19	1.34	0.17	0.006	0.006	0.005	0.008	0.018
	2.07	1.95	1.30	1.47	0.19	0.008	0.007	0.006	0.010	0.020
Total REE	32.18	30.82	25.54	23.61	3.24	0.074	0.064	0.053	0.0511	0.187
Th	14.8	11.4	12.5	18.2	1.1	0.01	0.01	0.01	0.53	1.25
U	1.0	1.9	1.8	1.0	0.2	<0.2	<0.01	<0.01	0.07	0.4
Total $REE_{/Th}$	2.2	2.7	2.0	1.3	3.0	7.4	6.4	5.3	0.1	0.2
$Th_{/U}$	14.8	6.0	6.9	18.2	5.5	--	--	--	7.6	3.1

Table V-3. U-Th-REE minerals identified in the Roy Creek prospect

[Minerals identified by: M.H. Staatz, USGS; Mark Robinson, Mineral Industries Research Lab.; P.J. Burton (1981); and T.J. Armbrustmacher, USGS]

Allanite	(Ce,Ca,Y)2(Al,Fe+3)3(SiO4)3(OH)
Bastnaesite	(Ce,La)(CO3)F
Britholite	(Ce,Ca)5(SiO4,PO4)3(OH,F)
Monazite	(Ce,La,Nd,Th)PO4
Parisite	(Ce,La)2Ca(CO3)3F2
Synchysite	(Ce,La)Ca(CO)3)2F
Thorianite	ThO2
Thorite	ThSiO4
Uraninite	UO2
Xenotime	YPO4
Neodymian phosphate	NdPO4

composed mainly of rare earth oxides. The 5th and 95th percentiles of the estimates are 0 and 6,500,000 tons for undiscovered thorium-bearing ore, 0 and 25,000 tons for contained ThO_2, and 0 and 25,000 tons for contained REO.

POTENTIAL FOR TUNGSTEN SKARN DEPOSITS

Deposits of this type which have been extensively investigated and described by Einaudi and others (1981), and Einaudi and Burt (1982), are generated through contact metasomatism of calcareous rocks where these rocks are intruded by generally leucocratic granitoid rocks. The calcareous rock is typically converted to a complex granoblastic host assemblage of calc-silicate minerals that commonly includes garnet, diopside, and epidote. The principal ore mineral is scheelite. The median size of tungsten skarn deposits is small, on the order of a million tons of ore. The largest known deposits are on the order of 25 million tons. Average grade varies from less than 0.5 percent WO_3 to 1.5 percent WO_3.

The area surrounding the Victoria Mountain pluton (Tract III, in pl. V) in the WMNRA is identified as being permissive for the occurrence of undiscovered tungsten-bearing skarn deposits for the following reasons:

(1) The pluton is a leucocratic intrusive body that has developed a hornfels aureole in the surrounding mainly pelitic country rock;
(2) Thin carbonate lenses are sparsely and sporadically distributed through the pelitic rocks and locally are converted to sulfide-bearing skarn assemblages;
(3) Abundant scheelite and cassiterite are present in pan concentrate samples taken from streams that drain the pluton;
(4) A 10-man-day study of the Victoria Mountain area by the U.S. Bureau of Mines (J.C. Barker, 1983, written commun.), mainly a search for cobalt that was found during earlier regional stream sediment sampling, yielded analyses of sulfide-bearing skarn from upper Sand Creek that showed a maximum of 30 ppm W.

The principal negative factor in assessing the potential for the occurrence of tungsten-bearing skarn deposits is the absence of carbonate lenses in the host pelite. There might be carbonate, however, in the rock units underlying the pelite. In addition, the tungsten concentration is low as are the other metals, that is, Ag, Au, Co, Pd, Pt, and Zn.

In view of the lack of direct evidence of mineralization, we estimate there is only a 5 percent probability that Tract III contains at least one undiscovered tungsten skarn deposit. Using this probability and the grade-tonnage model for tungsten skarn deposits compiled by Menzie and Jones (1986) in the MARK3 program, we estimate there are an expected 290,000 tons of undiscovered tungsten-bearing ore containing 2,100 tons of WO_3. The 5th and 95th percentiles for both estimates is 0.

Table V-4. Tonnage and grade statistics for known thorium vein districts in the United States based on data from Staatz (1979)

District	Tons (x 10E6)	Average grade percent ThO2	Average grade percent total Re2O3
Lemhi Pass, Idaho-Montana	34.8	0.53	0.53
Wet Mountains, Colorado	48.8	0.46	0.21
Powderhorn, Colorado	6.24	0.17	0.40
Hall Mountain, Idaho	.77	4.0	0.04
Diamond Creek, Idaho	6.31	.21	1.22
Bear Lodge, Wyoming	.36	.09	.50
Mountain Pass, California (vein deposits only)	.44	.40	2.00

POTENTIAL FOR HIGH-CALCIUM LIMESTONE

High-calcium limestone is the principal source for lime which has possibly the greatest number of diverse uses of any chemical or mineral commodity (Boynton and others, 1983). Although lime to the average person still connotes a mortar, plaster, or agricultural material and although it still enjoys these formerly predominant uses, most lime today, over 90 percent, is utilized by the chemical and metallurgical industries. High-calcium limestone is generally defined as having a minimum of 93 percent carbonate content. The value of a limestone for most purposes is dependent upon its available lime content (CaO). The higher the lime content the greater its value. Only a small fraction of the known limestone deposits have greater than 99 percent carbonate content and it is for this reason that such limestones are the ones most actively sought in this country. In addition to purity of the limestone in the manufacturing of lime, impurities are a consideration. The major impurities are silica, iron, alumina, and sulfur. Depending on the end product, each of these impurities affects the manufacturing process differently. However their effect, the higher the purity of the limestone, the less chance there is of any impurity detracting from its value. Therefore, any high-calcium limestone deposit can be regarded as a potentially valuable resource.

The Tolovana Limestone comprises the core of the White Mountains. The generalized outline of the unit is shown as Tract IV in plate V. Within the WMNRA study area, it covers an area of approximately 36 square miles. The thickness of the Tolovana Limestone in the White Mountains is in excess of 4,000 ft (Church and Durfee, 1961). We collected 10 grab samples of the unit and submitted them for chemical analysis. The locations of the samples are shown in plate V. The results of the analyses are shown in table V-5. For these 10 samples, the purity of the limestone is consistently very high. The average is 98.56 percent calcium carbonate (55.19 percent CaO). This average composition can be compared with the reported analyses of 2,829 samples of high-calcium limestone (defined as greater than 90 percent carbonate) in Alaska, Idaho, Oregon, and Washington (Hill and others, 1972). Of these, 787 samples were from Alaska (Hill and others, 1972, Table 25). From an examination of the cumulative frequency curve in Figure 32 of their report showing the proportion of all analyses of high-calcium limestone that contain as much as, but not more than, the indicated percentage, it is inferred that as many as 99 percent of the samples contained less than the average calcium carbonate percentage for the 10 grab samples from the Tolovana Limestone.

In order to estimate the size or endowment of the Tolovana Limestone as a high-calcium limestone resource within the WMNRA study area, we used the method described by Finch and McCammon (1987). The input values in the endowment equation and the results of the calculations are given in table V-6.

Based on these results, we estimate the endowment of high-calcium limestone to be 27 billion tons. The 5th and 95th percentiles of this estimate are 8.4 billion tons and 45 billions tons, respectively. Considering that the annual lime production in the United States is around 16 thousand tons, it can be concluded that the Tolovana Limestone represents an enormous potential resource for high-calcium limestone.

It must be recognized that this estimate of endowment is preliminary and that a comprehensive sampling program would be needed to determine more accurately the extent and thickness of the high-calcium layers within the Tolovana Limestone. The number of samples and the coring that would be required in such a sampling program are far beyond the scope of this report.

POTENTIAL FOR POLYMETALLIC VEIN DEPOSITS

Polymetallic vein deposits have been described by Sangster (1984) and by Cox (1986) as consisting of narrow, subvertical structures such as fractures, shears, or faults which are filled, either partially or completely, with sulfide minerals and associated silicates, carbonates, or sulfates. The veins are discordant where they occur in layered host rocks; veins in plutonic rocks appear to be later than all phases of intrusions. Whatever their occurrence, the veins are considered to be related to felsic and intermediate hypabyssal intrusions in sedimentary and metamorphic terranes, or to metamorphic fluids forming during waning regional metamorphism. The primary ore minerals are argentiferous galena, sphalerite, argentite, tetrahedrite, and pyrargyrite. The principal metals are Ag, Pb, and to a lesser extent, Zn. The size of such deposits is small, ranging from 10 tons to two million tons with a modal size of about 100,000 tons. Typical grades are: 10 to 30 oz/t Ag, 4 to 8 percent Pb, and 2 to 4 percent Zn (Sangster, 1984). Notable examples of polymetallic veins in east-central Alaska are the Quigley Ridge, Banjo, Spruce Creek, and Stampede deposits in the Kantishna district, and the Cleary Summit and Ester Dome deposits in the Fairbanks district (Nokleberg and others, in press). Polymetallic veins of the same type occur throughout the Yukon Territory in Canada, the most important being the deposits in the Keno Hill - Galena Hill District (K. Watson, 1987, written commun.).

Tracts VA and VB in the WMNRA study area are identified as areas favorable for the occurrence of undiscovered polymetallic vein deposits (pl. V). Tract VA is situated in the west-central part of the study area in a portion of the White Mountains that is underlain by the Fossil Creek Volcanics and the Globe quartzite. This tract is judged favorable for the following reasons:

(1) presence of galena, sphalerite, stibnite, pyrite, cinnabar, cassiterite, and abundant scheelite and barite in heavy-mineral pan-concentrate samples along Beaver Creek (table V-1);
(2) proximity of the Tertiary felsic intrusion at Cache Mountain;
(3) relatively similar geologic setting to that in the Keno-Hill - Galena Hill area in the Yukon Territory where a thick sequence of Paleozoic clastic sedimentary rocks is near a Tertiary felsic igneous intrusion.

What is lacking is the presence of faults or fractures and known occurrences of Ag-Pb-Zn veins. Tract VB is situated in the northeast part of the study area in a portion of the White Mountains that is also underlain by the Fossil Creek Volcanics and the Globe quartzite. This tract is judged favorable for the following reasons:

Table V-5. Chemical analyses of the Tolovana Limestone

[Analyses determined by X-ray fluorescence after method described by Taggart and others (1981)]

Sample	Lat	Long	CaCO3 1	MgCO3 2	SiO2	FeTO3	Al2O3
86MC25	65-36-33	147-20-00	98.88	1.03	<0.10	<0.04	0.40
86MC26	65-36-32	147-20-45	97.66	0.85	<0.10	<0.04	0.30
86MC27	65-36-42	147-20-55	98.88	1.00	0.14	<0.04	0.15
86MC28	65-36-32	147-23-15	99.40	0.90	<0.10	<0.04	<0.10
86MC29	65-36-48	147-23-13	99.05	1.13	<0.10	<0.04	<0.10
86MC30	65-36-36	147-24-38	98.01	0.88	<0.10	<0.04	0.24
86MC32	65-37-16	147-23-00	97.83	1.28	0.41	<0.04	0.19
86MC33	65-37-07	147-22-48	98.53	0.93	0.24	<0.04	0.14
86MC34B	65-37-03	147-22-45	98.70	1.25	<0.10	<0.04	<0.10
86MC35	65-38-03	147-18-18	98.70	0.75	<0.10	<0.04	<0.10
Minimum			97.66				
Average			98.56				
Maximum			99.40				

1 Recalculated from CaO based on G. Frederic Smith Standard

2 Recalculated from MgO

Table V-6. Estimation of endowment of high-calcium limestone for the Tolovana Limestone within the WMNRA study area

Endowment is estimated by the following equation:

$$E = A \times F \times T$$

where

E = endowment in tons of high-calcium limestone

A = projected surface area of favorable area in square miles

F = the fraction of A that is underlain by endowment

T = tons of endowed rock per square mile within A x F (estimated by multiplying the thickness in feet of the limestone by a weight-to-volume factor; for limestone, the factor is 5280 x 5280 / 11.8)

Summary of the input values

Factor	Lower (.05)	Most likely	Upper (.95)
A	-	36	-
F	.7	.8	.9
T	2E8	10E8	16E8

Odds are 9 to 1 that the values lie between the lower and upper estimates.

Using the computer program described by Finch and McCammon (in press), the endowment was calculated using the above equation. The mean value of the endowment of high-calcium limestone is 2.7E10 tons. The probability distribution for the endowment is:

Limestone (tons)	Probability (in percent)	Limestone (tons)	Probability (in percent)
.84E10	.05	2.85E10	.55
1.21E10	.10	3.00E10	.60
1.48E10	.15	3.16E10	.65
1.70E10	.20	3.32E10	.70
1.90E10	.25	3.50E10	.75
2.07E10	.30	3.69E10	.80
2.24E10	.35	3.91E10	.85
2.39E10	.40	4.17E10	.90
2.55E10	.45	4.54E10	.95
2.70E10	.50		

Thus, the odds are 9 to 1 that the true endowment of high-calcium limestone within the WMNRA is between .84E10 and 4.54E10 tons.

(1) presence of sphalerite, stibnite, pyrite, cassiterite, scheelite, and abundant barite in heavy-mineral pan-concentrate samples along Warren Creek and its tributaries (table V-1);
(2) proximity of the Tertiary felsic intrusion, at Lime Peak to the south;
(3) relatively similar geologic setting to that in the Keno-Hill - Galena Hill area in the Yukon Territory in which a thick sequence of Paleozoic clastic sedimentary rocks is near a Tertiary felsic igneous intrusion;
(4) presence of major fault in area.

What is lacking is the presence of fractures and known occurrences of Ag-Pb-Zn veins. Using the Keno Hill - Galena Hill District in the Yukon Territory as an analog area, it is estimated that there is a 50 percent probability there exists at least one undiscovered deposit in tracts VA and VB of the type known in the Keno Hill - Galena Hill District. Given the existence of one or more deposits, it is estimated there is a 5 percent probability that there are at least two such deposits. These probabilistic estimates are based on the similarity of the geologic setting of both tracts and the Keno Hill - Galena Hill District, the relative sizes of the tracts, and the difficulty in identifying concealed vein fault structures during exploration for this type of deposit. Using these probabilities and grade-tonnage data for 33 deposits in the Keno Hill - Galena Hill District (K. Watson, 1987, written commun.) in the MARK3 program, it is estimated that there is an expected 89,000 tons of ore-bearing rock in undiscovered polymetallic vein deposits that contain 4,200,000 oz of Ag, 11,000 tons of Pb, and 2,900 tons of Zn. The 5th and 95th percentiles of these estimates are 0 and 330,000 tons of ore-bearing rock, 0 and 14,000,000 oz of Ag, 0 and 20,000 tons of Pb, and 0 and 5,600 tons of Zn, respectively.

POTENTIAL FOR LODE GOLD OCCURRENCES

Low-sulfide Au-quartz veins are described by Berger (1985) as being mainly veins in regionally metamorphosed volcanic and volcanic sedimentary rocks. The veins in these deposits are generally post-metamorphic and locally cut granitic rocks. The depositional environment is low-grade metamorphic belts. The size of these deposits is small, ranging from a few thousand to as much as a million tons of ore. Average gold grades range from 0.1 oz/t Au to 40 oz/t Au. Notable examples of low-sulfide Au-quartz veins in Alaska are the Big Hurrah mine on the Seward Peninsula, the Chandalar district mines in the southern Brooks Range, and certain of the quartz-vein deposits in the Fairbanks mining district (Nokleberg and others, 1987).

The area considered prospective for low-sulfide Au-quartz vein deposits within the WMNRA is shown as Tract VI in plate V. The main reason for this area being considered prospective is the probable presence of the Cleary sequence, a distinctive 360 ft-thick section of probable volcanogenic beds that consists of "interlensing felsic schist, laminated white micaceous quartzite, actinolitic greenschist, graphitic schist, metabasite, metarhyolite, and calcsilicate beds" (Robinson and others, 1982, p. 228). The Cleary sequence is considered the source for most of the gold in placer deposits in the

Fairbanks Mining District (Smith and others, 1981). Similar and possibly correlative rocks are recognized near Mount Prindle (T.E. Smith, oral commun., 1986). Based on the regional northeast strike, these rocks project southwestward roughly parallel to Nome Creek. Cady and Weber (1983) determined that linear magnetic highs reflect magnetic chloritic schists within the Fairbanks schist (probably the Cleary sequence). These highs are interpreted as crests of antiforms that bring magnetic schist close to the surface. Such linear magnetic highs extend southwestward from Mount Prindle toward the heads of Trail and Ophir Creeks and are coincident with a known antiform. Although the Cleary sequence most likely is present in this structure, it was not recognized in the meager outcrops.

Of second major importance for Tract VI being considered prospective for lode gold are granitic and associated felsic hypabyssal intrusions near Mount Prindle that occur in the axis of a magnetic low. This belt of magnetic lows extend southwestward from Mount Prindle toward a strong low that occurs near the headwaters of Ophir and Trail Creeks. Cady and Weber (1983) suggested that the magnetic lows indicate continuity of nonmagnetic plutons at depth. Light and others (1987) suggested that the inferred buried plutons may have caused hydrothermal remobilization and concentration of disseminated gold from the Cleary sequence to form lode deposits near the headwaters of Ophir and Trail Creeks. However, a resistivity cross-section constructed from Audiomagnetotelluric and Magnetotelluric soundings (Long and Miyaoka, section III, fig. III-4) indicates that there are no plutons within at least 2 km of the surface along the line of their traverse. Additional data from traverses across upper Ophir and Trail Creeks in the central portion of the aeromagnetic low reported by Cady and Weber (1983) and Cady and others (section III) are needed to assess the presence of the inferred pluton.

It is plausible that the intrusion of Cretaceous and/or Tertiary plutons, inferred from the aeromagnetic lows, caused hydrothermal remobilization of gold from the Cleary sequence buried along the northwestern flank of an antiform. Hydrothermal fluids migrating through dilatant fractures caused by warping associated with the intrusion could have formed gold-bearing veins and stringers. Because of the lesser degree of erosion as compared to the head of Nome Creek, gold-bearing veins may still be in place in the area delineated as Tract VI on plate V. Conversely, if no buried plutons exist in this area, the placer gold in Trail and Ophir Creeks may simply have been derived from the Cleary sequence, thus diminishing the potential for lode gold deposits in this area. The second senario, however, does not explain the source of the high concentrations of gold in Trail and Ophir Creeks relative to similar nearby drainages.

Based on the available data and comparison with areas outside the WMNRA known to contain low-sulfide Au-quartz vein deposits, we estimate there is a 10 percent probability that one or more deposits of this type occurs within the WMNRA. Given that such deposits do exist, we estimate there is a 5 percent probability that there are at least two such deposits. Using these probabilities and the grade-tonnage model for low-sulfide Au-quartz veins compiled by Bliss (1986) in the MARK3 program, it is estimated there are 230,000 tons of ore-bearing rock in undiscovered deposits of this type that

contain 34,000 oz Au. The 5th and 95th percentiles for these estimates are 0 and 35,000 tons of ore-bearing rock and 0 and 15,000 oz Au, respectively.

POTENTIAL FOR PLACER GOLD OCCURRENCES

Placer gold was reported in the upper tributaries of Beaver Creek prior to the turn of the century. The first substantial gold discovery in the area was in 1910 when mineable deposits were found on Ophir Creek (Ellsworth and Parker, 1911). Subsequently, gold was discovered on Nome Creek and Trail Creek. The deposits along both Ophir and Trail Creeks proved to be limited in extent. The known production to date is 33 oz Au and 4 oz Ag (MAS, U.S. Bur. Mines). Dredges were operated on Nome Creek for many years, beginning in 1926 (Cobb, 1973), and gold was recovered from a 6 mile stretch upstream from the confluence with Moose Creek. The upstream extent of placer mining coincides with the maximum extent of Pleistocene glacial ice from Mount Prindle (Weber and Hamilton, 1984) that scoured the creek bed and served to concentrate gold below the terminus of the glacier. The cumulative production prior to 1948 from Nome Creek is 28,957 oz Au and 2,711 oz Ag (MAS, U.S. Bur. Mines). In recent years, mining using dozer-backhoe-sluicebox systems has occurred, and chiefly has been confined to ground that has been mined with these methods has been in ground that the dredge missed. The abundance of colors observed in heavy-mineral concentrate samples from Nome, Ophir, and Trail Creeks suggests that much of the fine-grained and flour gold may still remain in the tailings. Using the relationship described by Bliss and others (1987) for estimating the remaining gold in placers suitable for large-volume mining based on the gold reported from earlier small-volume mining, we estimate the amount of gold remaining in Nome Creek to be 6,500 oz. Within the WMNRA study area, we estimate there is a 50 percent probability of at least one more undiscovered placer deposit, and given this occurrence, we estimate that there is a 50 percent probability there are at least two and a 10 percent probability there are at least three placer deposits. Using these probabilities and the tonnage-grade model for small-volume placer deposits described by Orris and Bliss (1986) in the MARK3 program, we estimate there are 4,700 oz Au in undiscovered placer deposits. The 5th and 95th percentiles for the amount of gold in undiscovered placer deposits is 0 and 21,000 oz, respectively. The drainage shown as Tract VII in plate V delineates the prospective drainages. The locations where gold is known to occur are also shown.

POTENTIAL FOR SEDIMENTARY EXHALATIVE ZINC-LEAD (ZN-PB) DEPOSITS

Deposits of this type have been described by Briskey (1986), Sangster (1986), and by Lydon and Sangster (1984) as stratiform basinal accumulations of sulfide and sulfate minerals interbedded with euxinic marine sediments. These deposits form sheet or lens-like tabular ore bodies up to several tens of feet thick, and may be distributed through a stratigraphic interval over several thousand feet. They are considered to have formed in a subaqueous environment, usually submarine, by precipitation of metal sulfides from hot, aqueous solutions emanating from fissures on the seafloor. The principal ore minerals are sphalerite, galena, and barite. The size of such deposits can be very large, up to 500 million tons. Typical grades are: 6 percent Zn and 3

percent Pb although in some cases, the grades are up to 18 percent Zn and 13 percent Pb (Lydon and Sangster, 1984). Notable examples of sedimentary exhalative Zn-Pb deposits in Alaska are the Lik and Red Dog Creek deposits in the northwestern Brooks range (Nokleberg and others, 1987). Zn-Pb deposits of the same type occur throughout the Selwyn Basin in the Yukon Territory in Canada and constitute one of the major sources of these metals worldwide. A displacement model with large-scale right-separation on the Tintina-Victoria

Creek fault system would allow the White Mountains study area to have counterparts to resources known in the Selwyn basin, and mineral exploration, evaluation, and development techniques used successfully that might be applicatle here.

Tract VIII shown in plate V is identified as being favorable for the occurrence of undiscovered sedimentary exhalative Zn-Pb deposits (Menzie and others, 1983). Tract VIII is situated in the northeasternmost part of the WMNRA study area that is underlain principally by the Vrain unit which is composed of mostly argillite with minor quartzite and slaty argillite. In some parts of the area, the Vrain unit is characterized by tuffaceous rocks associated with black or dark gray argillite and conglomerate. Sulfides and limonite are locally abundant although in much of the tract due to intense chemical weathering, the sulfides have been removed leaving casts in the rocks and staining the rocks along fractures. The area is judged favorable for the following reasons:

(1) presence of galena, sphalerite, pyrite, and extensive barite in heavy-mineral pan-concentrate samples along Beaver Creek and its tributaries (pl. IV-R);
(2) presence of tuffaceous rocks associated with black or dark gray argillite and conglomerate;
(3) relatively similar geologic setting to that in the Selwyn Basin in the Yukon Territory in Canada in which several deposits of this type have been discovered.

What is lacking is any direct evidence of the presence of single or stacked sulfide layers. Despite the limited exposures in the area and the intense weathering of the rocks that are exposed, the probability that such layers exist is nevertheless real. It is estimated there is a 10 percent probability that there is at least one undiscovered sedimentary-exhalative Zn-Pb deposit in the area. Using this probability and the grade-tonnage model compiled by Menzie and Mosier (1986) in the MARK3 program, it is estimated there is an expected 4,300,000 tons of ore-bearing rock that contains 310,000 tons of Zn and 170,000 tons of Pb. The 5th and 95th percentiles of these estimates are 0 and 18,000,000 tons of ore-bearing rock, 0 and 1,100,000 tons of Zn and 0 and 540,000 tons of Pb, respectively.

POTENTIAL FOR SERPENTINE-HOSTED ASBESTOS/STRATIFORM MAFIC-ULTRAMAFIC (BUSHVELD) CR DEPOSITS

Serpentine-hosted asbestos deposits have been described by Page (1986a) as consisting of stockworks of asbestos in serpentinized ultramafic rocks. The

depositional environment is usually an ophiolite sequence, sometimes with later deformation or igneous intrusion. The major rock types are serpentinite, dunite, harzburgite, and pyroxenite. The notable example of a serpentine-hosted asbestos deposit in Alaska is the Fortymile deposit in east-central Alaska (Foster and Keith, 1974). Stratiform mafic-ultramafic deposits have been described by Page (1986b) and by Duke (1984) as consisting of layered chromitite in zones of large repetitively layered mafic-ultramafic intrusions. Chromitite seams are most commonly hosted by peridotite or its serpentinized equivalent. The intrusions occur in a variety of tectonic settings. The nearest example of this type of deposit is the Stillwater Complex in Montana (Page and Zientek, 1985). The reason for considering both types of deposits simultaneously is that both asbestos and chromitite have been reported in the serpentinized ultramafic rocks in the WMNRA.

Tract X in plate V is underlain by mafic and ultramafic rocks most of which are serpentinite. The serpentinite follows a northeasterly trend and conforms generally to the regional structural grain. Pyroxenite cobbles containing as much as one-half inch in thickness veins of amphibole asbestos found along Beaver Creek are reported by Barker (1978), and the location is shown on plate V. A grab rock sample found nearby, also contained chromitite (Foster, 1969). Other rocks collected in this area contained chromium and nickel in amounts ranging from 1000 to 5000 ppm (Foster, 1969; this report, pl. V). The area was the focus of extensive exploration for chromium and platinum during the seventies (Barker, 1978). In a recent report by Cathrall and others (1987), platinum has been found in gold samples collected from the nearby Tolovana mining district. Much earlier, Mertie (1937) noted that a small nugget of platinum reportedly was found on one of the placer creeks there in this district. Just as we were writing this report, we received the results of analyses for platinum in 23 pan concentrate samples collected along streams which drain the ultramafic belt within the WMNRA study area. Only 8 of the 23 samples, contained detectable but unmeasurable amounts of platinum. In these analyses the threshold of detection for platinum was in the range of 2-15 ppb. To date, no major discoveries of asbestos, chromium, nickel, or platinum within the WMNRA have been announced. We believe that tract X unlikely to contain undiscovered serpentine-hosted asbestos or stratiform mafic/ultramafic Cr deposits for the following reasons:

(1) relatively thin (<5,000 ft) mafic-ultramafic complex;
(2) separate trend and different age rock from ultramafic rocks which comprise the Seventymile terrane of Foster and others (in press);
(3) lack of any discovery of significant amounts of asbestos, chromium, nickel, or platinum despite intensive exploration in an area in which the rocks are well exposed.

We do not regard tract X as a potential resource for asbestos, chromium, or nickel. The occurrence of platinum in gold samples from the nearby Tolovana mining district, however, makes platinum worthy of further consideration as a potential metallic resource.

POTENTIAL FOR PLACER DIAMOND OCCURRENCES

Three diamonds, ranging in weight from 0.3 to 1.4 carats, have been recovered from placer gold operations on Crooked Creek in the Circle Mining District, near Central, Alaska (Forbes and others, 1987). The Crooked Creek discoveries are 50-60 mi (80-100 km) east of the WMNRA study area. The source of the diamonds recovered from Crooked Creek is not known, but most diamonds are associated with either kimberlites or lamproites and occur in diatremes of only local extent (less than one-half mile diameter). Chrome diopside, pyrope garnet, and magnesium-chromium rich ilmenite are pathfinder minerals used in the exploration for diamond-bearing kimberlites (Forbes and others, 1987).

Chrome diopside is present in a heavy mineral concentrate sample from Fossil Creek (sample LA429C). This occurrence together with the presence of alkaline and syenitic rocks suggest that the geologic environment is permissive for the occurrence of kimberlites. If the Tintina and Beaver Creek fault zones can be inferred to be deep crustal flaws, then they may act as conduits for the emplacement of diamond-bearing diatremes. A detailed, systematic study of the heavy-mineral concentrates in stream and soils along these major fault zones and subsequent surface magnetometer surveys could identify the most favorable areas for concealed diatremes.

Based on our present knowledge, we conclude that there is less than a 5 percent probability that undiscovered diamond-bearing diatremes occur in the WMNRA study area.

Summary

A summary of the probabilistic estimates of the existence and the number of undiscovered deposits within the WMNRA study area of most deposit types for the deposit types we considered is given in table V-7. The probability is low that one or more undiscovered deposits exist. This is due largely to the overall lack of evidence of mineralization in the rocks that are exposed at the surface. It is reasonable to assume that estimates of the existence and the number of undiscovered deposits might be different if more were known about the subsurface.

The deposit types considered in this report have enabled us to estimate the undiscovered endowments for eight metals and one nonmetallic commodity. The estimates of undiscovered endowment are shown in table V-8. For each metal and for the one nonmetallic commodity, the estimate of the mean undiscovered endowment and the 5th and 95th percentiles of the distribution of the undiscovered endowment are given. The two qualifications to be made for anyone using these figures are that we have assumed that future discovery of the types of deposits considered in our assessment will be of similar size and grade as those deposits already discovered and that the estimates we have made are based on our present knowledge about the deposit types we have considered.

Table V-7. Probability of existence and expected number of undiscovered deposits within the WMNRA study area.

Deposit Type	Probability that one or more undiscovered deposits exist	Given the existence of undiscovered deposits, probability that the expected number equals or exceeds a given number		
		.90	.50	.10
Sn greisen	0.1	1	1	1
REE	0.1	1	1	1
W Skarn	0.05	1	1	1
Polymetallic vein	0.5	1	1	2
Lode Au	0.1	1	1	2
Placer Au	0.5	1	2	3
Sedimentary exhalative	0.1	1	1	1

Table V-8. Estimates of undiscovered metal and nonmetallic endowment in the WMNRA

metal or nonmetallic commodity	unit of measure	mean undiscovered endowment	percentiles 95	5
Gold	oz	46,000	6,500	94,000
Silver	oz	4,200,000	0	14,000,000
Zinc	ton	310,000	0	1,200,000
Lead	ton	180,000	0	520,000
Tin	ton	500	0	1,100
Tungsten	ton	2,100	0	0
Thorium	ton	7,000	0	25,000
REO	ton	6,000	0	32,000
Total metallic ore-bearing material	ton	6,900,000	0	30,000,000
High-calcium limestone	ton	27 billion	8.4 billion	45 billion

REFERENCES CITED

Anderson, R.G., 1987, Plutonic rocks in the Dawson map area, Yukon Territory: Geol. Survey of Canada Paper 87-1A, p. 689-697.

Armbrustmacher, T.J., 1984, Rare-earth/thorium deposits associated with a complex of syenitic rocks near Mt. Prindle, East-central Alaska: Geological Society of America, Abstracts with Programs, v. 16, p. 266-267.

Barker, J.C., 1978, Mineral deposits of the Tanana - Yukon Uplands: A summary report: U.S. Bureau of Mines Open File Report 88-78, 33 p.

Barker, J.C., 1983, Potential for cobalt in skarn occurrences at Victoria Mountain, Circle quadrangle, Alaska: U.S. Bureau of Mines Field Report - January, 8 p.

Barker, J.C., and Clautice, K.H., 1977, Anomalous uranium concentrations in artesian spring and stream sediments in the Mount Prindle area, Alaska: U.S. Bureau of Mines OFR 130-77, 19 p.

Berger, B.R., 1986, Descriptive model of low-sulfide Au-quartz veins, in Cox, D.P., and Singer, D.A. (Editors), Mineral deposit models: U.S. Geological Survey Bulletin 1693, p. 239.

Bliss, J.D., 1986, Grade and tonnage model of low-sulfide Au-quartz veins, in Cox, D.P., and Singer, D.A. (Editors), Mineral deposit models: U.S. Geological Survey Bulletin 1693, p. 239-243.

Bliss, J.D., Orris, G.J., and Menzie, W.D., 1987, Changes in grade, volume, and contained gold during the mining life-cycle of gold placer deposits: Canadian Institute of Mining, v. 80, no. 903, p. 75-80.

Briskey, J.A., 1986, Descriptive model of sedimentary exhalative Zn-Pb, in Cox, D.P., and Singer, D.A. (Editors), Mineral deposit models: U.S. Geological Survey Bulletin 1693, p. 211-212.

Boynton, R.S., Gutschick, K.A., Freas, R.C., and Thompson, J.L., 1983, Lime: Industrial Minerals and Rocks 5th Edition Volume 2, Society of Mining Engineers, New York, p. 809-831.

Burton, P.J., 1981, Radioactive mineral occurrences, Mt. Prindle area, Yukon-Tanana uplands, Alaska: Ms. Thesis, University of Alaska, Fairbanks, 72 p.

Cady, J.W., and Weber, F.R., 1983, Aeromagnetic map and interpretation of magnetic and gravity data, Circle quadrangle, Alaska: U.S. Geological Survey Open-File Report 83-170-C, 29 p.

Chapman, R.M., and Weber, F.R., 1972, Geochemical analyses of bedrock and streamsediment samples from the Livengood quadrangle, Alaska: U.S. Geological Survey Open-File Report 72-067, 2 sheets, scale 1:250,000.

Church, R.E., and Durfee, M.C., 1961, Geology of the Fossil Creek area, White Mountains, Alaska: Ms. Thesis, University of Alaska, Fairbanks, 96 p.

Cobb, E.H., 1973, Placer deposits of Alaska: U.S. Geological Survey Bulletin 1374, 213 p.

Cox, D.P., 1986, Descriptive model of polymetallic veins, in Cox, D.P., and Singer, D.A. (Editors), Mineral deposit models: U.S. Geological Survey Bulletin 1693, p. 125-126.

Cox, D.P., and Singer, D.A. (Editors), 1986, Mineral deposit models: U.S. Geological Survey Bulletin 1693, 379 p.

Drew, L.J., Bliss, J.D., Bowen, R.W., Bridges, N.J., Cox, D.P., DeYoung, Jr., J.C., Houghton, J.C., Ludington, S., Menzie, W.D., Page, N J., Root,

D.H., and Singer, D.A., 1986, Quantitative estimation of undiscovered mineral resources--A case study of U.S. Forest Service Wilderness Tracts in the Pacific Mountain System: Economic Geology, v. 81, p. 80-88.

Duke, J.M., 1984, Mafic/ultramafic-hosted chromite, in Eckstrand, O.R., ed., Canadian mineral deposit types: A geological synopsis: Geological Survey of Canada Economic Geology Report 36, p. 43.

Einaudi, M.T., 1981, Skarns associated with porphyry plutons. I. Description of deposits, southwestern North America, II. General features and origin, in Titley, S.R., ed., Advances in geology of the porphyry copper deposits of southwestern North America: Tucson, University of Arizona Press, p. 139-183.

Einaudi, M.T., and Burt, D.M., 1982, Introduction--terminology, classification, and composition of skarn deposits: Economic Geology, v. 77, p. 745-754.

Ellsworth, C.E., and Parker, G.L., 1911, Placer mining in the Yukon-Tanana region: U.S. Geological Survey Bulletin 480, p. 153-172.

Finch, W.I., and McCammon, R.B., 1987, Uranium resource assessment by the Geological Survey: Methodology and plan to update the National Resource Base: U.S. Geological Survey Circular 994, 31 p.

Forbes, R.B., Kline, J.T., and Clough, A.H., 1987, A preliminary evaluation of alluvial diamond discoveries in placer gravels of Crooked Creek, Circle district, Alaska: Div. Geol. and Geophys. Surveys Rept. of Investigations 87-1, 26 p.

Foster, H.L., and Keith, T.E.C., 1974, Ultramafic rocks of the Eagle quadrangle, east-central Alaska: U.S. Geological Survey Journal of Research, v. 2, no. 6, p. 667-669.

Foster, H.L., Keith, T.E.C., and Menzie, W.D., in press, Geology of east-central Alaska:

Foster, H.L., Laird, J., Keith, T.E.C., Cushing, G.W., and Menzie, W.D., 1983, Preliminary geologic map of the Circle quadrangle, Alaska; U.S. Geological Survey Open-File Report 83-170A, 29 p.

Foster, R.L., 1969, Nickeliferous serpentinite near Beaver Creek, East-central Alaska, in Some shorter mineral resource investigations in Alaska: U.S. Geological Survey Circular 615, p. 2-4.

Hill, T.P., and Werner, M.A., 1972, Chemical composition of sedimentary rocks in Alaska, Idaho, Oregon, and Washington: U.S. Geological Survey Professional Paper 771, 319 p.

Lydon, J.W., and Sangster, D.F., 1984, Sediment-hosted sulphide, in Eckstrand, O.R., ed., Canadian mineral deposit types: A geological synopsis: Geological Survey of Canada Economic Geology Report 36, p. 35.

MacKevett, E.M., Jr., 1963, Geology and ore deposits of the Bokan Mountain uranium-thorium area, southeastern Alaska: U.S. Geological Survey Bulletin 1154, 125 p.

Menzie, W.D., Foster, H.L., Tripp, R.B., and Yeend, W.E., 1983, Mineral resource assessment of the Circle Quadrangle, Alaska: U.S. Geological Survey Open-File Report 83-170-B, 57 p.

Menzie, W.D., and Jones, G.M., 1986, Grade and tonnage model of W skarn deposits, in Cox, D.P., and Singer, D.A., eds., Mineral deposit models: U.S. Geological Survey Bulletin 1693, p. 55-57.

Menzie, W.D., and Mosier, D.L., 1986, Grade and tonnage model of sedimentary exhalative Zn-Pb, in Cox, D.P., and Singer, D.A., eds., 1986, Mineral deposit models: U.S. Geological Survey Bulletin 1693, p. 212-215.

Menzie, W.D., and Reed, B.L., 1986, Grade and tonnage model of Sn greisen deposits: in Cox, D.P., and Singer, D.A. (Editors), Mineral deposit models: U.S. Geological Survey Bulletin 1693, p. 71-72.

Mertie, J.B., Jr., 1937, The Yukon-Tanana region, Alaska: U.S. Geological Survey Bulletin 872, 276 p.

Nokleberg, W.J., Bundtzen, T.K., Berg, H.C., Brew, D.A., Grybeck, D., Smith, T.E., and Yeend, W., 1987, Significant metalliferous lode deposits and placer districts of Alaska: U.S. Geological Survey Bulletin 1786, 104 p.

Olade, M.A., and Goodfellow, W.D., 1978, Lithogeochemistry and hydrogeochemistry of uranium and associated elements in the Tombstone batholith, Yukon, Canada: in Proceedings of the 7th International Geochemical Symposium, Golden, Colorado, p. 407-428.

Orris, G.J., and Bliss, J.D., 1986, Grade and tonnage model of placer Au-PGE, in Cox, D.P., and Singer, D.A. (Editors), Mineral deposit models: U.S. Geological Survey Bulletin 1693, p. 261-264.

Page, N.J, 1986a, Descriptive model of serpentine-hosted asbestos, in Cox, D.P., and Singer, D.A. (Editors), Mineral deposit models: U.S. Geological Survey Bulletin 1693, p. 46.

Page, N.J, 1986b, Descriptive model of Bushveld Cr, in Cox, D.P., and Singer, D.A. (Editors), Mineral deposit models: U.S. Geological Survey Bulletin 1693, p. 13.

Page, N.J, and Zientek, M.L., 1985, Geologic and structural setting of the Stillwater Complex, in Stillwater Complex: Montana Bureau of Mines and Geology Special Publication 92, p. 1-8.

Reed, B.L., 1986, Descriptive model of Sn greisen deposits, in Cox, D.P., and Singer, D.A. (Editors), Mineral deposit models: U.S. Geological Survey Bulletin 1693, p. 70.

Robinson, M.S., Smith, T.E., and Bundtzen, T.K., 1982, Cleary sequence of the Fairbanks mining district--Primary stratigraphic control of lode gold/antimony mineralization (abs.): Geol. Soc. America Abstracts with Programs, v. 14, no. 4, p. 228.

Sangster, D.F., 1984, Felsic intrusion-associated silver-lead-zinc veins, in Eckstrand, O.R., ed., Canadian mineral deposit types: A geological synopsis: Geological Survey of Canada, Economic Geology Report 36, p. 66.

Sangster, D.F., 1986, Classification, distribution and grade-tonnage summaries of Canadian lead-zinc deposits: Geological Survey of Canada Economic Geology Report 37, 68 p.

Smith, T.E., Robinson, M.S., Bundtzen, T.K., and Metz, P.A., 1981, Fairbanks mining district in 1981: New look at an old mineral province: The Alaska Miner, Jour. Alaska Miners Association, v.9, no. 11, p. 8-28.

Staatz, M.H., and others, 1979, Principal thorium resources in the United States: U.S. Geological Survey Circular 805, 42 p.

Taggart, J.E., Lichte, F.E., and Wahlberg, J.S., 1981, Methods of analysis of samples using x-ray fluorescence and induction-coupled plasma spectroscopy, in The 1980 eruptions of Mount St. Helens, Washington: U.S. Geological Survey Professional Paper 1250, p. 683-687.

Watson, K.W., 1986, Silver-lead-zinc deposits of the Keno Hill-Galena Hill area, Central Yukon: Yukon Geology Volume 1, Indian and Northern Affairs Canada, p. 83-88.

Appendix V-A. A brief note concerning modifications to the MARK3 program for purposes of the assessment described in this report.

R.B. McCammon, D.H. Root, and W.A. Scott, Jr.

MARK3 is a mineral assessment simulation program described by Drew and others (1986) that was developed for the purpose of estimating undiscovered mineral resources within large areas of the country. A number of the grade-tonnage models in MARK3 have been used to estimate the undiscovered mineral resources in the WMNRA. These are the models for Sn-greisen, sedimentary exhalative Zn-Pb, W-skarn, and lode and placer gold deposits. New models added for this assessment are polymetallic-vein and U/Th-REE deposits. In addition to the new models, changes to the program have been made that more nearly portray the properties of the empirical grade-tonnage distributions. In particular, the logarithm of the grade and the logarithm of the ore tonnage of the different deposit types are now simulated using a bivariate normal distribution. The correlation of the bivariate normals is chosen so that the mean metal in the simulated deposits equals the mean metal in the data for each deposit type. In addition to estimating the expected number of undiscovered deposits of a given type within an area, a separate estimate is now made for the probability that no undiscovered deposits exist. This has allowed us to estimate explicitly the risk of no deposits. Estimates for the total contained metal in undiscovered deposits in those cases where a metal occurs in more than one model are now obtained by convolving the probability distributions of the separate contained metal distributions.

OPEN-FILE REPORT NO. 88-284

APPENDIX IV-A

UNITED STATES DEPARTMENT OF THE INTERIOR

GEOLOGICAL SURVEY

Histograms and frequency distributions of rock sample data from the White Mountains National Recreation Area, Livengood and Circle quadrangles, east-central Alaska

1988

APPENDIX IV-A. HISTOGRAMS OF ROCK SAMPLE DATA, WHITE MTS NRA

COLUMN ID.: S-FE%

	VALUE	NO.	%	CUM.	CUM. %		TOT CUM	TOT CUM %	
1	.050	12	1.94	12	1.9	95.0	29	4.7	95.3
2	.070	10	1.61	22	3.5	93.4	39	6.3	93.7
3	.100	13	2.10	35	5.6	91.3	52	8.4	91.6
4	.150	9	1.45	44	7.1	89.8	61	9.8	90.2
5	.200	21	3.39	65	10.5	86.5	82	13.2	86.8
6	.300	8	1.29	73	11.8	85.2	90	14.5	85.5
7	.500	48	7.74	121	19.5	77.4	138	22.3	77.7
8	.700	34	5.48	155	25.0	71.9	172	27.7	72.3
9	1.000	62	10.00	217	35.0	61.9	234	37.7	62.3
10	1.500	28	4.52	245	39.5	57.4	262	42.3	57.7
11	2.000	84	13.55	329	53.1	43.9	346	55.8	44.2
12	3.000	68	10.97	397	64.0	32.9	414	66.8	33.2
13	5.000	105	16.94	502	81.0	16.0	519	83.7	16.3
14	7.000	39	6.29	541	87.3	9.7	558	90.0	10.0
15	10.000	30	4.84	571	92.1	4.8	588	94.8	5.2
16	15.000	24	3.87	595	96.0	1.0	612	98.7	1.3
17	20.000	6	.97	601	96.9	.0	618	99.7	.3

B	T	H	N	L	G	OTHER	UNQUAL	ANAL	read	
0	0	0	5	12	2	0	601	620	620	VALUES
.0	.0	.0	.8	1.9	.3	.0	96.9			PERCENT

MIN	MAX	AMEAN	SD	GMEAN	GD	VALUES
.050	20.00	3.515	3.88	1.769	3.90	601
.012	40.00	3.537	4.38	1.581	4.66	620

APPENDIX IV-A. HISTOGRAMS OF ROCK SAMPLE DATA, WHITE MTS NRA

COLUMN ID: S-FE%

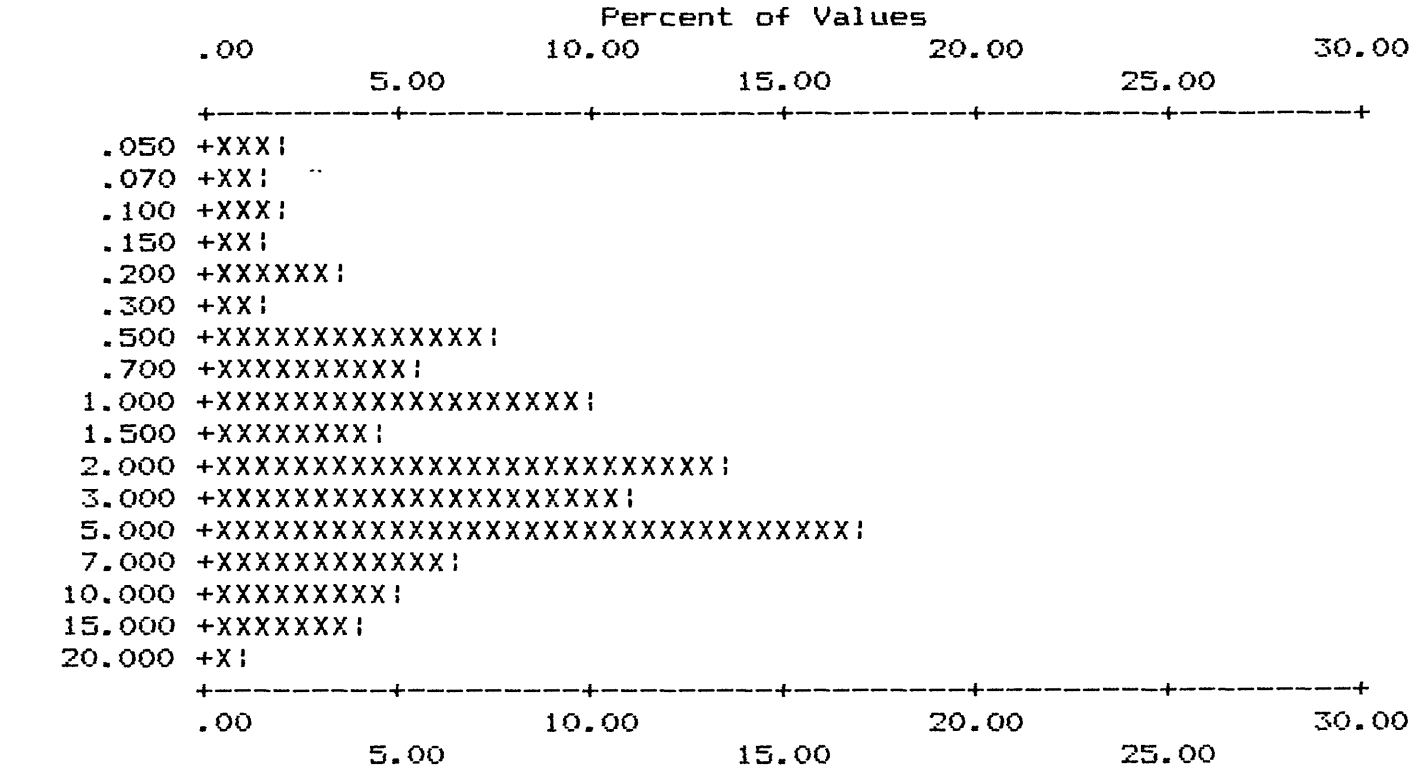

Each increment (each X or ! plotted) = .500 %

APPENDIX IV-A. HISTOGRAMS OF ROCK SAMPLE DATA, WHITE MTS NRA

COLUMN ID.: S-MG%

	VALUE	NO.	%	CUM.	CUM. %		TOT CUM	TOT CUM %	
1	.020	18	2.90	18	2.9	91.9	39	6.3	93.7
2	.030	12	1.94	30	4.8	90.0	51	8.2	91.8
3	.050	31	5.00	61	9.8	85.0	82	13.2	86.8
4	.070	13	2.10	74	11.9	82.9	95	15.3	84.7
5	.100	46	7.42	120	19.4	75.5	141	22.7	77.3
6	.150	11	1.77	131	21.1	73.7	152	24.5	75.5
7	.200	38	6.13	169	27.3	67.6	190	30.6	69.4
8	.300	27	4.35	196	31.6	63.2	217	35.0	65.0
9	.500	35	5.65	231	37.3	57.6	252	40.6	59.4
10	.700	35	5.65	266	42.9	51.9	287	46.3	53.7
11	1.000	60	9.68	326	52.6	42.3	347	56.0	44.0
12	1.500	50	8.06	376	60.6	34.2	397	64.0	36.0
13	2.000	103	16.61	479	77.3	17.6	500	80.6	19.4
14	3.000	39	6.29	518	83.5	11.3	539	86.9	13.1
15	5.000	40	6.45	558	90.0	4.8	579	93.4	6.6
16	7.000	16	2.58	574	92.6	2.3	595	96.0	4.0
17	10.000	14	2.26	588	94.8	.0	609	98.2	1.8

B	T	H	N	L	G	OTHER	UNQUAL	ANAL	read	
0	0	0	1	20	11	0	588	620	620	VALUES
.0	.0	.0	.2	3.2	1.8	.0	94.8			PERCENT

MIN	MAX	AMEAN	SD	GMEAN	GD	VALUES
.020	10.00	1.662	2.07	.671	4.91	588
.005	20.00	1.931	3.17	.617	5.99	620

APPENDIX IV-A. HISTOGRAMS OF ROCK SAMPLE DATA, WHITE MTS NRA

COLUMN ID: S-MG%

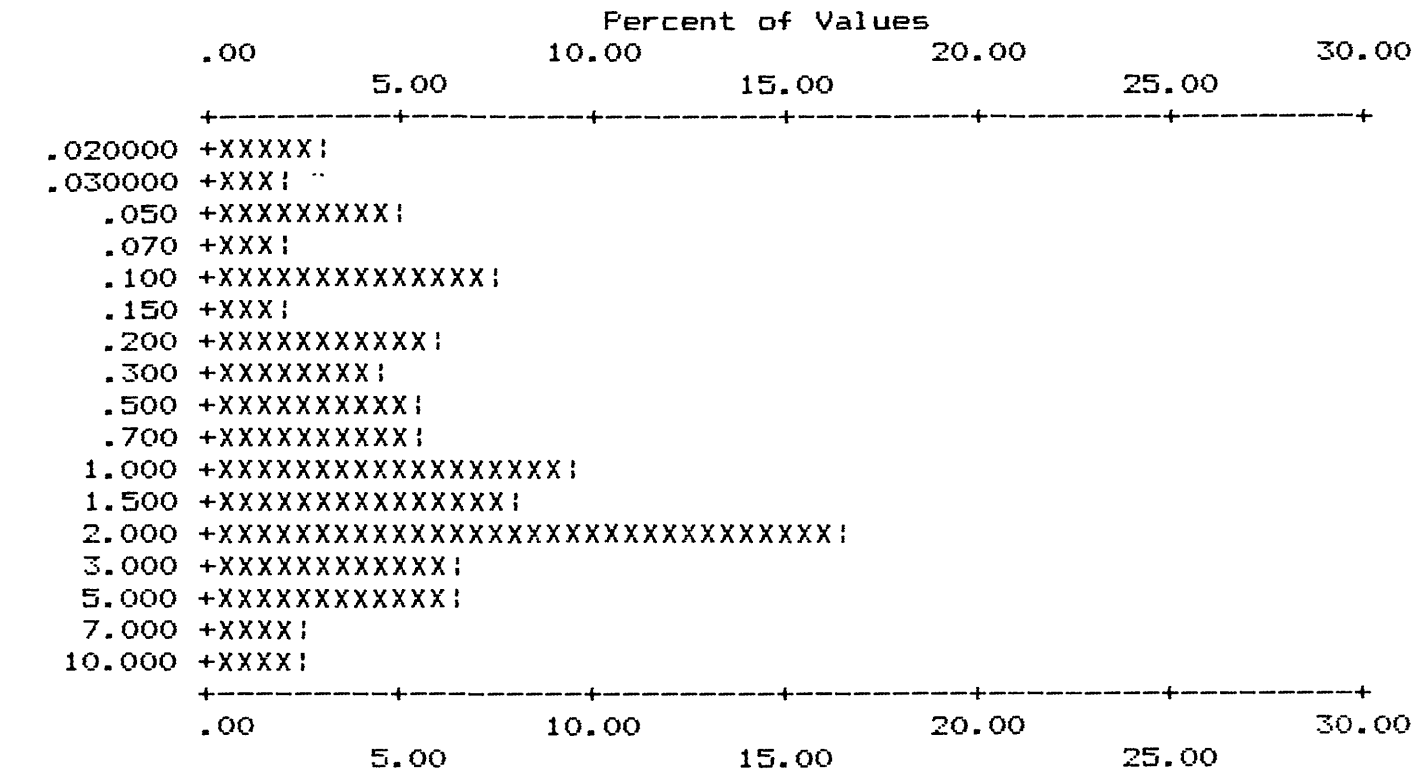

Each increment (each X or ¦ plotted) = .500 %

APPENDIX IV-A. HISTOGRAMS OF ROCK SAMPLE DATA, WHITE MTS NRA

COLUMN ID.: S-CA%

	VALUE	NO.	%	CUM.	CUM. %		TOT CUM	TOT CUM %	
1	.050	53	8.55	53	8.5	55.8	232	37.4	62.6
2	.070	18	2.90	71	11.5	52.9	250	40.3	59.7
3	.100	17	2.74	88	14.2	50.2	267	43.1	56.9
4	.150	31	5.00	119	19.2	45.2	298	48.1	51.9
5	.200	29	4.68	148	23.9	40.5	327	52.7	47.3
6	.300	10	1.61	158	25.5	38.9	337	54.4	45.6
7	.500	16	2.58	174	28.1	36.3	353	56.9	43.1
8	.700	11	1.77	185	29.8	34.5	364	58.7	41.3
9	1.000	30	4.84	215	34.7	29.7	394	63.5	36.5
10	1.500	20	3.23	235	37.9	26.5	414	66.8	33.2
11	2.000	51	8.23	286	46.1	18.2	465	75.0	25.0
12	3.000	28	4.52	314	50.6	13.7	493	79.5	20.5
13	5.000	29	4.68	343	55.3	9.0	522	84.2	15.8
14	7.000	9	1.45	352	56.8	7.6	531	85.6	14.4
15	10.000	20	3.23	372	60.0	4.4	551	88.9	11.1
16	15.000	2	.32	374	60.3	4.0	553	89.2	10.8
17	20.000	25	4.03	399	64.4	.0	578	93.2	6.8

B	T	H	N	L	G	OTHER	UNQUAL	ANAL	read	
0	0	0	41	138	42	0	399	620	620	VALUES
.0	.0	.0	6.6	22.3	6.8	.0	64.4			PERCENT

MIN	MAX	AMEAN	SD	GMEAN	GD	VALUES
.050	20.00	3.055	5.12	.752	6.47	399
.012	40.00	4.682	10.46	.352	12.63	620

APPENDIX IV-A. HISTOGRAMS OF ROCK SAMPLE DATA, WHITE MTS NRA

COLUMN ID: S-CA%

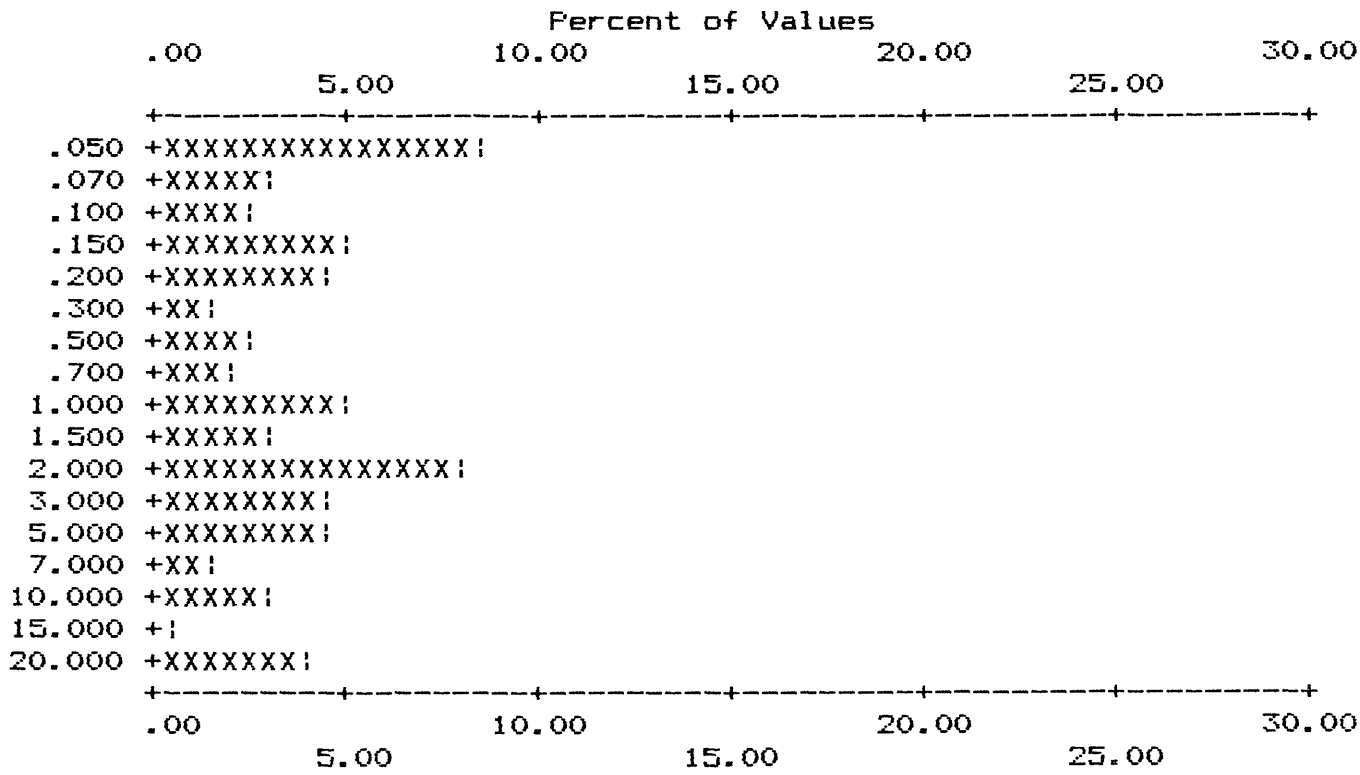

Each increment (each X or ! plotted) = .500 %

APPENDIX IV-A. HISTOGRAMS OF ROCK SAMPLE DATA, WHITE MTS NRA

COLUMN ID.: S-TI%

	VALUE	NO.	%	CUM.	CUM. %		TOT CUM	TOT CUM %	
1	.002	10	1.61	10	1.6	94.5	23	3.7	96.3
2	.003	4	.65	14	2.3	93.9	27	4.4	95.6
3	.005	13	2.10	27	4.4	91.8	40	6.5	93.5
4	.007	1	.16	28	4.5	91.6	41	6.6	93.4
5	.010	20	3.23	48	7.7	88.4	61	9.8	90.2
6	.015	5	.81	53	8.5	87.6	66	10.6	89.4
7	.020	14	2.26	67	10.8	85.3	80	12.9	87.1
8	.030	12	1.94	79	12.7	83.4	92	14.8	85.2
9	.050	40	6.45	119	19.2	76.9	132	21.3	78.7
10	.070	34	5.48	153	24.7	71.5	166	26.8	73.2
11	.100	75	12.10	228	36.8	59.4	241	38.9	61.1
12	.150	44	7.10	272	43.9	52.3	285	46.0	54.0
13	.200	71	11.45	343	55.3	40.8	356	57.4	42.6
14	.300	64	10.32	407	65.6	30.5	420	67.7	32.3
15	.500	76	12.26	483	77.9	18.2	496	80.0	20.0
16	.700	61	9.84	544	87.7	8.4	557	89.8	10.2
17	1.000	52	8.39	596	96.1	.0	609	98.2	1.8

B	T	H	N	L	G	OTHER	UNQUAL	ANAL	read	
0	0	0	2	11	11	0	596	620	620	VALUES
.0	.0	.0	.3	1.8	1.8	.0	96.1			PERCENT

MIN	MAX	AMEAN	SD	GMEAN	GD	VALUES
.002	1.00	.311	.30	.158	4.20	596
.001	2.00	.335	.37	.148	5.10	620

APPENDIX IV-A. HISTOGRAMS OF ROCK SAMPLE DATA, WHITE MTS NRA

COLUMN ID: S-TI%

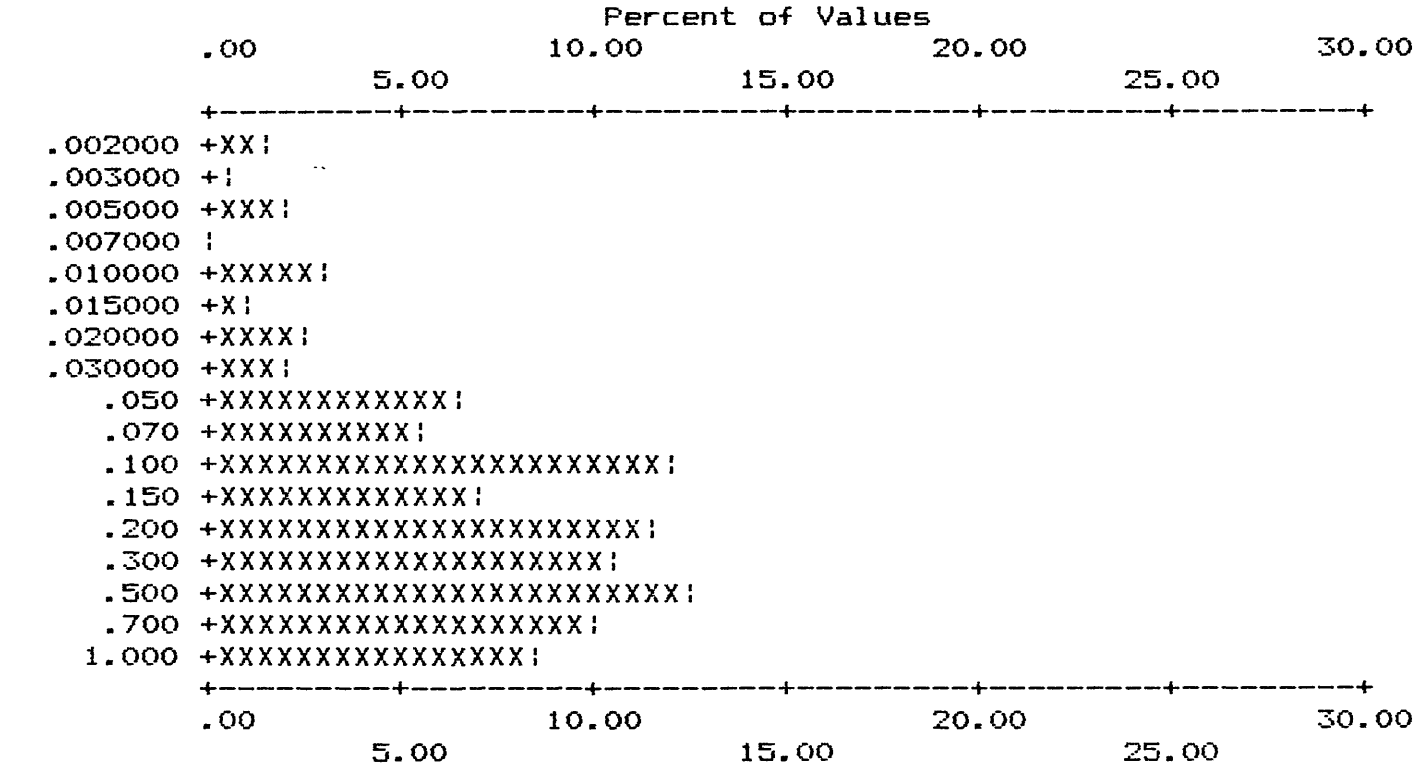

Each increment (each X or ! plotted) = .500 %

APPENDIX IV-A. HISTOGRAMS OF ROCK SAMPLE DATA, WHITE MTS NRA

COLUMN ID.: S-MN

	VALUE	NO.	%	CUM.	CUM. %		TOT CUM	TOT CUM %	
1	10.000	16	2.58	16	2.6	95.0	27	4.4	95.6
2	15.000	8	1.29	24	3.9	93.7	35	5.6	94.4
3	20.000	10	1.61	34	5.5	92.1	45	7.3	92.7
4	30.000	3	.48	37	6.0	91.6	48	7.7	92.3
5	50.000	24	3.87	61	9.8	87.7	72	11.6	88.4
6	70.000	22	3.55	83	13.4	84.2	94	15.2	84.8
7	100.000	53	8.55	136	21.9	75.6	147	23.7	76.3
8	150.000	45	7.26	181	29.2	68.4	192	31.0	69.0
9	200.000	61	9.84	242	39.0	58.5	253	40.8	59.2
10	300.000	58	9.35	300	48.4	49.2	311	50.2	49.8
11	500.000	76	12.26	376	60.6	36.9	387	62.4	37.6
12	700.000	70	11.29	446	71.9	25.6	457	73.7	26.3
13	1000.000	101	16.29	547	88.2	9.4	558	90.0	10.0
14	1500.000	28	4.52	575	92.7	4.8	586	94.5	5.5
15	2000.000	19	3.06	594	95.8	1.8	605	97.6	2.4
16	3000.000	9	1.45	603	97.3	.3	614	99.0	1.0
17	5000.000	2	.32	605	97.6	.0	616	99.4	.6

B	T	H	N	L	G	OTHER	UNQUAL	ANAL	read	
0	0	0	1	10	4	0	605	620	620	VALUES
.0	.0	.0	.2	1.6	.6	.0	97.6			PERCENT

MIN	MAX	AMEAN	SD	GMEAN	GD	VALUES
10.000	5000.00	578.446	618.76	312.993	3.59	605
2.500	10000.00	629.052	974.92	297.085	4.09	620

APPENDIX IV-A. HISTOGRAMS OF ROCK SAMPLE DATA, WHITE MTS NRA

COLUMN ID: S-MN

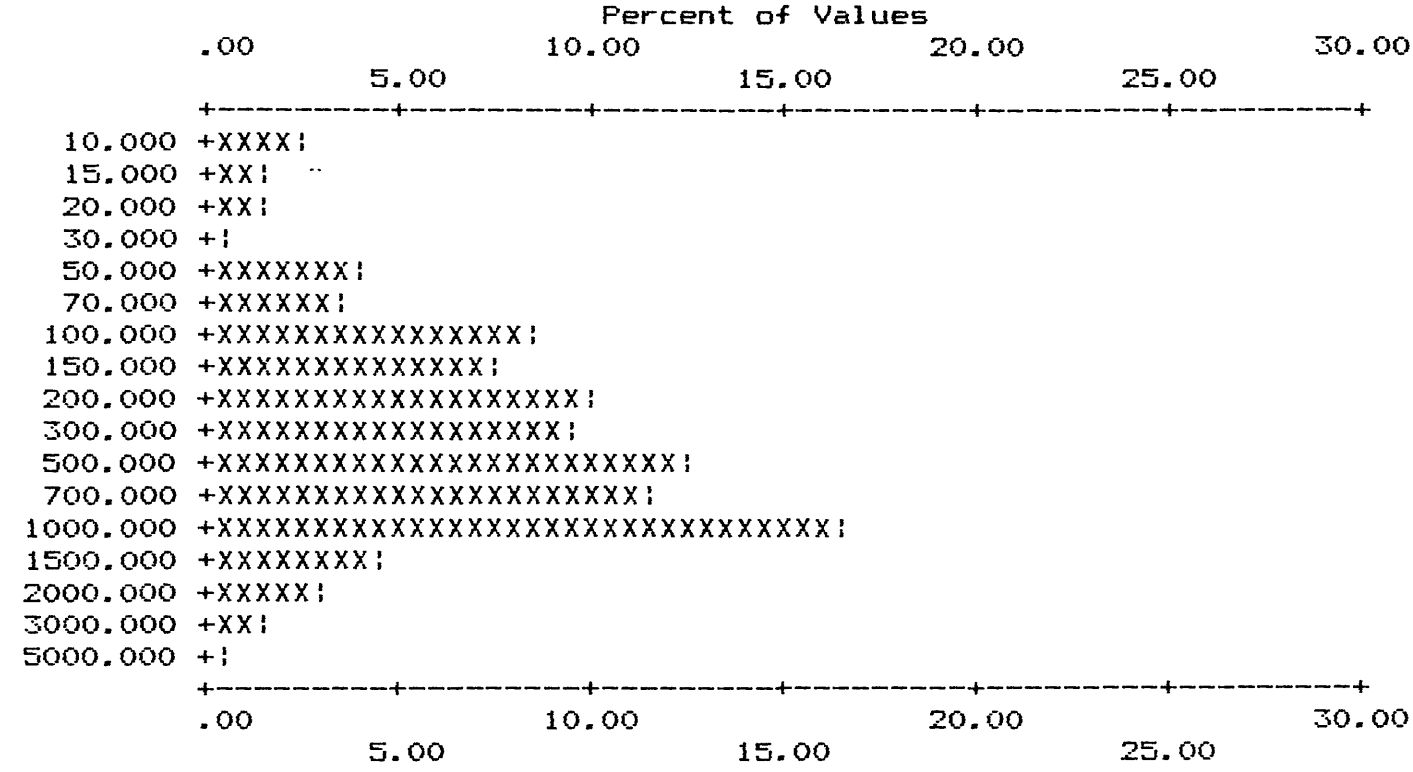

Each increment (each X or ! plotted) = .500 %

APPENDIX IV-A. HISTOGRAMS OF ROCK SAMPLE DATA, WHITE MTS NRA

COLUMN ID.: S-AG

	VALUE	NO.	%	CUM.	CUM. %		TOT CUM	TOT CUM %	
1	.500	15	2.42	15	2.4	3.7	597	96.3	3.7
2	.700	13	2.10	28	4.5	1.6	610	98.4	1.6
3	1.500	4	.65	32	5.2	1.0	614	99.0	1.0
4	2.000	1	.16	33	5.3	.8	615	99.2	.8
5	3.000	2	.32	35	5.6	.5	617	99.5	.5
6	7.000	2	.32	37	6.0	.2	619	99.8	.2
7	10.000	1	.16	38	6.1	.0	620	100.0	.0

B	T	H	N	L	G	OTHER	UNQUAL	ANAL	read	
0	0	0	537	45	0	0	38	620	620	VALUES
.0	.0	.0	86.6	7.3	.0	.0	6.1			PERCENT

MIN	MAX	AMEAN	SD	GMEAN	GD	VALUES
.500	10.00	1.437	2.08	.892	2.27	38
.125	10.00	.214	.60	.148	1.70	620

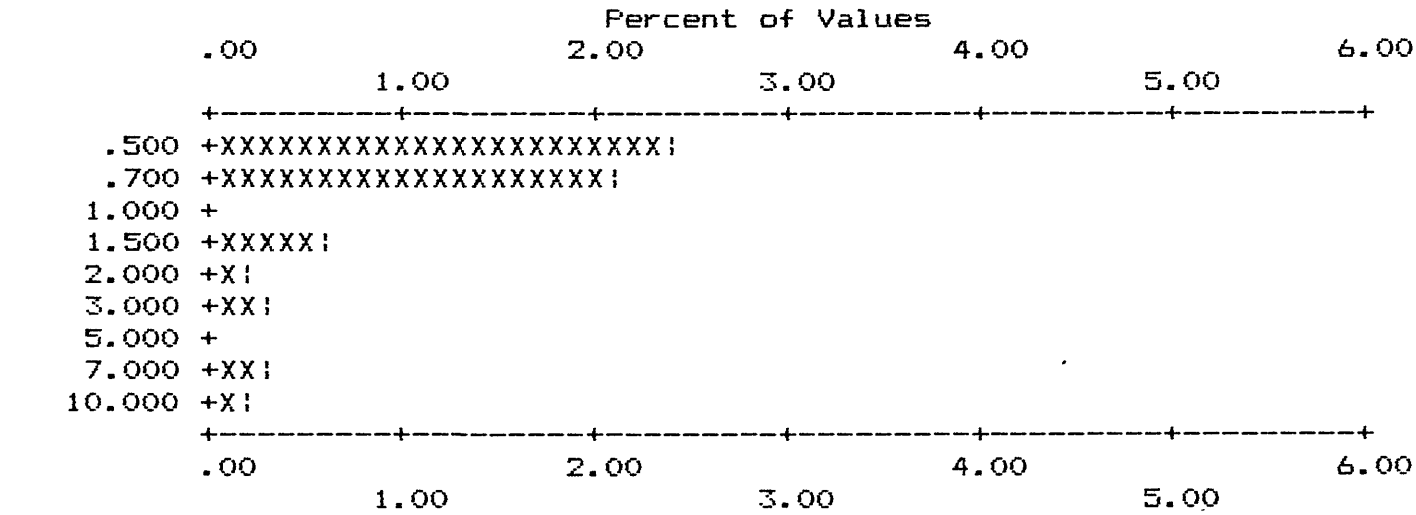

Each increment (each X or ¦ plotted) = .100 %

APPENDIX IV-A. HISTOGRAMS OF ROCK SAMPLE DATA, WHITE MTS NRA

COLUMN ID.: S-AS

	VALUE	NO.	%	CUM.	CUM. %	TOT CUM	TOT CUM %	
1	200.000	3	.48	3	.5	617	99.5	.5
2	1000.000	2	.32	5	.8	619	99.8	.2
3	5000.000	1	.16	6	1.0	620	100.0	.0

B	T	H	N	L	G	OTHER	UNQUAL	ANAL	read	
0	0	0	613	1	0	0	6	620	620	VALUES
.0	.0	.0	98.9	.2	.0	.0	1.0			PERCENT

MIN	MAX	AMEAN	SD	GMEAN	GD	VALUES
200.000	5000.00	1266.667	1870.47	584.803	3.72	6
50.000	5000.00	61.855	206.08	51.261	1.31	620

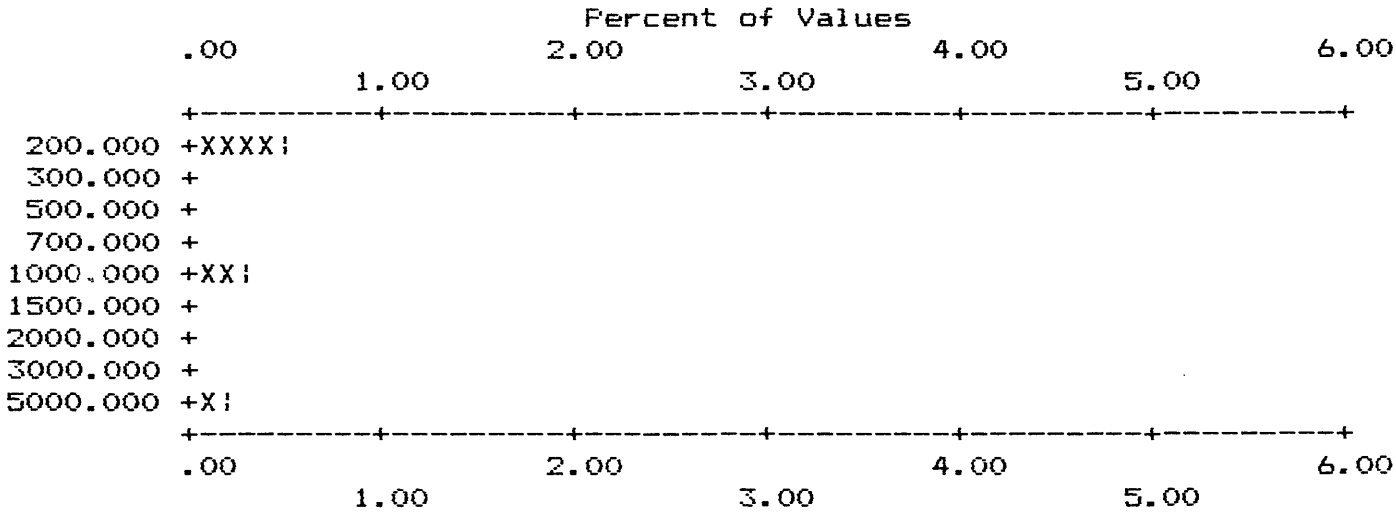

Each increment (each X or ! plotted) = .100 %

APPENDIX IV-A. HISTOGRAMS OF ROCK SAMPLE DATA, WHITE MTS NRA

COLUMN ID.: S-B

	VALUE	NO.	%	CUM.	CUM. %		TOT CUM	TOT CUM %	
1	10.000	87	14.03	87	14.0	64.8	218	35.2	64.8
2	15.000	45	7.26	132	21.3	57.6	263	42.4	57.6
3	20.000	107	17.26	239	38.5	40.3	370	59.7	40.3
4	30.000	54	8.71	293	47.3	31.6	424	68.4	31.6
5	50.000	74	11.94	367	59.2	19.7	498	80.3	19.7
6	70.000	30	4.84	397	64.0	14.8	528	85.2	14.8
7	100.000	43	6.94	440	71.0	7.9	571	92.1	7.9
8	150.000	23	3.71	463	74.7	4.2	594	95.8	4.2
9	200.000	17	2.74	480	77.4	1.5	611	98.5	1.5
10	300.000	4	.65	484	78.1	.8	615	99.2	.8
11	500.000	2	.32	486	78.4	.5	617	99.5	.5
12	700.000	2	.32	488	78.7	.2	619	99.8	.2
13	2000.000	1	.16	489	78.9	.0	620	100.0	.0

B	T	H	N	L	G	OTHER	UNQUAL	ANAL	read	
0	0	0	52	79	0	0	489	620	620	VALUES
.0	.0	.0	8.4	12.7	.0	.0	78.9			PERCENT

MIN	MAX	AMEAN	SD	GMEAN	GD	VALUES
10.000	2000.00	56.963	113.83	32.520	2.58	489
2.500	2000.00	45.774	103.36	20.658	3.41	620

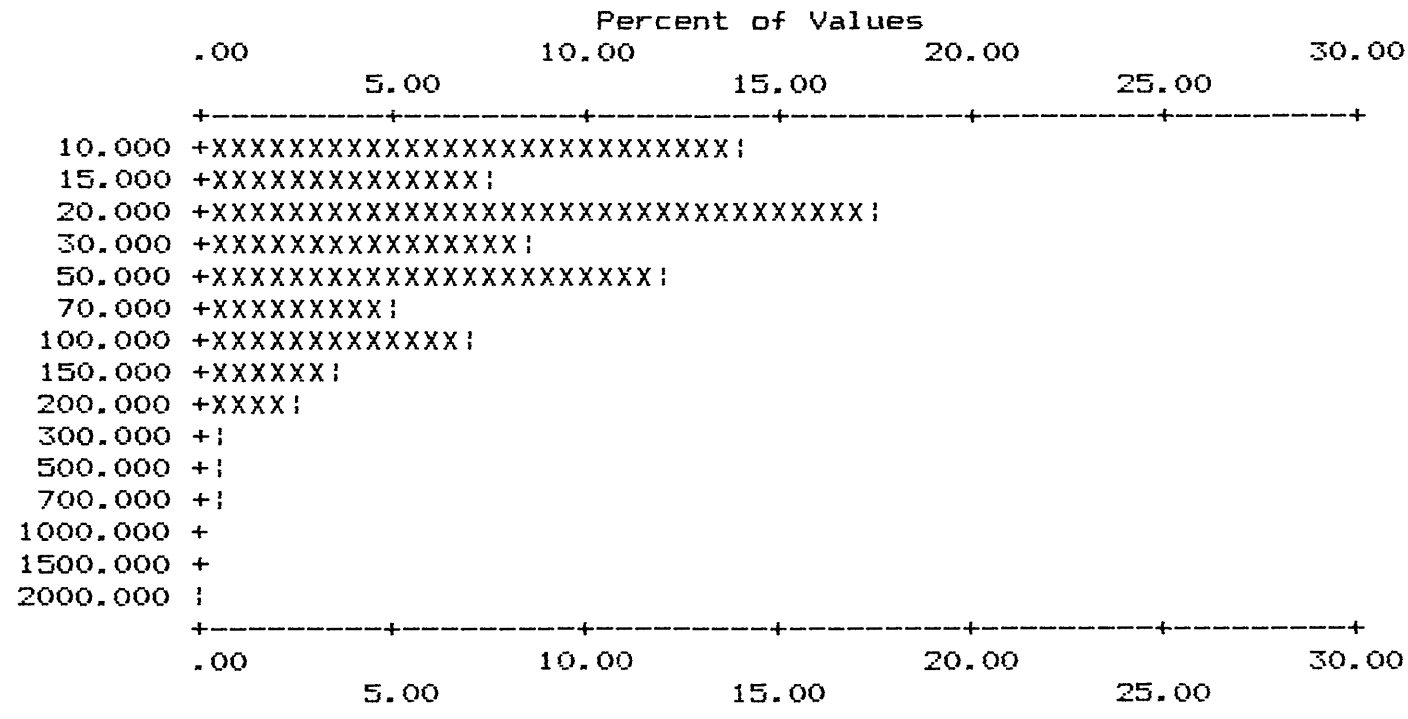

Each increment (each X or ¦ plotted) = .500 %

APPENDIX IV-A. HISTOGRAMS OF ROCK SAMPLE DATA, WHITE MTS NRA

COLUMN ID.: S-BA

	VALUE	NO.	%	CUM.	CUM. %		TOT CUM	TOT CUM %	
1	20.000	25	4.03	25	4.0	86.9	71	11.5	88.5
2	30.000	24	3.87	49	7.9	83.1	95	15.3	84.7
3	50.000	41	6.61	90	14.5	76.5	136	21.9	78.1
4	70.000	31	5.00	121	19.5	71.5	167	26.9	73.1
5	100.000	57	9.19	178	28.7	62.3	224	36.1	63.9
6	150.000	35	5.65	213	34.4	56.6	259	41.8	58.2
7	200.000	55	8.87	268	43.2	47.7	314	50.6	49.4
8	300.000	66	10.65	334	53.9	37.1	380	61.3	38.7
9	500.000	82	13.23	416	67.1	23.9	462	74.5	25.5
10	700.000	42	6.77	458	73.9	17.1	504	81.3	18.7
11	1000.000	45	7.26	503	81.1	9.8	549	88.5	11.5
12	1500.000	17	2.74	520	83.9	7.1	566	91.3	8.7
13	2000.000	23	3.71	543	87.6	3.4	589	95.0	5.0
14	3000.000	13	2.10	556	89.7	1.3	602	97.1	2.9
15	5000.000	8	1.29	564	91.0	.0	610	98.4	1.6

B	T	H	N	L	G	OTHER	UNQUAL	ANAL	read	
0	0	0	9	37	10	0	564	620	620	VALUES
.0	.0	.0	1.5	6.0	1.6	.0	91.0			PERCENT

MIN	MAX	AMEAN	SD	GMEAN	GD	VALUES
20.000	5000.00	555.124	809.92	253.210	3.70	564
5.000	10000.00	666.944	1430.87	209.282	4.99	620

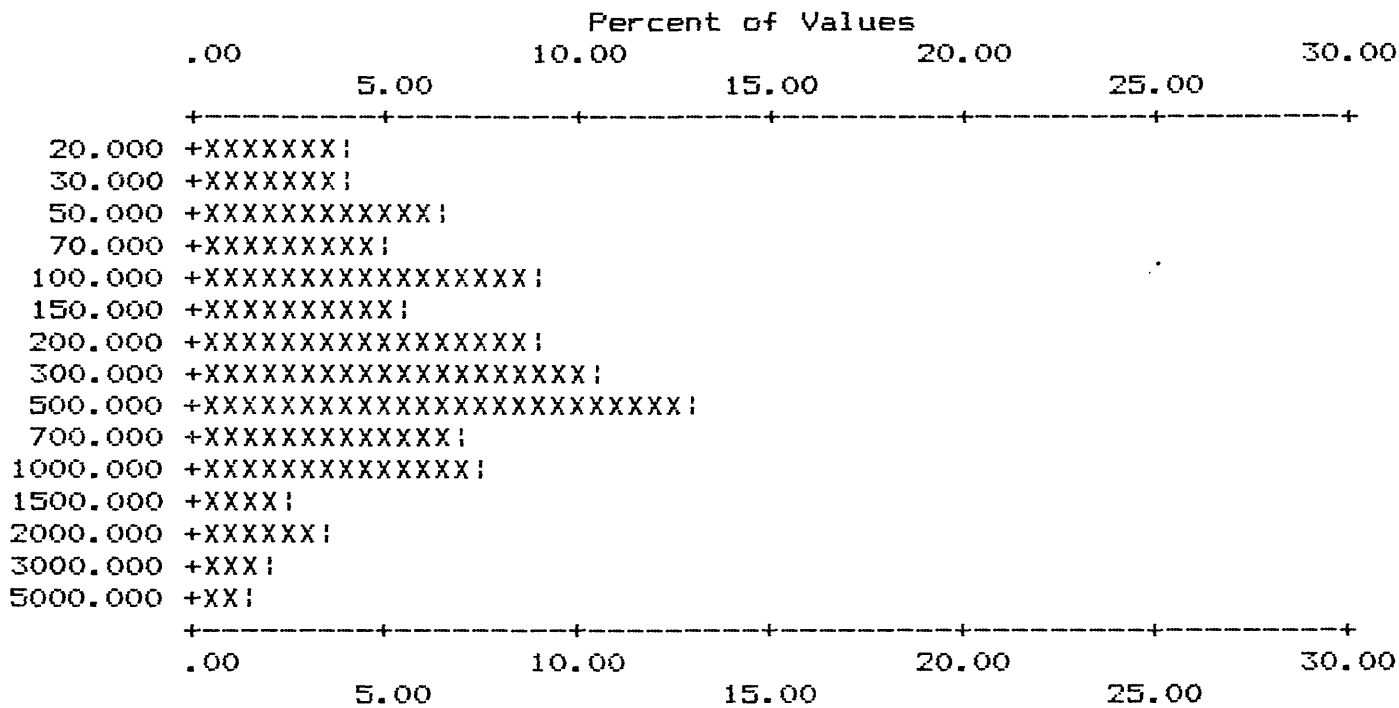

Each increment (each X or ¦ plotted) = .500 %

APPENDIX IV-A. HISTOGRAMS OF ROCK SAMPLE DATA, WHITE MTS NRA

COLUMN ID.: S-BE

	VALUE	NO.	%	CUM.	CUM. %		TOT CUM	TOT CUM %	
1	1.000	90	14.52	90	14.5	16.3	519	83.7	16.3
2	1.500	21	3.39	111	17.9	12.9	540	87.1	12.9
3	2.000	22	3.55	133	21.5	9.4	562	90.6	9.4
4	3.000	15	2.42	148	23.9	6.9	577	93.1	6.9
5	5.000	23	3.71	171	27.6	3.2	600	96.8	3.2
6	7.000	10	1.61	181	29.2	1.6	610	98.4	1.6
7	10.000	6	.97	187	30.2	.6	616	99.4	.6
8	15.000	1	.16	188	30.3	.5	617	99.5	.5
9	20.000	2	.32	190	30.6	.2	619	99.8	.2
10	30.000	1	.16	191	30.8	.0	620	100.0	.0

B	T	H	N	L	G	OTHER	UNQUAL	ANAL	read	
0	0	0	201	228	0	0	191	620	620	VALUES
.0	.0	.0	32.4	36.8	.0	.0	30.8			PERCENT

MIN	MAX	AMEAN	SD	GMEAN	GD	VALUES
1.000	30.00	2.830	3.57	1.900	2.21	191
.250	30.00	1.137	2.28	.603	2.53	620

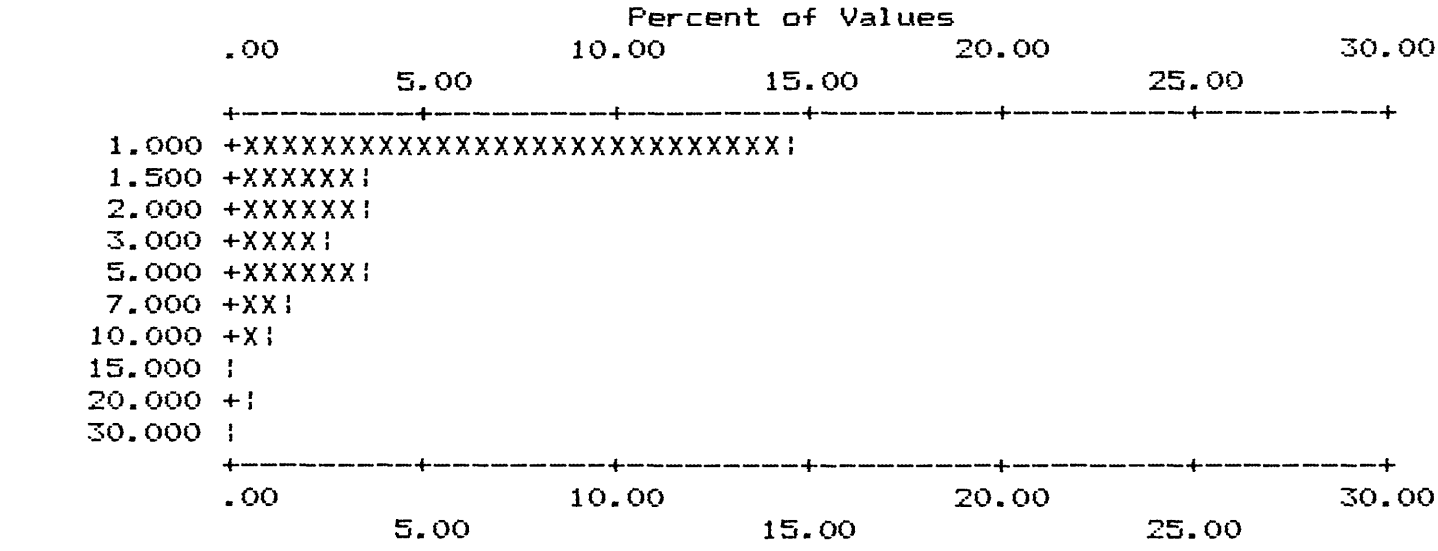

Each increment (each X or ¦ plotted) = .500 %

APPENDIX IV-A. HISTOGRAMS OF ROCK SAMPLE DATA, WHITE MTS NRA

COLUMN ID.: S-BI

	VALUE	NO.	%	CUM.	CUM. %	TOT CUM	TOT CUM %	
1	10.000	2	.32	2	.3	.5	617	99.5	.5
2	20.000	2	.32	4	.6	.2	619	99.8	.2
3	50.000	1	.16	5	.8	.0	620	100.0	.0

B	T	H	N	L	G	OTHER	UNQUAL	ANAL	read	
0	0	0	608	7	0	0	5	620	620	VALUES
.0	.0	.0	98.1	1.1	.0	.0	.8			PERCENT

MIN	MAX	AMEAN	SD	GMEAN	GD	VALUES
10.000	50.00	22.000	16.43	18.206	1.94	5
2.500	50.00	2.685	2.20	2.560	1.22	620

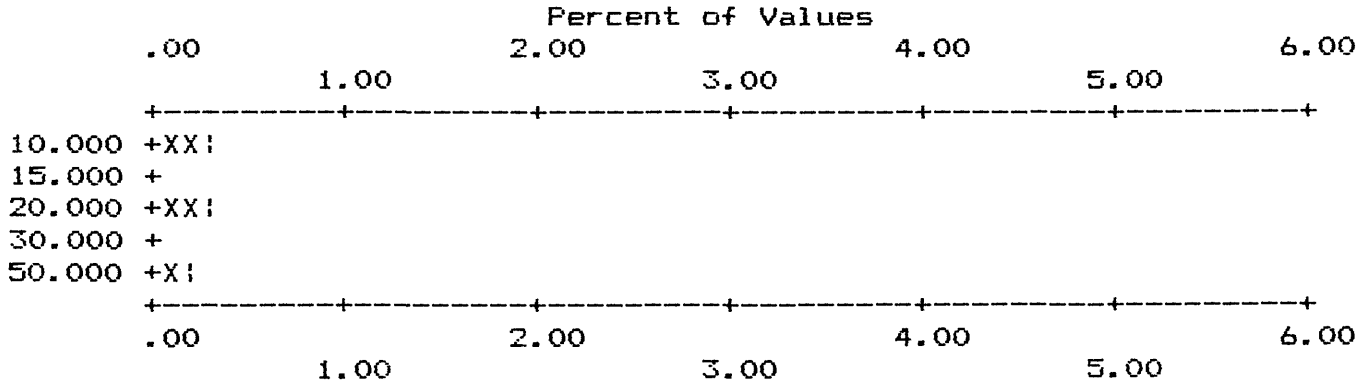

Each increment (each X or ! plotted) = .100 %

APPENDIX IV-A. HISTOGRAMS OF ROCK SAMPLE DATA, WHITE MTS NRA

COLUMN ID.: S-CD

	VALUE	NO.	%	CUM.	CUM. %	TOT CUM	TOT CUM %	
1	20.000	2	.32	2	.3	.3	618	99.7	.3
2	30.000	1	.16	3	.5	.2	619	99.8	.2
3	50.000	1	.16	4	.6	.0	620	100.0	.0

B	T	H	N	L	G	OTHER	UNQUAL	ANAL	read	
0	0	0	599	17	0	0	4	620	620	VALUES
.0	.0	.0	96.6	2.7	.0	.0	.6			PERCENT

MIN	MAX	AMEAN	SD	GMEAN	GD	VALUES
20.000	50.00	30.000	14.14	27.832	1.54	4
5.000	50.00	5.298	2.37	5.153	1.20	620

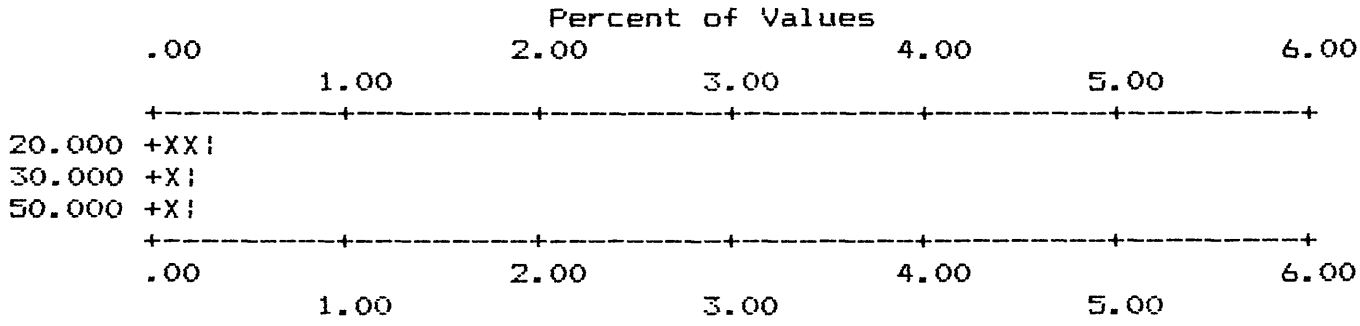

Each increment (each X or ! plotted) = .100 %

APPENDIX IV-A. HISTOGRAMS OF ROCK SAMPLE DATA, WHITE MTS NRA

COLUMN ID.: S-CO

	VALUE	NO.	%	CUM.	CUM. %		TOT CUM	TOT CUM %	
1	5.000	31	5.00	31	5.0	54.7	281	45.3	54.7
2	7.000	39	6.29	70	11.3	48.4	320	51.6	48.4
3	10.000	51	8.23	121	19.5	40.2	371	59.8	40.2
4	15.000	48	7.74	169	27.3	32.4	419	67.6	32.4
5	20.000	51	8.23	220	35.5	24.2	470	75.8	24.2
6	30.000	40	6.45	260	41.9	17.7	510	82.3	17.7
7	50.000	70	11.29	330	53.2	6.5	580	93.5	6.5
8	70.000	34	5.48	364	58.7	1.0	614	99.0	1.0
9	100.000	6	.97	370	59.7	.0	620	100.0	.0

B	T	H	N	L	G	OTHER	UNQUAL	ANAL	read	
0	0	0	213	37	0	0	370	620	620	VALUES
.0	.0	.0	34.4	6.0	.0	.0	59.7			PERCENT

MIN	MAX	AMEAN	SD	GMEAN	GD	VALUES
5.000	100.00	27.995	22.49	19.975	2.33	370
1.250	100.00	17.285	21.72	6.810	4.36	620

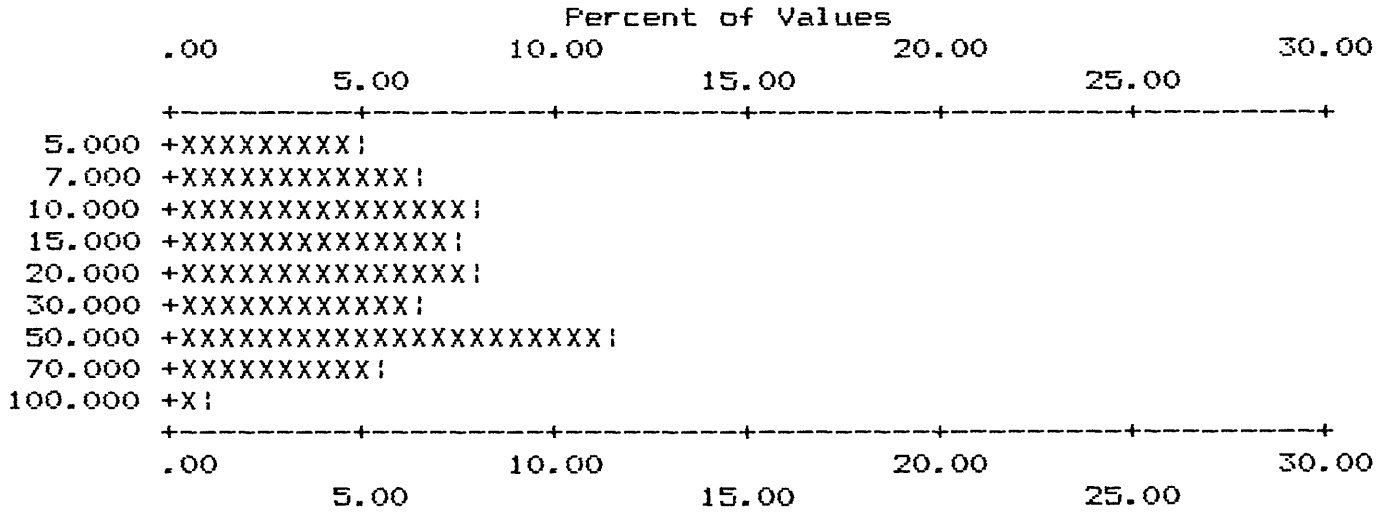

Each increment (each X or ¦ plotted) = .500 %

APPENDIX IV-A. HISTOGRAMS OF ROCK SAMPLE DATA, WHITE MTS NRA

COLUMN ID.: S-CR

	VALUE	NO.	%	CUM.	CUM. %		TOT CUM	TOT CUM %	
1	10.000	41	6.61	41	6.6	58.7	255	41.1	58.9
2	15.000	18	2.90	59	9.5	55.8	273	44.0	56.0
3	20.000	50	8.06	109	17.6	47.7	323	52.1	47.9
4	30.000	38	6.13	147	23.7	41.6	361	58.2	41.8
5	50.000	41	6.61	188	30.3	35.0	402	64.8	35.2
6	70.000	34	5.48	222	35.8	29.5	436	70.3	29.7
7	100.000	47	7.58	269	43.4	21.9	483	77.9	22.1
8	150.000	39	6.29	308	49.7	15.6	522	84.2	15.8
9	200.000	47	7.58	355	57.3	8.1	569	91.8	8.2
10	300.000	21	3.39	376	60.6	4.7	590	95.2	4.8
11	500.000	16	2.58	392	63.2	2.1	606	97.7	2.3
12	700.000	3	.48	395	63.7	1.6	609	98.2	1.8
13	1000.000	4	.65	399	64.4	1.0	613	98.9	1.1
14	1500.000	1	.16	400	64.5	.8	614	99.0	1.0
15	2000.000	4	.65	404	65.2	.2	618	99.7	.3
16	3000.000	1	.16	405	65.3	.0	619	99.8	.2

B	T	H	N	L	G	OTHER	UNQUAL	ANAL	read	
0	0	0	124	90	1	0	405	620	620	VALUES
.0	.0	.0	20.0	14.5	.2	.0	65.3			PERCENT

MIN	MAX	AMEAN	SD	GMEAN	GD	VALUES
10.000	3000.00	148.395	286.89	66.542	3.41	405
2.500	10000.00	114.290	465.40	23.900	5.82	620

APPENDIX IV-A. HISTOGRAMS OF ROCK SAMPLE DATA, WHITE MTS NRA

COLUMN ID: S-CR

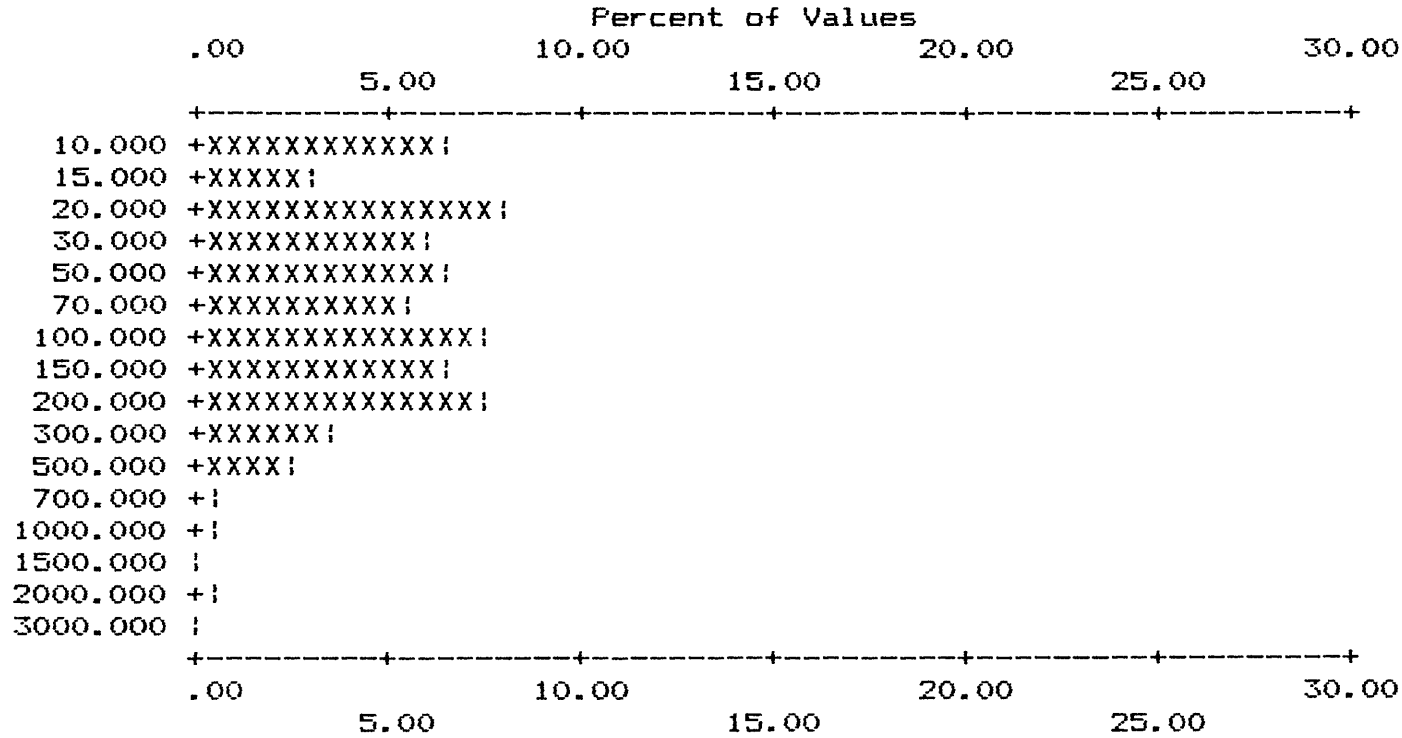

Each increment (each X or ¦ plotted) = .500 %

APPENDIX IV-A. HISTOGRAMS OF ROCK SAMPLE DATA, WHITE MTS NRA

COLUMN ID.: S-CU

	VALUE	NO.	%	CUM.	CUM. %		TOT CUM	TOT CUM %	
1	5.000	54	8.71	54	8.7	60.5	245	39.5	60.5
2	7.000	37	5.97	91	14.7	54.5	282	45.5	54.5
3	10.000	65	10.48	156	25.2	44.0	347	56.0	44.0
4	15.000	53	8.55	209	33.7	35.5	400	64.5	35.5
5	20.000	56	9.03	265	42.7	26.5	456	73.5	26.5
6	30.000	38	6.13	303	48.9	20.3	494	79.7	20.3
7	50.000	53	8.55	356	57.4	11.8	547	88.2	11.8
8	70.000	40	6.45	396	63.9	5.3	587	94.7	5.3
9	100.000	18	2.90	414	66.8	2.4	605	97.6	2.4
10	115.000	1	.16	415	66.9	2.3	606	97.7	2.3
11	150.000	9	1.45	424	68.4	.8	615	99.2	.8
12	200.000	4	.65	428	69.0	.2	619	99.8	.2
13	300.000	1	.16	429	69.2	.0	620	100.0	.0

B	T	H	N	L	G	OTHER	UNQUAL	ANAL	read	
0	0	0	77	114	0	0	429	620	620	VALUES
.0	.0	.0	12.4	18.4	.0	.0	69.2			PERCENT

MIN	MAX	AMEAN	SD	GMEAN	GD	VALUES
5.000	300.00	32.748	37.20	20.040	2.66	429
1.250	300.00	23.275	34.04	9.683	3.95	620

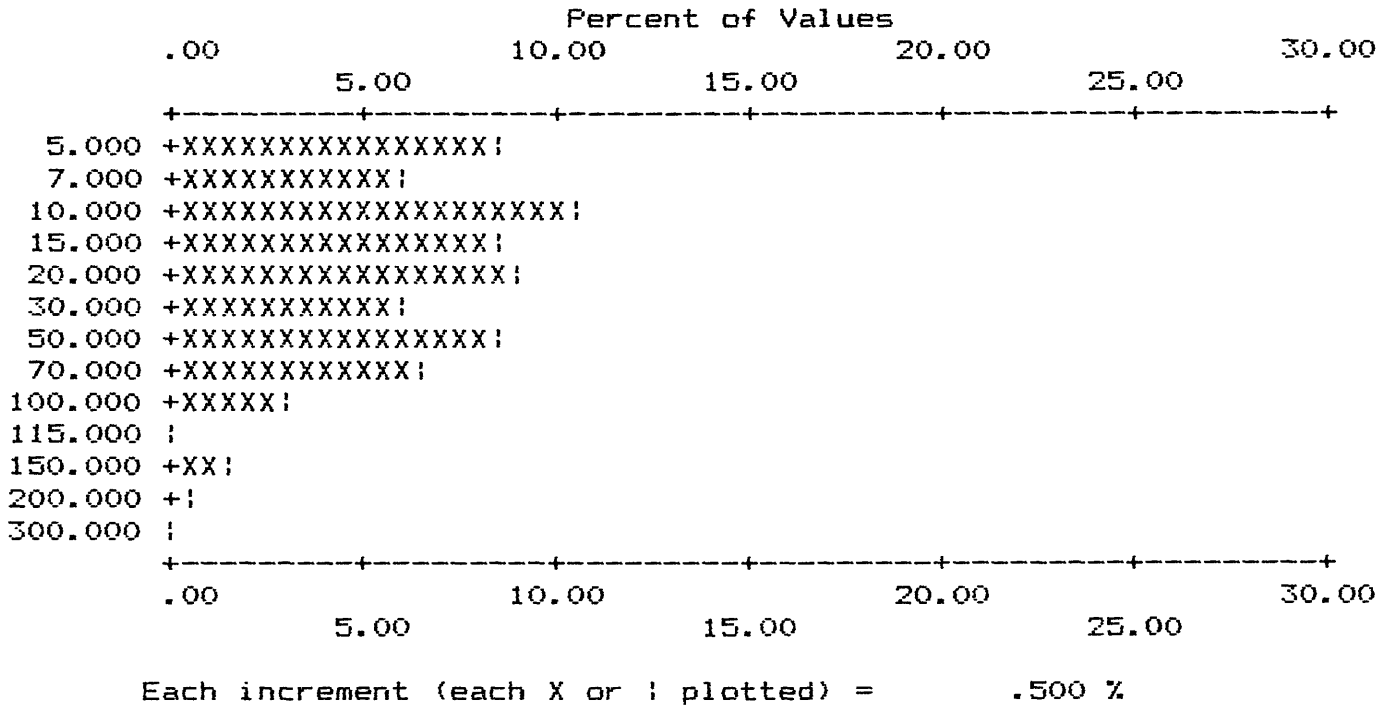

Each increment (each X or ¦ plotted) = .500 %

APPENDIX IV-A. HISTOGRAMS OF ROCK SAMPLE DATA, WHITE MTS NRA

COLUMN ID.: S-LA

	VALUE	NO.	%	CUM.	CUM. %		TOT CUM	TOT CUM %	
1	20.000	43	6.94	43	6.9	25.5	460	74.2	25.8
2	30.000	49	7.90	92	14.8	17.6	509	82.1	17.9
3	50.000	60	9.68	152	24.5	7.9	569	91.8	8.2
4	70.000	27	4.35	179	28.9	3.5	596	96.1	3.9
5	100.000	18	2.90	197	31.8	.6	614	99.0	1.0
6	200.000	1	.16	198	31.9	.5	615	99.2	.8
7	300.000	1	.16	199	32.1	.3	616	99.4	.6
8	500.000	1	.16	200	32.3	.2	617	99.5	.5
9	700.000	1	.16	201	32.4	.0	618	99.7	.3

B	T	H	N	L	G	OTHER	UNQUAL	ANAL	read	
0	0	0	381	36	2	0	201	620	620	VALUES
.0	.0	.0	61.5	5.8	.3	.0	32.4			PERCENT

MIN	MAX	AMEAN	SD	GMEAN	GD	VALUES
20.000	700.00	53.333	64.10	42.062	1.82	201
5.000	2000.00	27.395	120.19	10.585	2.95	620

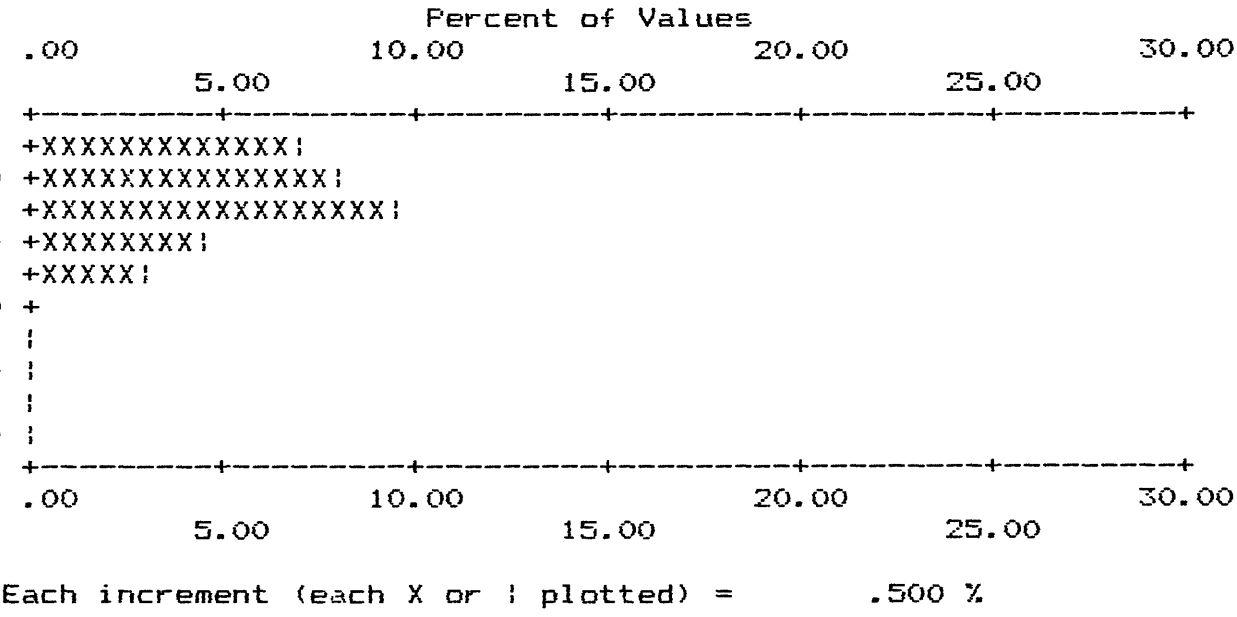

Each increment (each X or ¦ plotted) = .500 %

APPENDIX IV-A. HISTOGRAMS OF ROCK SAMPLE DATA, WHITE MTS NRA

COLUMN ID.: S-MO

	VALUE	NO.	%	CUM.	CUM. %		TOT CUM	TOT CUM %	
1	5.000	3	.48	3	.5	1.8	609	98.2	1.8
2	7.000	4	.65	7	1.1	1.1	613	98.9	1.1
3	10.000	3	.48	10	1.6	.6	616	99.4	.6
4	15.000	1	.16	11	1.8	.5	617	99.5	.5
5	20.000	1	.16	12	1.9	.3	618	99.7	.3
6	30.000	1	.16	13	2.1	.2	619	99.8	.2
7	50.000	1	.16	14	2.3	.0	620	100.0	.0

B	T	H	N	L	G	OTHER	UNQUAL	ANAL	read	
0	0	0	596	10	0	0	14	620	620	VALUES
.0	.0	.0	96.1	1.6	.0	.0	2.3			PERCENT

MIN	MAX	AMEAN	SD	GMEAN	GD	VALUES
5.000	50.00	13.429	12.62	10.217	2.02	14
1.250	50.00	1.545	2.58	1.325	1.40	620

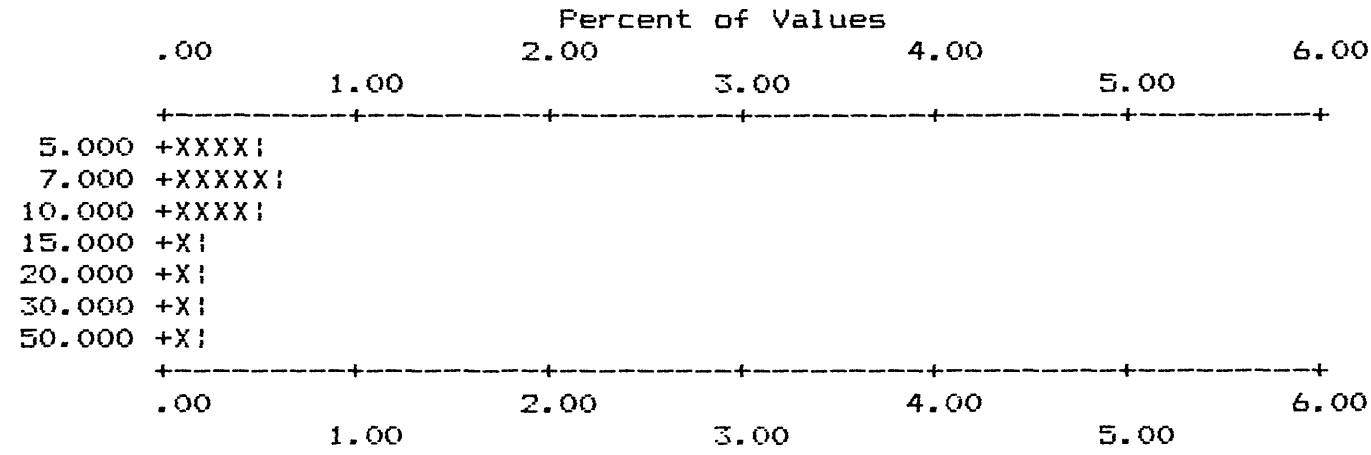

Each increment (each X or ! plotted) = .100 %

APPENDIX IV-A. HISTOGRAMS OF ROCK SAMPLE DATA, WHITE MTS NRA

COLUMN ID.: S-NB

	VALUE	NO.	%	CUM.	CUM. %		TOT CUM	TOT CUM %	
1	20.000	40	6.45	40	6.5	4.5	592	95.5	4.5
2	30.000	17	2.74	57	9.2	1.8	609	98.2	1.8
3	50.000	4	.65	61	9.8	1.1	613	98.9	1.1
4	70.000	5	.81	66	10.6	.3	618	99.7	.3
5	100.000	1	.16	67	10.8	.2	619	99.8	.2
6	200.000	1	.16	68	11.0	.0	620	100.0	.0

B	T	H	N	L	G	OTHER	UNQUAL	ANAL	read	
0	0	0	474	78	0	0	68	620	620	VALUES
.0	.0	.0	76.5	12.6	.0	.0	11.0			PERCENT

MIN	MAX	AMEAN	SD	GMEAN	GD	VALUES
20.000	200.00	31.765	26.54	27.130	1.62	68
5.000	200.00	8.565	12.06	6.567	1.77	620

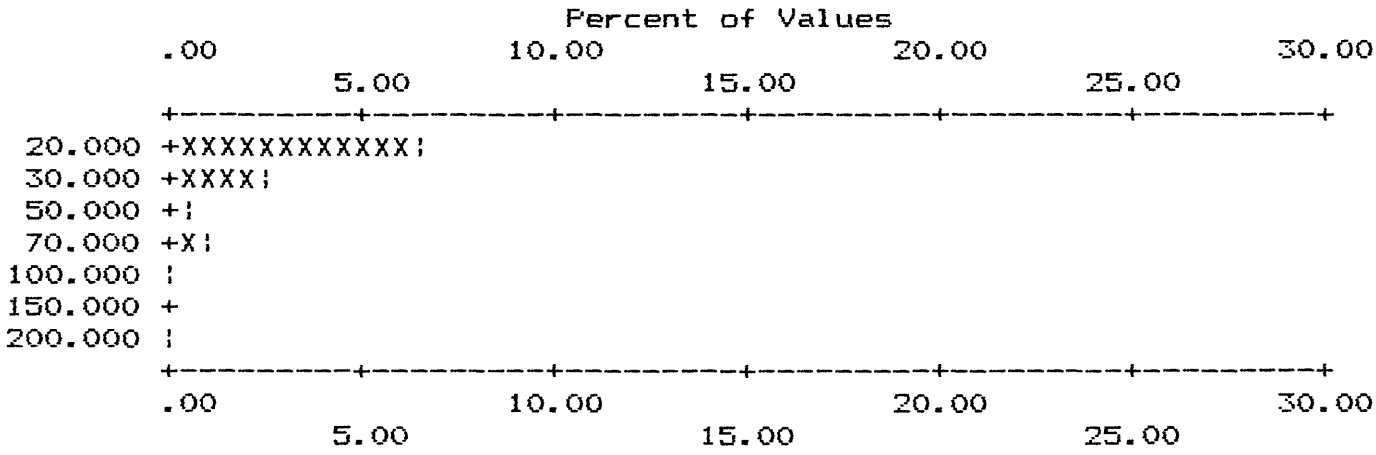

Each increment (each X or ¦ plotted) = .500 %

APPENDIX IV-A. HISTOGRAMS OF ROCK SAMPLE DATA, WHITE MTS NRA

COLUMN ID.: S-NI

	VALUE	NO.	%	CUM.	CUM. %	TOT CUM	TOT CUM %	
1	5.000	42	6.77	42	6.8	64.7	219	35.3	64.7
2	7.000	32	5.16	74	11.9	59.5	251	40.5	59.5
3	10.000	47	7.58	121	19.5	51.9	298	48.1	51.9
4	15.000	21	3.39	142	22.9	48.5	319	51.5	48.5
5	20.000	57	9.19	199	32.1	39.4	376	60.6	39.4
6	30.000	68	10.97	267	43.1	28.4	444	71.6	28.4
7	50.000	91	14.68	358	57.7	13.7	535	86.3	13.7
8	70.000	40	6.45	398	64.2	7.3	575	92.7	7.3
9	100.000	14	2.26	412	66.5	5.0	589	95.0	5.0
10	150.000	8	1.29	420	67.7	3.7	597	96.3	3.7
11	200.000	9	1.45	429	69.2	2.3	606	97.7	2.3
12	300.000	2	.32	431	69.5	1.9	608	98.1	1.9
13	500.000	4	.65	435	70.2	1.3	612	98.7	1.3
14	1000.000	7	1.13	442	71.3	.2	619	99.8	.2
15	5000.000	1	.16	443	71.5	.0	620	100.0	.0

B	T	H	N	L	G	OTHER	UNQUAL	ANAL	read	
0	0	0	121	56	0	0	443	620	620	VALUES
.0	.0	.0	19.5	9.0	.0	.0	71.5			PERCENT

MIN	MAX	AMEAN	SD	GMEAN	GD	VALUES
5.000	5000.00	69.411	270.10	27.508	3.07	443
1.250	5000.00	50.065	230.28	12.116	5.04	620

APPENDIX IV-A. HISTOGRAMS OF ROCK SAMPLE DATA, WHITE MTS NRA

COLUMN ID: S-NI

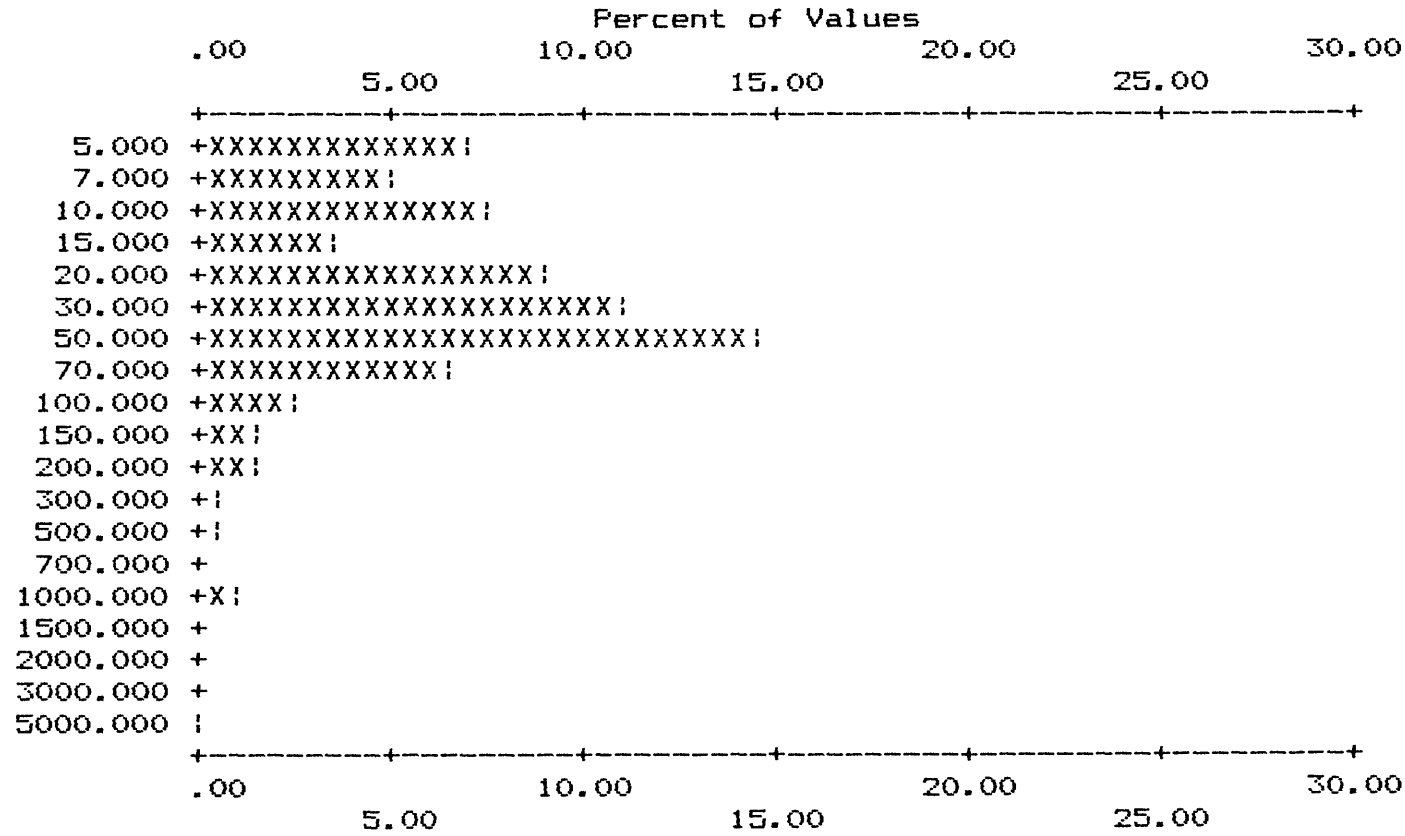

APPENDIX IV-A. HISTOGRAMS OF ROCK SAMPLE DATA, WHITE MTS NRA

COLUMN ID.: S-PB

	VALUE	NO.	%	CUM.	CUM. %		TOT CUM	TOT CUM %	
1	10.000	68	10.97	68	11.0	29.7	436	70.3	29.7
2	15.000	34	5.48	102	16.5	24.2	470	75.8	24.2
3	20.000	51	8.23	153	24.7	16.0	521	84.0	16.0
4	30.000	40	6.45	193	31.1	9.5	561	90.5	9.5
5	50.000	34	5.48	227	36.6	4.0	595	96.0	4.0
6	70.000	12	1.94	239	38.5	2.1	607	97.9	2.1
7	100.000	4	.65	243	39.2	1.5	611	98.5	1.5
8	150.000	2	.32	245	39.5	1.1	613	98.9	1.1
9	200.000	3	.48	248	40.0	.6	616	99.4	.6
10	300.000	3	.48	251	40.5	.2	619	99.8	.2
11	7000.000	1	.16	252	40.6	.0	620	100.0	.0

B	T	H	N	L	G	OTHER	UNQUAL	ANAL	read	
0	0	0	233	135	0	0	252	620	620	VALUES
.0	.0	.0	37.6	21.8	.0	.0	40.6			PERCENT

MIN	MAX	AMEAN	SD	GMEAN	GD	VALUES
10.000	7000.00	60.119	440.84	23.149	2.30	252
2.500	7000.00	26.464	282.10	7.184	3.11	620

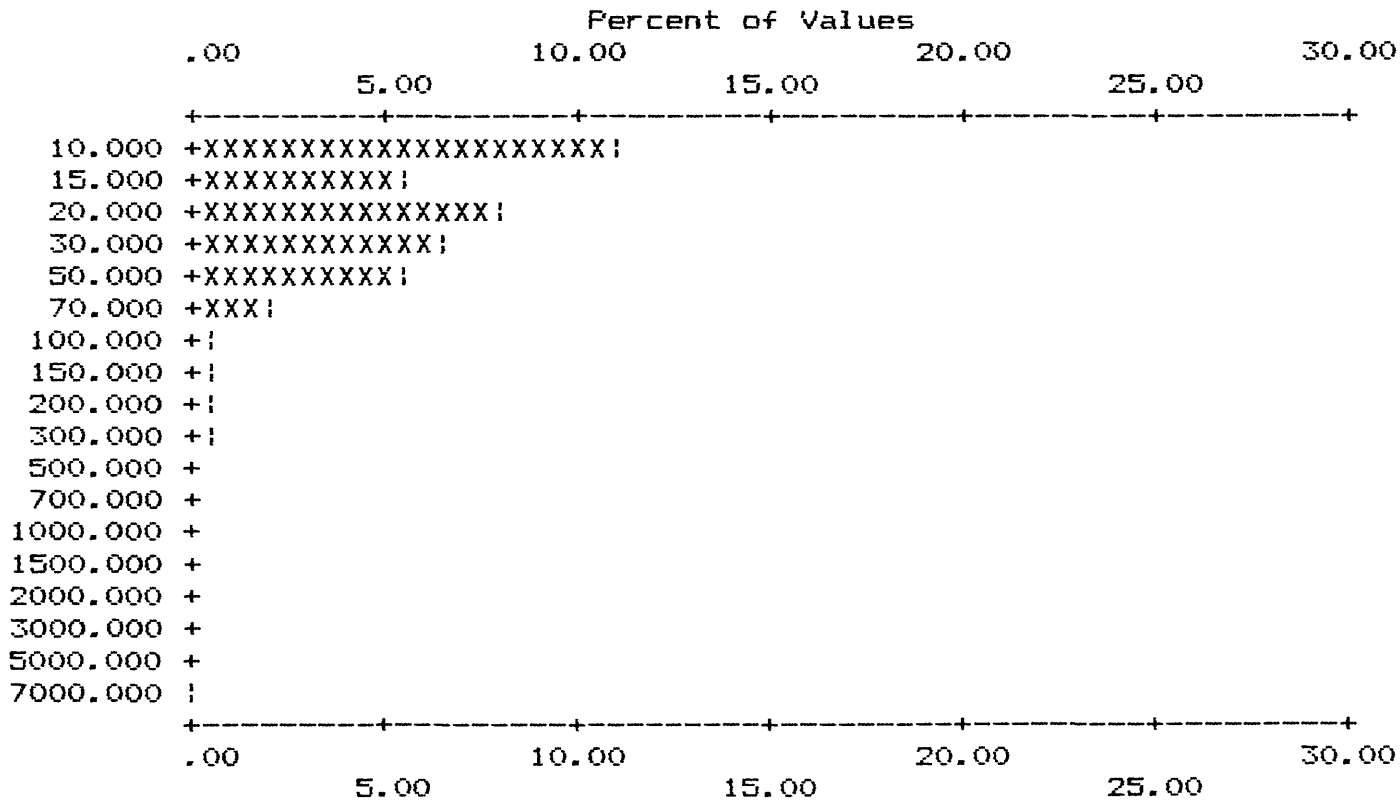

Each increment (each X or ! plotted) = .500 %

APPENDIX IV-A. HISTOGRAMS OF ROCK SAMPLE DATA, WHITE MTS NRA

COLUMN ID.: S-SB

	VALUE	NO.	%	CUM.	CUM. %	TOT CUM	TOT CUM %
1	100.000	3	.48	3	.5	620	100.0 .0

B	T	H	N	L	G	OTHER	UNQUAL	ANAL	read	
0	0	0	616	1	0	0	3	620	620	VALUES
.0	.0	.0	99.4	.2	.0	.0	.5			PERCENT

MIN	MAX	AMEAN	SD	GMEAN	GD	VALUES
100.000	100.00	100.000	.00	100.000	1.00	3
25.000	100.00	25.403	5.30	25.196	1.11	620

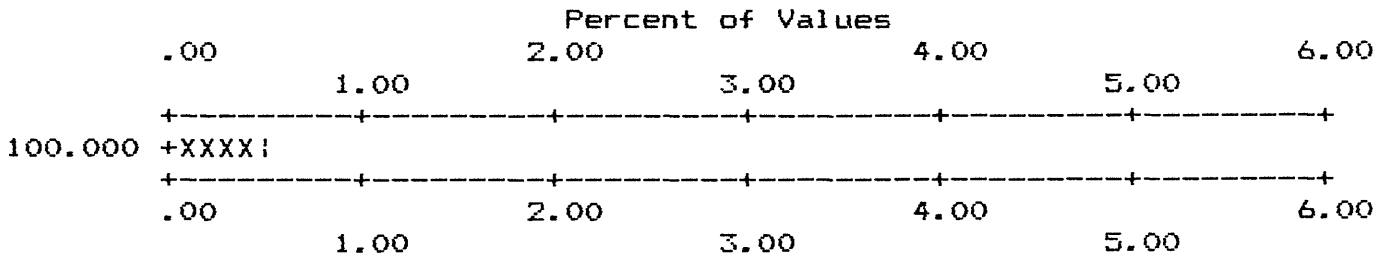

Each increment (each X or ¦ plotted) = .100 %

APPENDIX IV-A. HISTOGRAMS OF ROCK SAMPLE DATA, WHITE MTS NRA

COLUMN ID.: S-SC

	VALUE	NO.	%	CUM.	CUM. %		TOT CUM	TOT CUM %	
1	5.000	89	14.35	89	14.4	55.3	277	44.7	55.3
2	7.000	59	9.52	148	23.9	45.8	336	54.2	45.8
3	10.000	64	10.32	212	34.2	35.5	400	64.5	35.5
4	15.000	55	8.87	267	43.1	26.6	455	73.4	26.6
5	20.000	90	14.52	357	57.6	12.1	545	87.9	12.1
6	30.000	63	10.16	420	67.7	1.9	608	98.1	1.9
7	50.000	12	1.94	432	69.7	.0	620	100.0	.0

B	T	H	N	L	G	OTHER	UNQUAL	ANAL	read	
0	0	0	116	72	0	0	432	620	620	VALUES
.0	.0	.0	18.7	11.6	.0	.0	69.7			PERCENT

MIN	MAX	AMEAN	SD	GMEAN	GD	VALUES
5.000	50.00	15.308	10.26	12.330	1.94	432
1.250	50.00	11.190	10.60	6.676	3.00	620

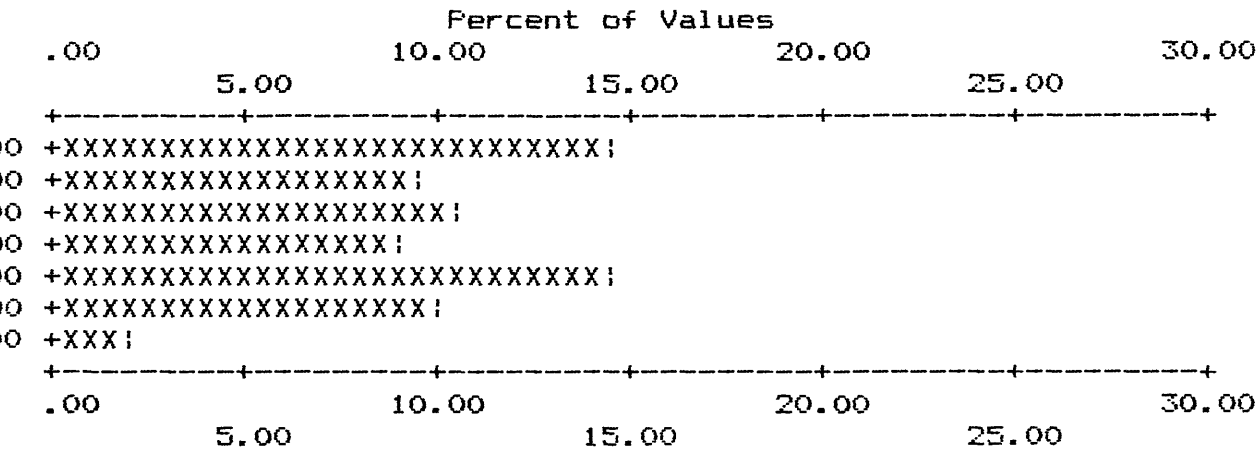

Each increment (each X or ¦ plotted) = .500 %

APPENDIX IV-A. HISTOGRAMS OF ROCK SAMPLE DATA, WHITE MTS NRA

COLUMN ID.: S-SN

	VALUE	NO.	%	CUM.	CUM. %		TOT CUM	TOT CUM %	
1	10.000	17	2.74	17	2.7	1.6	610	98.4	1.6
2	15.000	2	.32	19	3.1	1.3	612	98.7	1.3
3	20.000	4	.65	23	3.7	.6	616	99.4	.6
4	30.000	1	.16	24	3.9	.5	617	99.5	.5
5	70.000	1	.16	25	4.0	.3	618	99.7	.3
6	100.000	1	.16	26	4.2	.2	619	99.8	.2
7	150.000	1	.16	27	4.4	.0	620	100.0	.0

B	T	H	N	L	G	OTHER	UNQUAL	ANAL	read	
0	0	0	562	31	0	0	27	620	620	VALUES
.0	.0	.0	90.6	5.0	.0	.0	4.4			PERCENT

MIN	MAX	AMEAN	SD	GMEAN	GD	VALUES
10.000	150.00	23.333	32.43	15.389	2.13	27
2.500	150.00	3.532	7.90	2.801	1.53	620

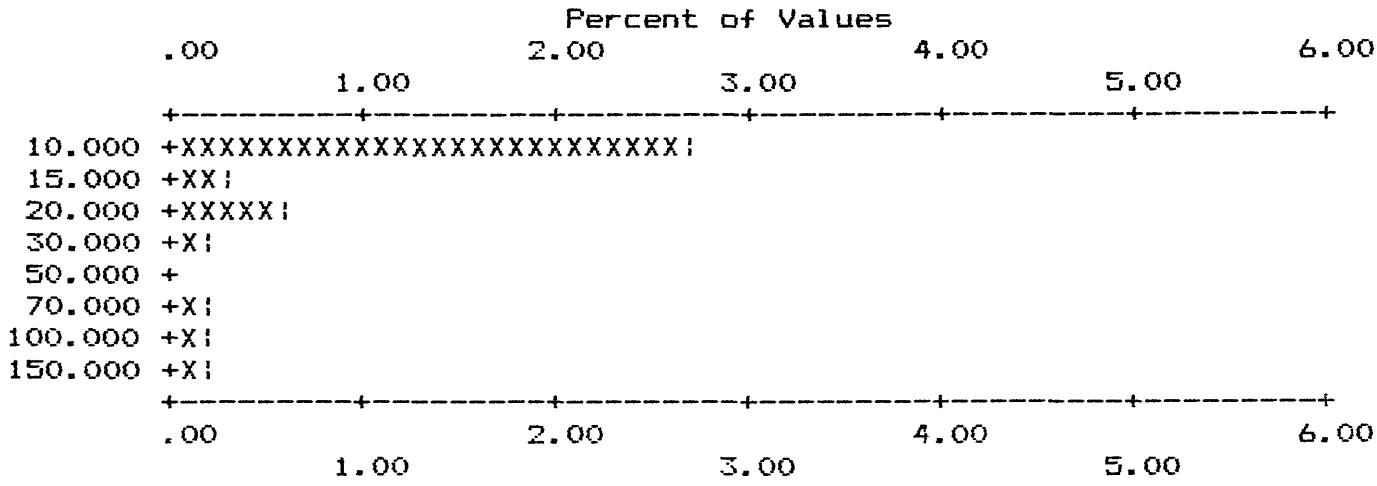

Each increment (each X or ¦ plotted) = .100 %

APPENDIX IV-A. HISTOGRAMS OF ROCK SAMPLE DATA, WHITE MTS NRA

COLUMN ID.: S-SR

	VALUE	NO.	%	CUM.	CUM. %		TOT CUM	TOT CUM %	
1	100.000	55	8.87	55	8.9	30.3	431	69.5	30.5
2	150.000	29	4.68	84	13.5	25.6	460	74.2	25.8
3	200.000	52	8.39	136	21.9	17.3	512	82.6	17.4
4	300.000	22	3.55	158	25.5	13.7	534	86.1	13.9
5	500.000	49	7.90	207	33.4	5.8	583	94.0	6.0
6	700.000	14	2.26	221	35.6	3.5	597	96.3	3.7
7	1000.000	12	1.94	233	37.6	1.6	609	98.2	1.8
8	1500.000	5	.81	238	38.4	.8	614	99.0	1.0
9	2000.000	3	.48	241	38.9	.3	617	99.5	.5
10	3000.000	1	.16	242	39.0	.2	618	99.7	.3
11	5000.000	1	.16	243	39.2	.0	619	99.8	.2

B	T	H	N	L	G	OTHER	UNQUAL	ANAL	read	
0	0	0	254	122	1	0	243	620	620	VALUES
.0	.0	.0	41.0	19.7	.2	.0	39.2			PERCENT

MIN	MAX	AMEAN	SD	GMEAN	GD	VALUES
100.000	5000.00	389.506	484.28	263.618	2.27	243
25.000	10000.00	188.871	527.08	72.834	3.33	620

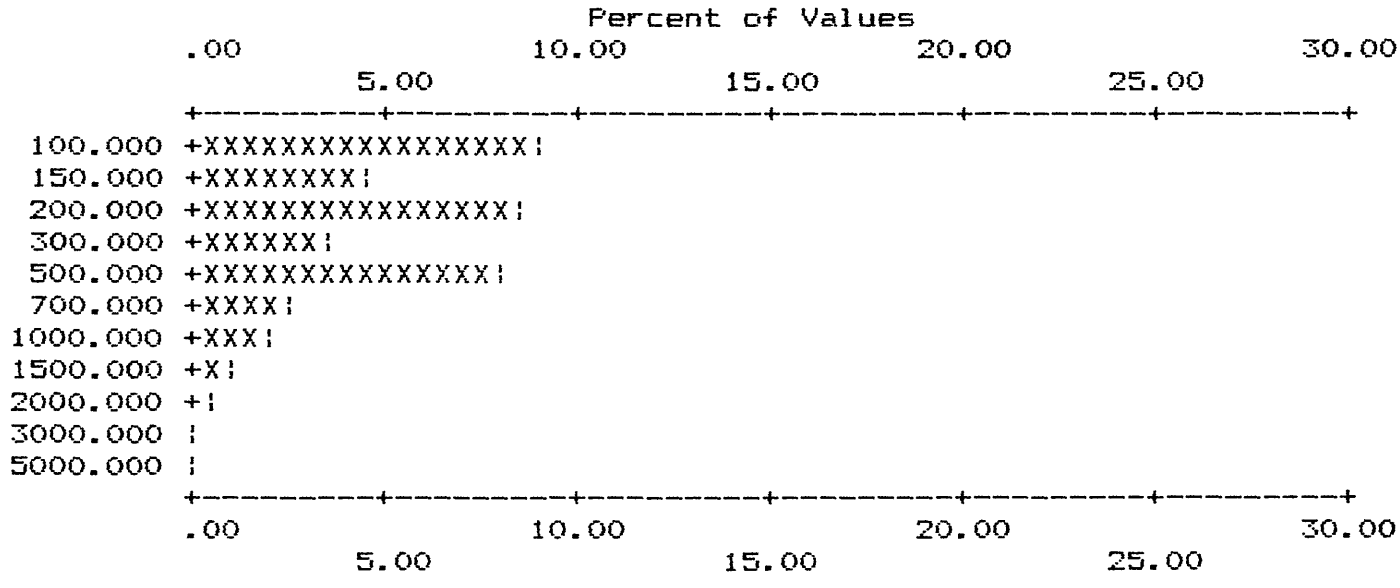

Each increment (each X or ¦ plotted) = .500 %

APPENDIX IV-A. HISTOGRAMS OF ROCK SAMPLE DATA, WHITE MTS NRA

COLUMN ID.: S-V

	VALUE	NO.	%	CUM.	CUM. %	TOT CUM	TOT CUM %	
1	10.000	57	9.19	57	9.2	81.5	115	18.5	81.5
2	15.000	29	4.68	86	13.9	76.8	144	23.2	76.8
3	20.000	61	9.84	147	23.7	66.9	205	33.1	66.9
4	30.000	32	5.16	179	28.9	61.8	237	38.2	61.8
5	50.000	54	8.71	233	37.6	53.1	291	46.9	53.1
6	70.000	61	9.84	294	47.4	43.2	352	56.8	43.2
7	100.000	95	15.32	389	62.7	27.9	447	72.1	27.9
8	150.000	67	10.81	456	73.5	17.1	514	82.9	17.1
9	200.000	76	12.26	532	85.8	4.8	590	95.2	4.8
10	300.000	19	3.06	551	88.9	1.8	609	98.2	1.8
11	500.000	9	1.45	560	90.3	.3	618	99.7	.3
12	700.000	2	.32	562	90.6	.0	620	100.0	.0

B	T	H	N	L	G	OTHER	UNQUAL	ANAL	read	
0	0	0	12	46	0	0	562	620	620	VALUES
.0	.0	.0	1.9	7.4	.0	.0	90.6			PERCENT

MIN	MAX	AMEAN	SD	GMEAN	GD	VALUES
10.000	700.00	100.543	96.79	62.621	2.87	562
2.500	700.00	91.556	96.30	48.775	3.57	620

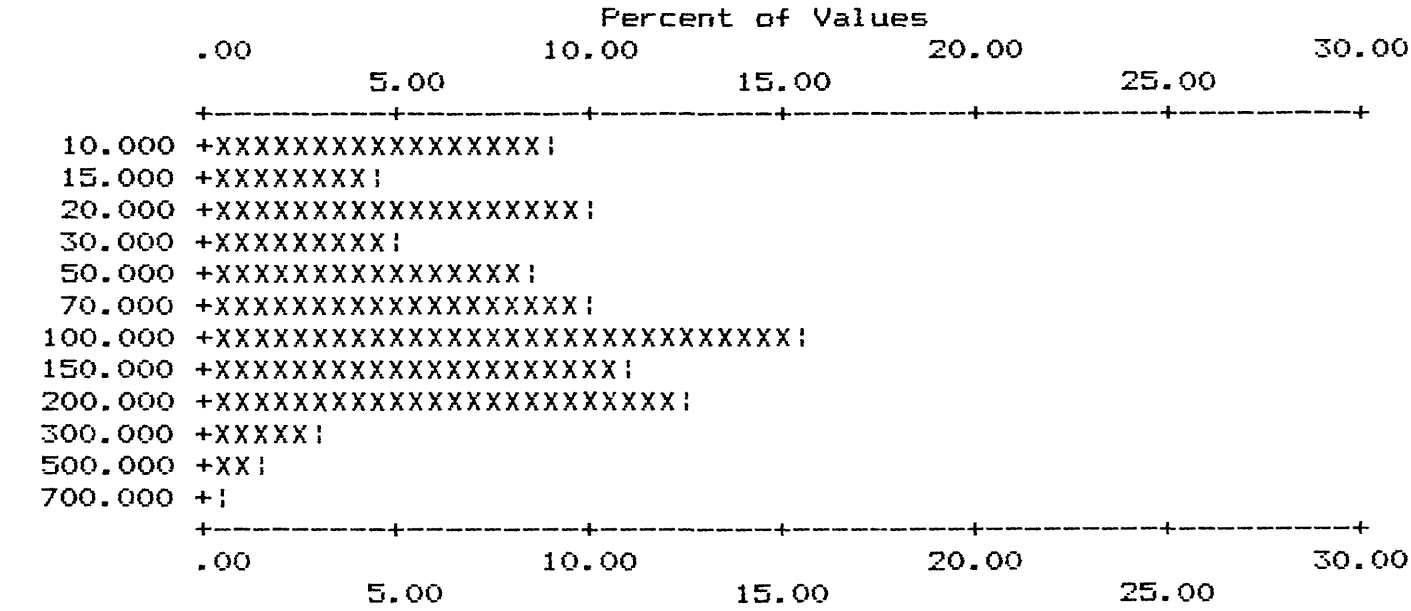

Each increment (each X or ! plotted) = .500 %

APPENDIX IV-A. HISTOGRAMS OF ROCK SAMPLE DATA, WHITE MTS NRA

COLUMN ID.: S-Y

	VALUE	NO.	%	CUM.	CUM. %		TOT CUM	TOT CUM %	
1	10.000	75	12.10	75	12.1	66.5	206	33.2	66.8
2	15.000	81	13.06	156	25.2	53.4	287	46.3	53.7
3	20.000	163	26.29	319	51.5	27.1	450	72.6	27.4
4	30.000	79	12.74	398	64.2	14.4	529	85.3	14.7
5	50.000	53	8.55	451	72.7	5.8	582	93.9	6.1
6	70.000	23	3.71	474	76.5	2.1	605	97.6	2.4
7	100.000	9	1.45	483	77.9	.6	614	99.0	1.0
8	150.000	3	.48	486	78.4	.2	617	99.5	.5
9	300.000	1	.16	487	78.5	.0	618	99.7	.3

B	T	H	N	L	G	OTHER	UNQUAL	ANAL	read	
0	0	0	80	51	2	0	487	620	620	VALUES
.0	.0	.0	12.9	8.2	.3	.0	78.5			PERCENT

MIN	MAX	AMEAN	SD	GMEAN	GD	VALUES
10.000	300.00	27.731	24.01	22.500	1.81	487
2.500	4000.00	35.419	226.94	15.226	2.75	620

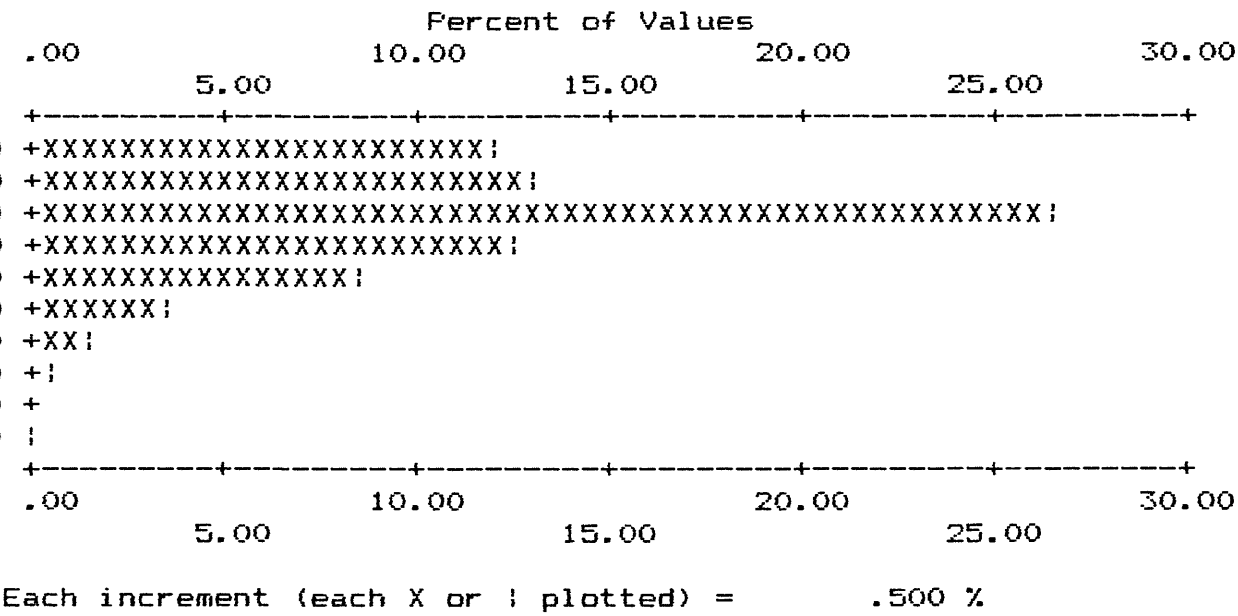

Each increment (each X or ¦ plotted) = .500 %

APPENDIX IV-A. HISTOGRAMS OF ROCK SAMPLE DATA, WHITE MTS NRA

COLUMN ID.: S-ZN

	VALUE	NO.	%	CUM.	CUM. %		TOT CUM	TOT CUM %	
1	200.000	20	3.23	20	3.2	2.1	607	97.9	2.1
2	300.000	5	.81	25	4.0	1.3	612	98.7	1.3
3	500.000	3	.48	28	4.5	.8	615	99.2	.8
4	1000.000	3	.48	31	5.0	.3	618	99.7	.3
5	2000.000	2	.32	33	5.3	.0	620	100.0	.0

B	T	H	N	L	G	OTHER	UNQUAL	ANAL	read	
0	0	0	565	22	0	0	33	620	620	VALUES
.0	.0	.0	91.1	3.5	.0	.0	5.3			PERCENT

MIN	MAX	AMEAN	SD	GMEAN	GD	VALUES
200.000	2000.00	424.242	469.73	307.634	2.01	33
50.000	2000.00	71.694	135.98	56.448	1.57	620

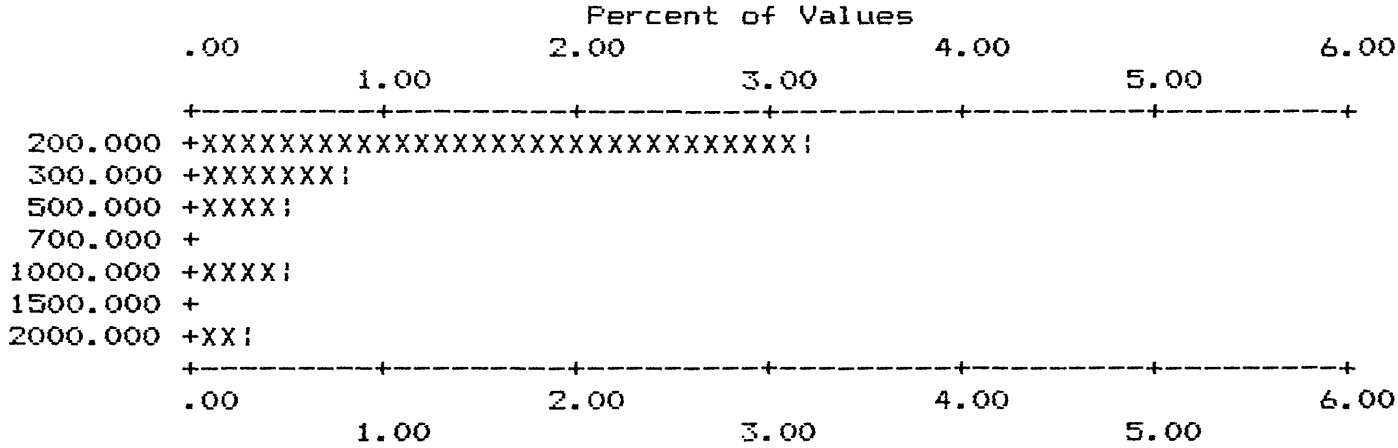

Each increment (each X or ¦ plotted) = .100 %

APPENDIX IV-A. HISTOGRAMS OF ROCK SAMPLE DATA, WHITE MTS NRA

COLUMN ID.: S-ZR

	VALUE	NO.	%	CUM.	CUM. %		TOT CUM	TOT CUM %	
1	10.000	29	4.68	29	4.7	84.7	91	14.7	85.3
2	15.000	6	.97	35	5.6	83.7	97	15.6	84.4
3	20.000	24	3.87	59	9.5	79.8	121	19.5	80.5
4	30.000	13	2.10	72	11.6	77.7	134	21.6	78.4
5	50.000	47	7.58	119	19.2	70.2	181	29.2	70.8
6	70.000	76	12.26	195	31.5	57.9	257	41.5	58.5
7	100.000	146	23.55	341	55.0	34.4	403	65.0	35.0
8	150.000	78	12.58	419	67.6	21.8	481	77.6	22.4
9	200.000	63	10.16	482	77.7	11.6	544	87.7	12.3
10	300.000	48	7.74	530	85.5	3.9	592	95.5	4.5
11	500.000	16	2.58	546	88.1	1.3	608	98.1	1.9
12	700.000	4	.65	550	88.7	.6	612	98.7	1.3
13	1000.000	4	.65	554	89.4	.0	616	99.4	.6

B	T	H	N	L	G	OTHER	UNQUAL	ANAL	read	
0	0	0	45	17	4	0	554	620	620	VALUES
.0	.0	.0	7.3	2.7	.6	.0	89.4			PERCENT

MIN	MAX	AMEAN	SD	GMEAN	GD	VALUES
10.000	1000.00	139.025	133.28	96.220	2.51	554
2.500	2000.00	137.448	200.23	69.420	3.99	620

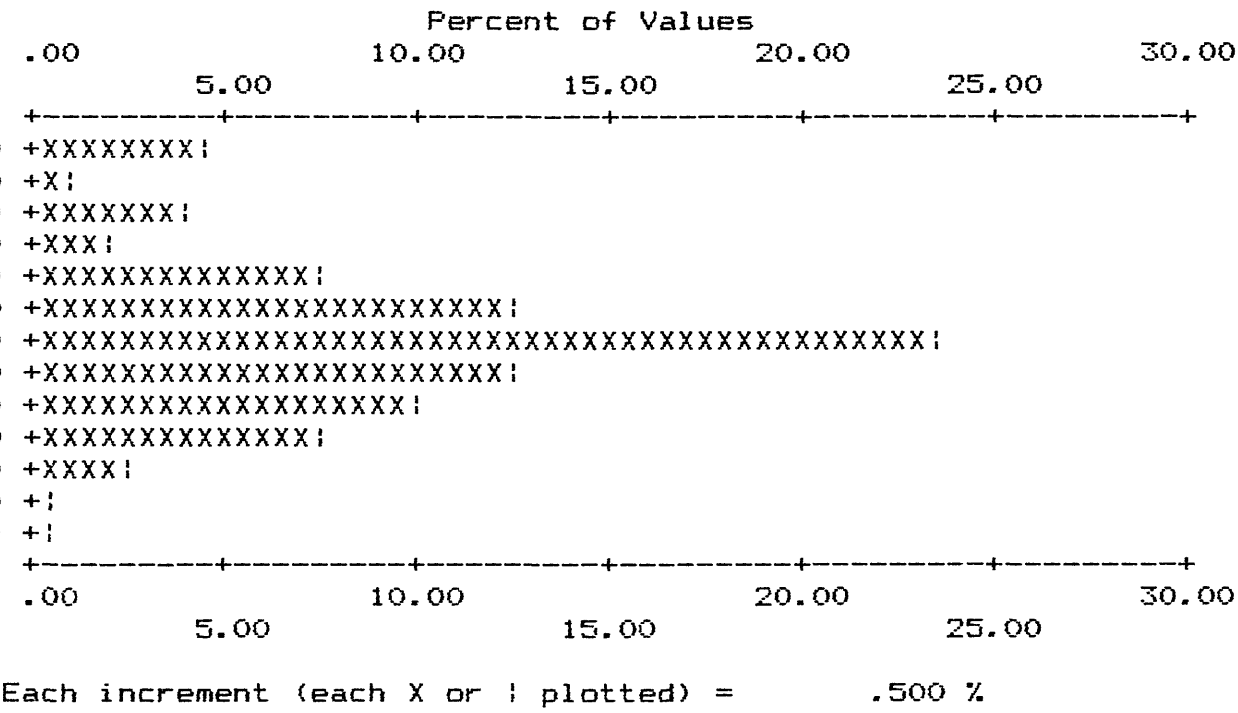

Each increment (each X or ! plotted) = .500 %

APPENDIX IV-A. HISTOGRAMS OF ROCK SAMPLE DATA, WHITE MTS NRA

COLUMN ID.: S-TH

	VALUE	NO.	%	CUM.	CUM. %	TOT CUM	TOT CUM %
1	200.000	2	.32	2	.3	618	99.7 .3

B	T	H	N	L	G	OTHER	UNQUAL	ANAL	read	
0	0	0	616	0	2	0	2	620	620	VALUES
.0	.0	.0	99.4	.0	.3	.0	.3			PERCENT

MIN	MAX	AMEAN	SD	GMEAN	GD	VALUES
200.000	200.00	200.000	.00	200.000	1.00	2
25.000	4000.00	38.387	225.77	25.584	1.37	620

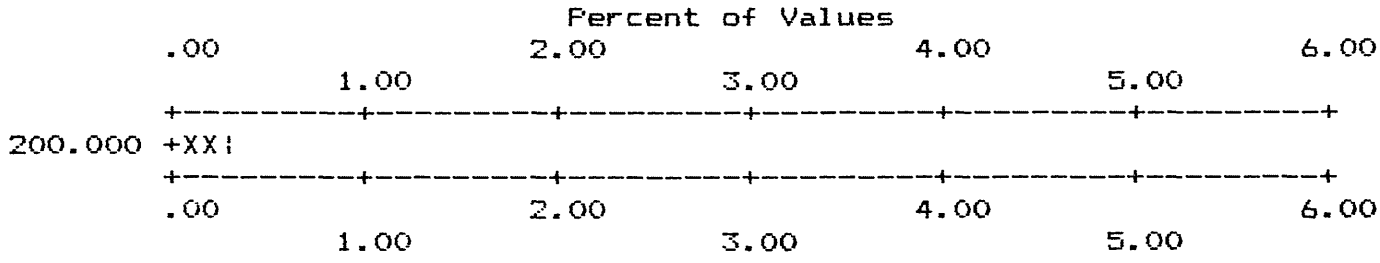

Each increment (each X or ! plotted) = .100 %

APPENDIX IV-A. HISTOGRAMS OF ROCK SAMPLE DATA, WHITE MTS NRA

COLUMN ID.: AA-AU-P

	VALUE	NO.	%	CUM.	CUM. %	TOT CUM	TOT CUM %
1	.150	1	1.64	1	1.6	.0	61	100.0	.0

B	T	H	N	L	G	OTHER	UNQUAL	ANAL	read	
559	0	0	60	0	0	0	1	61	620	VALUES
90.2	.0	.0	9.7	.0	.0	.0	.2			PERCENT

MIN	MAX	AMEAN	SD	GMEAN	GD	VALUES
.150	.15	.150	.00	.150	********	1
.012	.15	.015	.02	.013	1.37	61

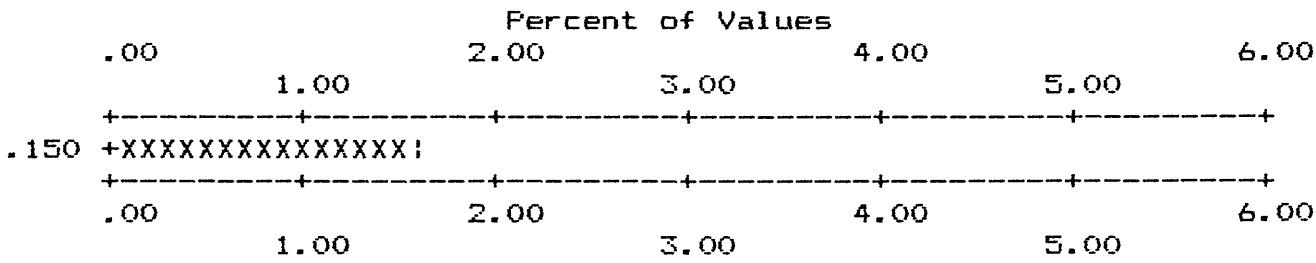

Each increment (each X or ! plotted) = .100 %

APPENDIX IV-A. HISTOGRAMS OF ROCK SAMPLE DATA, WHITE MTS NRA

COLUMN ID.: AA-AS-P

	VALUE	NO.	%	CUM.	CUM. %		TOT CUM	TOT CUM %	
1	10.000	51	10.56	51	10.6	7.7	444	91.9	8.1
2	20.000	16	3.31	67	13.9	4.3	460	95.2	4.8
3	30.000	5	1.04	72	14.9	3.3	465	96.3	3.7
4	40.000	4	.83	76	15.7	2.5	469	97.1	2.9
5	50.000	3	.62	79	16.4	1.9	472	97.7	2.3
6	70.000	2	.41	81	16.8	1.4	474	98.1	1.9
7	100.000	1	.21	82	17.0	1.2	475	98.3	1.7
8	120.000	1	.21	83	17.2	1.0	476	98.6	1.4
9	150.000	1	.21	84	17.4	.8	477	98.8	1.2
10	180.000	2	.41	86	17.8	.4	479	99.2	.8
11	500.000	1	.21	87	18.0	.2	480	99.4	.6
12	1000.000	1	.21	88	18.2	.0	481	99.6	.4

B	T	H	N	L	G	OTHER	UNQUAL	ANAL	read	
137	0	0	393	0	2	0	88	483	620	VALUES
22.1	.0	.0	63.4	.0	.3	.0	14.2			PERCENT

MIN	MAX	AMEAN	SD	GMEAN	GD	VALUES
10.000	1000.00	41.591	119.83	18.189	2.57	88
2.500	4000.00	26.175	261.95	3.700	2.65	483

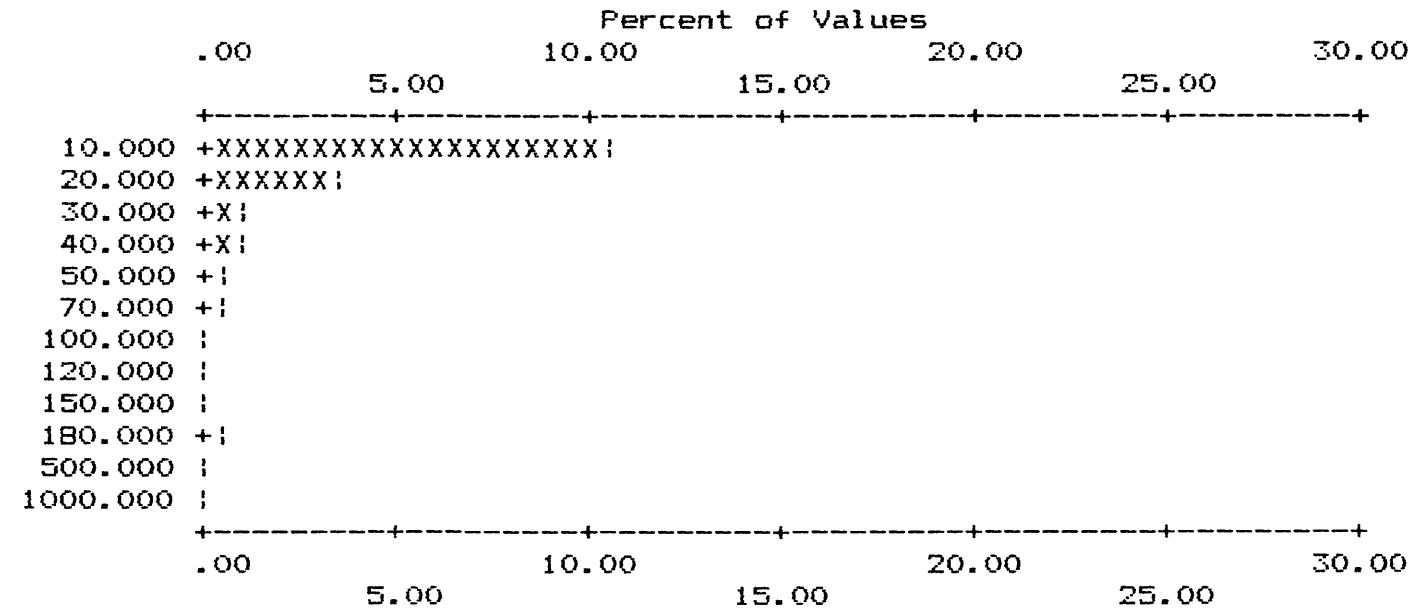

Each increment (each X or ¦ plotted) = .500 %

APPENDIX IV-A. HISTOGRAMS OF ROCK SAMPLE DATA, WHITE MTS NRA

COLUMN ID.: AA-BI-P

	VALUE	NO.	%	CUM.	CUM. %	TOT CUM	TOT CUM %	
1	1.000	2	.41	2	.4	3.1	468	96.9	3.1
2	2.000	5	1.04	7	1.4	2.1	473	97.9	2.1
3	3.000	4	.83	11	2.3	1.2	477	98.8	1.2
4	6.000	2	.41	13	2.7	.8	479	99.2	.8
5	10.000	1	.21	14	2.9	.6	480	99.4	.6
6	20.000	2	.41	16	3.3	.2	482	99.8	.2
7	56.000	1	.21	17	3.5	.0	483	100.0	.0

B	T	H	N	L	G	OTHER	UNQUAL	ANAL	read	
137	0	0	466	0	0	0	17	483	620	VALUES
22.1	.0	.0	75.2	.0	.0	.0	2.7			PERCENT

MIN	MAX	AMEAN	SD	GMEAN	GD	VALUES
1.000	56.00	8.353	13.65	4.046	3.05	17
.250	56.00	.535	2.90	.276	1.74	483

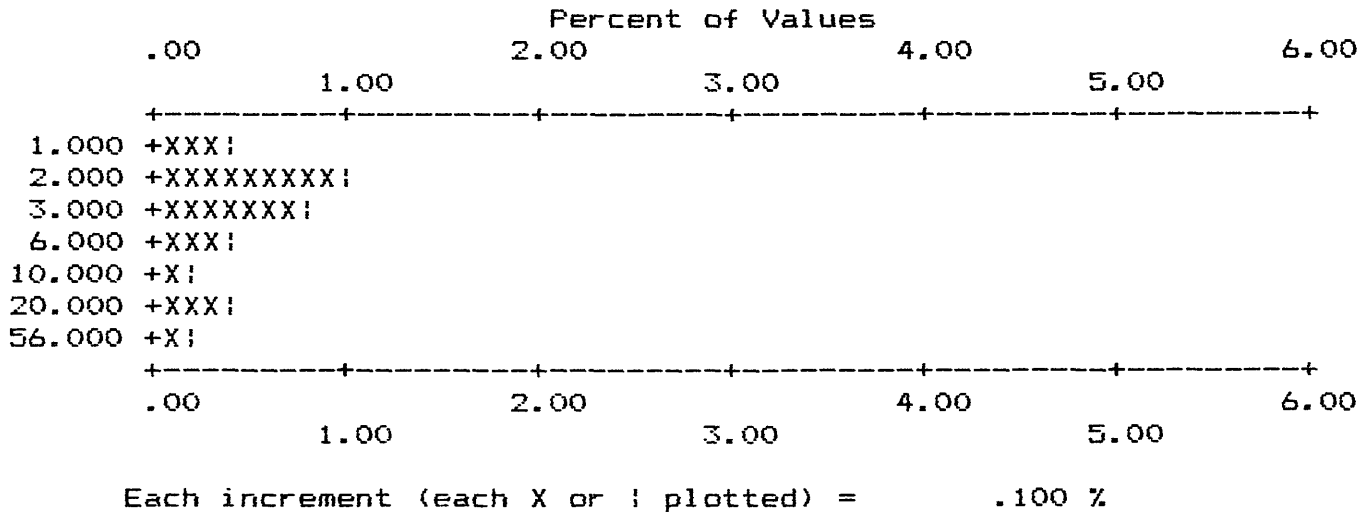

Each increment (each X or ! plotted) = .100 %

APPENDIX IV-A. HISTOGRAMS OF ROCK SAMPLE DATA, WHITE MTS NRA

COLUMN ID.: AA-CD-P

	VALUE	NO.	%	CUM.	CUM. %		TOT CUM	TOT CUM %	
1	.100	97	20.08	97	20.1	33.3	322	66.7	33.3
2	.200	70	14.49	167	34.6	18.8	392	81.2	18.8
3	.250	1	.21	168	34.8	18.6	393	81.4	18.6
4	.300	22	4.55	190	39.3	14.1	415	85.9	14.1
5	.400	9	1.86	199	41.2	12.2	424	87.8	12.2
6	.500	8	1.66	207	42.9	10.6	432	89.4	10.6
7	.600	7	1.45	214	44.3	9.1	439	90.9	9.1
8	.700	4	.83	218	45.1	8.3	443	91.7	8.3
9	.800	2	.41	220	45.5	7.9	445	92.1	7.9
10	.900	2	.41	222	46.0	7.5	447	92.5	7.5
11	1.000	1	.21	223	46.2	7.2	448	92.8	7.2
12	1.100	3	.62	226	46.8	6.6	451	93.4	6.6
13	1.200	1	.21	227	47.0	6.4	452	93.6	6.4
14	1.300	1	.21	228	47.2	6.2	453	93.8	6.2
15	1.400	2	.41	230	47.6	5.8	455	94.2	5.8
16	1.500	1	.21	231	47.8	5.6	456	94.4	5.6
17	1.600	1	.21	232	48.0	5.4	457	94.6	5.4
18	1.700	1	.21	233	48.2	5.2	458	94.8	5.2
19	2.000	3	.62	236	48.9	4.6	461	95.4	4.6
20	2.100	1	.21	237	49.1	4.3	462	95.7	4.3
21	2.300	3	.62	240	49.7	3.7	465	96.3	3.7
22	2.400	1	.21	241	49.9	3.5	466	96.5	3.5
23	2.500	2	.41	243	50.3	3.1	468	96.9	3.1
24	2.600	2	.41	245	50.7	2.7	470	97.3	2.7
25	3.000	4	.83	249	51.6	1.9	474	98.1	1.9
26	3.500	1	.21	250	51.8	1.7	475	98.3	1.7
27	3.700	1	.21	251	52.0	1.4	476	98.6	1.4
28	4.000	1	.21	252	52.2	1.2	477	98.8	1.2
29	4.100	1	.21	253	52.4	1.0	478	99.0	1.0
30	6.100	1	.21	254	52.6	.8	479	99.2	.8
31	8.900	1	.21	255	52.8	.6	480	99.4	.6
32	15.000	1	.21	256	53.0	.4	481	99.6	.4
33	26.000	1	.21	257	53.2	.2	482	99.8	.2
34	33.000	1	.21	258	53.4	.0	483	100.0	.0

B	T	H	N	L	G	OTHER	UNQUAL	ANAL	read	
137	0	0	209	16	0	0	258	483	620	VALUES
22.1	.0	.0	33.7	2.6	.0	.0	41.6			PERCENT

MIN	MAX	AMEAN	SD	GMEAN	GD	VALUES
.100	33.00	.802	2.88	.260	3.13	258
.025	33.00	.441	2.14	.089	4.14	483

APPENDIX IV-A. HISTOGRAMS OF ROCK SAMPLE DATA, WHITE MTS NRA

COLUMN ID: AA-CD-P

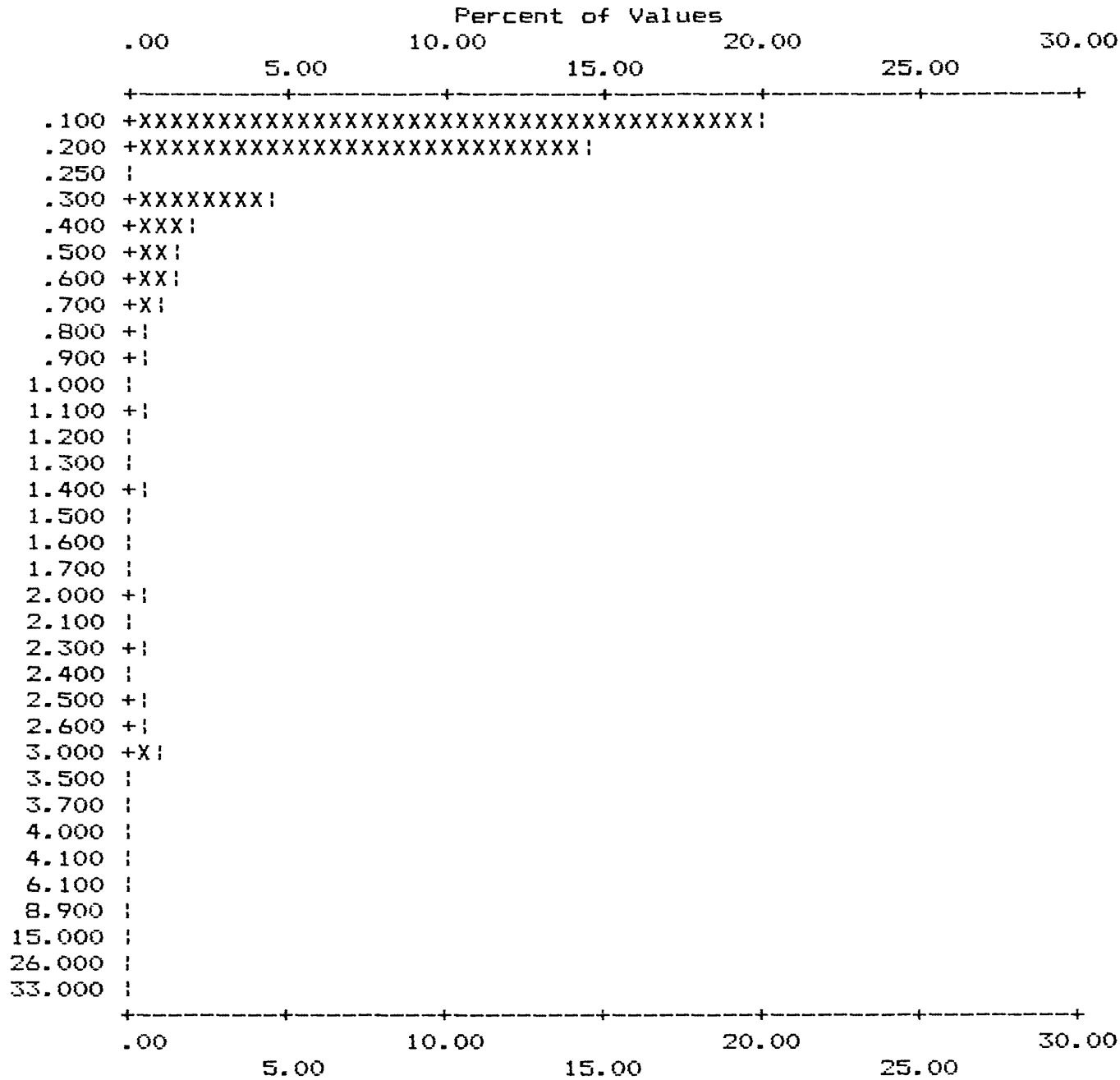

Each increment (each X or ! plotted) = .500 %

APPENDIX IV-A. HISTOGRAMS OF ROCK SAMPLE DATA, WHITE MTS NRA

COLUMN ID.: AA-SB-P

	VALUE	NO.	%	CUM.	CUM. %		TOT CUM	TOT CUM %	
1	2.000	37	7.66	37	7.7	9.5	437	90.5	9.5
2	4.000	15	3.11	52	10.8	6.4	452	93.6	6.4
3	6.000	9	1.86	61	12.6	4.6	461	95.4	4.6
4	8.000	2	.41	63	13.0	4.1	463	95.9	4.1
5	10.000	5	1.04	68	14.1	3.1	468	96.9	3.1
6	12.000	1	.21	69	14.3	2.9	469	97.1	2.9
7	14.000	2	.41	71	14.7	2.5	471	97.5	2.5
8	15.000	1	.21	72	14.9	2.3	472	97.7	2.3
9	16.000	1	.21	73	15.1	2.1	473	97.9	2.1
10	22.000	1	.21	74	15.3	1.9	474	98.1	1.9
11	26.000	1	.21	75	15.5	1.7	475	98.3	1.7
12	30.000	2	.41	77	15.9	1.2	477	98.8	1.2
13	32.000	1	.21	78	16.1	1.0	478	99.0	1.0
14	38.000	2	.41	80	16.6	.6	480	99.4	.6
15	46.000	1	.21	81	16.8	.4	481	99.6	.4
16	82.000	1	.21	82	17.0	.2	482	99.8	.2
17	120.000	1	.21	83	17.2	.0	483	100.0	.0

B	T	H	N	L	G	OTHER	UNQUAL	ANAL	read	
137	0	0	400	0	0	0	83	483	620	VALUES
22.1	.0	.0	64.5	.0	.0	.0	13.4			PERCENT

MIN	MAX	AMEAN	SD	GMEAN	GD	VALUES
2.000	120.00	9.506	17.45	4.697	2.78	83
.500	120.00	2.048	7.96	.735	2.57	483

APPENDIX IV-A. HISTOGRAMS OF ROCK SAMPLE DATA, WHITE MTS NRA

COLUMN ID: AA-SB-P

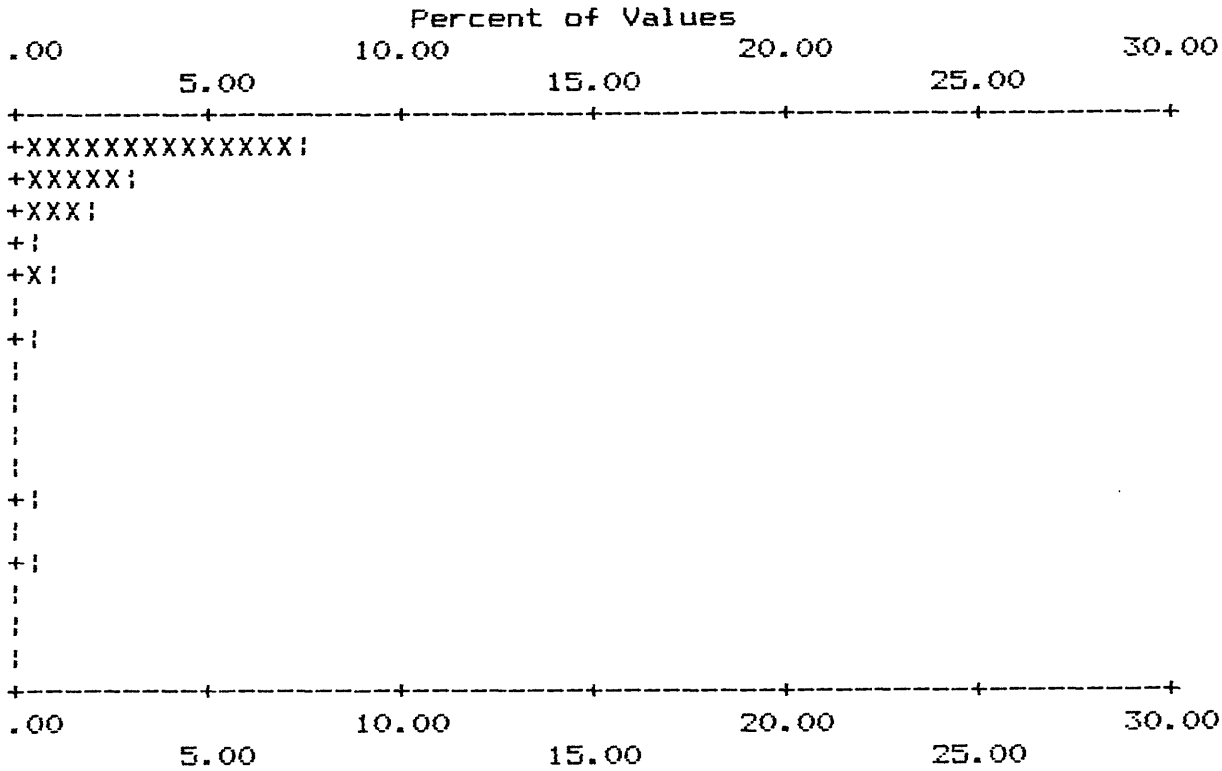

Each increment (each X or ! plotted) = .500 %

APPENDIX IV-A. HISTOGRAMS OF ROCK SAMPLE DATA, WHITE MTS NRA

COLUMN ID.: AA-ZN-P

	VALUE	NO.	%	CUM.	CUM. %		TOT CUM	TOT CUM %	
1	5.000	22	4.55	22	4.6	88.4	54	11.2	88.8
2	10.000	30	6.21	52	10.8	82.2	84	17.4	82.6
3	15.000	27	5.59	79	16.4	76.6	111	23.0	77.0
4	20.000	32	6.63	111	23.0	70.0	143	29.6	70.4
5	25.000	26	5.38	137	28.4	64.6	169	35.0	65.0
6	30.000	31	6.42	168	34.8	58.2	200	41.4	58.6
7	35.000	15	3.11	183	37.9	55.1	215	44.5	55.5
8	40.000	12	2.48	195	40.4	52.6	227	47.0	53.0
9	45.000	19	3.93	214	44.3	48.7	246	50.9	49.1
10	50.000	19	3.93	233	48.2	44.7	265	54.9	45.1
11	55.000	23	4.76	256	53.0	40.0	288	59.6	40.4
12	60.000	17	3.52	273	56.5	36.4	305	63.1	36.9
13	65.000	15	3.11	288	59.6	33.3	320	66.3	33.7
14	70.000	15	3.11	303	62.7	30.2	335	69.4	30.6
15	75.000	12	2.48	315	65.2	27.7	347	71.8	28.2
16	80.000	15	3.11	330	68.3	24.6	362	74.9	25.1
17	85.000	12	2.48	342	70.8	22.2	374	77.4	22.6
18	90.000	8	1.66	350	72.5	20.5	382	79.1	20.9
19	95.000	11	2.28	361	74.7	18.2	393	81.4	18.6
20	100.000	17	3.52	378	78.3	14.7	410	84.9	15.1
21	110.000	10	2.07	388	80.3	12.6	420	87.0	13.0
22	115.000	1	.21	389	80.5	12.4	421	87.2	12.8
23	120.000	2	.41	391	81.0	12.0	423	87.6	12.4
24	130.000	9	1.86	400	82.8	10.1	432	89.4	10.6
25	135.000	2	.41	402	83.2	9.7	434	89.9	10.1
26	140.000	3	.62	405	83.9	9.1	437	90.5	9.5
27	150.000	3	.62	408	84.5	8.5	440	91.1	8.9
28	160.000	1	.21	409	84.7	8.3	441	91.3	8.7
29	170.000	2	.41	411	85.1	7.9	443	91.7	8.3
30	190.000	4	.83	415	85.9	7.0	447	92.5	7.5
31	200.000	2	.41	417	86.3	6.6	449	93.0	7.0
32	220.000	2	.41	419	86.7	6.2	451	93.4	6.6
33	240.000	1	.21	420	87.0	6.0	452	93.6	6.4
34	250.000	4	.83	424	87.8	5.2	456	94.4	5.6
35	260.000	1	.21	425	88.0	5.0	457	94.6	5.4
36	270.000	1	.21	426	88.2	4.8	458	94.8	5.2
37	280.000	1	.21	427	88.4	4.6	459	95.0	5.0
38	290.000	1	.21	428	88.6	4.3	460	95.2	4.8
39	300.000	1	.21	429	88.8	4.1	461	95.4	4.6
40	310.000	1	.21	430	89.0	3.9	462	95.7	4.3
41	320.000	4	.83	434	89.9	3.1	466	96.5	3.5
42	330.000	1	.21	435	90.1	2.9	467	96.7	3.3
43	340.000	1	.21	436	90.3	2.7	468	96.9	3.1
44	350.000	1	.21	437	90.5	2.5	469	97.1	2.9
45	420.000	1	.21	438	90.7	2.3	470	97.3	2.7
46	430.000	1	.21	439	90.9	2.1	471	97.5	2.5
47	540.000	2	.41	441	91.3	1.7	473	97.9	2.1
48	560.000	1	.21	442	91.5	1.4	474	98.1	1.9
49	570.000	1	.21	443	91.7	1.2	475	98.3	1.7
50	620.000	1	.21	444	91.9	1.0	476	98.6	1.4

APPENDIX IV-A. HISTOGRAMS OF ROCK SAMPLE DATA, WHITE MTS NRA

COLUMN ID.: AA-ZN-P

51	810.000	1	.21	445	92.1	.8	477	98.8	1.2
52	900.000	1	.21	446	92.3	.6	478	99.0	1.0
53	980.000	1	.21	447	92.5	.4	479	99.2	.8
54	1100.000	1	.21	448	92.8	.2	480	99.4	.6
55	1300.000	1	.21	449	93.0	.0	481	99.6	.4

B	T	H	N	L	G	OTHER	UNQUAL	ANAL	read	
137	0	0	25	7	2	0	449	483	620	VALUES
22.1	.0	.0	4.0	1.1	.3	.0	72.4			PERCENT

MIN	MAX	AMEAN	SD	GMEAN	GD	VALUES
5.000	1300.00	81.570	131.82	45.393	2.85	449
1.250	4000.00	92.492	283.14	36.817	3.90	483

Percent of Values

```
          .00          10.00          20.00          30.00
                5.00          15.00          25.00
          +---------+---------+---------+---------+---------+---------+
  5.000 +XXXXXXXX¦
 10.000 +XXXXXXXXXXX¦
 15.000 +XXXXXXXXXX¦
 20.000 +XXXXXXXXXXXX¦
 25.000 +XXXXXXXXXX¦
 30.000 +XXXXXXXXXXX¦
 35.000 +XXXXX¦
 40.000 +XXXX¦
 45.000 +XXXXXXX¦
 50.000 +XXXXXXX¦
 55.000 +XXXXXXXXX¦
 60.000 +XXXXXX¦
 65.000 +XXXXX¦
 70.000 +XXXXX¦
 75.000 +XXXX¦
 80.000 +XXXXX¦
 85.000 +XXXX¦
 90.000 +XX¦
 95.000 +XXXX¦
100.000 +XXXXXX¦
110.000 +XXX¦
115.000 ¦
120.000 +¦
130.000 +XXX¦
135.000 +¦
140.000 +¦
150.000 +¦
160.000 ¦
170.000 +¦
190.000 +X¦
200.000 +¦
220.000 +¦
240.000 ¦
250.000 +X¦
```

APPENDIX IV-A. HISTOGRAMS OF ROCK SAMPLE DATA, WHITE MTS NRA

COLUMN ID.: AA-ZN-P

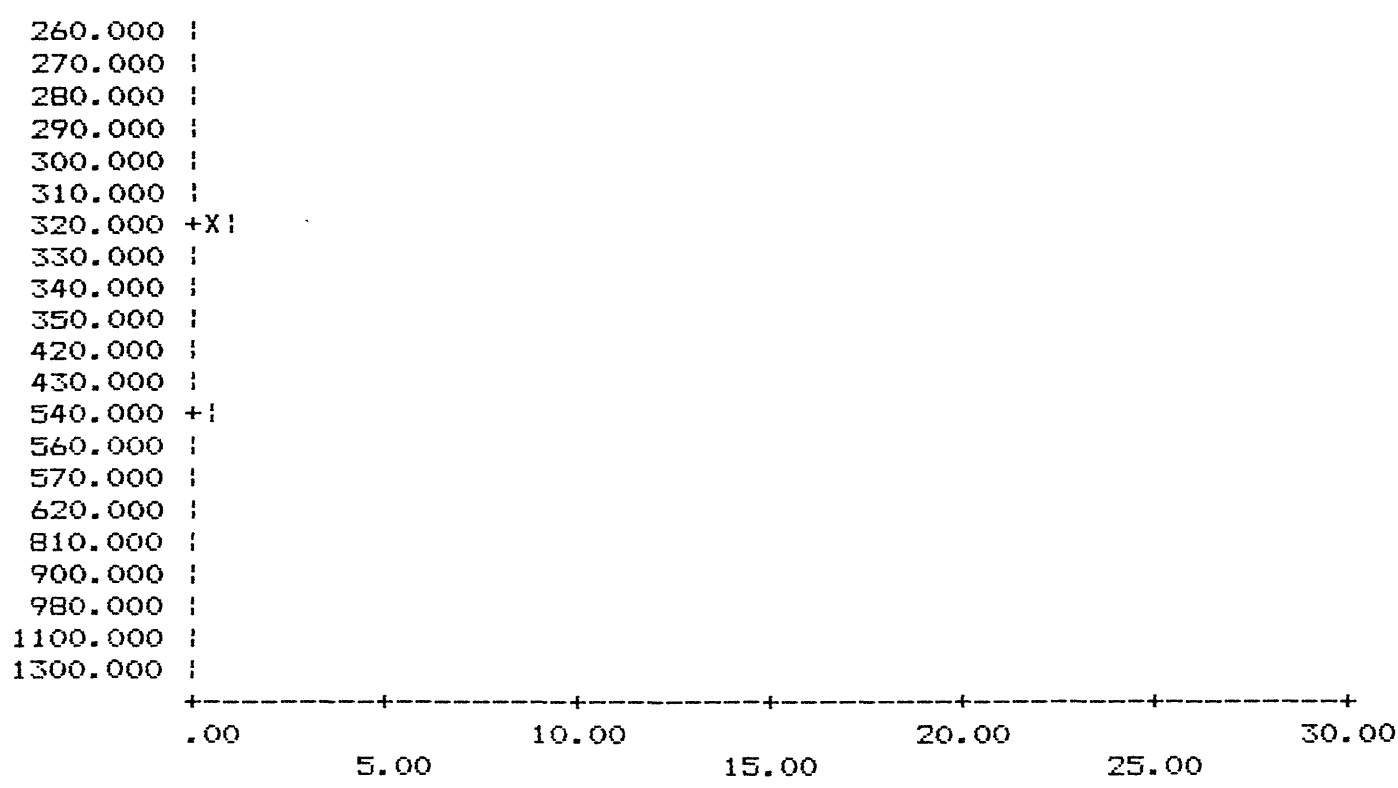

Each increment (each X or ¦ plotted) = .500 %

OPEN-FILE REPORT NO. 88-284

APPENDIX IV-B

UNITED STATES DEPARTMENT OF THE INTERIOR

GEOLOGICAL SURVEY

Histograms and frequency distributions of heavy-mineral-concentrate sample data from the White Mountains National Recreation Area, Livengood and Circle quadrangles, east-central Alaska

This report is preliminary and has not been reviewed for conformity with U.S. Geological Survey editorial standards and stratigraphic nomenclature. Any use of trade names is for descriptive purposes only and does not imply endorsement by the USGS.

1988

APPENDIX IV-B. HISTOGRAMS OF HEAVY-MINERAL-CONCENTRATE DATA, WHITE MTS NRA

COLUMN ID.: S-FE%

	VALUE	NO.	%	CUM.	CUM. %		TOT CUM	TOT CUM %	
1	.100	54	15.88	54	15.9	77.4	77	22.6	77.4
2	.150	25	7.35	79	23.2	70.0	102	30.0	70.0
3	.200	103	30.29	182	53.5	39.7	205	60.3	39.7
4	.300	31	9.12	213	62.6	30.6	236	69.4	30.6
5	.500	48	14.12	261	76.8	16.5	284	83.5	16.5
6	.700	11	3.24	272	80.0	13.2	295	86.8	13.2
7	1.000	19	5.59	291	85.6	7.6	314	92.4	7.6
8	1.500	3	.88	294	86.5	6.8	317	93.2	6.8
9	2.000	10	2.94	304	89.4	3.8	327	96.2	3.8
10	3.000	4	1.18	308	90.6	2.6	331	97.4	2.6
11	5.000	2	.59	310	91.2	2.1	333	97.9	2.1
12	10.000	2	.59	312	91.8	1.5	335	98.5	1.5
13	15.000	2	.59	314	92.4	.9	337	99.1	.9
14	20.000	2	.59	316	92.9	.3	339	99.7	.3
15	30.000	1	.29	317	93.2	.0	340	100.0	.0

B	T	H	N	L	G	OTHER	UNQUAL	ANAL	read	
0	0	0	1	22	0	0	317	340	340	VALUES
.0	.0	.0	.3	6.5	.0	.0	93.2			PERCENT

MIN	MAX	AMEAN	SD	GMEAN	GD	VALUES
.100	30.00	.808	2.71	.305	2.80	317
.025	30.00	.757	2.62	.269	2.99	340

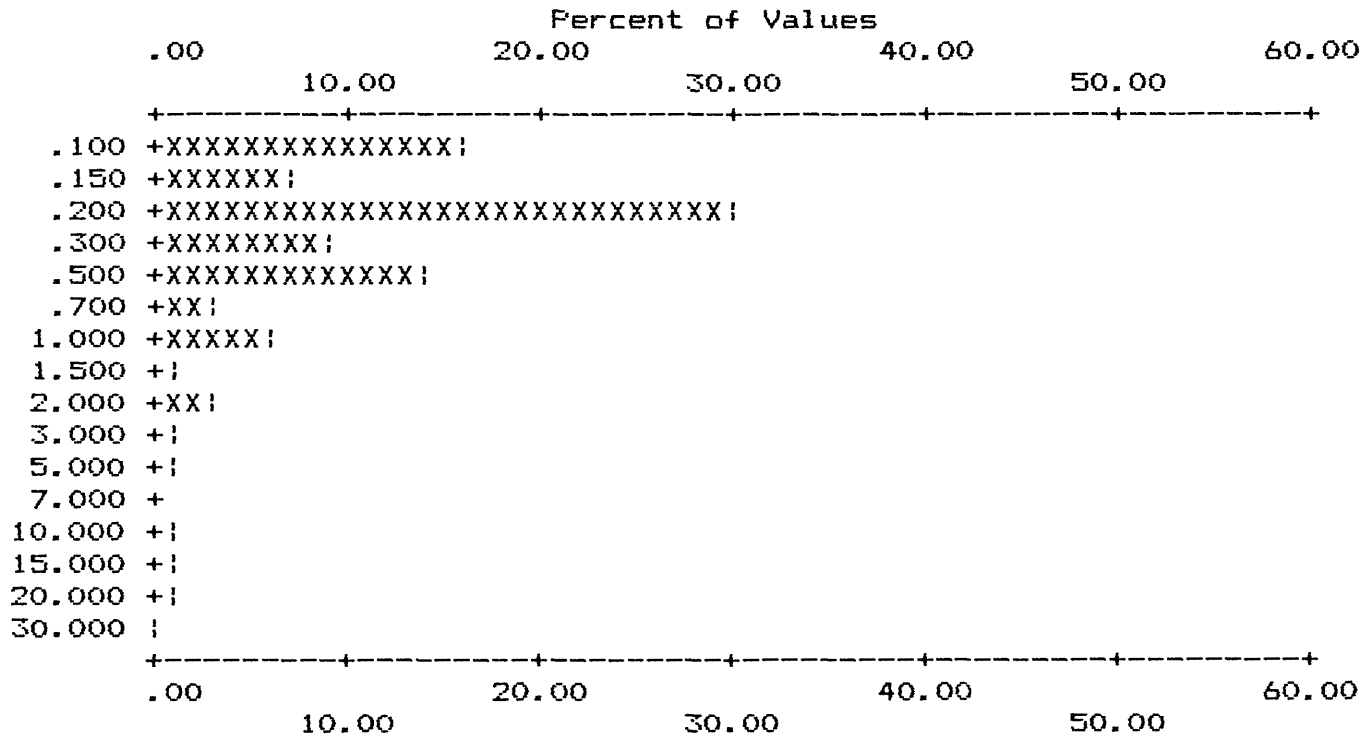

Each increment (each X or ! plotted) = 1.000 %

APPENDIX IV-B. HISTOGRAMS OF HEAVY-MINERAL-CONCENTRATE DATA, WHITE MTS NRA

COLUMN ID.: S-MG%

	VALUE	NO.	%	CUM.	CUM. %		TOT CUM	TOT CUM %	
1	.050	77	22.65	77	22.6	60.0	136	40.0	60.0
2	.070	39	11.47	116	34.1	48.5	175	51.5	48.5
3	.100	68	20.00	184	54.1	28.5	243	71.5	28.5
4	.150	25	7.35	209	61.5	21.2	268	78.8	21.2
5	.200	31	9.12	240	70.6	12.1	299	87.9	12.1
6	.300	9	2.65	249	73.2	9.4	308	90.6	9.4
7	.500	11	3.24	260	76.5	6.2	319	93.8	6.2
8	.700	6	1.76	266	78.2	4.4	325	95.6	4.4
9	1.000	3	.88	269	79.1	3.5	328	96.5	3.5
10	1.500	4	1.18	273	80.3	2.4	332	97.6	2.4
11	2.000	3	.88	276	81.2	1.5	335	98.5	1.5
12	3.000	3	.88	279	82.1	.6	338	99.4	.6
13	7.000	1	.29	280	82.4	.3	339	99.7	.3
14	15.000	1	.29	281	82.6	.0	340	100.0	.0

B	T	H	N	L	G	OTHER	UNQUAL	ANAL	read	
0	0	0	0	59	0	0	281	340	340	VALUES
.0	.0	.0	.0	17.4	.0	.0	82.6			PERCENT

MIN	MAX	AMEAN	SD	GMEAN	GD	VALUES
.050	15.00	.291	1.05	.119	2.64	281
.025	15.00	.245	.96	.091	2.90	340

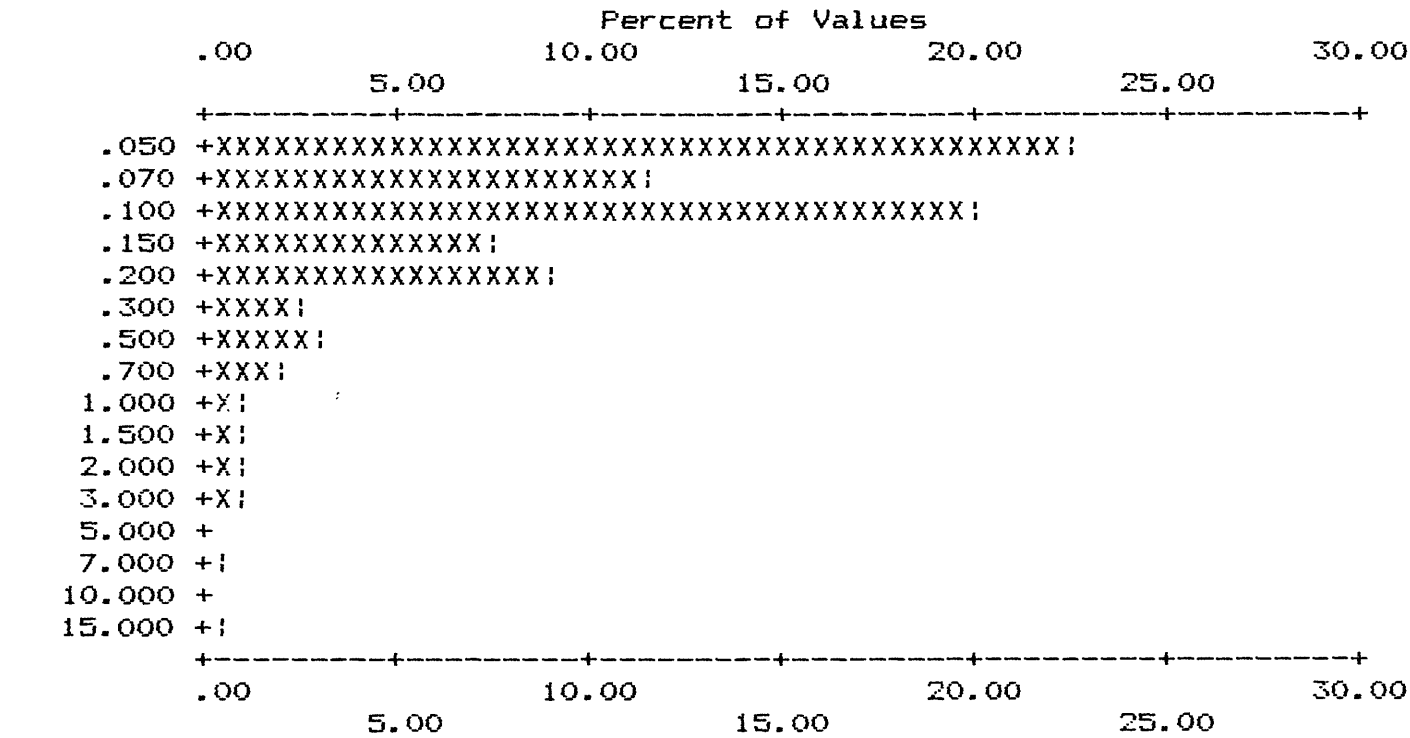

Each increment (each X or ¦ plotted) = .500 %

APPENDIX IV-B. HISTOGRAMS OF HEAVY-MINERAL-CONCENTRATE DATA, WHITE MTS NRA

COLUMN ID.: S-CA%

	VALUE	NO.	%	CUM.	CUM. %		TOT CUM	TOT CUM %	
1	.100	31	9.12	31	9.1	87.1	44	12.9	87.1
2	.150	15	4.41	46	13.5	82.6	59	17.4	82.6
3	.200	30	8.82	76	22.4	73.8	89	26.2	73.8
4	.300	24	7.06	100	29.4	66.8	113	33.2	66.8
5	.500	51	15.00	151	44.4	51.8	164	48.2	51.8
6	.700	30	8.82	181	53.2	42.9	194	57.1	42.9
7	1.000	41	12.06	222	65.3	30.9	235	69.1	30.9
8	1.500	18	5.29	240	70.6	25.6	253	74.4	25.6
9	2.000	25	7.35	265	77.9	18.2	278	81.8	18.2
10	3.000	6	1.76	271	79.7	16.5	284	83.5	16.5
11	5.000	16	4.71	287	84.4	11.8	300	88.2	11.8
12	7.000	16	4.71	303	89.1	7.1	316	92.9	7.1
13	10.000	17	5.00	320	94.1	2.1	333	97.9	2.1
14	15.000	4	1.18	324	95.3	.9	337	99.1	.9
15	20.000	3	.88	327	96.2	.0	340	100.0	.0

B	T	H	N	L	G	OTHER	UNQUAL	ANAL	read	
0	0	0	3	10	0	0	327	340	340	VALUES
.0	.0	.0	.9	2.9	.0	.0	96.2			PERCENT

MIN	MAX	AMEAN	SD	GMEAN	GD	VALUES
.100	20.00	2.089	3.42	.793	3.94	327
.025	20.00	2.011	3.38	.709	4.29	340

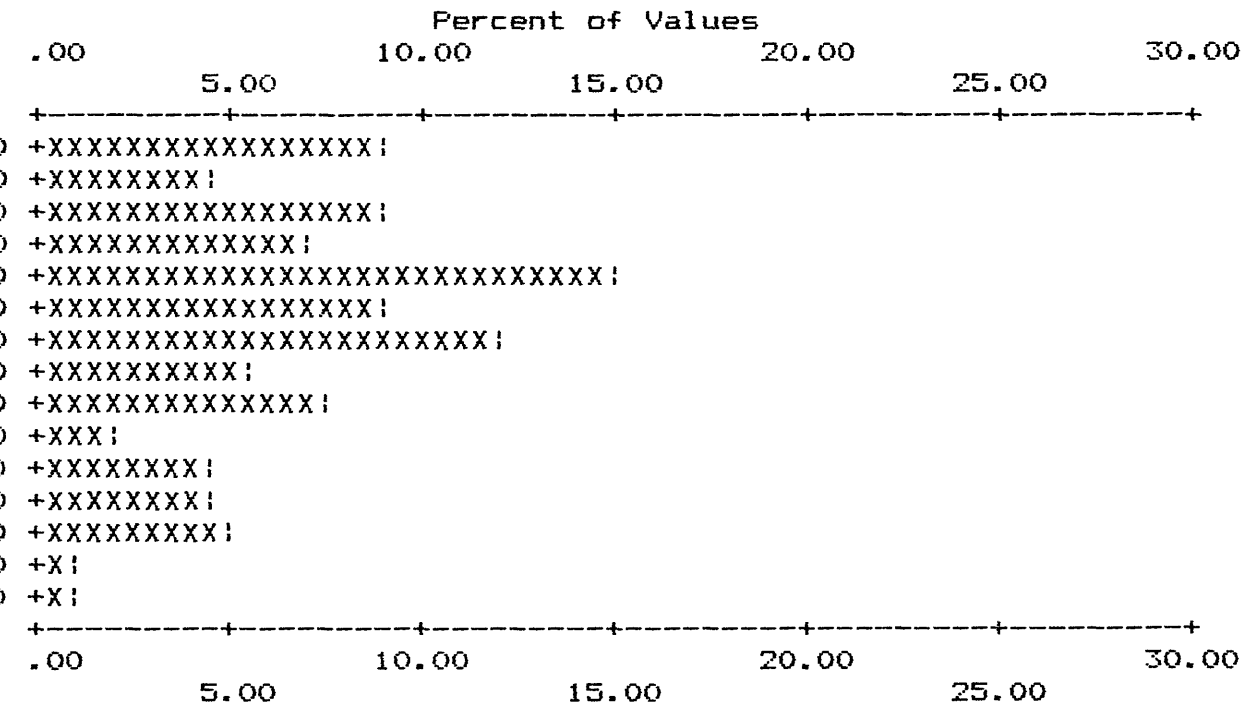

Each increment (each X or ! plotted) = .500 %

APPENDIX IV-B. HISTOGRAMS OF HEAVY-MINERAL-CONCENTRATE DATA, WHITE MTS NRA

COLUMN ID.: S-TI%

	VALUE	NO.	%	CUM.	CUM. %		TOT CUM	TOT CUM %	
1	.100	2	.59	2	.6	30.9	2	.6	99.4
2	.150	1	.29	3	.9	30.6	3	.9	99.1
3	.200	3	.88	6	1.8	29.7	6	1.8	98.2
4	.300	11	3.24	17	5.0	26.5	17	5.0	95.0
5	.500	8	2.35	25	7.4	24.1	25	7.4	92.6
6	.700	9	2.65	34	10.0	21.5	34	10.0	90.0
7	1.000	11	3.24	45	13.2	18.2	45	13.2	86.8
8	1.500	14	4.12	59	17.4	14.1	59	17.4	82.6
9	2.000	48	14.12	107	31.5	.0	107	31.5	68.5

B	T	H	N	L	G	OTHER	UNQUAL	ANAL	read	
0	0	0	0	0	233	0	107	340	340	VALUES
.0	.0	.0	.0	.0	68.5	.0	31.5			PERCENT

MIN	MAX	AMEAN	SD	GMEAN	GD	VALUES
.100	2.00	1.332	.70	1.054	2.23	107
.100	4.00	3.160	1.30	2.629	2.15	340

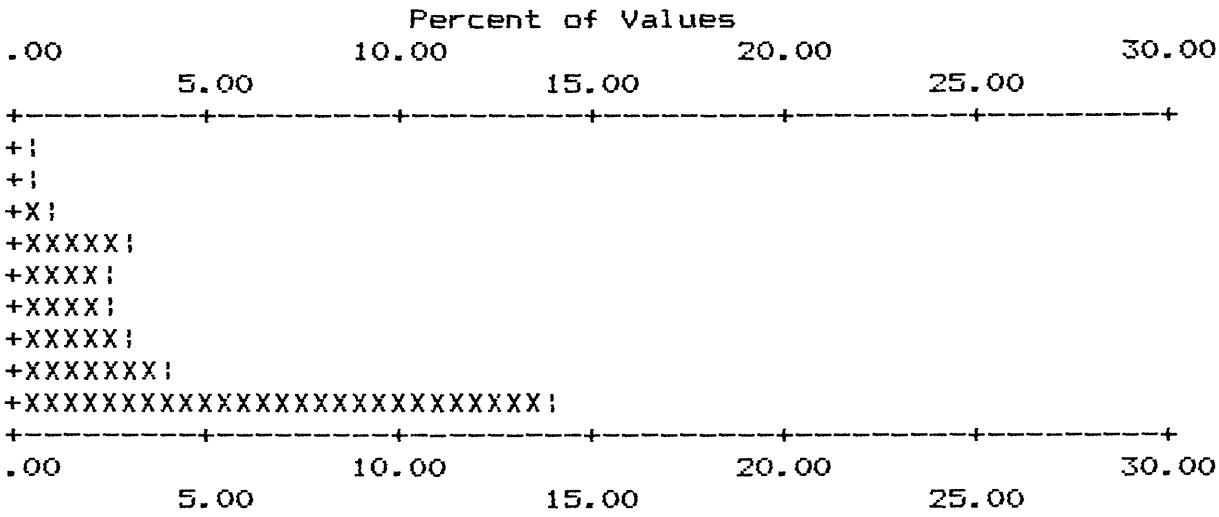

Each increment (each X or ¦ plotted) = .500 %

APPENDIX IV-B. HISTOGRAMS OF HEAVY-MINERAL-CONCENTRATE DATA, WHITE MTS NRA

COLUMN ID.: S-MN

	VALUE	NO.	%	CUM.	CUM. %		TOT CUM	TOT CUM %	
1	20.000	4	1.18	4	1.2	98.5	5	1.5	98.5
2	50.000	9	2.65	13	3.8	95.9	14	4.1	95.9
3	70.000	25	7.35	38	11.2	88.5	39	11.5	88.5
4	100.000	95	27.94	133	39.1	60.6	134	39.4	60.6
5	150.000	67	19.71	200	58.8	40.9	201	59.1	40.9
6	200.000	85	25.00	285	83.8	15.9	286	84.1	15.9
7	300.000	35	10.29	320	94.1	5.6	321	94.4	5.6
8	500.000	13	3.82	333	97.9	1.8	334	98.2	1.8
9	700.000	1	.29	334	98.2	1.5	335	98.5	1.5
10	1000.000	2	.59	336	98.8	.9	337	99.1	.9
11	10000.000	3	.88	339	99.7	.0	340	100.0	.0

B	T	H	N	L	G	OTHER	UNQUAL	ANAL	read	
0	0	0	0	1	0	0	339	340	340	VALUES
.0	.0	.0	.0	.3	.0	.0	99.7			PERCENT

MIN	MAX	AMEAN	SD	GMEAN	GD	VALUES
20.000	10000.00	261.150	929.11	153.029	2.00	339
10.000	10000.00	260.412	927.83	151.806	2.03	340

```
                          Percent of Values
          .00                10.00               20.00               30.00
                    5.00               15.00               25.00
          +---------+---------+---------+---------+---------+---------+
   20.000 +X|
   30.000 +
   50.000 +XXXX|
   70.000 +XXXXXXXXXXXXXX|
  100.000 +XXXXXXXXXXXXXXXXXXXXXXXXXXXXXXXXXXXXXXXXXXXXXXXXXXXXXXX|
  150.000 +XXXXXXXXXXXXXXXXXXXXXXXXXXXXXXXXXXXXXX|
  200.000 +XXXXXXXXXXXXXXXXXXXXXXXXXXXXXXXXXXXXXXXXXXXXXXXXX|
  300.000 +XXXXXXXXXXXXXXXXXXXX|
  500.000 +XXXXXXX|
  700.000 +|
 1000.000 +|
 1500.000 +
 2000.000 +
 3000.000 +
 5000.000 +
 7000.000 +
10000.000 +X|
          +---------+---------+---------+---------+---------+---------+
          .00                10.00               20.00               30.00
                    5.00               15.00               25.00

         Each increment (each X or | plotted) =       .500 %
```

APPENDIX IV-B. HISTOGRAMS OF HEAVY-MINERAL-CONCENTRATE DATA, WHITE MTS NRA

COLUMN ID.: S-AG

	VALUE	NO.	%	CUM.	CUM. %		TOT CUM	TOT CUM %	
1	1.000	4	1.18	4	1.2	14.1	292	85.9	14.1
2	1.500	1	.29	5	1.5	13.8	293	86.2	13.8
3	2.000	13	3.82	18	5.3	10.0	306	90.0	10.0
4	5.000	9	2.65	27	7.9	7.4	315	92.6	7.4
5	7.000	3	.88	30	8.8	6.5	318	93.5	6.5
6	10.000	3	.88	33	9.7	5.6	321	94.4	5.6
7	15.000	2	.59	35	10.3	5.0	323	95.0	5.0
8	20.000	5	1.47	40	11.8	3.5	328	96.5	3.5
9	30.000	1	.29	41	12.1	3.2	329	96.8	3.2
10	50.000	4	1.18	45	13.2	2.1	333	97.9	2.1
11	70.000	1	.29	46	13.5	1.8	334	98.2	1.8
12	100.000	1	.29	47	13.8	1.5	335	98.5	1.5
13	150.000	1	.29	48	14.1	1.2	336	98.8	1.2
14	300.000	1	.29	49	14.4	.9	337	99.1	.9
15	500.000	1	.29	50	14.7	.6	338	99.4	.6
16	2000.000	2	.59	52	15.3	.0	340	100.0	.0

B	T	H	N	L	G	OTHER	UNQUAL	ANAL	read	
0	0	0	287	1	0	0	52	340	340	VALUES
.0	.0	.0	84.4	.3	.0	.0	15.3			PERCENT

MIN	MAX	AMEAN	SD	GMEAN	GD	VALUES
1.000	2000.00	107.837	390.75	9.501	6.44	52
.250	2000.00	16.705	156.44	.437	4.47	340

APPENDIX IV-B. HISTOGRAMS OF HEAVY-MINERAL-CONCENTRATE DATA, WHITE MTS NRA

COLUMN ID: S-AG

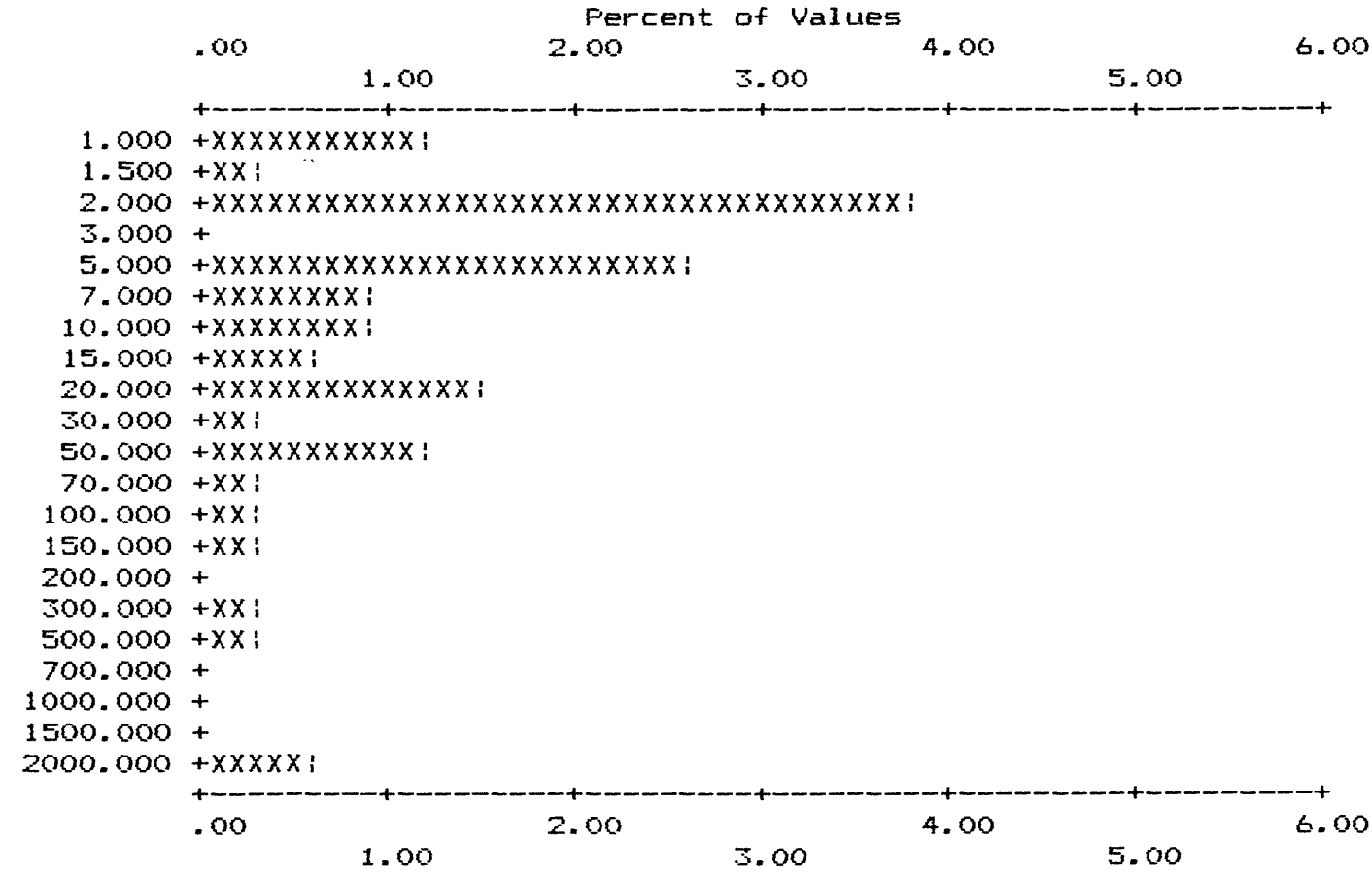

Each increment (each X or ! plotted) = .100 %

APPENDIX IV-B. HISTOGRAMS OF HEAVY-MINERAL-CONCENTRATE DATA, WHITE MTS NRA

COLUMN ID.: S-AS

	VALUE	NO.	%	CUM.	CUM. %	TOT CUM	TOT CUM %	
1	500.000	3	.88	3	.9	.6	338	99.4	.6
2	1000.000	1	.29	4	1.2	.3	339	99.7	.3
3	2000.000	1	.29	5	1.5	.0	340	100.0	.0

B	T	H	N	L	G	OTHER	UNQUAL	ANAL	read	
0	0	0	334	1	0	0	5	340	340	VALUES
.0	.0	.0	98.2	.3	.0	.0	1.5			PERCENT

MIN	MAX	AMEAN	SD	GMEAN	GD	VALUES
500.000	2000.00	900.000	651.92	757.857	1.86	5
125.000	2000.00	136.765	117.39	128.619	1.26	340

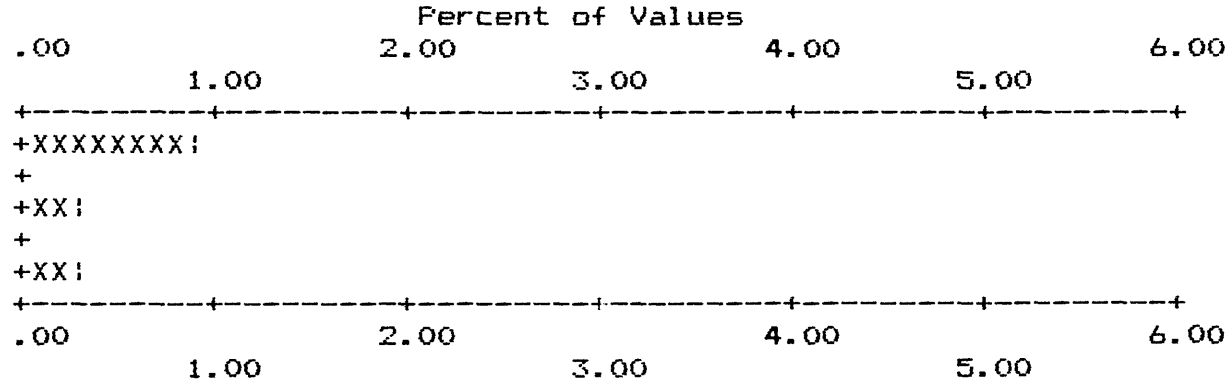

Each increment (each X or ! plotted) = .100 %

APPENDIX IV-B. HISTOGRAMS OF HEAVY-MINERAL-CONCENTRATE DATA, WHITE MTS NRA

COLUMN ID.: S-AU

	VALUE	NO.	%	CUM.	CUM. %		TOT CUM	TOT CUM %	
1	20.000	3	.88	3	.9	4.1	323	95.0	5.0
2	50.000	3	.88	6	1.8	3.2	326	95.9	4.1
3	70.000	1	.29	7	2.1	2.9	327	96.2	3.8
4	100.000	1	.29	8	2.4	2.6	328	96.5	3.5
5	150.000	1	.29	9	2.6	2.4	329	96.8	3.2
6	200.000	1	.29	10	2.9	2.1	330	97.1	2.9
7	300.000	3	.88	13	3.8	1.2	333	97.9	2.1
8	700.000	1	.29	14	4.1	.9	334	98.2	1.8
9	1000.000	3	.88	17	5.0	.0	337	99.1	.9

B	T	H	N	L	G	OTHER	UNQUAL	ANAL	read	
0	0	0	311	9	3	0	17	340	340	VALUES
.0	.0	.0	91.5	2.6	.9	.0	5.0			PERCENT

MIN	MAX	AMEAN	SD	GMEAN	GD	VALUES
20.000	1000.00	313.529	368.70	142.188	4.04	17
5.000	2000.00	38.162	212.86	6.347	2.62	340

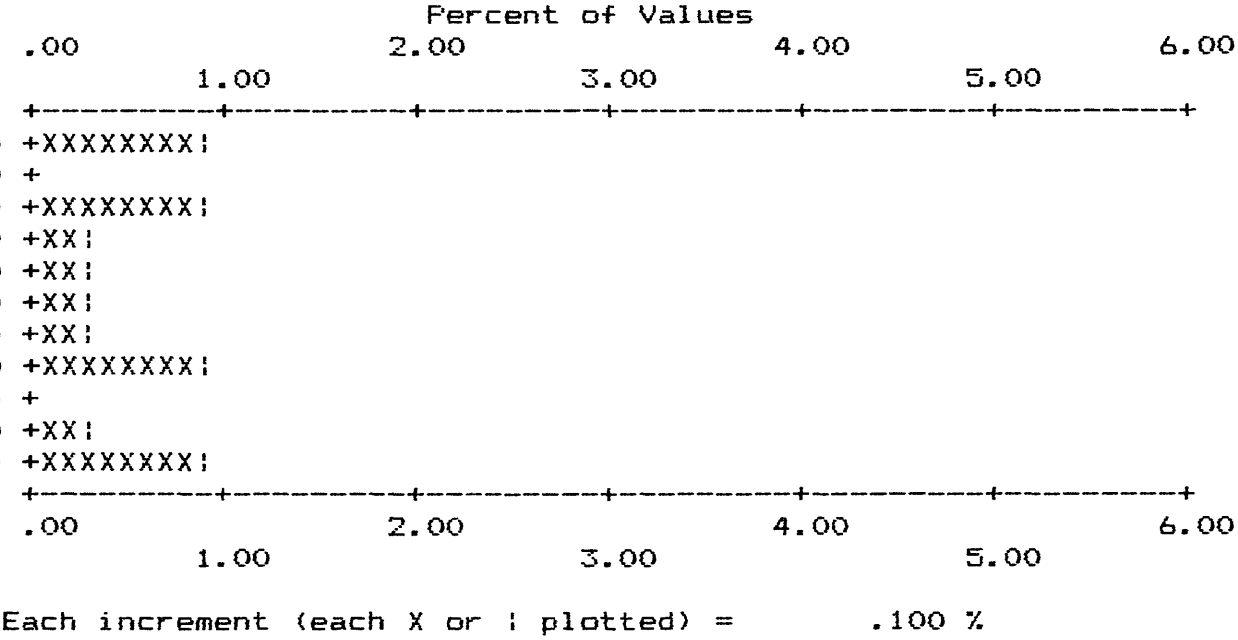

Each increment (each X or ¦ plotted) = .100 %

APPENDIX IV-B. HISTOGRAMS OF HEAVY-MINERAL-CONCENTRATE DATA, WHITE MTS NRA

COLUMN ID.: S-B

	VALUE	NO.	%	CUM.	CUM. %		TOT CUM	TOT CUM %	
1	20.000	37	10.88	37	10.9	84.4	53	15.6	84.4
2	30.000	18	5.29	55	16.2	79.1	71	20.9	79.1
3	50.000	60	17.65	115	33.8	61.5	131	38.5	61.5
4	70.000	57	16.76	172	50.6	44.7	188	55.3	44.7
5	100.000	70	20.59	242	71.2	24.1	258	75.9	24.1
6	150.000	28	8.24	270	79.4	15.9	286	84.1	15.9
7	200.000	23	6.76	293	86.2	9.1	309	90.9	9.1
8	300.000	11	3.24	304	89.4	5.9	320	94.1	5.9
9	500.000	12	3.53	316	92.9	2.4	332	97.6	2.4
10	700.000	3	.88	319	93.8	1.5	335	98.5	1.5
11	1000.000	3	.88	322	94.7	.6	338	99.4	.6
12	1500.000	1	.29	323	95.0	.3	339	99.7	.3
13	2000.000	1	.29	324	95.3	.0	340	100.0	.0

B	T	H	N	L	G	OTHER	UNQUAL	ANAL	read	
0	0	0	0	16	0	0	324	340	340	VALUES
.0	.0	.0	.0	4.7	.0	.0	95.3			PERCENT

MIN	MAX	AMEAN	SD	GMEAN	GD	VALUES
20.000	2000.00	129.537	192.62	81.571	2.40	324
10.000	2000.00	123.912	189.72	73.899	2.62	340

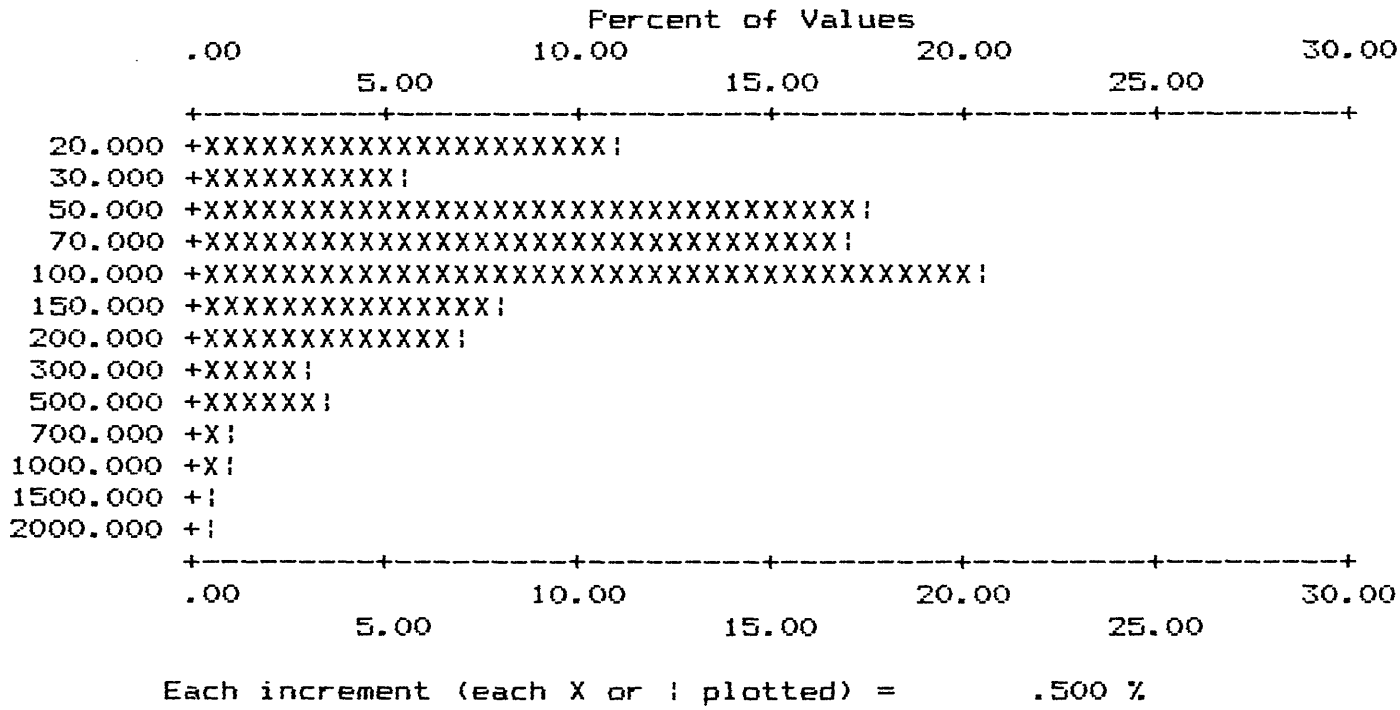

Each increment (each X or ! plotted) = .500 %

APPENDIX IV-B. HISTOGRAMS OF HEAVY-MINERAL-CONCENTRATE DATA, WHITE MTS NRA

COLUMN ID.: S-BA

	VALUE	NO.	%	CUM.	CUM. %		TOT CUM	TOT CUM %	
1	50.000	6	1.76	6	1.8	62.6	8	2.4	97.6
2	70.000	15	4.41	21	6.2	58.2	23	6.8	93.2
3	100.000	13	3.82	34	10.0	54.4	36	10.6	89.4
4	150.000	10	2.94	44	12.9	51.5	46	13.5	86.5
5	200.000	18	5.29	62	18.2	46.2	64	18.8	81.2
6	300.000	16	4.71	78	22.9	41.5	80	23.5	76.5
7	500.000	44	12.94	122	35.9	28.5	124	36.5	63.5
8	700.000	21	6.18	143	42.1	22.4	145	42.6	57.4
9	1000.000	16	4.71	159	46.8	17.6	161	47.4	52.6
10	1500.000	5	1.47	164	48.2	16.2	166	48.8	51.2
11	2000.000	12	3.53	176	51.8	12.6	178	52.4	47.6
12	3000.000	8	2.35	184	54.1	10.3	186	54.7	45.3
13	5000.000	10	2.94	194	57.1	7.4	196	57.6	42.4
14	7000.000	11	3.24	205	60.3	4.1	207	60.9	39.1
15	10000.000	14	4.12	219	64.4	.0	221	65.0	35.0

B	T	H	N	L	G	OTHER	UNQUAL	ANAL	read	
0	0	0	0	2	119	0	219	340	340	VALUES
.0	.0	.0	.0	.6	35.0	.0	64.4			PERCENT

MIN	MAX	AMEAN	SD	GMEAN	GD	VALUES
50.000	10000.00	1770.548	2770.76	621.610	4.32	219
25.000	20000.00	8140.590	8995.00	2055.598	7.83	340

```
                                Percent of Values
          .00                  10.00                  20.00                  30.00
                   5.00                  15.00                  25.00
          +---------+---------+---------+---------+---------+---------+
   50.000 +XXX!
   70.000 +XXXXXXXX!
  100.000 +XXXXXXX!
  150.000 +XXXXX!
  200.000 +XXXXXXXXXX!
  300.000 +XXXXXXXX!
  500.000 +XXXXXXXXXXXXXXXXXXXXXXXXX!
  700.000 +XXXXXXXXXXX!
 1000.000 +XXXXXXXX!
 1500.000 +XX!
 2000.000 +XXXXXX!
 3000.000 +XXXX!
 5000.000 +XXXXX!
 7000.000 +XXXXX!
10000.000 +XXXXXXX!
          +---------+---------+---------+---------+---------+---------+
          .00                  10.00                  20.00                  30.00
                   5.00                  15.00                  25.00

        Each increment (each X or ! plotted) =       .500 %
```

APPENDIX IV-B. HISTOGRAMS OF HEAVY-MINERAL-CONCENTRATE DATA, WHITE MTS NRA

COLUMN ID.: S-BE

	VALUE	NO.	%	CUM.	CUM. %	TOT CUM	TOT CUM %	
1	2.000	63	18.53	63	18.5	3.2	329	96.8	3.2
2	3.000	2	.59	65	19.1	2.6	331	97.4	2.6
3	5.000	4	1.18	69	20.3	1.5	335	98.5	1.5
4	10.000	1	.29	70	20.6	1.2	336	98.8	1.2
5	20.000	1	.29	71	20.9	.9	337	99.1	.9
6	50.000	1	.29	72	21.2	.6	338	99.4	.6
7	500.000	2	.59	74	21.8	.0	340	100.0	.0

B	T	H	N	L	G	OTHER	UNQUAL	ANAL	read	
0	0	0	124	142	0	0	74	340	340	VALUES
.0	.0	.0	36.5	41.8	.0	.0	21.8			PERCENT

MIN	MAX	AMEAN	SD	GMEAN	GD	VALUES
2.000	500.00	16.649	81.33	2.716	2.77	74
.500	500.00	4.224	38.31	.965	2.19	340

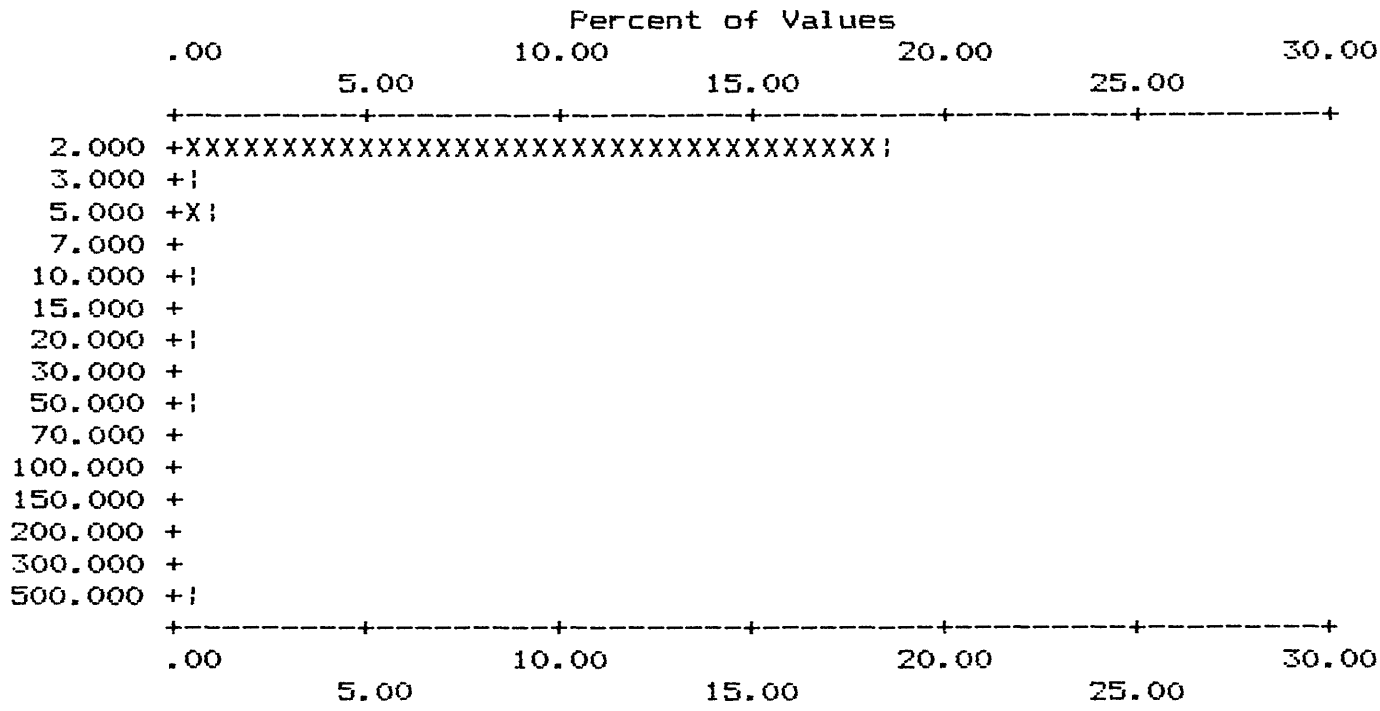

Each increment (each X or ¦ plotted) = .500 %

APPENDIX IV-B. HISTOGRAMS OF HEAVY-MINERAL-CONCENTRATE DATA, WHITE MTS NRA

COLUMN ID.: S-BI

	VALUE	NO.	%	CUM.	CUM. %		TOT CUM	TOT CUM %	
1	20.000	7	2.06	7	2.1	9.4	306	90.0	10.0
2	30.000	3	.88	10	2.9	8.5	309	90.9	9.1
3	50.000	5	1.47	15	4.4	7.1	314	92.4	7.6
4	70.000	3	.88	18	5.3	6.2	317	93.2	6.8
5	100.000	4	1.18	22	6.5	5.0	321	94.4	5.6
6	150.000	2	.59	24	7.1	4.4	323	95.0	5.0
7	200.000	8	2.35	32	9.4	2.1	331	97.4	2.6
8	300.000	3	.88	35	10.3	1.2	334	98.2	1.8
9	500.000	2	.59	37	10.9	.6	336	98.8	1.2
10	2000.000	2	.59	39	11.5	.0	338	99.4	.6

B	T	H	N	L	G	OTHER	UNQUAL	ANAL	read	
0	0	0	280	19	2	0	39	340	340	VALUES
.0	.0	.0	82.4	5.6	.6	.0	11.5			PERCENT

MIN	MAX	AMEAN	SD	GMEAN	GD	VALUES
20.000	2000.00	227.949	434.72	98.596	3.37	39
5.000	4000.00	54.353	344.41	7.610	3.13	340

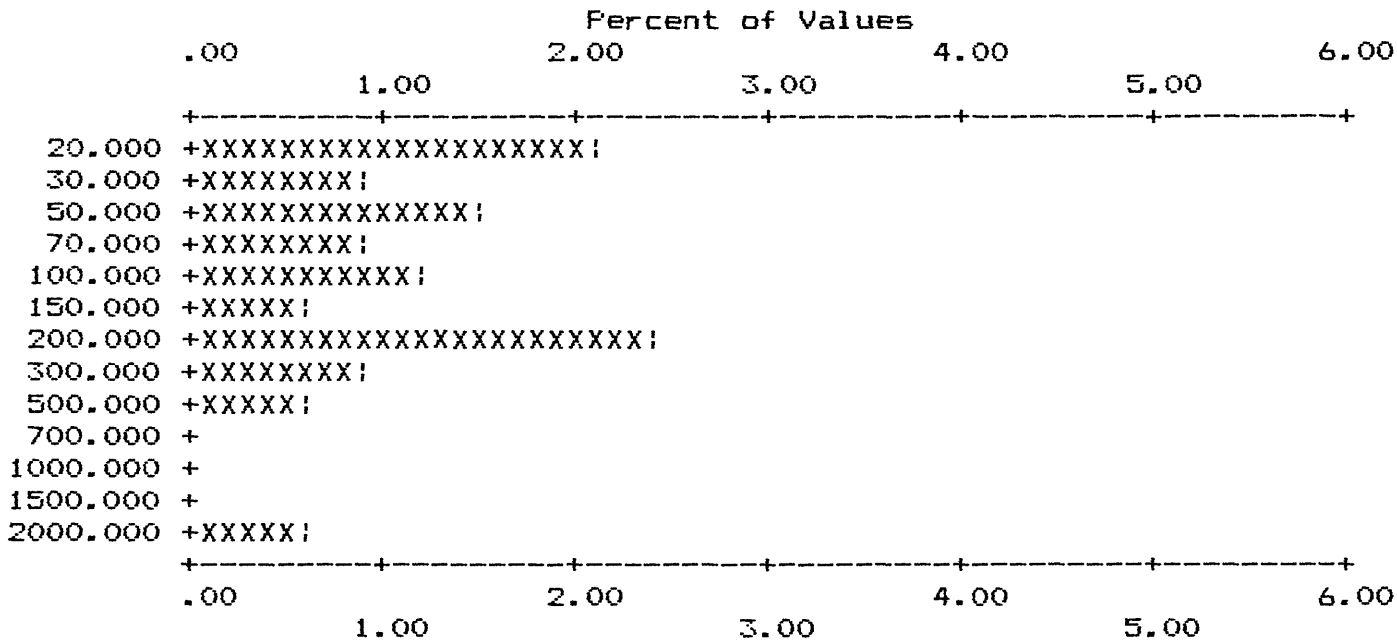

Each increment (each X or ! plotted) = .100 %

APPENDIX IV-B. HISTOGRAMS OF HEAVY-MINERAL-CONCENTRATE DATA, WHITE MTS NRA

COLUMN ID.: S-CD

	VALUE	NO.	%	CUM.	CUM. %		TOT CUM	TOT CUM %	
1	50.000	14	4.12	14	4.1	8.2	312	91.8	8.2
2	70.000	6	1.76	20	5.9	6.5	318	93.5	6.5
3	100.000	7	2.06	27	7.9	4.4	325	95.6	4.4
4	150.000	2	.59	29	8.5	3.8	327	96.2	3.8
5	200.000	4	1.18	33	9.7	2.6	331	97.4	2.6
6	300.000	3	.88	36	10.6	1.8	334	98.2	1.8
7	500.000	4	1.18	40	11.8	.6	338	99.4	.6
8	1000.000	2	.59	42	12.4	.0	340	100.0	.0

B	T	H	N	L	G	OTHER	UNQUAL	ANAL	read	
0	0	0	283	15	0	0	42	340	340	VALUES
.0	.0	.0	83.2	4.4	.0	.0	12.4			PERCENT

MIN	MAX	AMEAN	SD	GMEAN	GD	VALUES
50.000	1000.00	186.190	229.18	115.572	2.47	42
12.500	1000.00	34.507	98.03	16.963	2.22	340

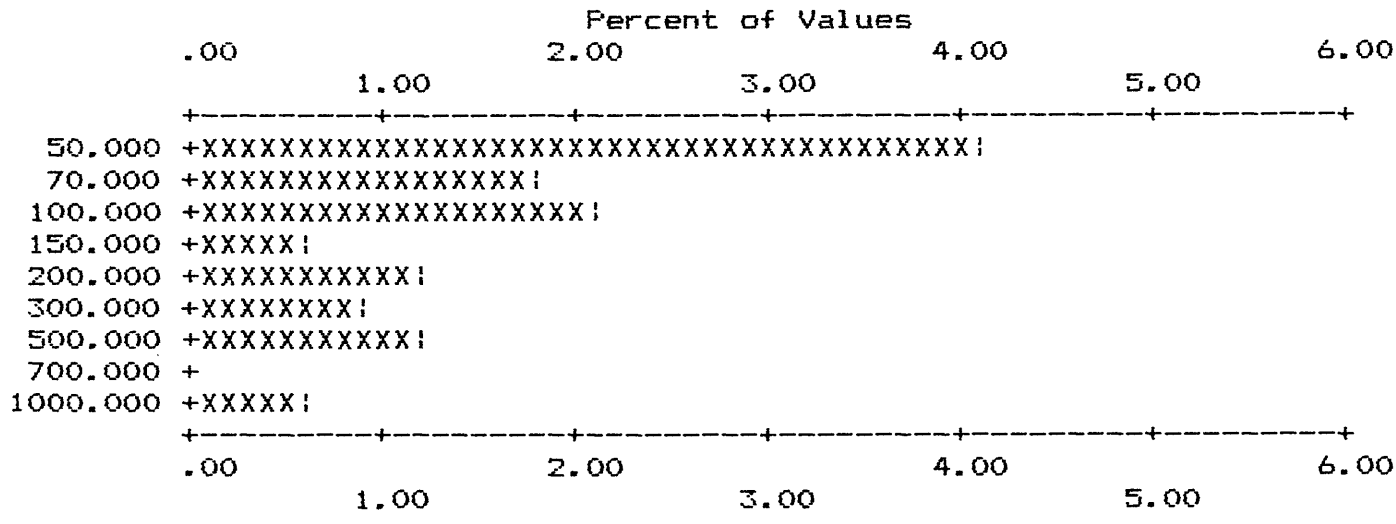

Each increment (each X or ¦ plotted) = .100 %

APPENDIX IV-B. HISTOGRAMS OF HEAVY-MINERAL-CONCENTRATE DATA, WHITE MTS NRA

COLUMN ID.: S-CO

	VALUE	NO.	%	CUM.	CUM. %		TOT CUM	TOT CUM %	
1	10.000	13	3.82	13	3.8	10.6	304	89.4	10.6
2	15.000	10	2.94	23	6.8	7.6	314	92.4	7.6
3	20.000	12	3.53	35	10.3	4.1	326	95.9	4.1
4	30.000	4	1.18	39	11.5	2.9	330	97.1	2.9
5	50.000	7	2.06	46	13.5	.9	337	99.1	.9
6	70.000	1	.29	47	13.8	.6	338	99.4	.6
7	100.000	1	.29	48	14.1	.3	339	99.7	.3
8	700.000	1	.29	49	14.4	.0	340	100.0	.0

B	T	H	N	L	G	OTHER	UNQUAL	ANAL	read	
0	0	0	273	18	0	0	49	340	340	VALUES
.0	.0	.0	80.3	5.3	.0	.0	14.4			PERCENT

MIN	MAX	AMEAN	SD	GMEAN	GD	VALUES
10.000	700.00	37.959	98.29	21.075	2.21	49
2.500	700.00	7.743	39.02	3.526	2.24	340

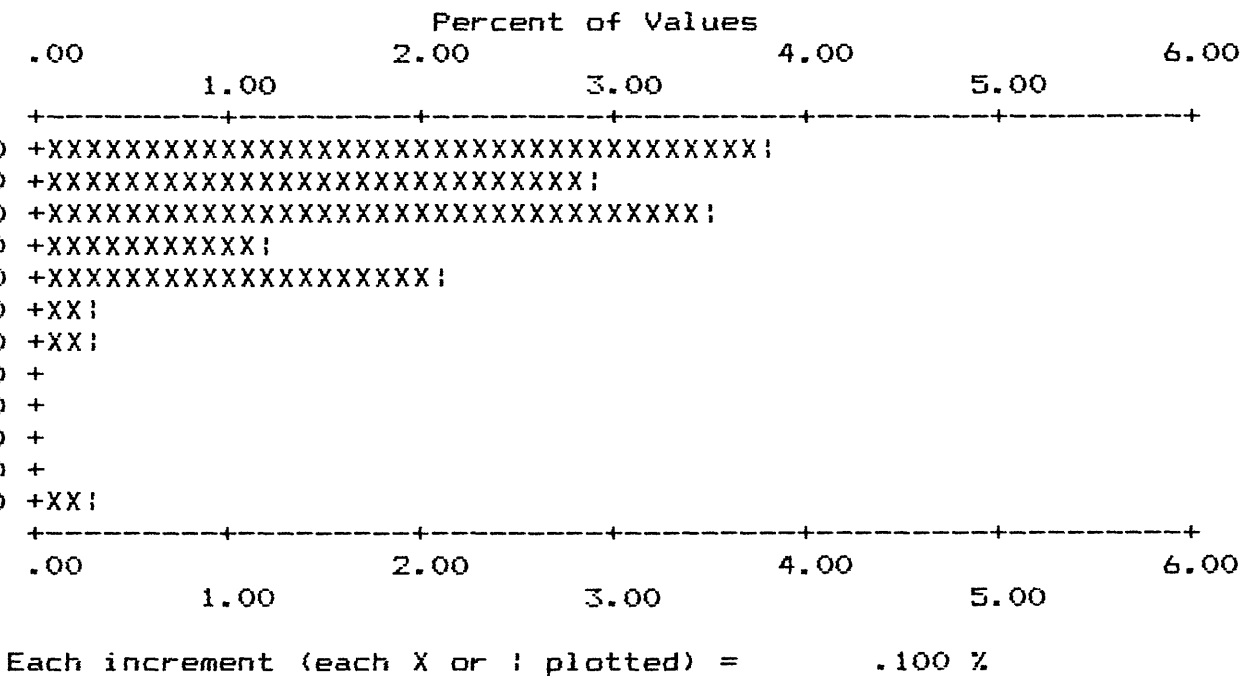

Each increment (each X or ! plotted) = .100 %

APPENDIX IV-B. HISTOGRAMS OF HEAVY-MINERAL-CONCENTRATE DATA, WHITE MTS NRA

COLUMN ID.: S-CR

	VALUE	NO.	%	CUM.	CUM. %		TOT CUM	TOT CUM %	
1	10.000	1	.29	1	.3	82.1	61	17.9	82.1
2	20.000	42	12.35	43	12.6	69.7	103	30.3	69.7
3	30.000	22	6.47	65	19.1	63.2	125	36.8	63.2
4	50.000	81	23.82	146	42.9	39.4	206	60.6	39.4
5	70.000	58	17.06	204	60.0	22.4	264	77.6	22.4
6	100.000	42	12.35	246	72.4	10.0	306	90.0	10.0
7	150.000	12	3.53	258	75.9	6.5	318	93.5	6.5
8	200.000	13	3.82	271	79.7	2.6	331	97.4	2.6
9	300.000	3	.88	274	80.6	1.8	334	98.2	1.8
10	500.000	3	.88	277	81.5	.9	337	99.1	.9
11	1000.000	1	.29	278	81.8	.6	338	99.4	.6
12	3000.000	2	.59	280	82.4	.0	340	100.0	.0

B	T	H	N	L	G	OTHER	UNQUAL	ANAL	read	
0	0	0	6	54	0	0	280	340	340	VALUES
.0	.0	.0	1.8	15.9	.0	.0	82.4			PERCENT

MIN	MAX	AMEAN	SD	GMEAN	GD	VALUES
10.000	3000.00	98.643	261.16	60.197	2.17	280
5.000	3000.00	82.912	239.35	43.320	2.73	340

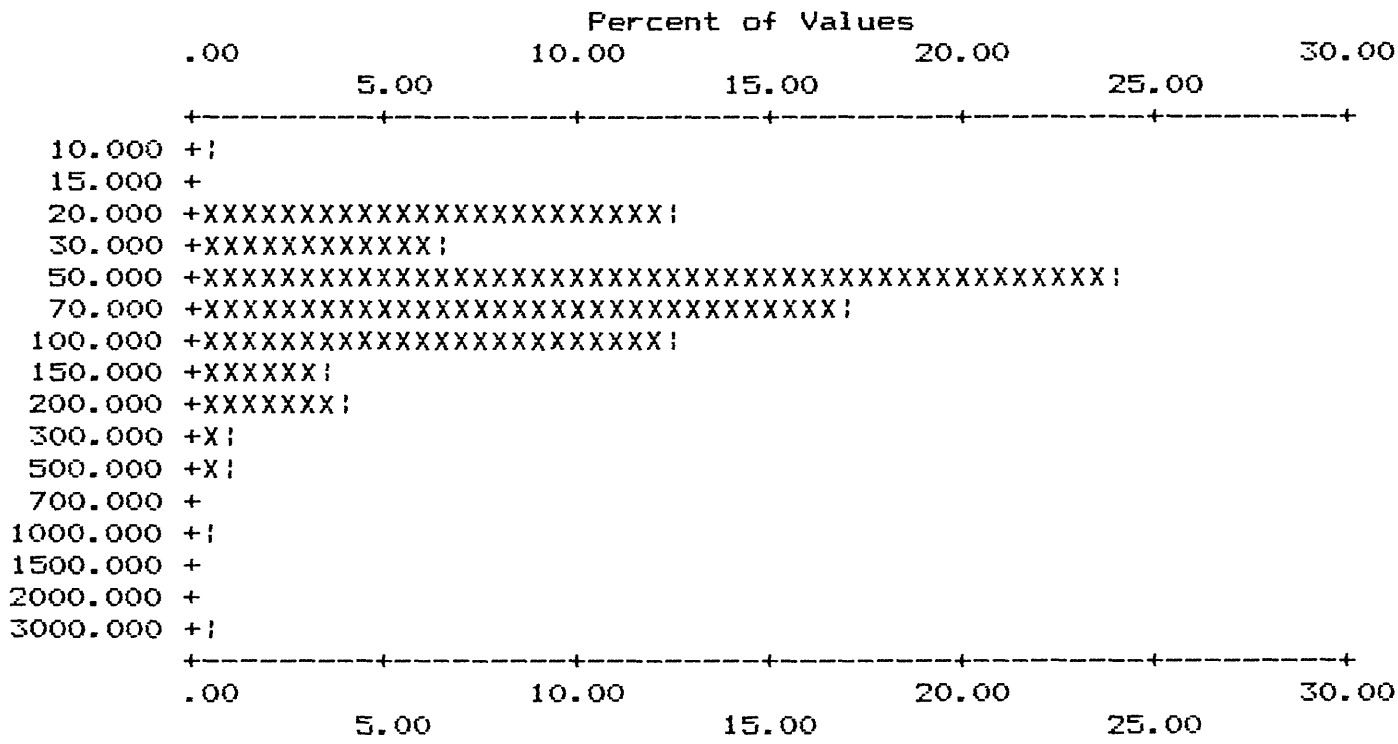

Each increment (each X or ¦ plotted) = .500 %

APPENDIX IV-B. HISTOGRAMS OF HEAVY-MINERAL-CONCENTRATE DATA, WHITE MTS NRA

COLUMN ID.: S-CU

	VALUE	NO.	%	CUM.	CUM. %		TOT CUM	TOT CUM %	
1	10.000	41	12.06	41	12.1	20.9	269	79.1	20.9
2	15.000	13	3.82	54	15.9	17.1	282	82.9	17.1
3	20.000	20	5.88	74	21.8	11.2	302	88.8	11.2
4	30.000	11	3.24	85	25.0	7.9	313	92.1	7.9
5	50.000	12	3.53	97	28.5	4.4	325	95.6	4.4
6	70.000	1	.29	98	28.8	4.1	326	95.9	4.1
7	100.000	9	2.65	107	31.5	1.5	335	98.5	1.5
8	150.000	1	.29	108	31.8	1.2	336	98.8	1.2
9	200.000	2	.59	110	32.4	.6	338	99.4	.6
10	1000.000	1	.29	111	32.6	.3	339	99.7	.3
11	2000.000	1	.29	112	32.9	.0	340	100.0	.0

B	T	H	N	L	G	OTHER	UNQUAL	ANAL	read	
0	0	0	132	96	0	0	112	340	340	VALUES
.0	.0	.0	38.8	28.2	.0	.0	32.9			PERCENT

MIN	MAX	AMEAN	SD	GMEAN	GD	VALUES
10.000	2000.00	57.634	209.68	22.698	2.67	112
2.500	2000.00	21.368	122.66	6.288	3.00	340

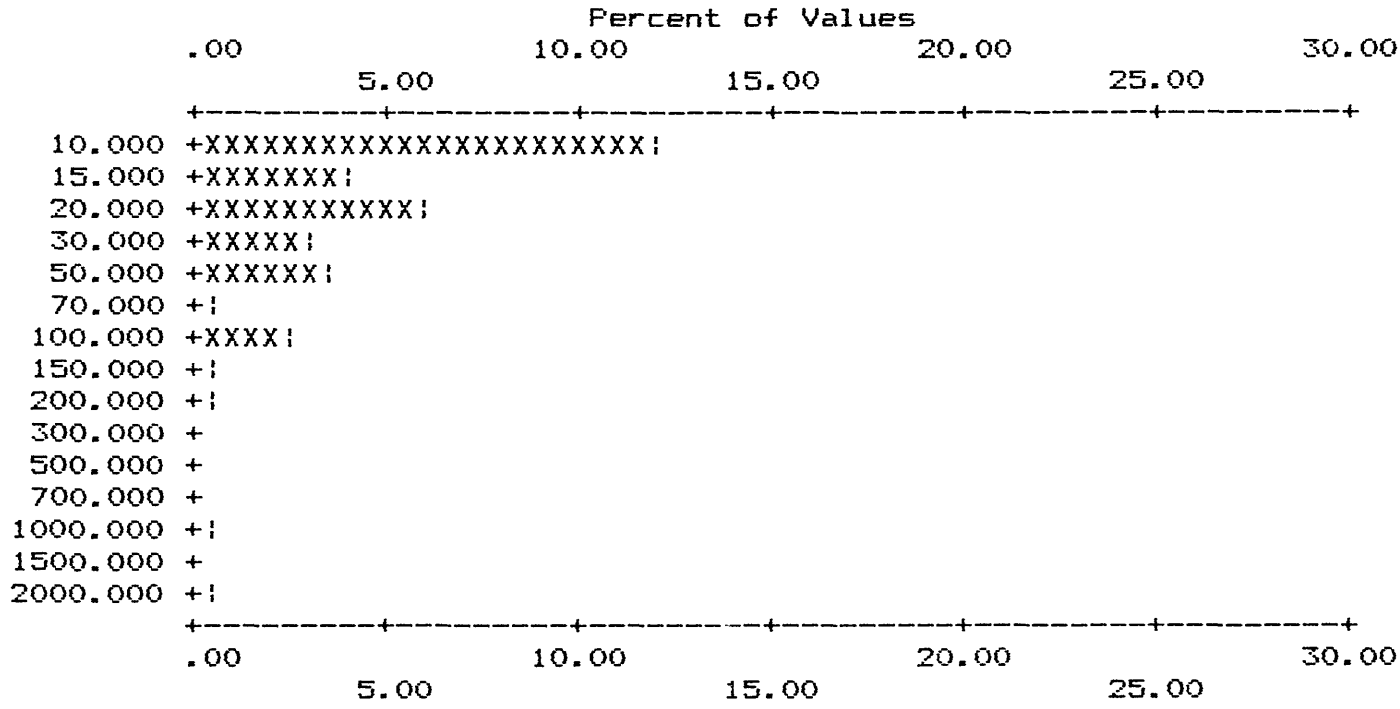

Each increment (each X or ! plotted) = .500 %

APPENDIX IV-B. HISTOGRAMS OF HEAVY-MINERAL-CONCENTRATE DATA, WHITE MTS NRA

COLUMN ID.: S-LA

	VALUE	NO.	%	CUM.	CUM. %		TOT CUM	TOT CUM %	
1	50.000	37	10.88	37	10.9	53.2	159	46.8	53.2
2	70.000	45	13.24	82	24.1	40.0	204	60.0	40.0
3	100.000	50	14.71	132	38.8	25.3	254	74.7	25.3
4	150.000	26	7.65	158	46.5	17.6	280	82.4	17.6
5	200.000	23	6.76	181	53.2	10.9	303	89.1	10.9
6	300.000	13	3.82	194	57.1	7.1	316	92.9	7.1
7	500.000	14	4.12	208	61.2	2.9	330	97.1	2.9
8	700.000	4	1.18	212	62.4	1.8	334	98.2	1.8
9	1000.000	2	.59	214	62.9	1.2	336	98.8	1.2
10	1500.000	2	.59	216	63.5	.6	338	99.4	.6
11	2000.000	2	.59	218	64.1	.0	340	100.0	.0

B	T	H	N	L	G	OTHER	UNQUAL	ANAL	read	
0	0	0	95	27	0	0	218	340	340	VALUES
.0	.0	.0	27.9	7.9	.0	.0	64.1			PERCENT

MIN	MAX	AMEAN	SD	GMEAN	GD	VALUES
50.000	2000.00	188.991	268.65	123.152	2.23	218
12.500	2000.00	126.654	230.59	57.259	3.39	340

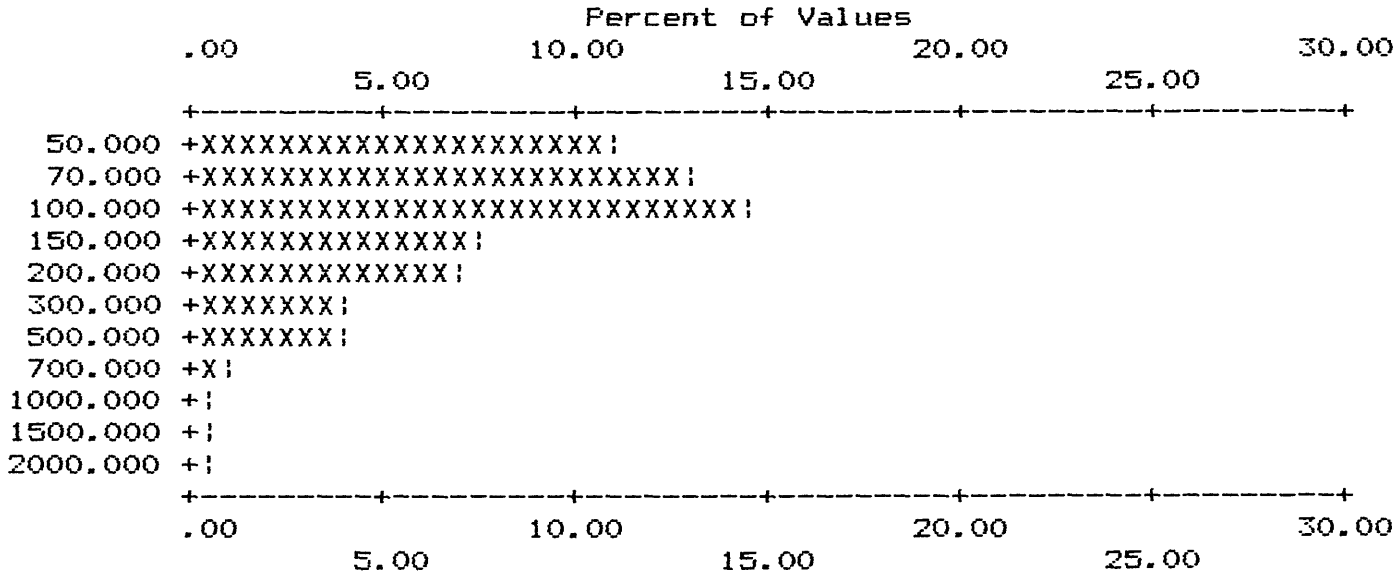

Each increment (each X or ¦ plotted) = .500 %

APPENDIX IV-B. HISTOGRAMS OF HEAVY-MINERAL-CONCENTRATE DATA, WHITE MTS NRA

COLUMN ID.: S-MO

	VALUE	NO.	%	CUM.	CUM. %	TOT CUM	TOT CUM %	
1	10.000	1	.29	1	.3	.9	337	99.1	.9
2	15.000	1	.29	2	.6	.6	338	99.4	.6
3	20.000	2	.59	4	1.2	.0	340	100.0	.0

B	T	H	N	L	G	OTHER	UNQUAL	ANAL	read	
0	0	0	333	3	0	0	4	340	340	VALUES
.0	.0	.0	97.9	.9	.0	.0	1.2			PERCENT

MIN	MAX	AMEAN	SD	GMEAN	GD	VALUES
10.000	20.00	16.250	4.79	15.651	1.39	4
2.500	20.00	2.684	1.57	2.570	1.23	340

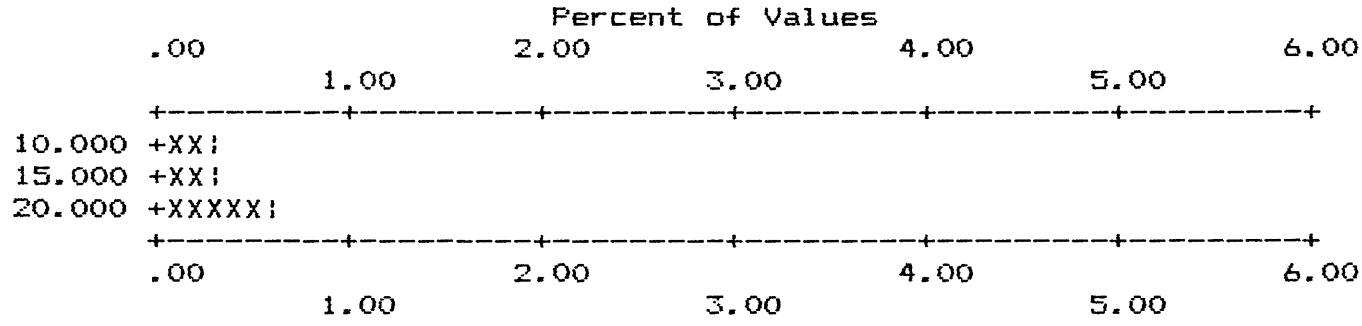

Each increment (each X or ! plotted) = .100 %

APPENDIX IV-B. HISTOGRAMS OF HEAVY-MINERAL-CONCENTRATE DATA, WHITE MTS NRA

COLUMN ID.: S-NB

	VALUE	NO.	%	CUM.	CUM. %		TOT CUM	TOT CUM %	
1	50.000	111	32.65	111	32.6	34.1	224	65.9	34.1
2	70.000	60	17.65	171	50.3	16.5	284	83.5	16.5
3	100.000	38	11.18	209	61.5	5.3	322	94.7	5.3
4	150.000	5	1.47	214	62.9	3.8	327	96.2	3.8
5	200.000	7	2.06	221	65.0	1.8	334	98.2	1.8
6	300.000	3	.88	224	65.9	.9	337	99.1	.9
7	500.000	3	.88	227	66.8	.0	340	100.0	.0

B	T	H	N	L	G	OTHER	UNQUAL	ANAL	read	
0	0	0	28	85	0	0	227	340	340	VALUES
.0	.0	.0	8.2	25.0	.0	.0	66.8			PERCENT

MIN	MAX	AMEAN	SD	GMEAN	GD	VALUES
50.000	500.00	79.736	63.83	69.272	1.57	227
12.500	500.00	60.515	58.91	46.630	2.00	340

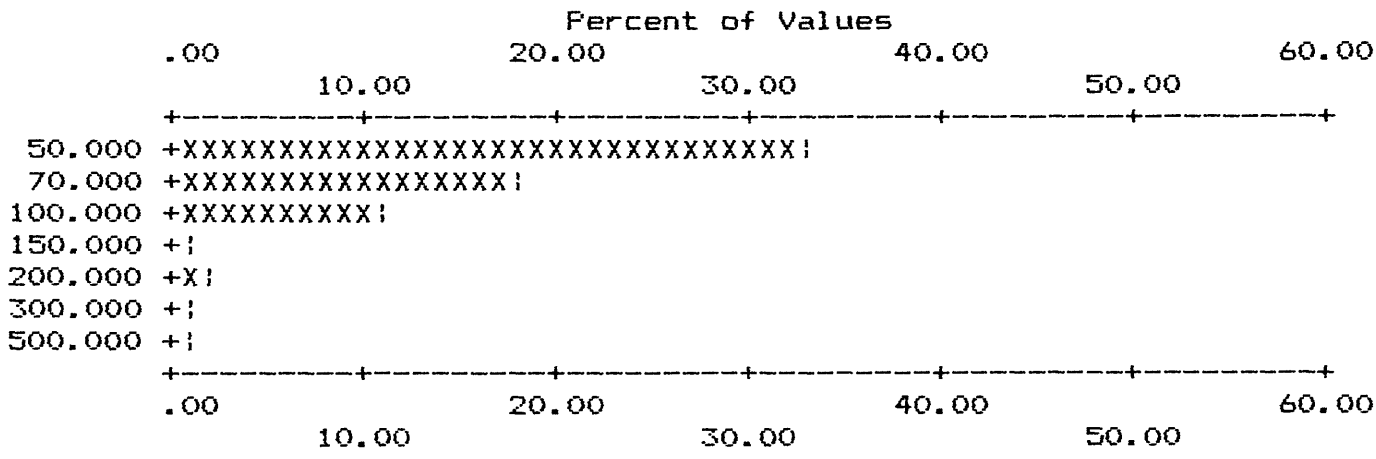

Each increment (each X or ¦ plotted) = 1.000 %

APPENDIX IV-B. HISTOGRAMS OF HEAVY-MINERAL-CONCENTRATE DATA, WHITE MTS NRA

COLUMN ID.: S-NI

	VALUE	NO.	%	CUM.	CUM. %	TOT CUM	TOT CUM %
1	10.000	1	.29	1	.3	13.2	295	86.8	13.2
2	20.000	10	2.94	11	3.2	10.3	305	89.7	10.3
3	30.000	9	2.65	20	5.9	7.6	314	92.4	7.6
4	50.000	11	3.24	31	9.1	4.4	325	95.6	4.4
5	70.000	4	1.18	35	10.3	3.2	329	96.8	3.2
6	100.000	6	1.76	41	12.1	1.5	335	98.5	1.5
7	150.000	1	.29	42	12.4	1.2	336	98.8	1.2
8	200.000	2	.59	44	12.9	.6	338	99.4	.6
9	500.000	1	.29	45	13.2	.3	339	99.7	.3
10	700.000	1	.29	46	13.5	.0	340	100.0	.0

B	T	H	N	L	G	OTHER	UNQUAL	ANAL	read	
0	0	0	292	2	0	0	46	340	340	VALUES
.0	.0	.0	85.9	.6	.0	.0	13.5			PERCENT

MIN	MAX	AMEAN	SD	GMEAN	GD	VALUES
10.000	700.00	79.565	122.07	48.869	2.38	46
2.500	700.00	12.941	51.72	3.753	2.90	340

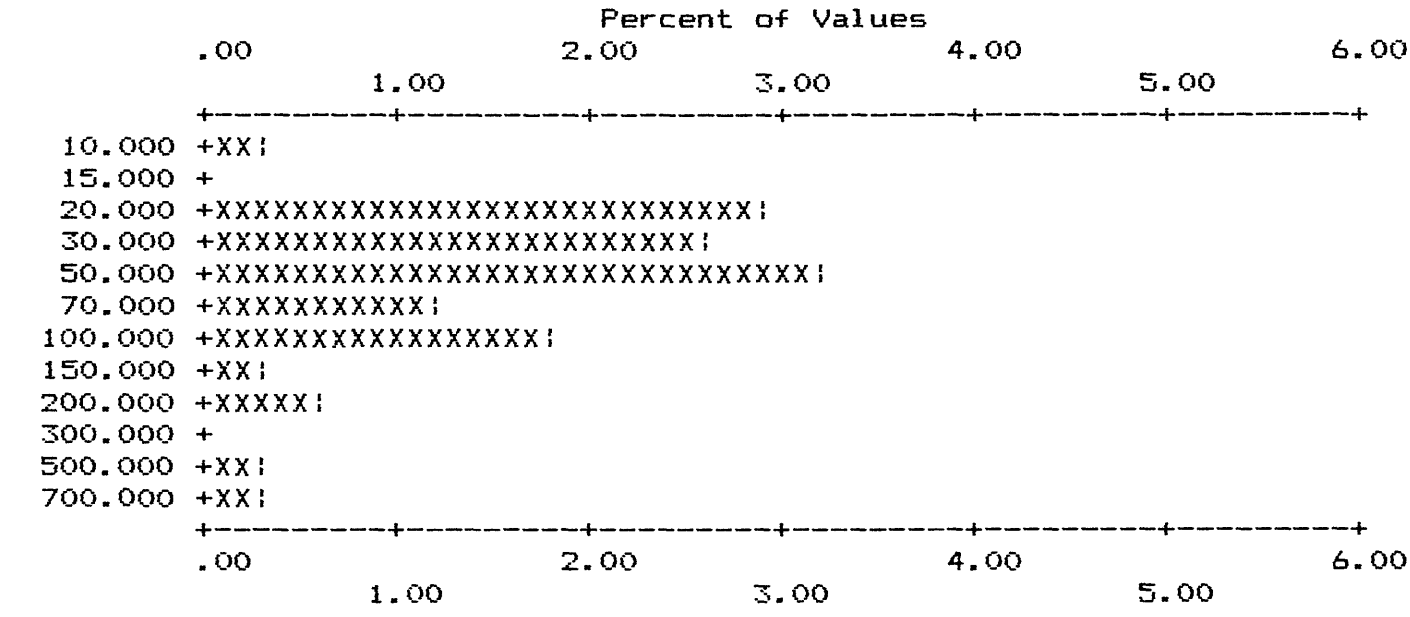

Each increment (each X or ¦ plotted) = .100 %

APPENDIX IV-B. HISTOGRAMS OF HEAVY-MINERAL-CONCENTRATE DATA, WHITE MTS NRA

COLUMN ID.: S-PB

	VALUE	NO.	%	CUM.	CUM. %		TOT CUM	TOT CUM %	
1	20.000	71	20.88	71	20.9	37.1	214	62.9	37.1
2	30.000	38	11.18	109	32.1	25.9	252	74.1	25.9
3	50.000	37	10.88	146	42.9	15.0	289	85.0	15.0
4	70.000	8	2.35	154	45.3	12.6	297	87.4	12.6
5	100.000	14	4.12	168	49.4	8.5	311	91.5	8.5
6	150.000	4	1.18	172	50.6	7.4	315	92.6	7.4
7	200.000	12	3.53	184	54.1	3.8	327	96.2	3.8
8	300.000	4	1.18	188	55.3	2.6	331	97.4	2.6
9	500.000	5	1.47	193	56.8	1.2	336	98.8	1.2
10	700.000	1	.29	194	57.1	.9	337	99.1	.9
11	1000.000	2	.59	196	57.6	.3	339	99.7	.3
12	2000.000	1	.29	197	57.9	.0	340	100.0	.0

B	T	H	N	L	G	OTHER	UNQUAL	ANAL	read	
0	0	0	51	92	0	0	197	340	340	VALUES
.0	.0	.0	15.0	27.1	.0	.0	57.9			PERCENT

MIN	MAX	AMEAN	SD	GMEAN	GD	VALUES
20.000	2000.00	90.203	194.32	45.163	2.61	197
5.000	2000.00	55.721	153.23	21.589	3.17	340

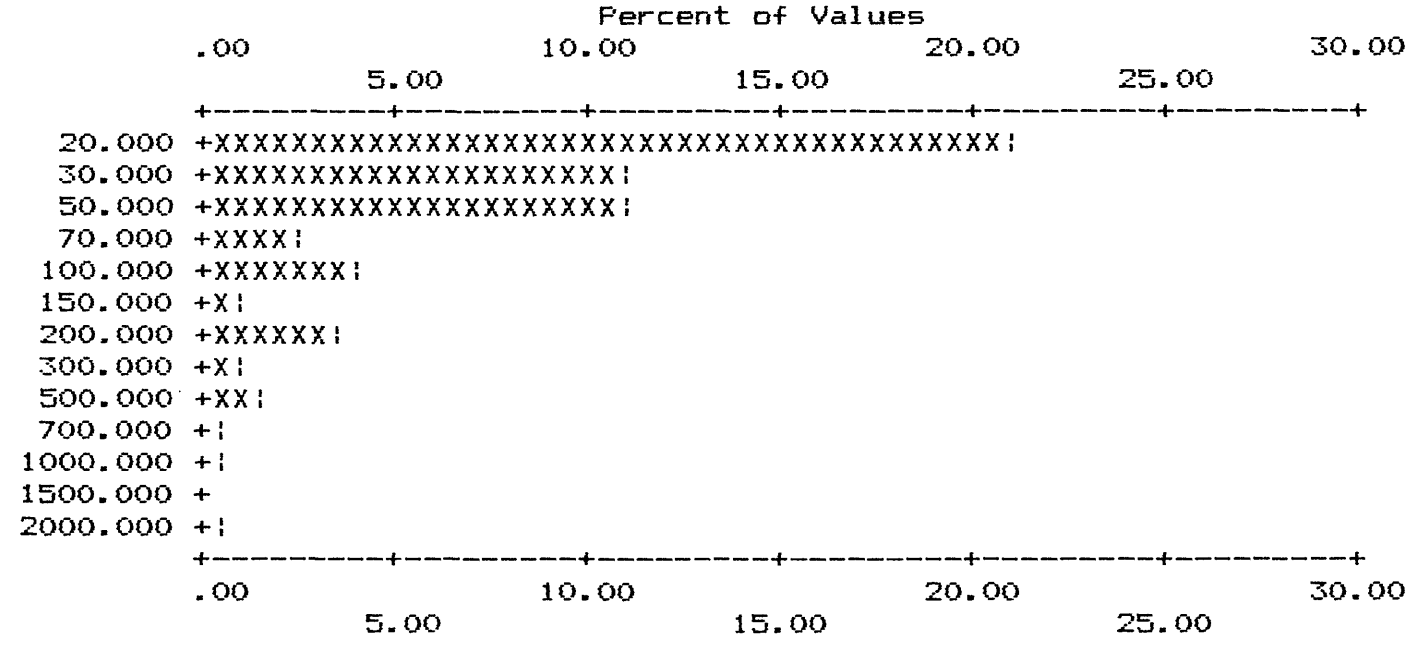

Each increment (each X or ¦ plotted) = .500 %

APPENDIX IV-B. HISTOGRAMS OF HEAVY-MINERAL-CONCENTRATE DATA, WHITE MTS NRA

COLUMN ID.: S-SB

	VALUE	NO.	%	CUM.	CUM. %	TOT CUM	TOT CUM %	
1	200.000	5	1.47	5	1.5	2.4	332	97.6	2.4
2	300.000	2	.59	7	2.1	1.8	334	98.2	1.8
3	500.000	1	.29	8	2.4	1.5	335	98.5	1.5
4	700.000	3	.88	11	3.2	.6	338	99.4	.6
5	2000.000	1	.29	12	3.5	.3	339	99.7	.3
6	7000.000	1	.29	13	3.8	.0	340	100.0	.0

B	T	H	N	L	G	OTHER	UNQUAL	ANAL	read	
0	0	0	321	6	0	0	13	340	340	VALUES
.0	.0	.0	94.4	1.8	.0	.0	3.8			PERCENT

MIN	MAX	AMEAN	SD	GMEAN	GD	VALUES
200.000	7000.00	1015.385	1864.07	478.611	2.94	13
50.000	7000.00	87.794	396.67	55.181	1.62	340

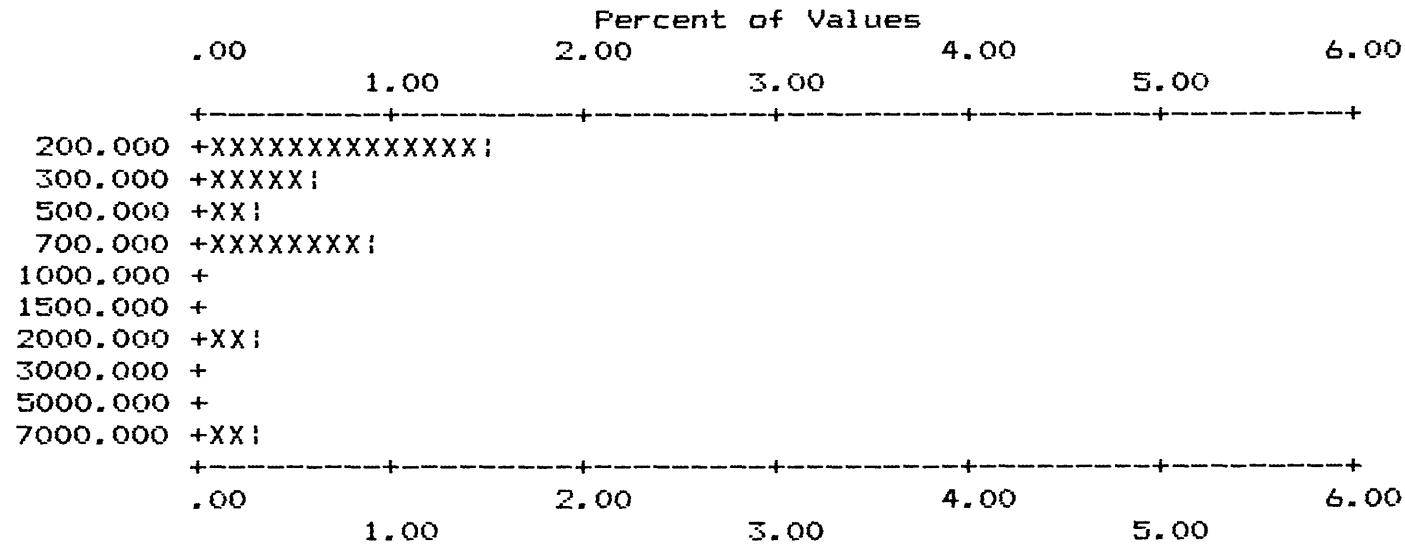

Each increment (each X or ! plotted) = .100 %

APPENDIX IV-B. HISTOGRAMS OF HEAVY-MINERAL-CONCENTRATE DATA, WHITE MTS NRA

COLUMN ID.: S-SC

	VALUE	NO.	%	CUM.	CUM. %	TOT CUM	TOT CUM %	
1	7.000	1	.29	1	.3	85.9	48	14.1	85.9
2	10.000	17	5.00	18	5.3	80.9	65	19.1	80.9
3	15.000	50	14.71	68	20.0	66.2	115	33.8	66.2
4	20.000	61	17.94	129	37.9	48.2	176	51.8	48.2
5	30.000	54	15.88	183	53.8	32.4	230	67.6	32.4
6	50.000	68	20.00	251	73.8	12.4	298	87.6	12.4
7	70.000	27	7.94	278	81.8	4.4	325	95.6	4.4
8	100.000	12	3.53	290	85.3	.9	337	99.1	.9
9	150.000	3	.88	293	86.2	.0	340	100.0	.0

B	T	H	N	L	G	OTHER	UNQUAL	ANAL	read	
0	0	0	36	11	0	0	293	340	340	VALUES
.0	.0	.0	10.6	3.2	.0	.0	86.2			PERCENT

MIN	MAX	AMEAN	SD	GMEAN	GD	VALUES
7.000	150.00	36.543	25.14	29.732	1.89	293
2.500	150.00	31.918	26.04	21.593	2.72	340

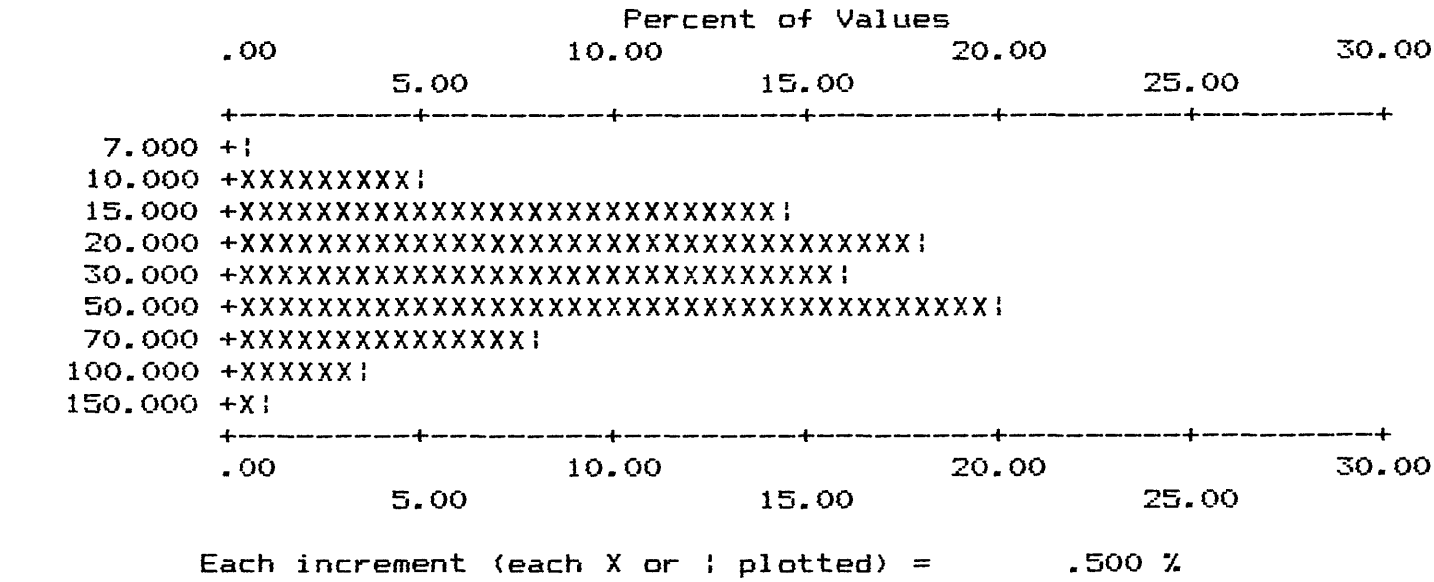

Each increment (each X or ¦ plotted) = .500 %

APPENDIX IV-B. HISTOGRAMS OF HEAVY-MINERAL-CONCENTRATE DATA, WHITE MTS NRA

COLUMN ID.: S-SN

	VALUE	NO.	%	CUM.	CUM. %		TOT CUM	TOT CUM %	
1	20.000	21	6.18	21	6.2	43.8	87	25.6	74.4
2	30.000	9	2.65	30	8.8	41.2	96	28.2	71.8
3	50.000	26	7.65	56	16.5	33.5	122	35.9	64.1
4	70.000	9	2.65	65	19.1	30.9	131	38.5	61.5
5	100.000	14	4.12	79	23.2	26.8	145	42.6	57.4
6	150.000	10	2.94	89	26.2	23.8	155	45.6	54.4
7	200.000	18	5.29	107	31.5	18.5	173	50.9	49.1
8	300.000	4	1.18	111	32.6	17.4	177	52.1	47.9
9	500.000	17	5.00	128	37.6	12.4	194	57.1	42.9
10	700.000	18	5.29	146	42.9	7.1	212	62.4	37.6
11	1000.000	9	2.65	155	45.6	4.4	221	65.0	35.0
12	1500.000	2	.59	157	46.2	3.8	223	65.6	34.4
13	2000.000	13	3.82	170	50.0	.0	236	69.4	30.6

B	T	H	N	L	G	OTHER	UNQUAL	ANAL	read	
0	0	0	38	28	104	0	170	340	340	VALUES
.0	.0	.0	11.2	8.2	30.6	.0	50.0			PERCENT

MIN	MAX	AMEAN	SD	GMEAN	GD	VALUES
20.000	2000.00	408.353	553.59	162.495	4.19	170
5.000	4000.00	1429.088	1759.73	233.184	11.68	340

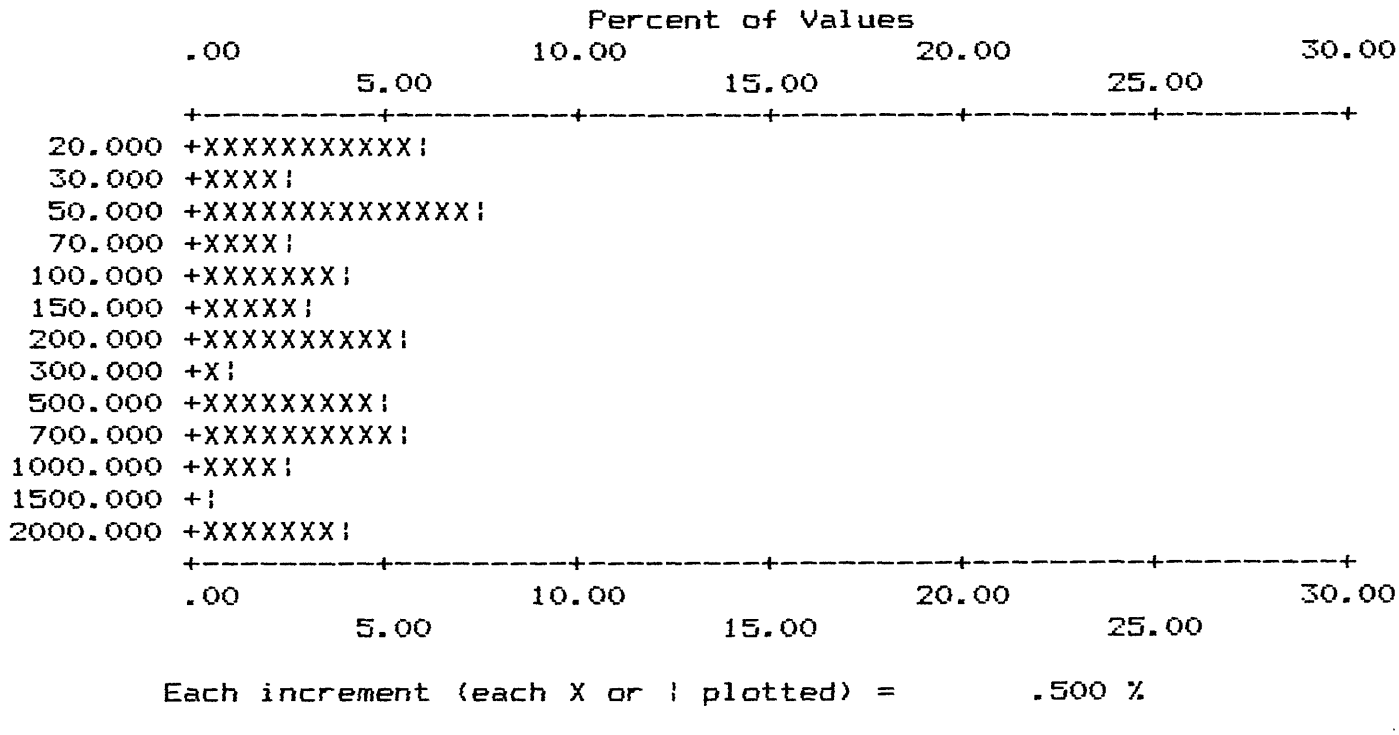

Each increment (each X or ! plotted) = .500 %

APPENDIX IV-B. HISTOGRAMS OF HEAVY-MINERAL-CONCENTRATE DATA, WHITE MTS NRA

COLUMN ID.: S-SR

	VALUE	NO.	%	CUM.	CUM. %		TOT CUM	TOT CUM %	
1	200.000	34	10.00	34	10.0	46.5	182	53.5	46.5
2	300.000	16	4.71	50	14.7	41.8	198	58.2	41.8
3	500.000	25	7.35	75	22.1	34.4	223	65.6	34.4
4	700.000	24	7.06	99	29.1	27.4	247	72.6	27.4
5	1000.000	58	17.06	157	46.2	10.3	305	89.7	10.3
6	1500.000	22	6.47	179	52.6	3.8	327	96.2	3.8
7	2000.000	10	2.94	189	55.6	.9	337	99.1	.9
8	5000.000	3	.88	192	56.5	.0	340	100.0	.0

B	T	H	N	L	G	OTHER	UNQUAL	ANAL	read	
0	0	0	122	26	0	0	192	340	340	VALUES
.0	.0	.0	35.9	7.6	.0	.0	56.5			PERCENT

MIN	MAX	AMEAN	SD	GMEAN	GD	VALUES
200.000	5000.00	869.271	717.14	662.016	2.13	192
50.000	5000.00	516.471	672.21	226.742	3.89	340

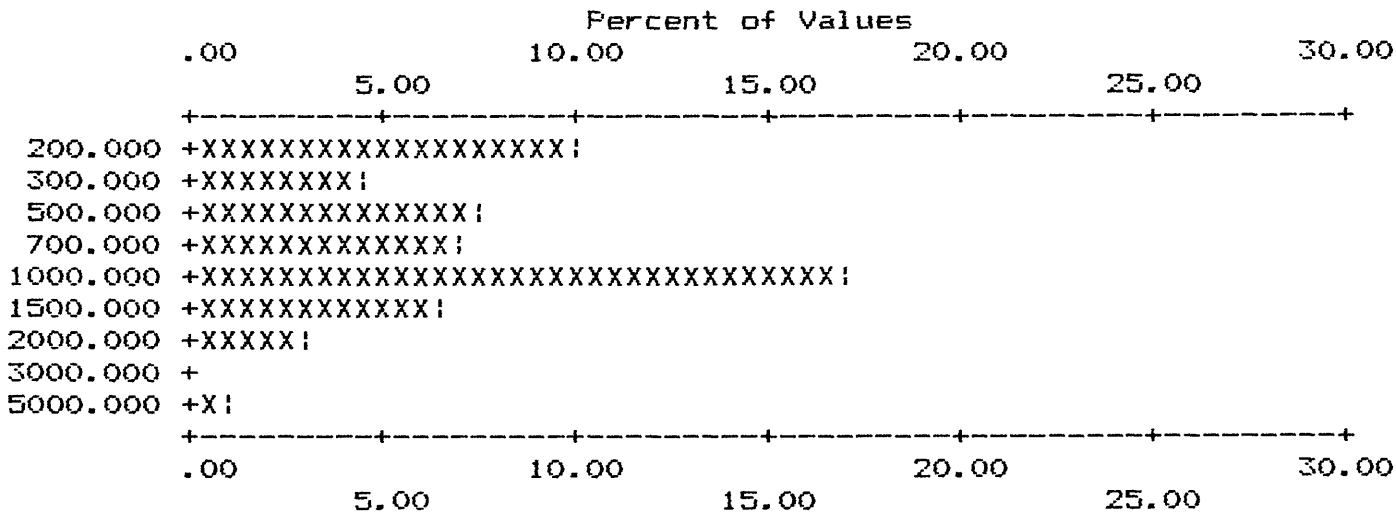

Each increment (each X or ! plotted) = .500 %

APPENDIX IV-B. HISTOGRAMS OF HEAVY-MINERAL-CONCENTRATE DATA, WHITE MTS NRA

COLUMN ID.: S-V

	VALUE	NO.	%	CUM.	CUM. %		TOT CUM	TOT CUM %	
1	20.000	63	18.53	63	18.5	75.6	83	24.4	75.6
2	30.000	47	13.82	110	32.4	61.8	130	38.2	61.8
3	50.000	71	20.88	181	53.2	40.9	201	59.1	40.9
4	70.000	58	17.06	239	70.3	23.8	259	76.2	23.8
5	100.000	49	14.41	288	84.7	9.4	308	90.6	9.4
6	150.000	19	5.59	307	90.3	3.8	327	96.2	3.8
7	200.000	11	3.24	318	93.5	.6	338	99.4	.6
8	300.000	1	.29	319	93.8	.3	339	99.7	.3
9	500.000	1	.29	320	94.1	.0	340	100.0	.0

B	T	H	N	L	G	OTHER	UNQUAL	ANAL	read	
0	0	0	2	18	0	0	320	340	340	VALUES
.0	.0	.0	.6	5.3	.0	.0	94.1			PERCENT

MIN	MAX	AMEAN	SD	GMEAN	GD	VALUES
20.000	500.00	65.719	51.46	51.904	1.97	320
5.000	500.00	62.412	51.64	46.920	2.17	340

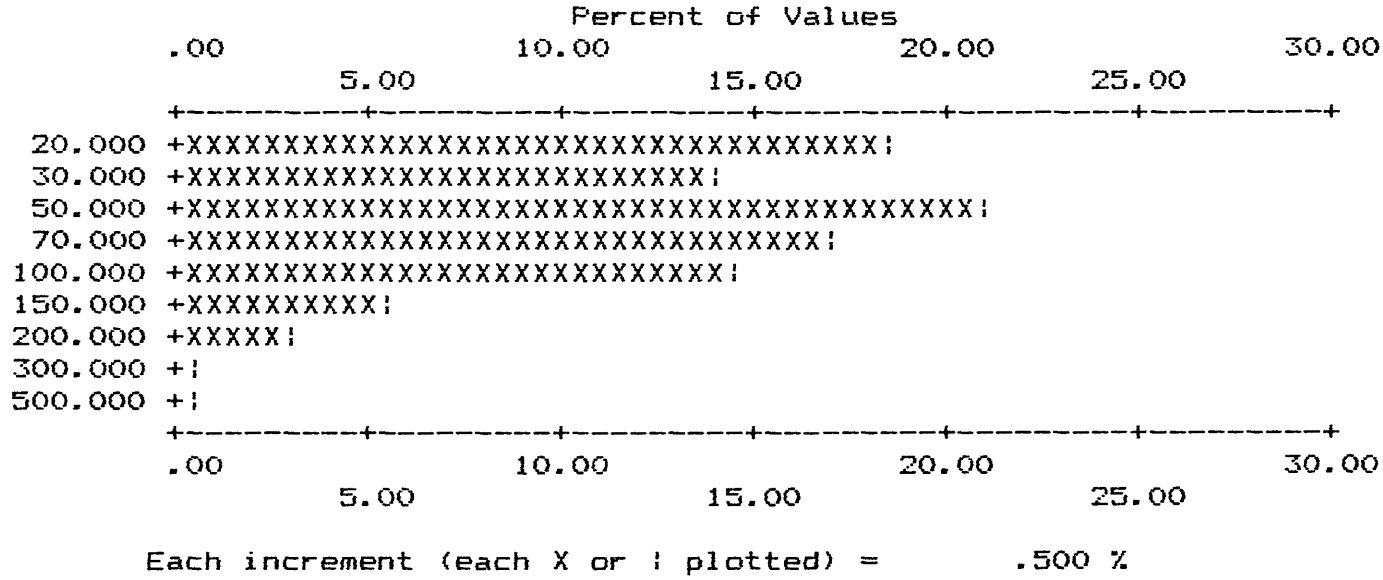

Each increment (each X or ¦ plotted) = .500 %

APPENDIX IV-B. HISTOGRAMS OF HEAVY-MINERAL-CONCENTRATE DATA, WHITE MTS NRA

COLUMN ID.: S-W

	VALUE	NO.	%	CUM.	CUM. %		TOT CUM	TOT CUM %	
1	100.000	31	9.12	31	9.1	16.5	284	83.5	16.5
2	150.000	10	2.94	41	12.1	13.5	294	86.5	13.5
3	200.000	13	3.82	54	15.9	9.7	307	90.3	9.7
4	300.000	5	1.47	59	17.4	8.2	312	91.8	8.2
5	500.000	7	2.06	66	19.4	6.2	319	93.8	6.2
6	700.000	2	.59	68	20.0	5.6	321	94.4	5.6
7	1000.000	3	.88	71	20.9	4.7	324	95.3	4.7
8	2000.000	10	2.94	81	23.8	1.8	334	98.2	1.8
9	3000.000	2	.59	83	24.4	1.2	336	98.8	1.2
10	5000.000	2	.59	85	25.0	.6	338	99.4	.6
11	10000.000	2	.59	87	25.6	.0	340	100.0	.0

B	T	H	N	L	G	OTHER	UNQUAL	ANAL	read	
0	0	0	210	43	0	0	87	340	340	VALUES
.0	.0	.0	61.8	12.6	.0	.0	25.6			PERCENT

MIN	MAX	AMEAN	SD	GMEAN	GD	VALUES
100.000	10000.00	834.483	1720.77	296.023	3.57	87
25.000	10000.00	235.294	935.42	51.365	3.43	340

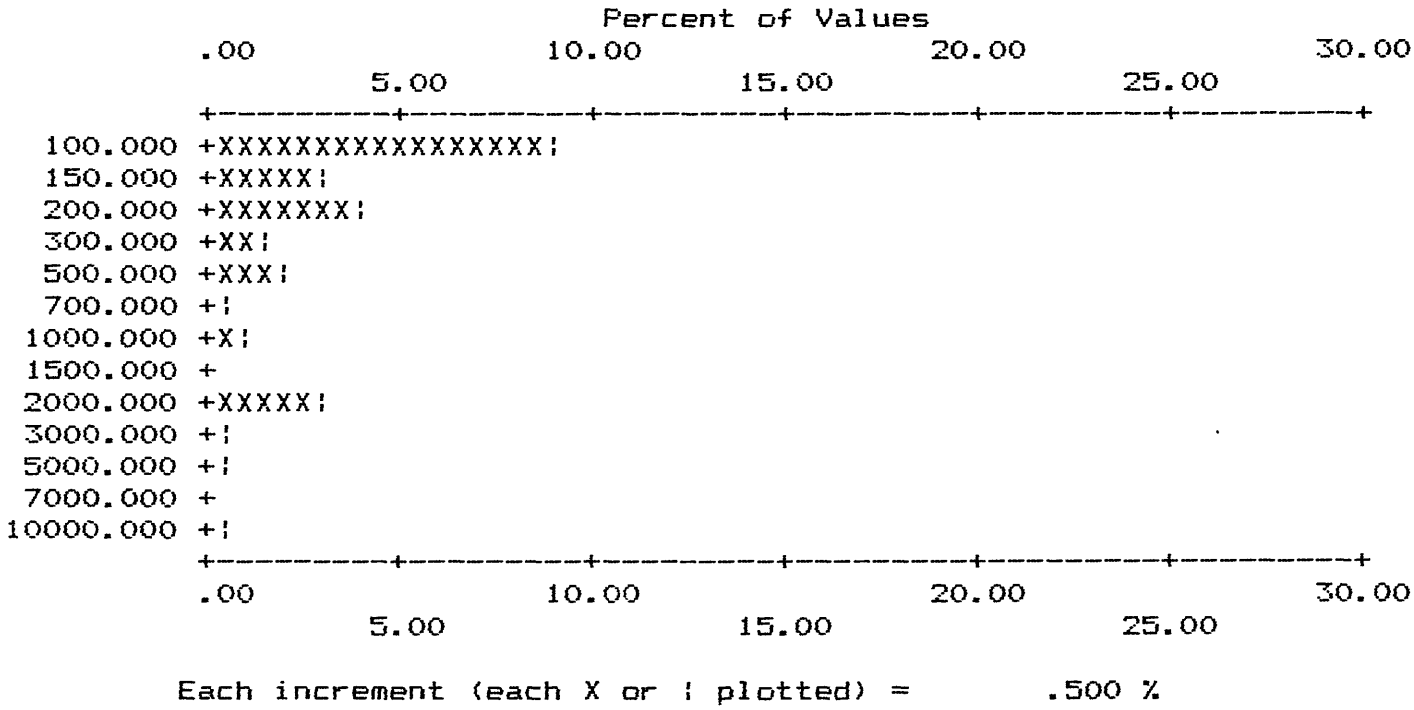

Each increment (each X or ! plotted) = .500 %

APPENDIX IV-B. HISTOGRAMS OF HEAVY-MINERAL-CONCENTRATE DATA, WHITE MTS NRA

COLUMN ID.: S-Y

	VALUE	NO.	%	CUM.	CUM. %		TOT CUM	TOT CUM %	
1	20.000	12	3.53	12	3.5	95.0	17	5.0	95.0
2	30.000	14	4.12	26	7.6	90.9	31	9.1	90.9
3	50.000	21	6.18	47	13.8	84.7	52	15.3	84.7
4	70.000	20	5.88	67	19.7	78.8	72	21.2	78.8
5	100.000	58	17.06	125	36.8	61.8	130	38.2	61.8
6	150.000	47	13.82	172	50.6	47.9	177	52.1	47.9
7	200.000	78	22.94	250	73.5	25.0	255	75.0	25.0
8	300.000	41	12.06	291	85.6	12.9	296	87.1	12.9
9	500.000	35	10.29	326	95.9	2.6	331	97.4	2.6
10	700.000	6	1.76	332	97.6	.9	337	99.1	.9
11	1000.000	3	.88	335	98.5	.0	340	100.0	.0

B	T	H	N	L	G	OTHER	UNQUAL	ANAL	read	
0	0	0	1	4	0	0	335	340	340	VALUES
.0	.0	.0	.3	1.2	.0	.0	98.5			PERCENT

MIN	MAX	AMEAN	SD	GMEAN	GD	VALUES
20.000	1000.00	204.657	166.63	149.727	2.31	335
5.000	1000.00	201.779	167.07	143.592	2.46	340

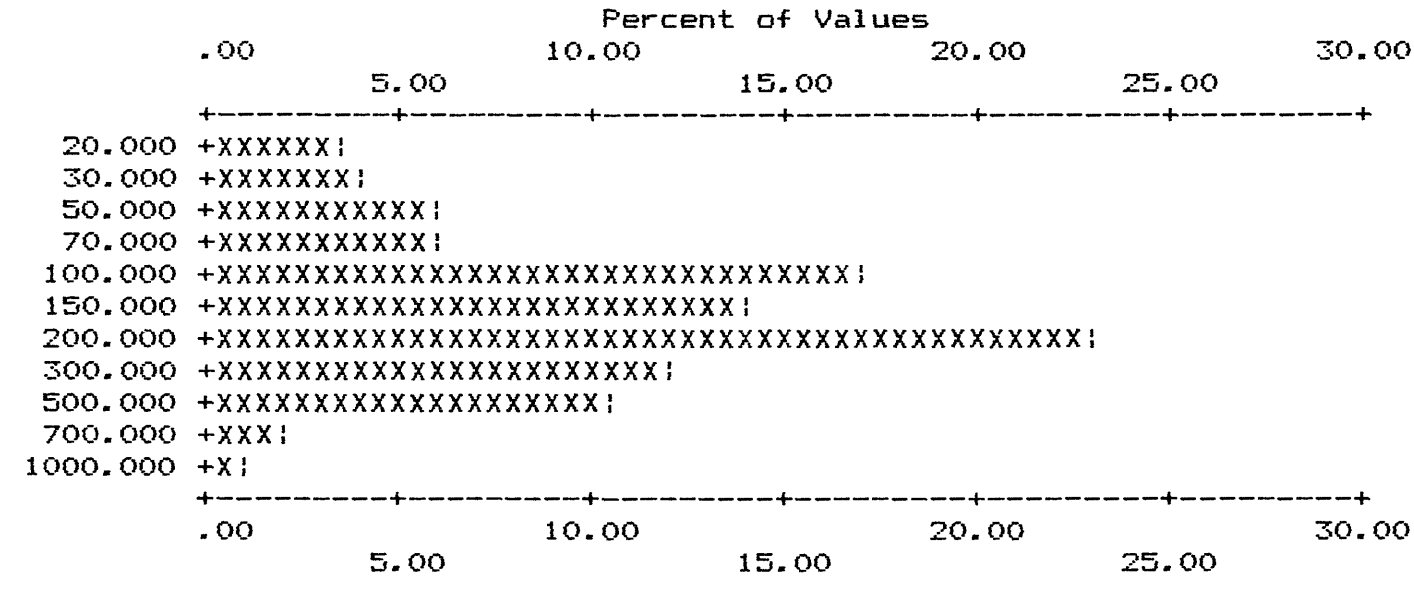

Each increment (each X or ¦ plotted) = .500 %

APPENDIX IV-B. HISTOGRAMS OF HEAVY-MINERAL-CONCENTRATE DATA, WHITE MTS NRA

COLUMN ID.: S-ZN

	VALUE	NO.	%	CUM.	CUM. %		TOT CUM	TOT CUM %	
1	500.000	13	3.82	13	3.8	17.9	278	81.8	18.2
2	700.000	13	3.82	26	7.6	14.1	291	85.6	14.4
3	1000.000	12	3.53	38	11.2	10.6	303	89.1	10.9
4	1500.000	9	2.65	47	13.8	7.9	312	91.8	8.2
5	2000.000	8	2.35	55	16.2	5.6	320	94.1	5.9
6	3000.000	5	1.47	60	17.6	4.1	325	95.6	4.4
7	5000.000	9	2.65	69	20.3	1.5	334	98.2	1.8
8	10000.000	1	.29	70	20.6	1.2	335	98.5	1.5
9	15000.000	2	.59	72	21.2	.6	337	99.1	.9
10	20000.000	2	.59	74	21.8	.0	339	99.7	.3

B	T	H	N	L	G	OTHER	UNQUAL	ANAL	read	
0	0	0	257	8	1	0	74	340	340	VALUES
.0	.0	.0	75.6	2.4	.3	.0	21.8			PERCENT

MIN	MAX	AMEAN	SD	GMEAN	GD	VALUES
500.000	20000.00	2663.513	4001.52	1484.479	2.64	74
125.000	40000.00	797.721	3015.21	221.441	3.16	340

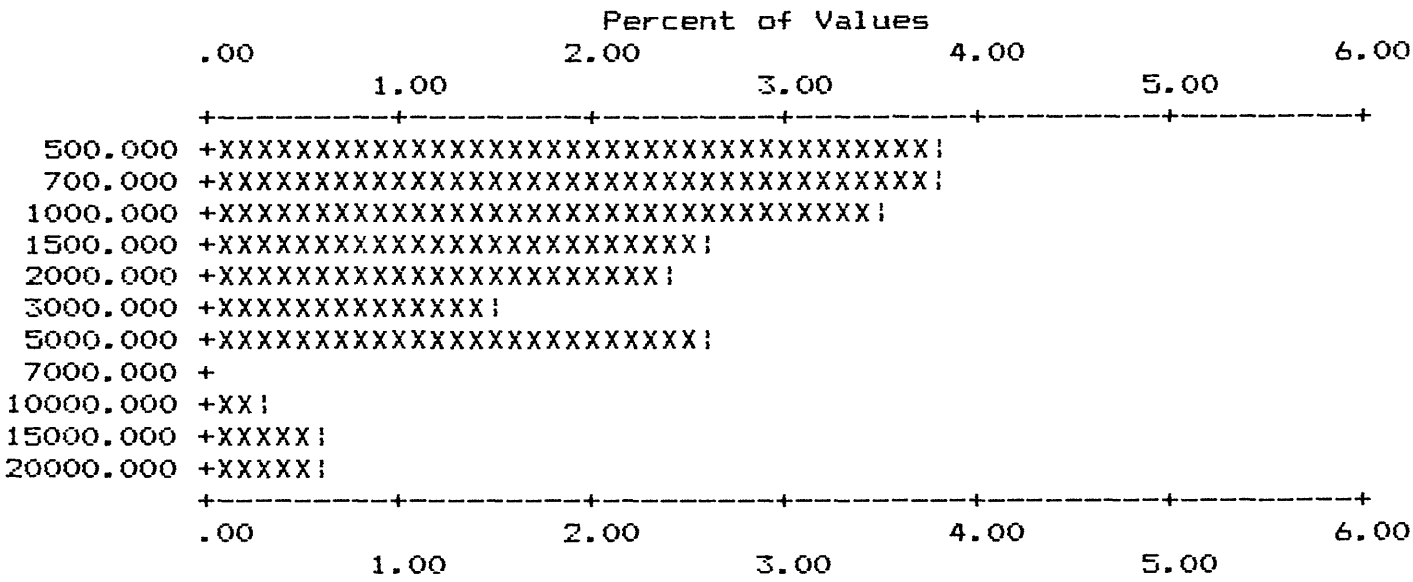

Each increment (each X or ¦ plotted) = .100 %

APPENDIX IV-B. HISTOGRAMS OF HEAVY-MINERAL-CONCENTRATE DATA, WHITE MTS NRA

COLUMN ID.: S-ZR

	VALUE	NO.	%	CUM.	CUM. %	TOT CUM	TOT CUM %
1	20.000	2	.59	2	.6 17.6	2	.6 99.4
2	100.000	1	.29	3	.9 17.4	3	.9 99.1
3	150.000	1	.29	4	1.2 17.1	4	1.2 98.8
4	200.000	5	1.47	9	2.6 15.6	9	2.6 97.4
5	300.000	4	1.18	13	3.8 14.4	13	3.8 96.2
6	500.000	7	2.06	20	5.9 12.4	20	5.9 94.1
7	700.000	8	2.35	28	8.2 10.0	28	8.2 91.8
8	1000.000	10	2.94	38	11.2 7.1	38	11.2 88.8
9	1500.000	9	2.65	47	13.8 4.4	47	13.8 86.2
10	2000.000	15	4.41	62	18.2 .0	62	18.2 81.8

B	T	H	N	L	G	OTHER	UNQUAL	ANAL	read	
0	0	0	0	0	278	0	62	340	340	VALUES
.0	.0	.0	.0	.0	81.8	.0	18.2			PERCENT

MIN	MAX	AMEAN	SD	GMEAN	GD	VALUES
20.000	2000.00	1049.839	679.67	741.464	2.82	62
20.000	4000.00	3462.029	1176.69	2941.591	2.20	340

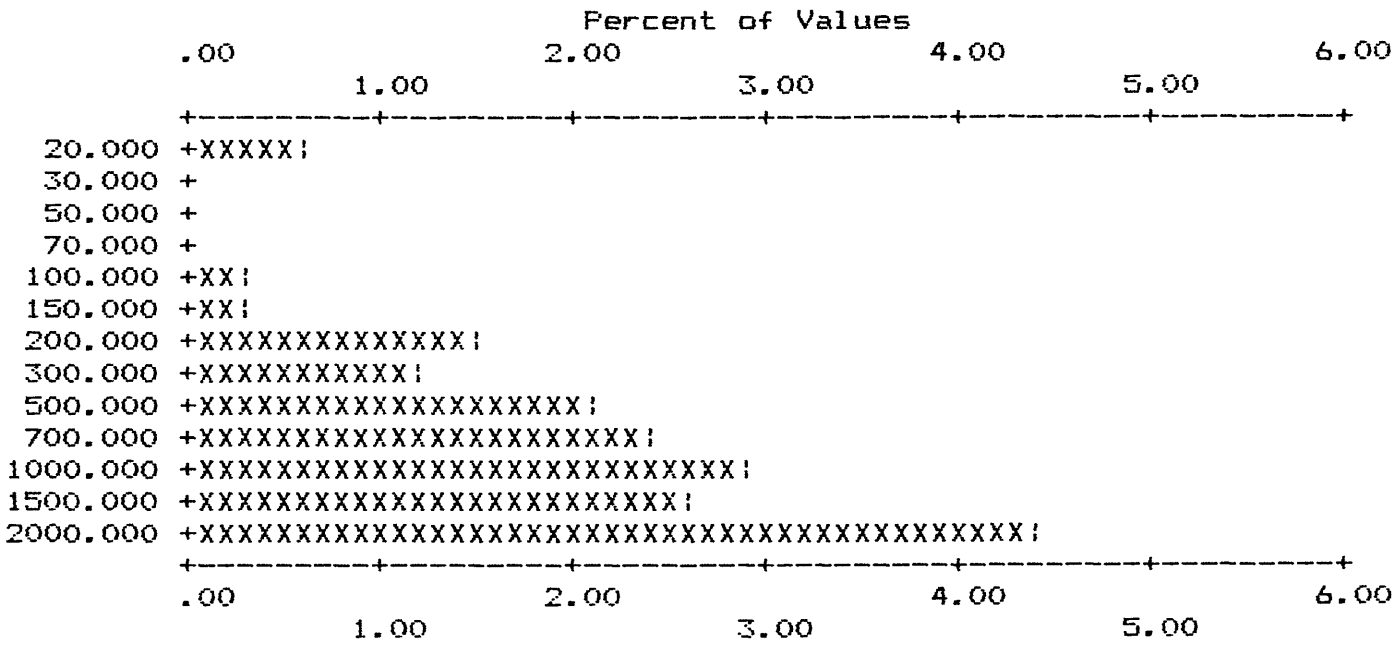

Each increment (each X or ! plotted) = .100 %

APPENDIX IV-B. HISTOGRAMS OF HEAVY-MINERAL-CONCENTRATE DATA, WHITE MTS NRA

COLUMN ID.: S-TH

	VALUE	NO.	%	CUM.	CUM. %		TOT CUM	TOT CUM %	
1	200.000	4	1.18	4	1.2	5.3	322	94.7	5.3
2	300.000	3	.88	7	2.1	4.4	325	95.6	4.4
3	500.000	11	3.24	18	5.3	1.2	336	98.8	1.2
4	700.000	2	.59	20	5.9	.6	338	99.4	.6
5	2000.000	2	.59	22	6.5	.0	340	100.0	.0

B	T	H	N	L	G	OTHER	UNQUAL	ANAL	read	
0	0	0	302	16	0	0	22	340	340	VALUES
.0	.0	.0	88.8	4.7	.0	.0	6.5			PERCENT

MIN	MAX	AMEAN	SD	GMEAN	GD	VALUES
200.000	2000.00	572.727	485.19	461.724	1.86	22
50.000	2000.00	86.176	176.41	59.649	1.79	340

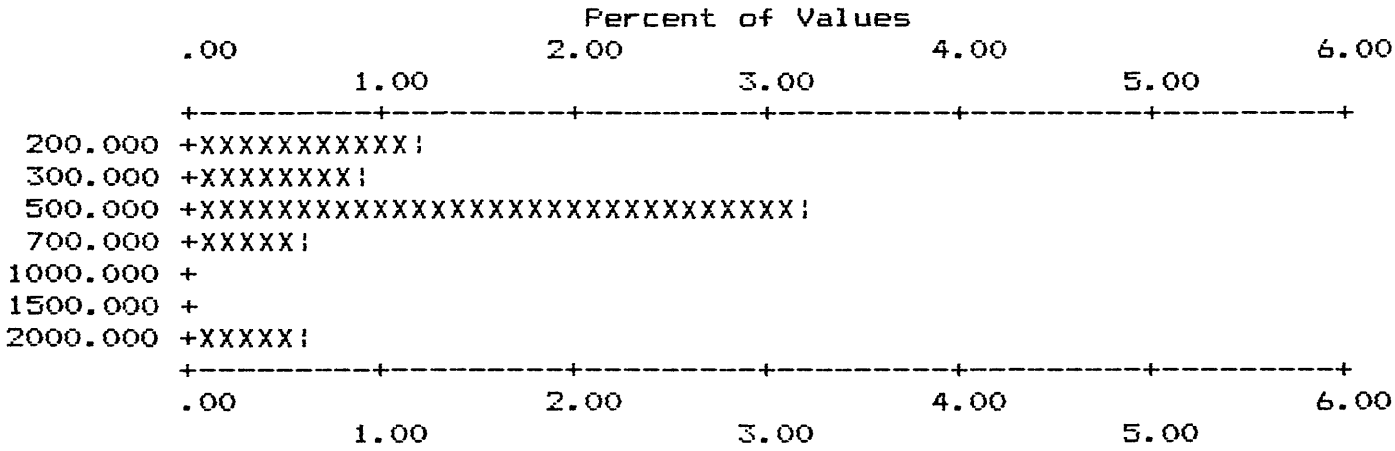

Each increment (each X or ¦ plotted) = .100 %

OPEN-FILE REPORT NO. 88-284

APPENDIX IV-C

UNITED STATES DEPARTMENT OF THE INTERIOR

GEOLOGICAL SURVEY

Histograms and frequency distributions of stream-sediment sample data from the White Mountains National Recreation Area, Livengood and Circle quadrangles, east-central Alaska

This report is preliminary and has not been reviewed for conformity with U.S. Geological Survey editorial standards and stratigraphic nomenclature. Any use of trade names is for descriptive purposes only and does not imply endorsement by the USGS.

1988

APPENDIX IV-C. HISTOGRAMS OF STREAM-SEDIMENT SAMPLE DATA, WHITE MTS NRA

COLUMN ID.: S-FE%

	VALUE	NO.	%	CUM.	CUM. %		TOT CUM	TOT CUM %	
1	.500	2	.43	2	.4	99.6	2	.4	99.6
2	.700	4	.87	6	1.3	98.7	6	1.3	98.7
3	1.000	22	4.77	28	6.1	93.9	28	6.1	93.9
4	1.500	48	10.41	76	16.5	83.5	76	16.5	83.5
5	2.000	209	45.34	285	61.8	38.2	285	61.8	38.2
6	3.000	130	28.20	415	90.0	10.0	415	90.0	10.0
7	5.000	39	8.46	454	98.5	1.5	454	98.5	1.5
8	7.000	3	.65	457	99.1	.9	457	99.1	.9
9	10.000	4	.87	461	100.0	.0	461	100.0	.0

B	T	H	N	L	G	OTHER	UNQUAL	ANAL	read	
0	0	0	0	0	0	0	461	461	461	VALUES
.0	.0	.0	.0	.0	.0	.0	100.0			PERCENT

MIN	MAX	AMEAN	SD	GMEAN	GD	VALUES
.500	10.00	2.520	1.26	2.291	1.53	461

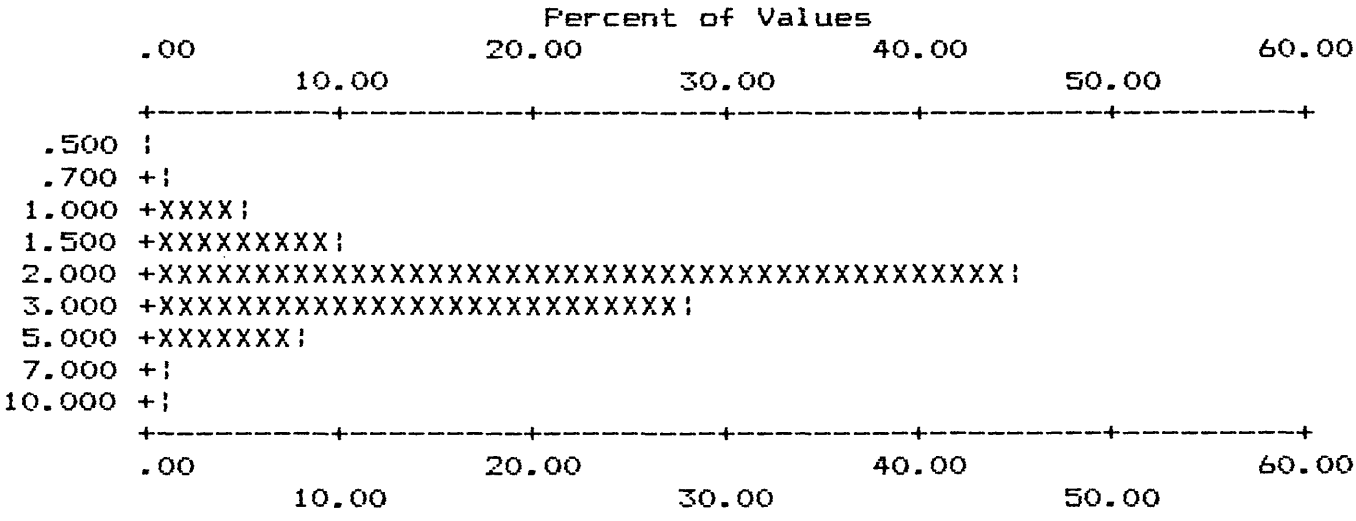

Each increment (each X or ¦ plotted) = 1.000 %

APPENDIX IV-C. HISTOGRAMS OF STREAM-SEDIMENT SAMPLE DATA, WHITE MTS NRA

COLUMN ID.: S-MG%

	VALUE	NO.	%	CUM.	CUM. %		TOT CUM	TOT CUM %	
1	.070	1	.22	1	.2	99.8	1	.2	99.8
2	.100	1	.22	2	.4	99.6	2	.4	99.6
3	.150	4	.87	6	1.3	98.7	6	1.3	98.7
4	.200	17	3.69	23	5.0	95.0	23	5.0	95.0
5	.300	45	9.76	68	14.8	85.2	68	14.8	85.2
6	.500	139	30.15	207	44.9	55.1	207	44.9	55.1
7	.700	146	31.67	353	76.6	23.4	353	76.6	23.4
8	1.000	69	14.97	422	91.5	8.5	422	91.5	8.5
9	1.500	13	2.82	435	94.4	5.6	435	94.4	5.6
10	2.000	21	4.56	456	98.9	1.1	456	98.9	1.1
11	3.000	2	.43	458	99.3	.7	458	99.3	.7
12	5.000	3	.65	461	100.0	.0	461	100.0	.0

B	T	H	N	L	G	OTHER	UNQUAL	ANAL	read	
0	0	0	0	0	0	0	461	461	461	VALUES
.0	.0	.0	.0	.0	.0	.0	100.0			PERCENT

MIN	MAX	AMEAN	SD	GMEAN	GD	VALUES
.070	5.00	.739	.54	.626	1.75	461

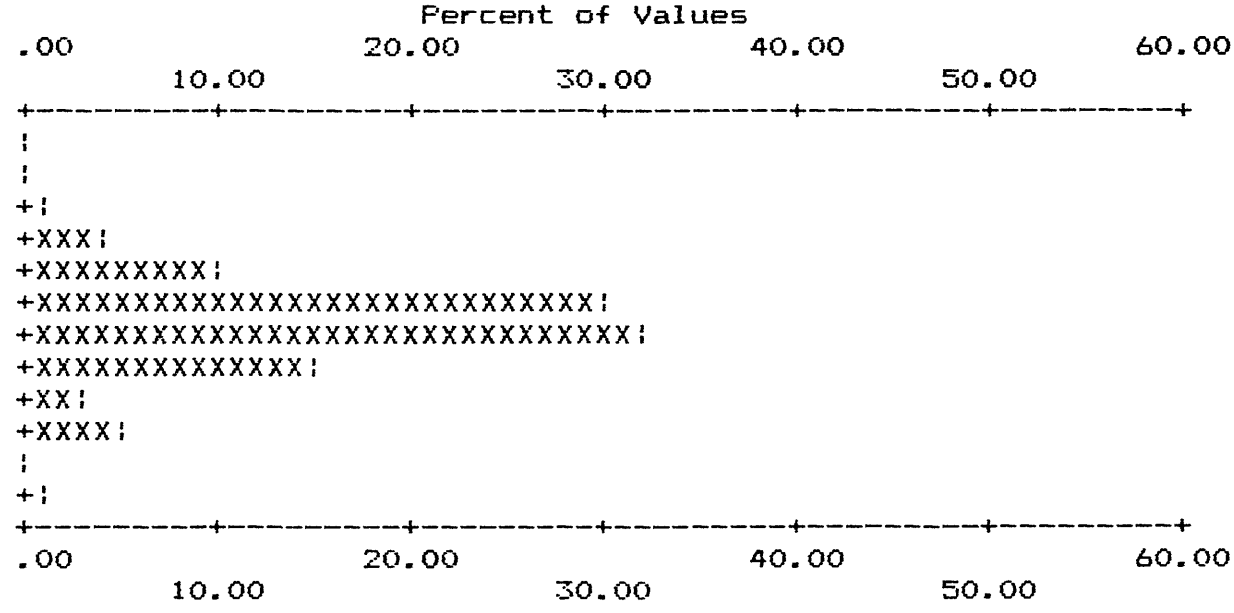

Each increment (each X or ¦ plotted) = 1.000 %

APPENDIX IV-C. HISTOGRAMS OF STREAM-SEDIMENT SAMPLE DATA, WHITE MTS NRA

COLUMN ID.: S-CA%

	VALUE	NO.	%	CUM.	CUM. %		TOT CUM	TOT CUM %	
1	.050	52	11.28	52	11.3	81.3	86	18.7	81.3
2	.070	19	4.12	71	15.4	77.2	105	22.8	77.2
3	.100	44	9.54	115	24.9	67.7	149	32.3	67.7
4	.150	56	12.15	171	37.1	55.5	205	44.5	55.5
5	.200	88	19.09	259	56.2	36.4	293	63.6	36.4
6	.300	43	9.33	302	65.5	27.1	336	72.9	27.1
7	.500	76	16.49	378	82.0	10.6	412	89.4	10.6
8	.700	22	4.77	400	86.8	5.9	434	94.1	5.9
9	1.000	16	3.47	416	90.2	2.4	450	97.6	2.4
10	1.500	6	1.30	422	91.5	1.1	456	98.9	1.1
11	2.000	1	.22	423	91.8	.9	457	99.1	.9
12	5.000	2	.43	425	92.2	.4	459	99.6	.4
13	15.000	1	.22	426	92.4	.2	460	99.8	.2
14	20.000	1	.22	427	92.6	.0	461	100.0	.0

B	T	H	N	L	G	OTHER	UNQUAL	ANAL	read	
0	0	0	0	34	0	0	427	461	461	VALUES
.0	.0	.0	.0	7.4	.0	.0	92.6			PERCENT

MIN	MAX	AMEAN	SD	GMEAN	GD	VALUES
.050	20.00	.404	1.26	.215	2.58	427
.025	20.00	.376	1.22	.184	2.92	461

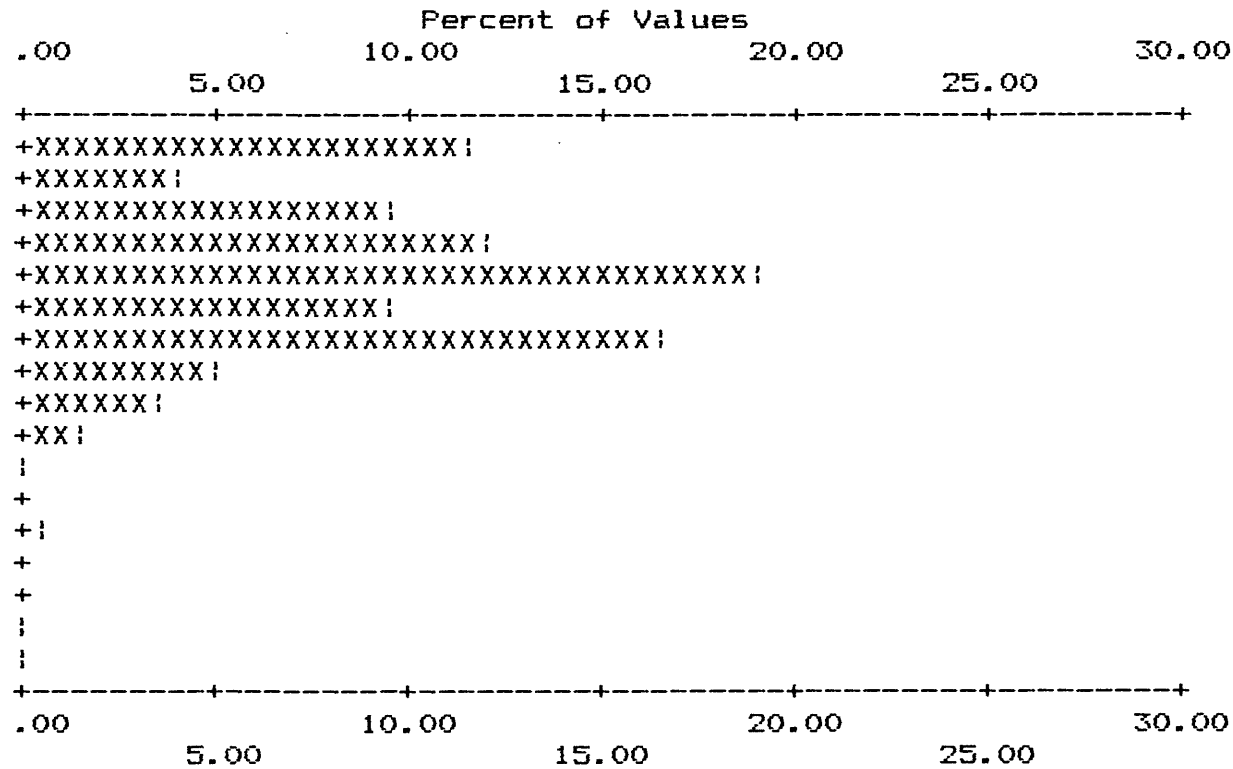

Each increment (each X or ¦ plotted) = .500 %

APPENDIX IV-C. HISTOGRAMS OF STREAM-SEDIMENT SAMPLE DATA, WHITE MTS NRA

COLUMN ID.: S-TI%

	VALUE	NO.	%	CUM.	CUM. %		TOT CUM	TOT CUM %	
1	.050	1	.22	1	.2	99.8	1	.2	99.8
2	.070	1	.22	2	.4	99.6	2	.4	99.6
3	.100	2	.43	4	.9	99.1	4	.9	99.1
4	.150	7	1.52	11	2.4	97.6	11	2.4	97.6
5	.200	53	11.50	64	13.9	86.1	64	13.9	86.1
6	.300	122	26.46	186	40.3	59.7	186	40.3	59.7
7	.500	234	50.76	420	91.1	8.9	420	91.1	8.9
8	.700	37	8.03	457	99.1	.9	457	99.1	.9
9	1.000	4	.87	461	100.0	.0	461	100.0	.0

B	T	H	N	L	G	OTHER	UNQUAL	ANAL	read	
0	0	0	0	0	0	0	461	461	461	VALUES
.0	.0	.0	.0	.0	.0	.0	100.0			PERCENT

MIN	MAX	AMEAN	SD	GMEAN	GD	VALUES
.050	1.00	.424	.15	.393	1.52	461

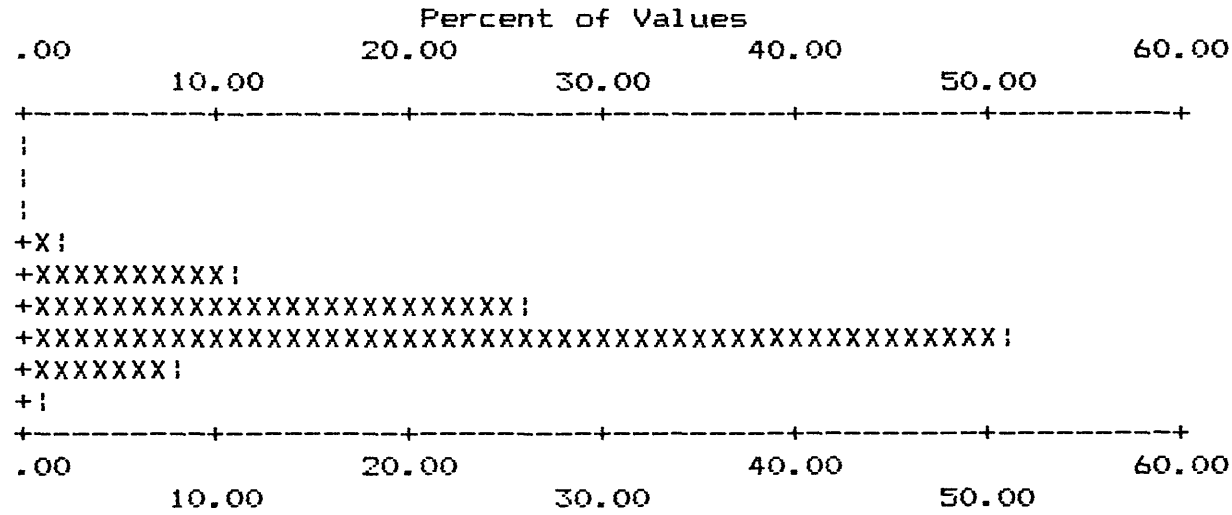

Each increment (each X or ¦ plotted) = 1.000 %

APPENDIX IV-C. HISTOGRAMS OF STREAM-SEDIMENT SAMPLE DATA, WHITE MTS NRA

COLUMN ID.: S-MN

	VALUE	NO.	%	CUM.	CUM. %	TOT CUM	TOT CUM %
1	70.000	2	.43	2	.4 98.9	2	.4 99.6
2	100.000	9	1.95	11	2.4 97.0	11	2.4 97.6
3	150.000	9	1.95	20	4.3 95.0	20	4.3 95.7
4	200.000	62	13.45	82	17.8 81.6	82	17.8 82.2
5	300.000	106	22.99	188	40.8 58.6	188	40.8 59.2
6	500.000	142	30.80	330	71.6 27.8	330	71.6 28.4
7	700.000	64	13.88	394	85.5 13.9	394	85.5 14.5
8	1000.000	50	10.85	444	96.3 3.0	444	96.3 3.7
9	1500.000	9	1.95	453	98.3 1.1	453	98.3 1.7
10	2000.000	2	.43	455	98.7 .7	455	98.7 1.3
11	3000.000	2	.43	457	99.1 .2	457	99.1 .9
12	5000.000	1	.22	458	99.3 .0	458	99.3 .7

B	T	H	N	L	G	OTHER	UNQUAL	ANAL	read	
0	0	0	0	0	3	0	458	461	461	VALUES
.0	.0	.0	.0	.0	.7	.0	99.3			PERCENT

MIN	MAX	AMEAN	SD	GMEAN	GD	VALUES
70.000	5000.00	525.961	401.67	433.397	1.85	458
70.000	10000.00	587.614	861.31	442.341	1.94	461

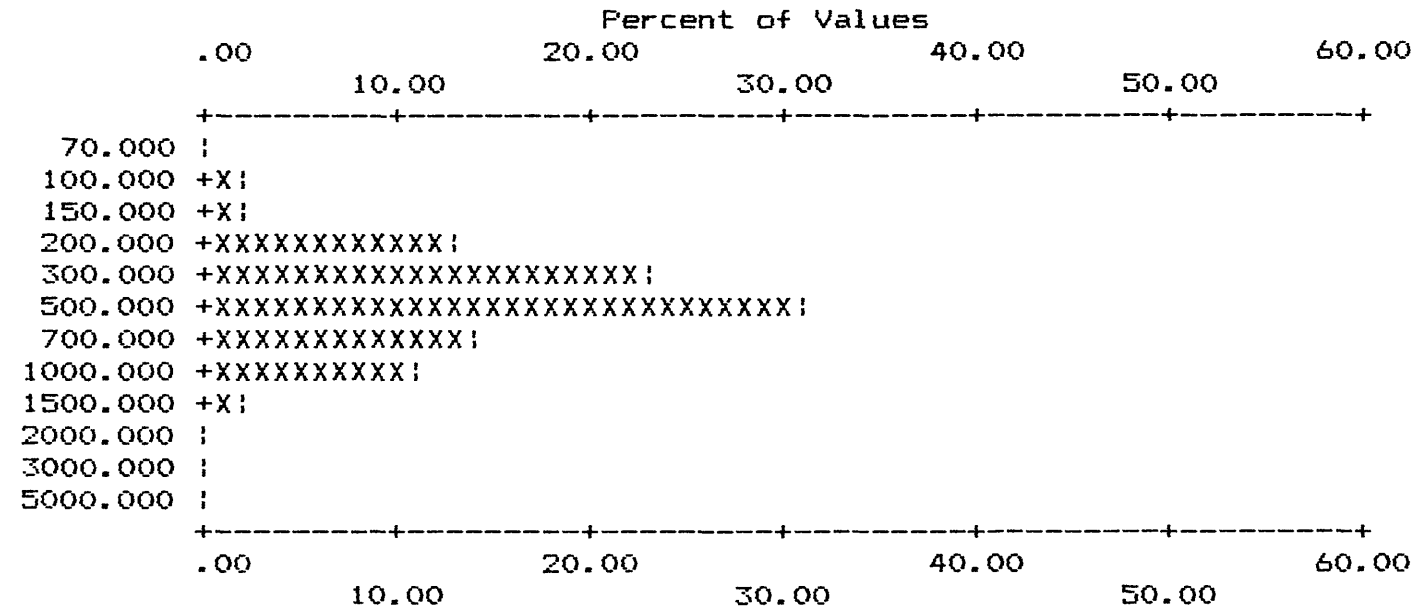

Each increment (each X or ¦ plotted) = 1.000 %

APPENDIX IV-C. HISTOGRAMS OF STREAM-SEDIMENT SAMPLE DATA, WHITE MTS NRA

COLUMN ID.: S-AG

	VALUE	NO.	%	CUM.	CUM. %		TOT CUM	TOT CUM %	
1	.500	25	5.42	25	5.4	2.4	450	97.6	2.4
2	.700	7	1.52	32	6.9	.9	457	99.1	.9
3	1.000	3	.65	35	7.6	.2	460	99.8	.2
4	1.500	1	.22	36	7.8	.0	461	100.0	.0

B	T	H	N	L	G	OTHER	UNQUAL	ANAL	read	
0	0	0	355	70	0	0	36	461	461	VALUES
.0	.0	.0	77.0	15.2	.0	.0	7.8			PERCENT

MIN	MAX	AMEAN	SD	GMEAN	GD	VALUES
.500	1.50	.608	.21	.583	1.31	36
.125	1.50	.182	.14	.157	1.59	461

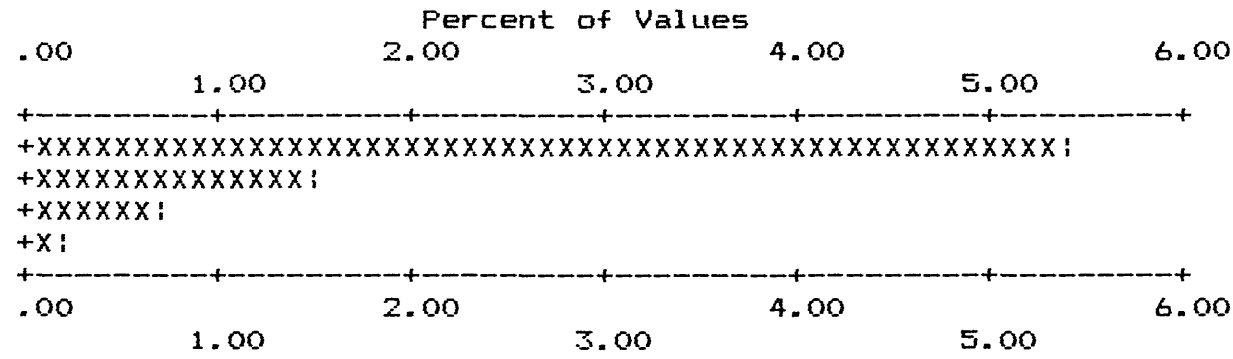

Each increment (each X or ¦ plotted) = .100 %

APPENDIX IV-C. HISTOGRAMS OF STREAM-SEDIMENT SAMPLE DATA, WHITE MTS NRA

COLUMN ID.: S-AS

	VALUE	NO.	%	CUM.	CUM. %	TOT CUM	TOT CUM %
1	200.000	1	.22	1	.2	461	100.0
					.0		.0

B	T	H	N	L	G	OTHER	UNQUAL	ANAL	read	
0	0	0	460	0	0	0	1	461	461	VALUES
.0	.0	.0	99.8	.0	.0	.0	.2			PERCENT

MIN	MAX	AMEAN	SD	GMEAN	GD	VALUES
200.000	200.00	200.000	.00	200.000	********	1
50.000	200.00	50.325	6.99	50.150	1.07	461

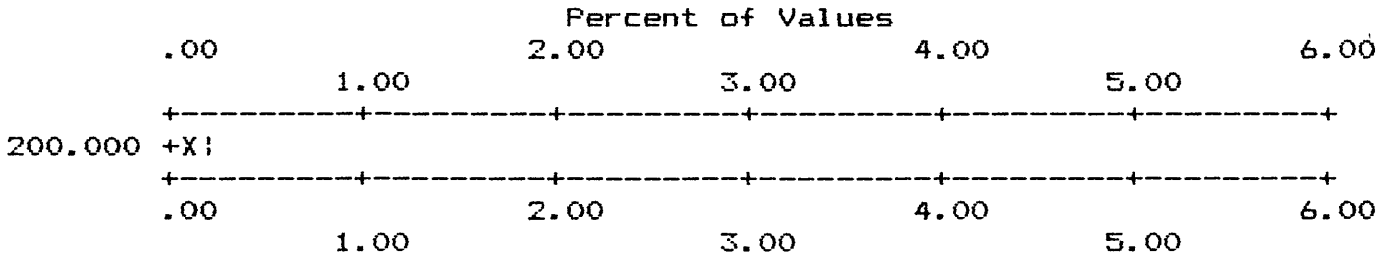

Each increment (each X or ! plotted) = .100 %

APPENDIX IV-C. HISTOGRAMS OF STREAM-SEDIMENT SAMPLE DATA, WHITE MTS NRA

COLUMN ID.: S-B

	VALUE	NO.	%	CUM.	CUM. %		TOT CUM	TOT CUM %	
1	10.000	1	.22	1	.2	99.8	1	.2	99.8
2	20.000	3	.65	4	.9	99.1	4	.9	99.1
3	30.000	15	3.25	19	4.1	95.9	19	4.1	95.9
4	50.000	94	20.39	113	24.5	75.5	113	24.5	75.5
5	70.000	140	30.37	253	54.9	45.1	253	54.9	45.1
6	100.000	158	34.27	411	89.2	10.8	411	89.2	10.8
7	150.000	40	8.68	451	97.8	2.2	451	97.8	2.2
8	200.000	10	2.17	461	100.0	.0	461	100.0	.0

B	T	H	N	L	G	OTHER	UNQUAL	ANAL	read	
0	0	0	0	0	0	0	461	461	461	VALUES
.0	.0	.0	.0	.0	.0	.0	100.0			PERCENT

MIN	MAX	AMEAN	SD	GMEAN	GD	VALUES
10.000	200.00	84.208	34.48	77.563	1.51	461

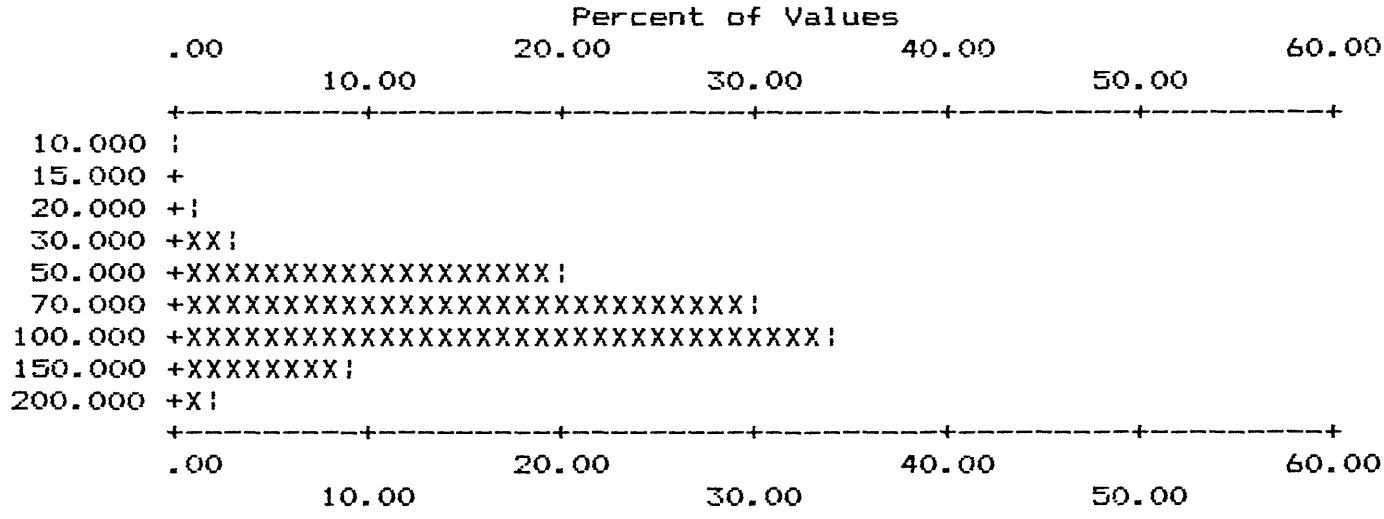

Each increment (each X or ¦ plotted) = 1.000 %

APPENDIX IV-C. HISTOGRAMS OF STREAM-SEDIMENT SAMPLE DATA, WHITE MTS NRA

COLUMN ID.: S-BA

	VALUE	NO.	%	CUM.	CUM. %	TOT CUM	TOT CUM %
1	100.000	2	.43	2	.4 99.6	2	.4 99.6
2	150.000	1	.22	3	.7 99.3	3	.7 99.3
3	200.000	25	5.42	28	6.1 93.9	28	6.1 93.9
4	300.000	109	23.64	137	29.7 70.3	137	29.7 70.3
5	500.000	200	43.38	337	73.1 26.9	337	73.1 26.9
6	700.000	65	14.10	402	87.2 12.8	402	87.2 12.8
7	1000.000	31	6.72	433	93.9 6.1	433	93.9 6.1
8	1500.000	11	2.39	444	96.3 3.7	444	96.3 3.7
9	2000.000	11	2.39	455	98.7 1.3	455	98.7 1.3
10	3000.000	4	.87	459	99.6 .4	459	99.6 .4
11	5000.000	2	.43	461	100.0 .0	461	100.0 .0

B	T	H	N	L	G	OTHER	UNQUAL	ANAL	read	
0	0	0	0	0	0	0	461	461	461	VALUES
.0	.0	.0	.0	.0	.0	.0	100.0			PERCENT

MIN	MAX	AMEAN	SD	GMEAN	GD	VALUES
100.000	5000.00	596.638	498.58	499.408	1.72	461

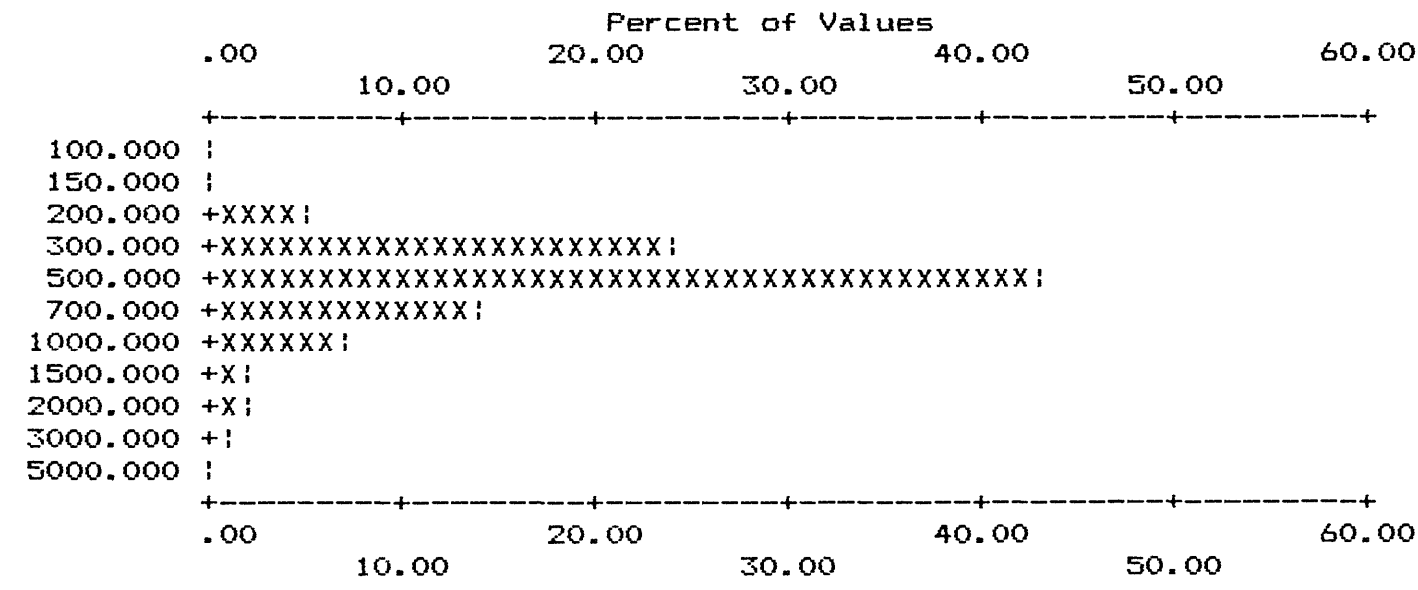

Each increment (each X or ¦ plotted) = 1.000 %

APPENDIX IV-C. HISTOGRAMS OF STREAM-SEDIMENT SAMPLE DATA, WHITE MTS NRA

COLUMN ID.: S-BE

	VALUE	NO.	%	CUM.	CUM. %	TOT CUM	TOT CUM %	
1	1.000	245	53.15	245	53.1	39.7	278	60.3	39.7
2	1.500	83	18.00	328	71.1	21.7	361	78.3	21.7
3	2.000	66	14.32	394	85.5	7.4	427	92.6	7.4
4	3.000	18	3.90	412	89.4	3.5	445	96.5	3.5
5	5.000	12	2.60	424	92.0	.9	457	99.1	.9
6	7.000	1	.22	425	92.2	.7	458	99.3	.7
7	10.000	3	.65	428	92.8	.0	461	100.0	.0

B	T	H	N	L	G	OTHER	UNQUAL	ANAL	read	
0	0	0	0	33	0	0	428	461	461	VALUES
.0	.0	.0	.0	7.2	.0	.0	92.8			PERCENT

MIN	MAX	AMEAN	SD	GMEAN	GD	VALUES
1.000	10.00	1.525	1.10	1.347	1.54	428
.500	10.00	1.451	1.09	1.254	1.63	461

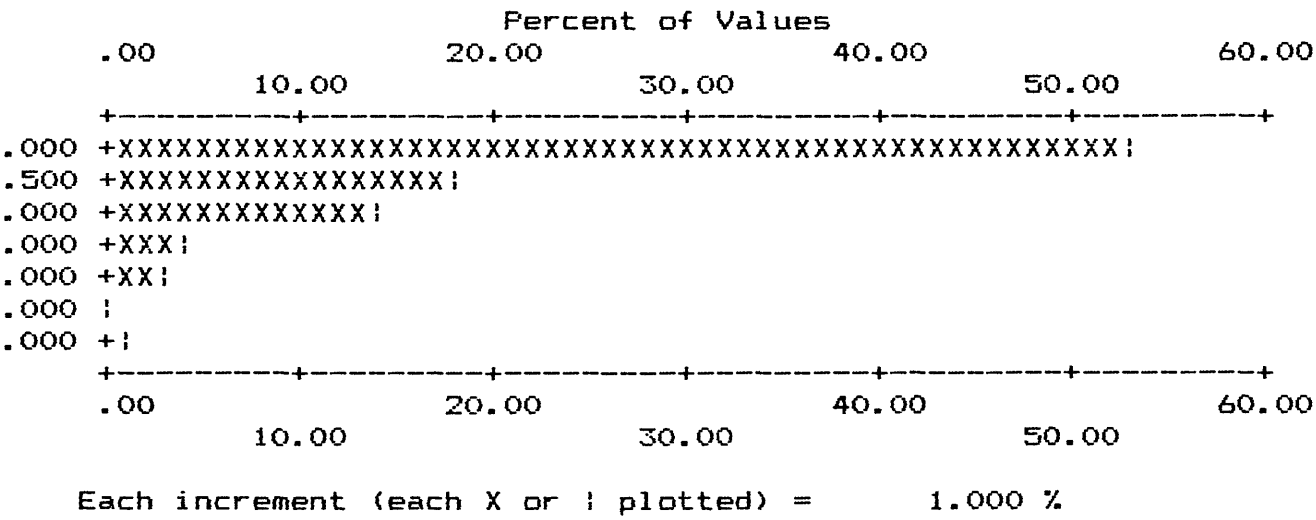

Each increment (each X or ¦ plotted) = 1.000 %

APPENDIX IV-C. HISTOGRAMS OF STREAM-SEDIMENT SAMPLE DATA, WHITE MTS NRA

COLUMN ID.: S-BI

	VALUE	NO.	%	CUM.	CUM. %	TOT CUM	TOT CUM %
1	10.000	1	.22	1	.2	461	100.0 .0

B	T	H	N	L	G	OTHER	UNQUAL	ANAL	read	
0	0	0	460	0	0	0	1	461	461	VALUES
.0	.0	.0	99.8	.0	.0	.0	.2			PERCENT

MIN	MAX	AMEAN	SD	GMEAN	GD	VALUES
10.000	10.00	10.000	.00	10.000	********	1
2.500	10.00	2.516	.35	2.508	1.07	461

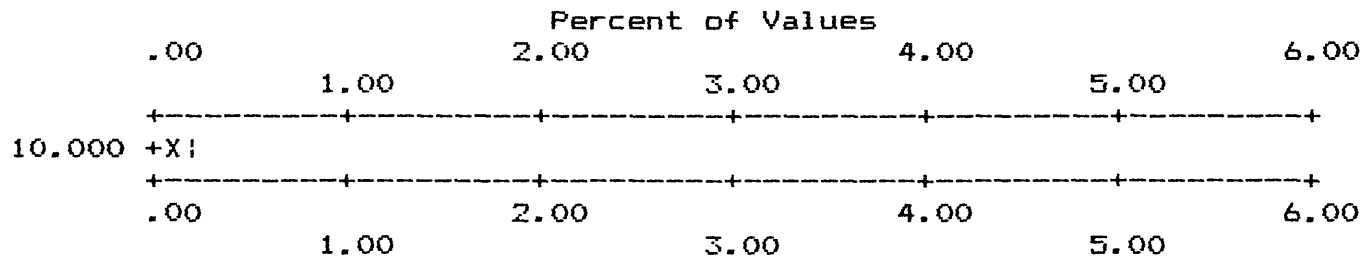

Each increment (each X or ¦ plotted) = .100 %

APPENDIX IV-C. HISTOGRAMS OF STREAM-SEDIMENT SAMPLE DATA, WHITE MTS NRA

COLUMN ID.: S-CO

	VALUE	NO.	%	CUM.	CUM. %		TOT CUM	TOT CUM %	
1	5.000	11	2.39	11	2.4	96.5	16	3.5	96.5
2	7.000	16	3.47	27	5.9	93.1	32	6.9	93.1
3	10.000	71	15.40	98	21.3	77.7	103	22.3	77.7
4	15.000	170	36.88	268	58.1	40.8	273	59.2	40.8
5	20.000	141	30.59	409	88.7	10.2	414	89.8	10.2
6	30.000	35	7.59	444	96.3	2.6	449	97.4	2.6
7	50.000	10	2.17	454	98.5	.4	459	99.6	.4
8	70.000	1	.22	455	98.7	.2	460	99.8	.2
9	100.000	1	.22	456	98.9	.0	461	100.0	.0

B	T	H	N	L	G	OTHER	UNQUAL	ANAL	read	
0	0	0	0	5	0	0	456	461	461	VALUES
.0	.0	.0	.0	1.1	.0	.0	98.9			PERCENT

MIN	MAX	AMEAN	SD	GMEAN	GD	VALUES
5.000	100.00	17.471	8.77	15.923	1.53	456
2.500	100.00	17.309	8.86	15.607	1.59	461

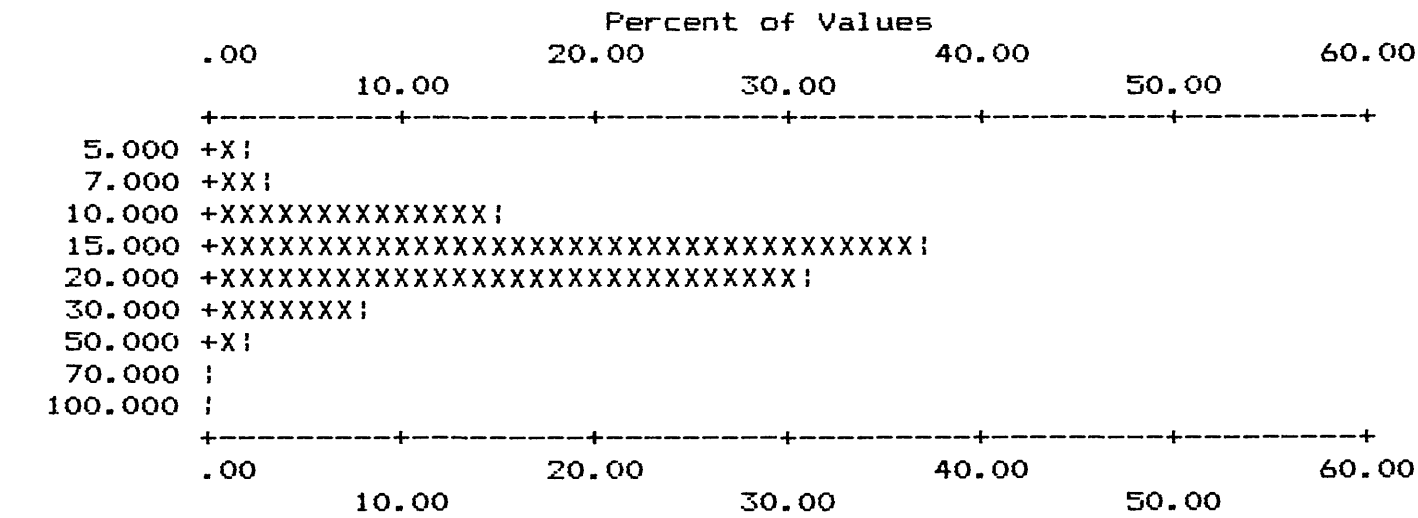

Each increment (each X or ¦ plotted) = 1.000 %

APPENDIX IV-C. HISTOGRAMS OF STREAM-SEDIMENT SAMPLE DATA, WHITE MTS NRA

COLUMN ID.: S-CR

	VALUE	NO.	%	CUM.	CUM. %		TOT CUM	TOT CUM %	
1	10.000	5	1.08	5	1.1	98.0	9	2.0	98.0
2	15.000	11	2.39	16	3.5	95.7	20	4.3	95.7
3	20.000	42	9.11	58	12.6	86.6	62	13.4	86.6
4	30.000	55	11.93	113	24.5	74.6	117	25.4	74.6
5	50.000	125	27.11	238	51.6	47.5	242	52.5	47.5
6	70.000	118	25.60	356	77.2	21.9	360	78.1	21.9
7	100.000	62	13.45	418	90.7	8.5	422	91.5	8.5
8	150.000	19	4.12	437	94.8	4.3	441	95.7	4.3
9	200.000	15	3.25	452	98.0	1.1	456	98.9	1.1
10	300.000	3	.65	455	98.7	.4	459	99.6	.4
11	500.000	1	.22	456	98.9	.2	460	99.8	.2
12	1500.000	1	.22	457	99.1	.0	461	100.0	.0

B	T	H	N	L	G	OTHER	UNQUAL	ANAL	read	
0	0	0	0	4	0	0	457	461	461	VALUES
.0	.0	.0	.0	.9	.0	.0	99.1			PERCENT

MIN	MAX	AMEAN	SD	GMEAN	GD	VALUES
10.000	1500.00	70.383	82.63	55.483	1.92	457
5.000	1500.00	69.816	82.50	54.337	1.99	461

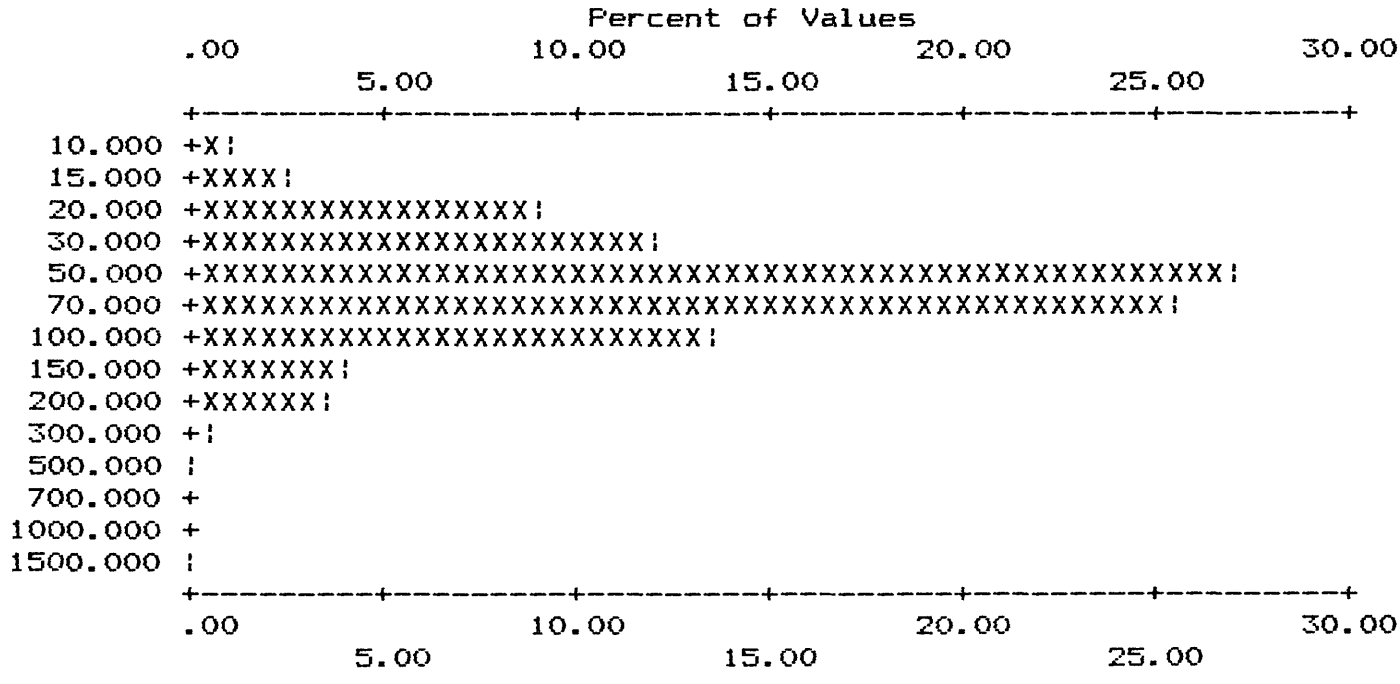

Each increment (each X or ! plotted) = .500 %

APPENDIX IV-C. HISTOGRAMS OF STREAM-SEDIMENT SAMPLE DATA, WHITE MTS NRA

COLUMN ID.: S-CU

	VALUE	NO.	%	CUM.	CUM. %		TOT CUM	TOT CUM %	
1	5.000	19	4.12	19	4.1	93.5	30	6.5	93.5
2	7.000	43	9.33	62	13.4	84.2	73	15.8	84.2
3	10.000	151	32.75	213	46.2	51.4	224	48.6	51.4
4	15.000	99	21.48	312	67.7	29.9	323	70.1	29.9
5	20.000	106	22.99	418	90.7	6.9	429	93.1	6.9
6	30.000	23	4.99	441	95.7	2.0	452	98.0	2.0
7	50.000	7	1.52	448	97.2	.4	459	99.6	.4
8	70.000	2	.43	450	97.6	.0	461	100.0	.0

B	T	H	N	L	G	OTHER	UNQUAL	ANAL	read	
0	0	0	0	11	0	0	450	461	461	VALUES
.0	.0	.0	.0	2.4	.0	.0	97.6			PERCENT

MIN	MAX	AMEAN	SD	GMEAN	GD	VALUES
5.000	70.00	14.869	8.29	13.218	1.60	450
2.500	70.00	14.574	8.41	12.703	1.70	461

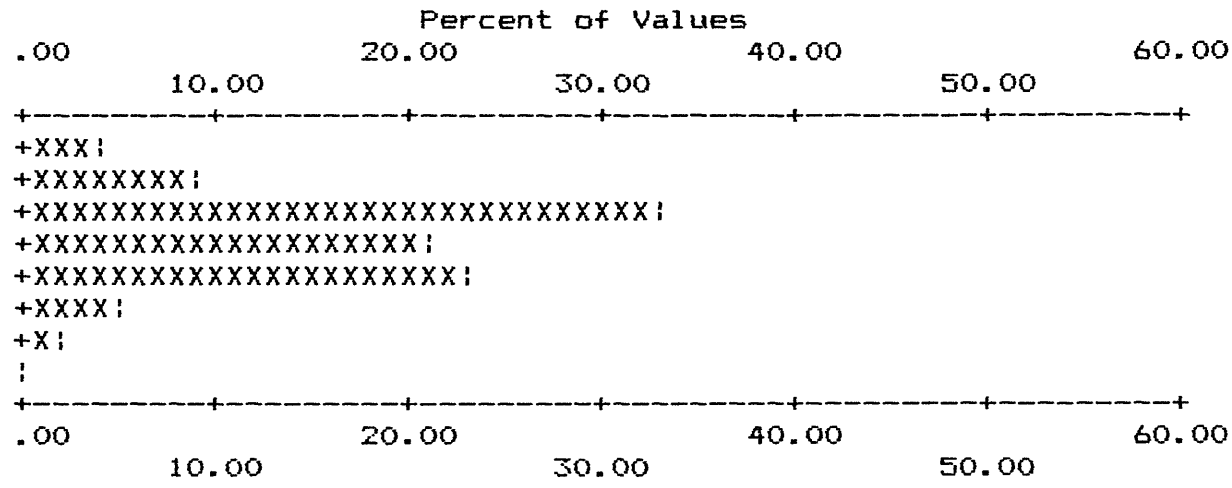

Each increment (each X or ! plotted) = 1.000 %

APPENDIX IV-C. HISTOGRAMS OF STREAM-SEDIMENT SAMPLE DATA, WHITE MTS NRA

COLUMN ID.: S-LA

	VALUE	NO.	%	CUM.	CUM. %		TOT CUM	TOT CUM %	
1	20.000	120	26.03	120	26.0	58.1	193	41.9	58.1
2	30.000	135	29.28	255	55.3	28.9	328	71.1	28.9
3	50.000	108	23.43	363	78.7	5.4	436	94.6	5.4
4	70.000	18	3.90	381	82.6	1.5	454	98.5	1.5
5	100.000	4	.87	385	83.5	.7	458	99.3	.7
6	150.000	1	.22	386	83.7	.4	459	99.6	.4
7	200.000	1	.22	387	83.9	.2	460	99.8	.2
8	300.000	1	.22	388	84.2	.0	461	100.0	.0

B	T	H	N	L	G	OTHER	UNQUAL	ANAL	read	
0	0	0	27	46	0	0	388	461	461	VALUES
.0	.0	.0	5.9	10.0	.0	.0	84.2			PERCENT

MIN	MAX	AMEAN	SD	GMEAN	GD	VALUES
20.000	300.00	36.495	22.93	32.612	1.55	388
5.000	300.00	32.007	23.46	25.969	1.97	461

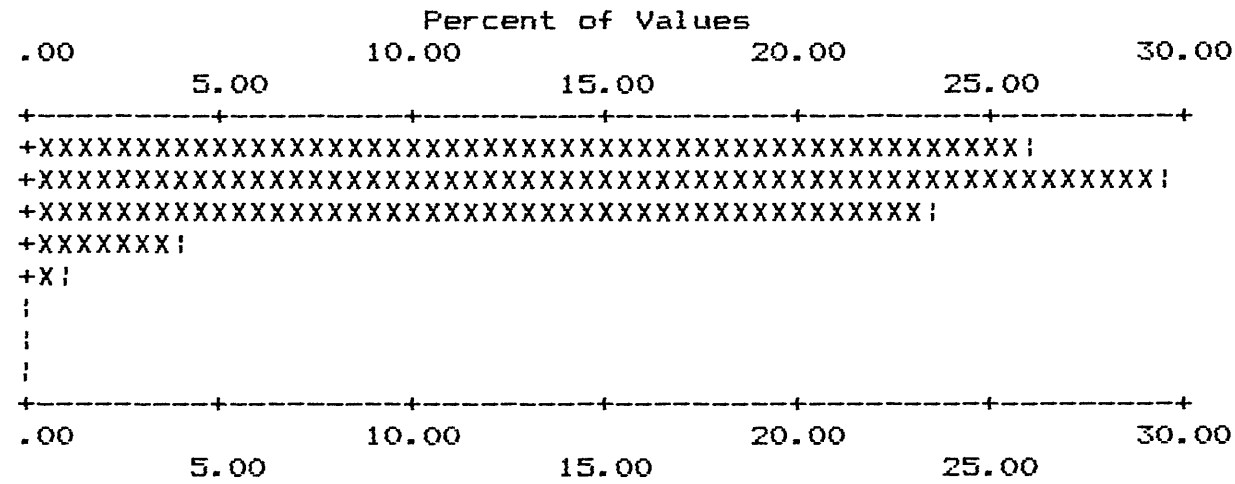

Each increment (each X or ¦ plotted) = .500 %

APPENDIX IV-C. HISTOGRAMS OF STREAM-SEDIMENT SAMPLE DATA, WHITE MTS NRA

COLUMN ID.: S-MO

	VALUE	NO.	%	CUM.	CUM. %		TOT CUM	TOT CUM %	
1	5.000	10	2.17	10	2.2	2.4	450	97.6	2.4
2	7.000	6	1.30	16	3.5	1.1	456	98.9	1.1
3	10.000	5	1.08	21	4.6	.0	461	100.0	.0

B	T	H	N	L	G	OTHER	UNQUAL	ANAL	read	
0	0	0	416	24	0	0	21	461	461	VALUES
.0	.0	.0	90.2	5.2	.0	.0	4.6			PERCENT

MIN	MAX	AMEAN	SD	GMEAN	GD	VALUES
5.000	10.00	6.762	2.05	6.492	1.33	21
1.250	10.00	1.566	1.25	1.397	1.45	461

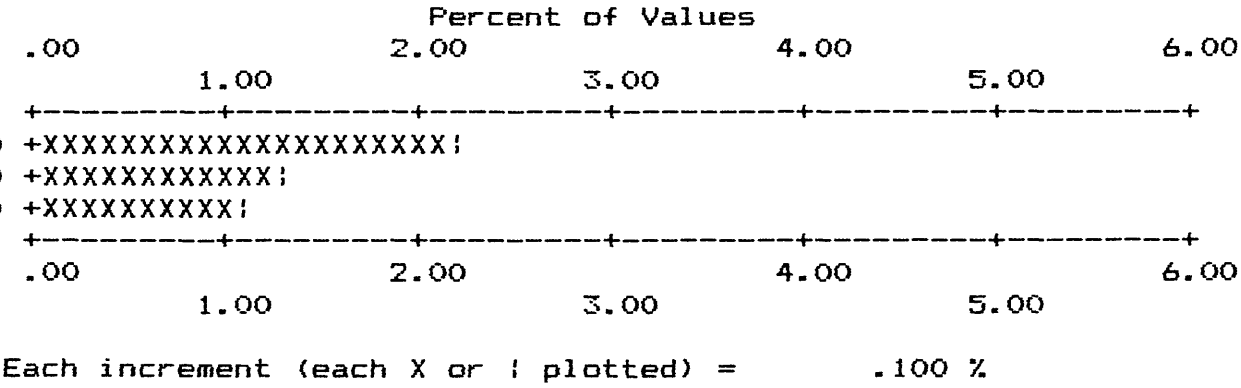

Each increment (each X or ¦ plotted) = .100 %

APPENDIX IV-C. HISTOGRAMS OF STREAM-SEDIMENT SAMPLE DATA, WHITE MTS NRA

COLUMN ID.: S-NB

	VALUE	NO.	%	CUM.	CUM. %	TOT CUM	TOT CUM %	
1	20.000	17	3.69	17	3.7	1.3	455	98.7	1.3
2	30.000	5	1.08	22	4.8	.2	460	99.8	.2
3	50.000	1	.22	23	5.0	.0	461	100.0	.0

B	T	H	N	L	G	OTHER	UNQUAL	ANAL	read	
0	0	0	363	75	0	0	23	461	461	VALUES
.0	.0	.0	78.7	16.3	.0	.0	5.0			PERCENT

MIN	MAX	AMEAN	SD	GMEAN	GD	VALUES
20.000	50.00	23.478	7.14	22.731	1.27	23
5.000	50.00	6.735	4.54	6.036	1.49	461

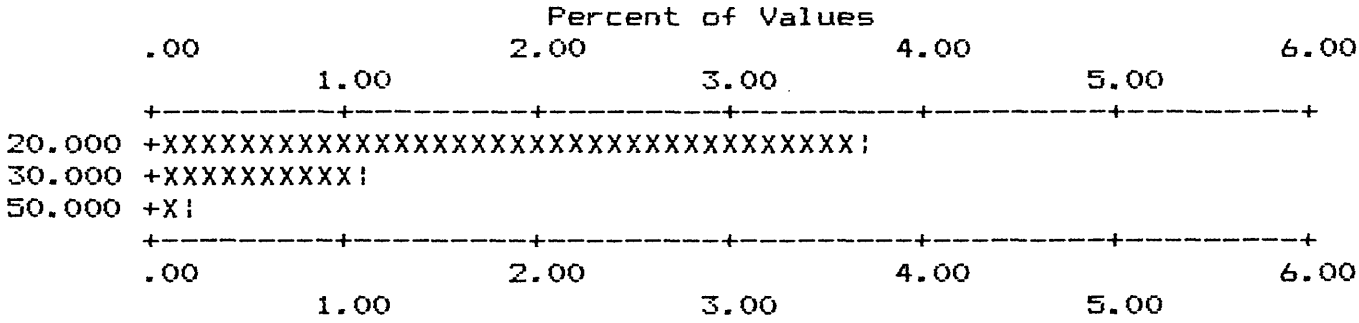

Each increment (each X or ¦ plotted) = .100 %

APPENDIX IV-C. HISTOGRAMS OF STREAM-SEDIMENT SAMPLE DATA, WHITE MTS NRA

COLUMN ID.: S-NI

	VALUE	NO.	%	CUM.	CUM. %		TOT CUM	TOT CUM %	
1	5.000	3	.65	3	.7	98.9	5	1.1	98.9
2	7.000	4	.87	7	1.5	98.0	9	2.0	98.0
3	10.000	30	6.51	37	8.0	91.5	39	8.5	91.5
4	15.000	30	6.51	67	14.5	85.0	69	15.0	85.0
5	20.000	147	31.89	214	46.4	53.1	216	46.9	53.1
6	30.000	137	29.72	351	76.1	23.4	353	76.6	23.4
7	50.000	80	17.35	431	93.5	6.1	433	93.9	6.1
8	70.000	24	5.21	455	98.7	.9	457	99.1	.9
9	100.000	2	.43	457	99.1	.4	459	99.6	.4
10	150.000	1	.22	458	99.3	.2	460	99.8	.2
11	200.000	1	.22	459	99.6	.0	461	100.0	.0

B	T	H	N	L	G	OTHER	UNQUAL	ANAL	read	
0	0	0	0	2	0	0	459	461	461	VALUES
.0	.0	.0	.0	.4	.0	.0	99.6			PERCENT

MIN	MAX	AMEAN	SD	GMEAN	GD	VALUES
5.000	200.00	30.660	18.73	26.471	1.71	459
2.500	200.00	30.538	18.78	26.202	1.75	461

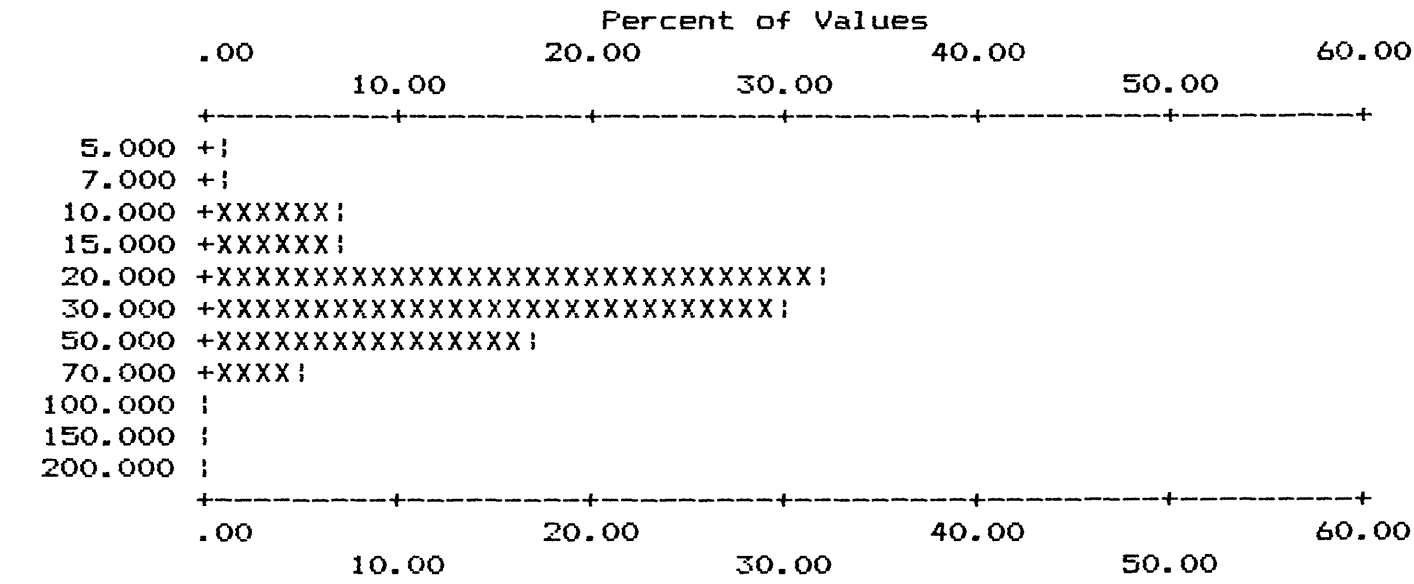

Each increment (each X or ¦ plotted) = 1.000 %

APPENDIX IV-C. HISTOGRAMS OF STREAM-SEDIMENT SAMPLE DATA, WHITE MTS NRA

COLUMN ID.: S-PB

	VALUE	NO.	%	CUM.	CUM. %		TOT CUM	TOT CUM %	
1	10.000	81	17.57	81	17.6	74.2	119	25.8	74.2
2	15.000	101	21.91	182	39.5	52.3	220	47.7	52.3
3	20.000	139	30.15	321	69.6	22.1	359	77.9	22.1
4	30.000	53	11.50	374	81.1	10.6	412	89.4	10.6
5	50.000	38	8.24	412	89.4	2.4	450	97.6	2.4
6	70.000	8	1.74	420	91.1	.7	458	99.3	.7
7	100.000	1	.22	421	91.3	.4	459	99.6	.4
8	150.000	1	.22	422	91.5	.2	460	99.8	.2
9	200.000	1	.22	423	91.8	.0	461	100.0	.0

B	T	H	N	L	G	OTHER	UNQUAL	ANAL	read	
0	0	0	3	35	0	0	423	461	461	VALUES
.0	.0	.0	.7	7.6	.0	.0	91.8			PERCENT

MIN	MAX	AMEAN	SD	GMEAN	GD	VALUES
10.000	200.00	22.707	17.05	19.397	1.67	423
2.500	200.00	21.231	17.06	17.268	1.88	461

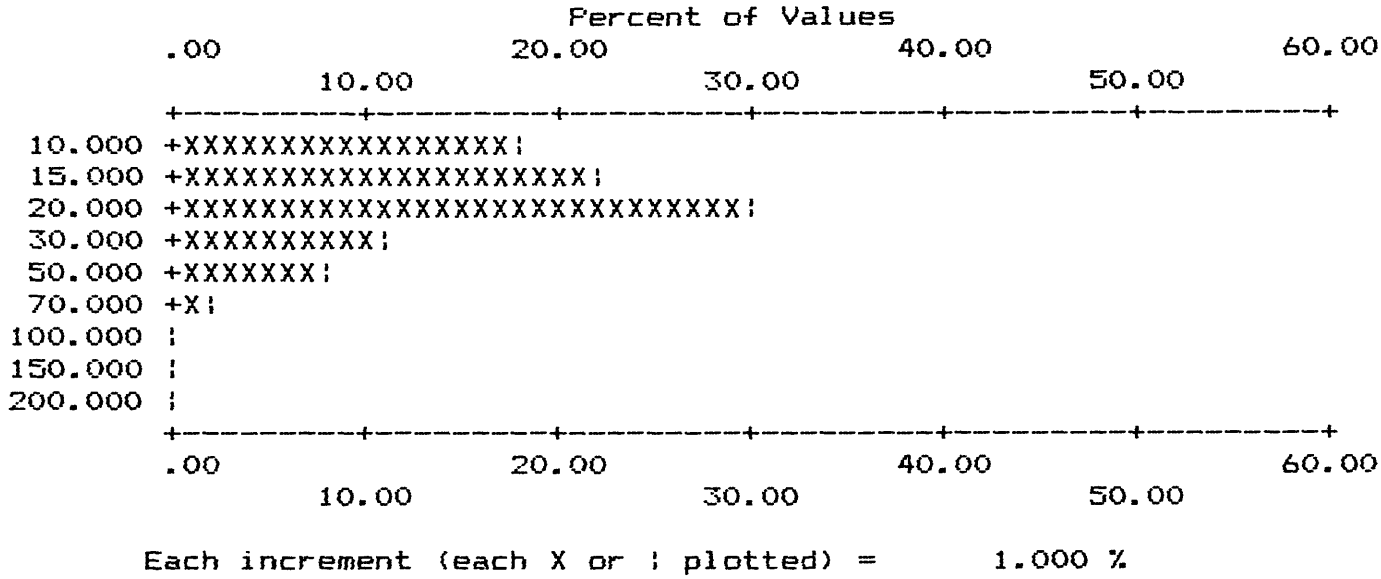

Each increment (each X or ¦ plotted) = 1.000 %

APPENDIX IV-C. HISTOGRAMS OF STREAM-SEDIMENT SAMPLE DATA, WHITE MTS NRA

COLUMN ID.: S-SC

	VALUE	NO.	%	CUM.	CUM. %		TOT CUM	TOT CUM %	
1	5.000	5	1.08	5	1.1	98.5	7	1.5	98.5
2	7.000	49	10.63	54	11.7	87.9	56	12.1	87.9
3	10.000	219	47.51	273	59.2	40.3	275	59.7	40.3
4	15.000	153	33.19	426	92.4	7.2	428	92.8	7.2
5	20.000	33	7.16	459	99.6	.0	461	100.0	.0

B	T	H	N	L	G	OTHER	UNQUAL	ANAL	read	
0	0	0	0	2	0	0	459	461	461	VALUES
.0	.0	.0	.0	.4	.0	.0	99.6			PERCENT

MIN	MAX	AMEAN	SD	GMEAN	GD	VALUES
5.000	20.00	12.011	3.57	11.495	1.35	459
2.500	20.00	11.970	3.62	11.420	1.37	461

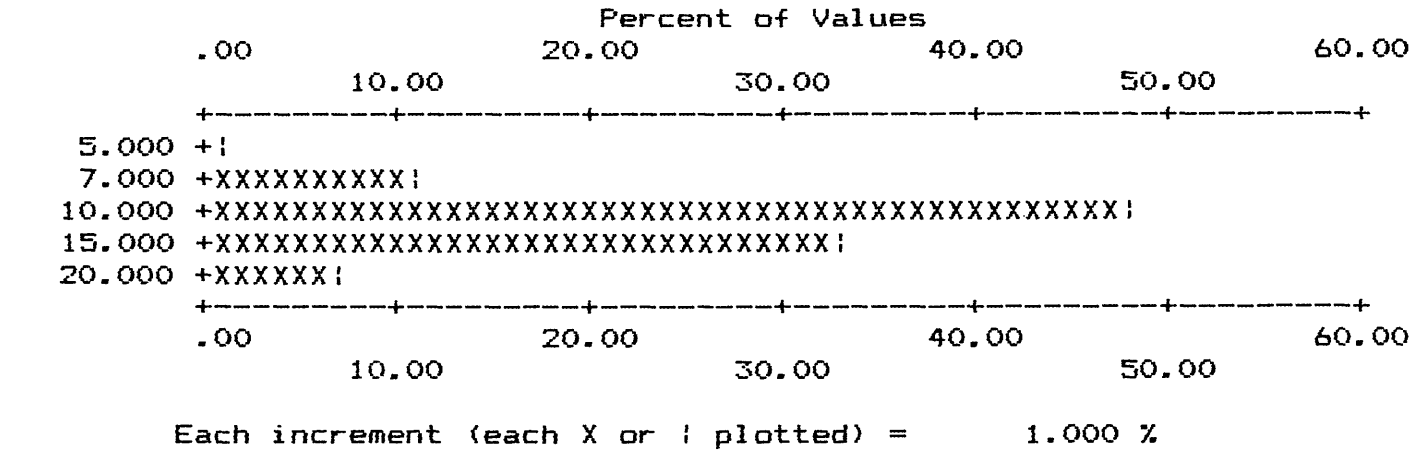

Each increment (each X or ¦ plotted) = 1.000 %

APPENDIX IV-C. HISTOGRAMS OF STREAM-SEDIMENT SAMPLE DATA, WHITE MTS NRA

COLUMN ID.: S-SN

	VALUE	NO.	%	CUM.	CUM. %		TOT CUM	TOT CUM %	
1	10.000	12	2.60	12	2.6	3.7	444	96.3	3.7
2	15.000	6	1.30	18	3.9	2.4	450	97.6	2.4
3	20.000	5	1.08	23	5.0	1.3	455	98.7	1.3
4	30.000	1	.22	24	5.2	1.1	456	98.9	1.1
5	50.000	1	.22	25	5.4	.9	457	99.1	.9
6	100.000	3	.65	28	6.1	.2	460	99.8	.2
7	700.000	1	.22	29	6.3	.0	461	100.0	.0

B	T	H	N	L	G	OTHER	UNQUAL	ANAL	read	
0	0	0	413	19	0	0	29	461	461	VALUES
.0	.0	.0	89.6	4.1	.0	.0	6.3			PERCENT

MIN	MAX	AMEAN	SD	GMEAN	GD	VALUES
10.000	700.00	47.931	128.36	19.768	2.70	29
2.500	700.00	5.461	33.53	2.930	1.77	461

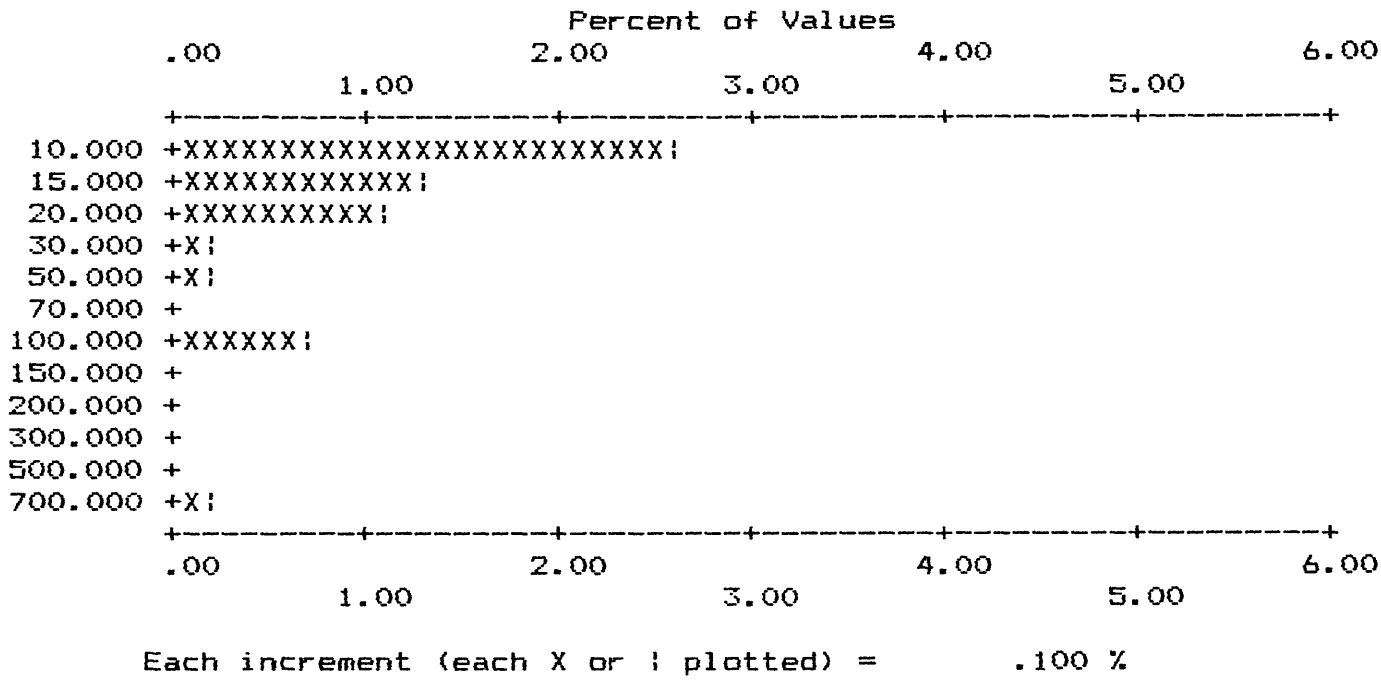

Each increment (each X or ¦ plotted) = .100 %

APPENDIX IV-C. HISTOGRAMS OF STREAM-SEDIMENT SAMPLE DATA, WHITE MTS NRA

COLUMN ID.: S-SR

	VALUE	NO.	%	CUM.	CUM. %		TOT CUM	TOT CUM %	
1	100.000	161	34.92	161	34.9	21.7	361	78.3	21.7
2	150.000	67	14.53	228	49.5	7.2	428	92.8	7.2
3	200.000	28	6.07	256	55.5	1.1	456	98.9	1.1
4	300.000	3	.65	259	56.2	.4	459	99.6	.4
5	500.000	1	.22	260	56.4	.2	460	99.8	.2
6	1000.000	1	.22	261	56.6	.0	461	100.0	.0

B	T	H	N	L	G	OTHER	UNQUAL	ANAL	read	
0	0	0	37	163	0	0	261	461	461	VALUES
.0	.0	.0	8.0	35.4	.0	.0	56.6			PERCENT

MIN	MAX	AMEAN	SD	GMEAN	GD	VALUES
100.000	1000.00	130.843	70.42	122.883	1.36	261
25.000	1000.00	93.764	68.13	78.688	1.80	461

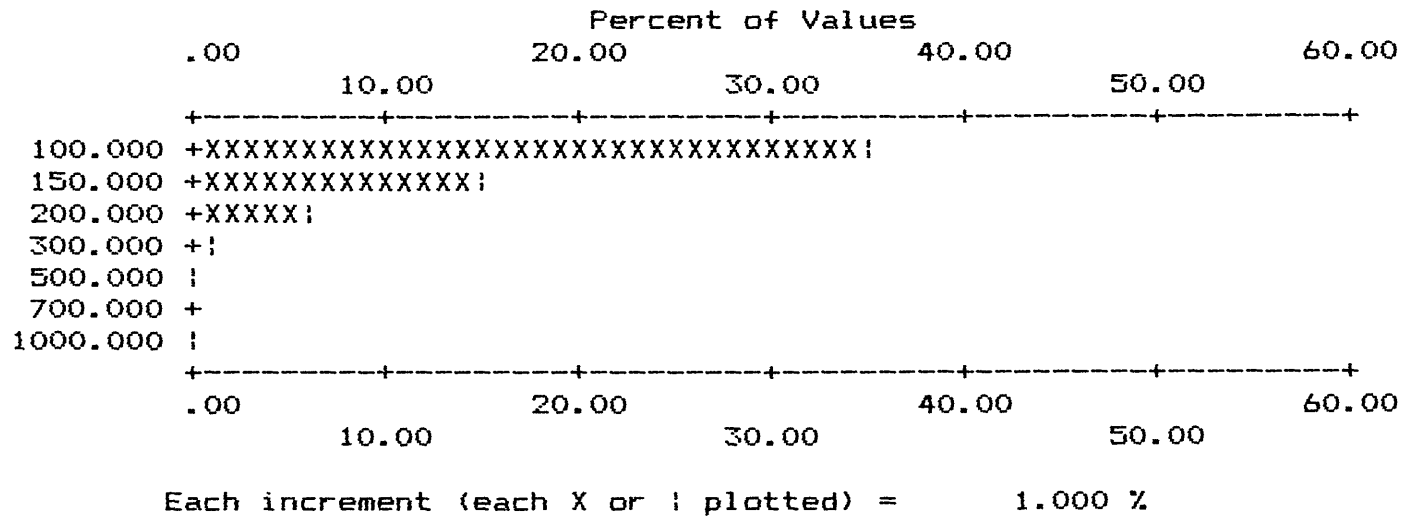

Each increment (each X or ¦ plotted) = 1.000 %

APPENDIX IV-C. HISTOGRAMS OF STREAM-SEDIMENT SAMPLE DATA, WHITE MTS NRA

COLUMN ID.: S-V

	VALUE	NO.	%	CUM.	CUM. %		TOT CUM	TOT CUM %	
1	10.000	2	.43	2	.4	99.6	2	.4	99.6
2	20.000	2	.43	4	.9	99.1	4	.9	99.1
3	30.000	1	.22	5	1.1	98.9	5	1.1	98.9
4	50.000	31	6.72	36	7.8	92.2	36	7.8	92.2
5	70.000	80	17.35	116	25.2	74.8	116	25.2	74.8
6	100.000	267	57.92	383	83.1	16.9	383	83.1	16.9
7	150.000	56	12.15	439	95.2	4.8	439	95.2	4.8
8	200.000	22	4.77	461	100.0	.0	461	100.0	.0

B	T	H	N	L	G	OTHER	UNQUAL	ANAL	read	
0	0	0	0	0	0	0	461	461	461	VALUES
.0	.0	.0	.0	.0	.0	.0	100.0			PERCENT

MIN	MAX	AMEAN	SD	GMEAN	GD	VALUES
10.000	200.00	101.388	34.34	95.527	1.44	461

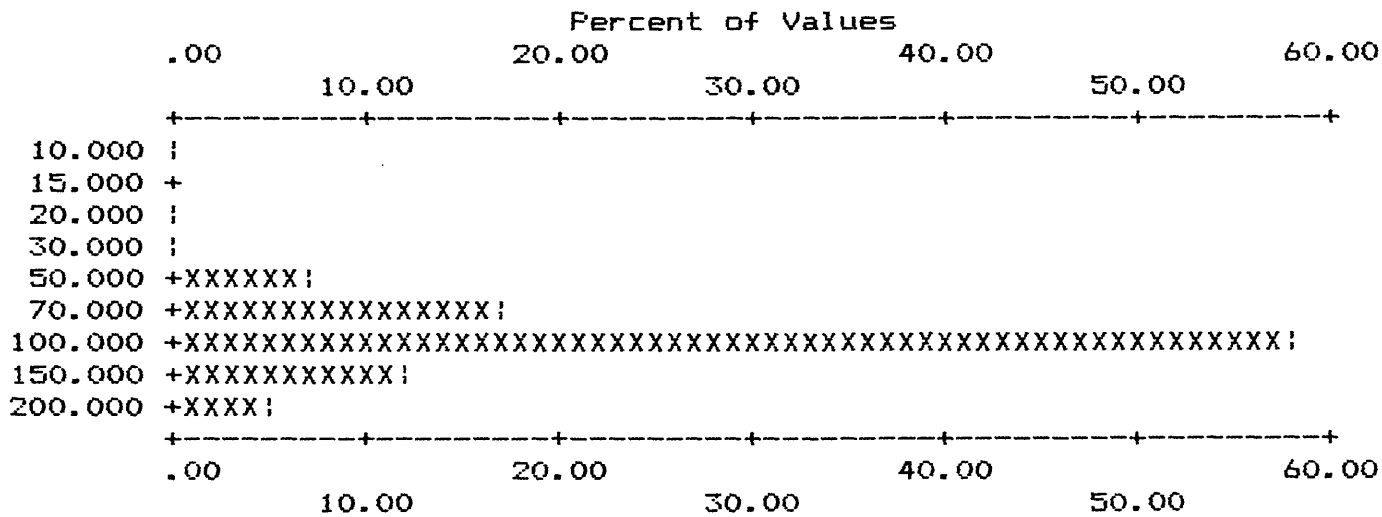

Each increment (each X or ¦ plotted) = 1.000 %

APPENDIX IV-C. HISTOGRAMS OF STREAM-SEDIMENT SAMPLE DATA, WHITE MTS NRA

COLUMN ID.: S-Y

	VALUE	NO.	%	CUM.	CUM. %		TOT CUM	TOT CUM %	
1	10.000	10	2.17	10	2.2	97.4	12	2.6	97.4
2	15.000	48	10.41	58	12.6	87.0	60	13.0	87.0
3	20.000	259	56.18	317	68.8	30.8	319	69.2	30.8
4	30.000	107	23.21	424	92.0	7.6	426	92.4	7.6
5	50.000	32	6.94	456	98.9	.7	458	99.3	.7
6	70.000	2	.43	458	99.3	.2	460	99.8	.2
7	100.000	1	.22	459	99.6	.0	461	100.0	.0

B	T	H	N	L	G	OTHER	UNQUAL	ANAL	read	
0	0	0	0	2	0	0	459	461	461	VALUES
.0	.0	.0	.0	.4	.0	.0	99.6			PERCENT

MIN	MAX	AMEAN	SD	GMEAN	GD	VALUES
10.000	100.00	24.074	9.97	22.599	1.40	459
5.000	100.00	23.991	10.02	22.452	1.42	461

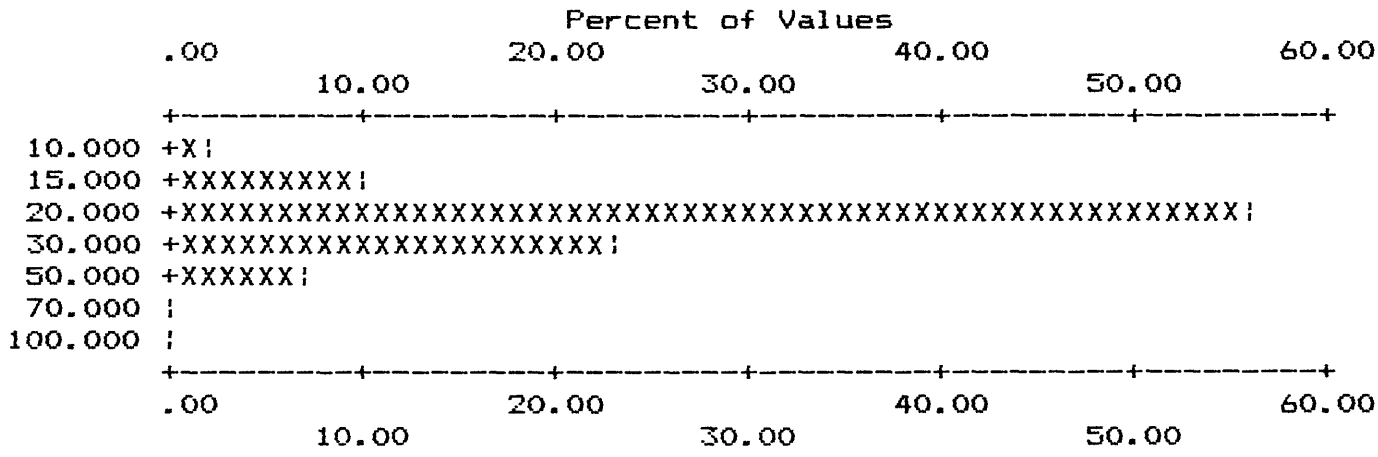

Each increment (each X or ¦ plotted) = 1.000 %

APPENDIX IV-C. HISTOGRAMS OF STREAM-SEDIMENT SAMPLE DATA, WHITE MTS NRA

COLUMN ID.: S-ZN

	VALUE	NO.	%	CUM.	CUM. %	TOT CUM	TOT CUM %	
1	200.000	15	3.25	15	3.3	459	99.6	.4
2	500.000	1	.22	16	3.5	460	99.8	.2
3	1000.000	1	.22	17	3.7	461	100.0	.0

B	T	H	N	L	G	OTHER	UNQUAL	ANAL	read	
0	0	0	402	42	0	0	17	461	461	VALUES
.0	.0	.0	87.2	9.1	.0	.0	3.7			PERCENT

MIN	MAX	AMEAN	SD	GMEAN	GD	VALUES
200.000	1000.00	264.706	202.92	232.035	1.55	17
50.000	1000.00	62.473	56.64	56.361	1.42	461

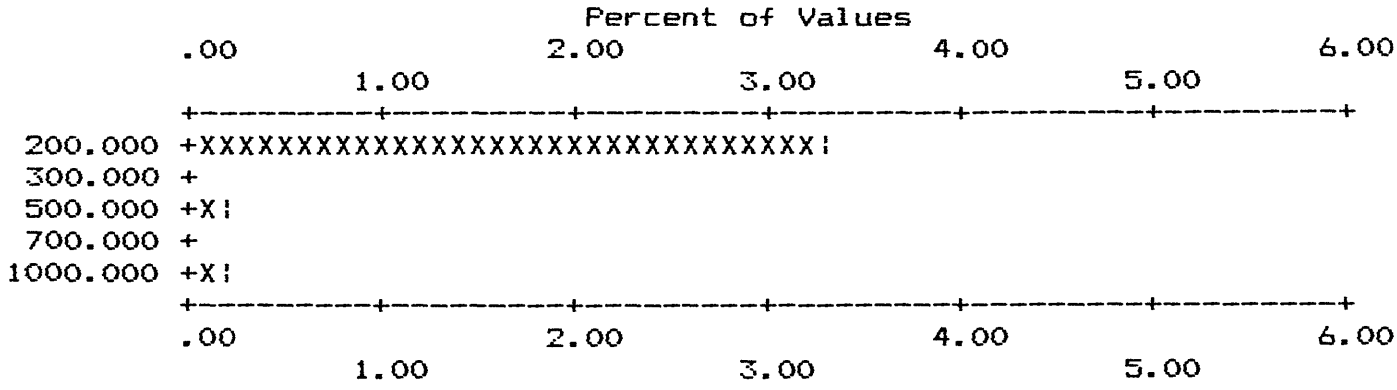

Each increment (each X or ¦ plotted) = .100 %

APPENDIX IV-C. HISTOGRAMS OF STREAM-SEDIMENT SAMPLE DATA, WHITE MTS NRA

COLUMN ID.: S-ZR

	VALUE	NO.	%	CUM.	CUM. %	TOT CUM	TOT CUM %
1	20.000	1	.22	1	.2 99.8	1	.2 99.8
2	50.000	2	.43	3	.7 99.3	3	.7 99.3
3	70.000	9	1.95	12	2.6 97.4	12	2.6 97.4
4	100.000	180	39.05	192	41.6 58.4	192	41.6 58.4
5	150.000	105	22.78	297	64.4 35.6	297	64.4 35.6
6	200.000	132	28.63	429	93.1 6.9	429	93.1 6.9
7	300.000	24	5.21	453	98.3 1.7	453	98.3 1.7
8	500.000	8	1.74	461	100.0 .0	461	100.0 .0

B	T	H	N	L	G	OTHER	UNQUAL	ANAL	read	
0	0	0	0	0	0	0	461	461	461	VALUES
.0	.0	.0	.0	.0	.0	.0	100.0			PERCENT

MIN	MAX	AMEAN	SD	GMEAN	GD	VALUES
20.000	500.00	156.399	71.86	143.689	1.50	461

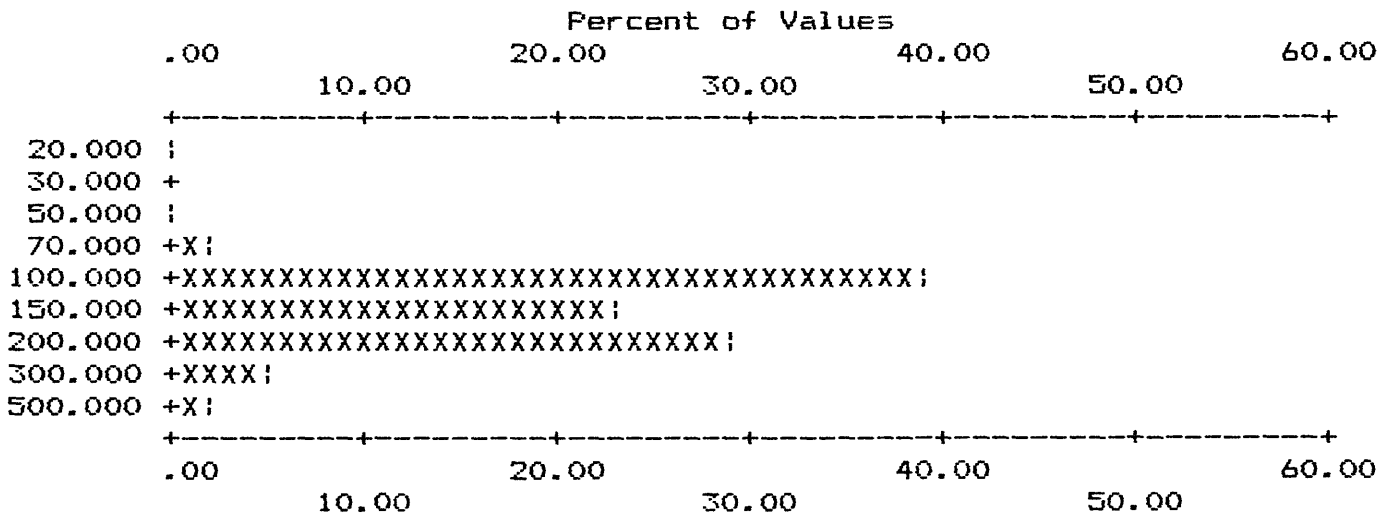

Each increment (each X or ¦ plotted) = 1.000 %

APPENDIX IV-C. HISTOGRAMS OF STREAM-SEDIMENT SAMPLE DATA, WHITE MTS NRA

COLUMN ID.: AA-AS-P

	VALUE	NO.	%	CUM.	CUM. %		TOT CUM	TOT CUM %	
1	10.000	191	41.43	191	41.4	33.8	305	66.2	33.8
2	20.000	107	23.21	298	64.6	10.6	412	89.4	10.6
3	30.000	30	6.51	328	71.1	4.1	442	95.9	4.1
4	40.000	7	1.52	335	72.7	2.6	449	97.4	2.6
5	50.000	6	1.30	341	74.0	1.3	455	98.7	1.3
6	60.000	1	.22	342	74.2	1.1	456	98.9	1.1
7	70.000	1	.22	343	74.4	.9	457	99.1	.9
8	80.000	1	.22	344	74.6	.7	458	99.3	.7
9	90.000	1	.22	345	74.8	.4	459	99.6	.4
10	110.000	2	.43	347	75.3	.0	461	100.0	.0

B	T	H	N	L	G	OTHER	UNQUAL	ANAL	read	
0	0	0	114	0	0	0	347	461	461	VALUES
.0	.0	.0	24.7	.0	.0	.0	75.3			PERCENT

MIN	MAX	AMEAN	SD	GMEAN	GD	VALUES
10.000	110.00	17.435	12.81	14.940	1.66	347
2.500	110.00	13.742	12.85	9.602	2.43	461

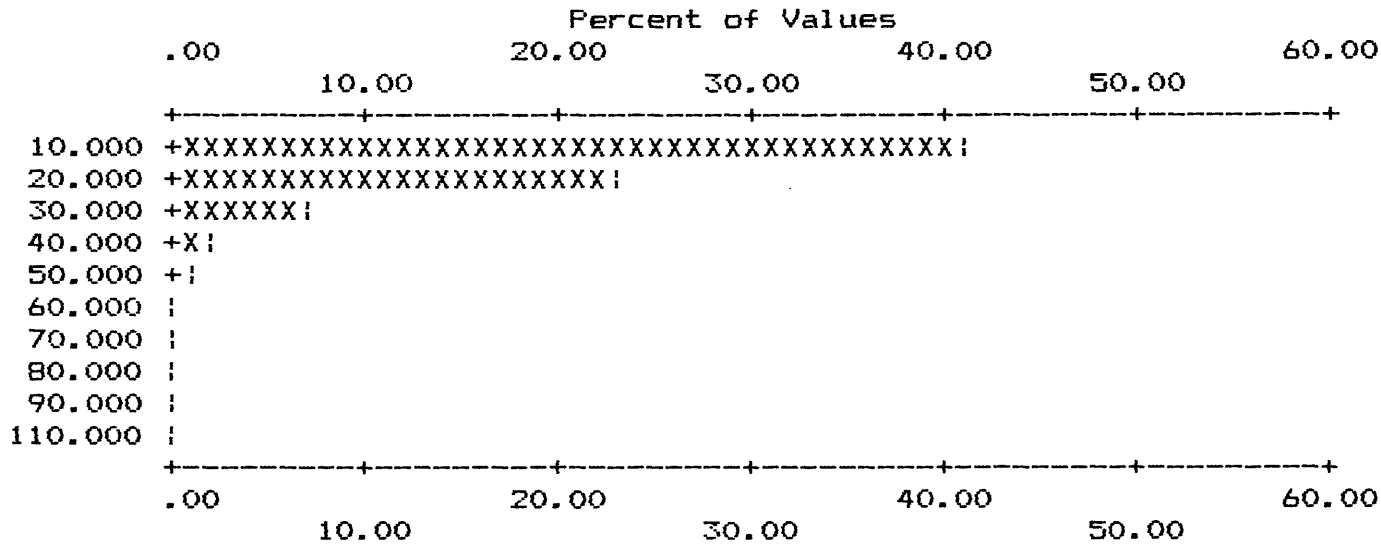

Each increment (each X or ¦ plotted) = 1.000 %

APPENDIX IV-C. HISTOGRAMS OF STREAM-SEDIMENT SAMPLE DATA, WHITE MTS NRA

COLUMN ID.: AA-BI-P

	VALUE	NO.	%	CUM.	CUM. %	TOT CUM	TOT CUM %	
1	1.000	6	1.30	6	1.3	.7	458	99.3	.7
2	2.000	1	.22	7	1.5	.4	459	99.6	.4
3	4.000	1	.22	8	1.7	.2	460	99.8	.2
4	14.000	1	.22	9	2.0	.0	461	100.0	.0

B	T	H	N	L	G	OTHER	UNQUAL	ANAL	read	
0	0	0	452	0	0	0	9	461	461	VALUES
.0	.0	.0	98.0	.0	.0	.0	2.0			PERCENT

MIN	MAX	AMEAN	SD	GMEAN	GD	VALUES
1.000	14.00	2.889	4.28	1.689	2.53	9
.250	14.00	.302	.67	.260	1.34	461

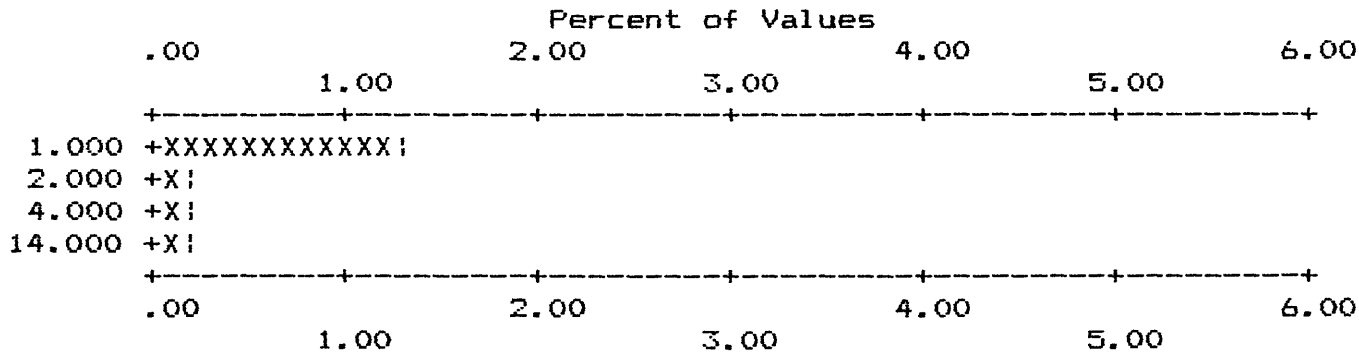

Each increment (each X or ! plotted) = .100 %

APPENDIX IV-C. HISTOGRAMS OF STREAM-SEDIMENT SAMPLE DATA, WHITE MTS NRA

COLUMN ID.: AA-CD-P

	VALUE	NO.	%	CUM.	CUM. %		TOT CUM	TOT CUM %	
1	.100	75	16.27	75	16.3	76.1	110	23.9	76.1
2	.200	120	26.03	195	42.3	50.1	230	49.9	50.1
3	.300	55	11.93	250	54.2	38.2	285	61.8	38.2
4	.400	47	10.20	297	64.4	28.0	332	72.0	28.0
5	.500	28	6.07	325	70.5	21.9	360	78.1	21.9
6	.600	22	4.77	347	75.3	17.1	382	82.9	17.1
7	.700	21	4.56	368	79.8	12.6	403	87.4	12.6
8	.800	10	2.17	378	82.0	10.4	413	89.6	10.4
9	.900	8	1.74	386	83.7	8.7	421	91.3	8.7
10	1.000	6	1.30	392	85.0	7.4	427	92.6	7.4
11	1.100	5	1.08	397	86.1	6.3	432	93.7	6.3
12	1.200	6	1.30	403	87.4	5.0	438	95.0	5.0
13	1.300	2	.43	405	87.9	4.6	440	95.4	4.6
14	1.400	2	.43	407	88.3	4.1	442	95.9	4.1
15	1.500	4	.87	411	89.2	3.3	446	96.7	3.3
16	1.600	1	.22	412	89.4	3.0	447	97.0	3.0
17	1.700	2	.43	414	89.8	2.6	449	97.4	2.6
18	1.800	1	.22	415	90.0	2.4	450	97.6	2.4
19	1.900	1	.22	416	90.2	2.2	451	97.8	2.2
20	2.000	2	.43	418	90.7	1.7	453	98.3	1.7
21	2.100	1	.22	419	90.9	1.5	454	98.5	1.5
22	2.300	1	.22	420	91.1	1.3	455	98.7	1.3
23	2.500	2	.43	422	91.5	.9	457	99.1	.9
24	4.000	1	.22	423	91.8	.7	458	99.3	.7
25	4.700	1	.22	424	92.0	.4	459	99.6	.4
26	4.900	1	.22	425	92.2	.2	460	99.8	.2
27	8.200	1	.22	426	92.4	.0	461	100.0	.0

B	T	H	N	L	G	OTHER	UNQUAL	ANAL	read	
0	0	0	20	15	0	0	426	461	461	VALUES
.0	.0	.0	4.3	3.3	.0	.0	92.4			PERCENT

MIN	MAX	AMEAN	SD	GMEAN	GD	VALUES
.100	8.20	.465	.64	.311	2.27	426
.025	8.20	.432	.63	.263	2.69	461

APPENDIX IV-C. HISTOGRAMS OF STREAM-SEDIMENT SAMPLE DATA, WHITE MTS NRA

COLUMN ID: AA-CD-P

```
                              Percent of Values
      .00              10.00              20.00              30.00
               5.00              15.00              25.00
      +---------+---------+---------+---------+---------+---------+
 .100 +XXXXXXXXXXXXXXXXXXXXXXXXXXXXXXXX!
 .200 +XXXXXXXXXXXXXXXXXXXXXXXXXXXXXXXXXXXXXXXXXXXXXXXXXXX!
 .300 +XXXXXXXXXXXXXXXXXXXXXXX!
 .400 +XXXXXXXXXXXXXXXXXXX!
 .500 +XXXXXXXXXXX!
 .600 +XXXXXXXXX!
 .700 +XXXXXXXX!
 .800 +XXX!
 .900 +XX!
1.000 +XX!
1.100 +X!
1.200 +XX!
1.300 +!
1.400 +!
1.500 +X!
1.600 !
1.700 +!
1.800 !
1.900 !
2.000 +!
2.100 !
2.300 !
2.500 +!
4.000 !
4.700 !
4.900 !
8.200 !
      +---------+---------+---------+---------+---------+---------+
      .00              10.00              20.00              30.00
               5.00              15.00              25.00

     Each increment (each X or ! plotted) =       .500 %
```

APPENDIX IV-C. HISTOGRAMS OF STREAM-SEDIMENT SAMPLE DATA, WHITE MTS NRA

COLUMN ID.: AA-SB-P

	VALUE	NO.	%	CUM.	CUM. %		TOT CUM	TOT CUM %	
1	2.000	62	13.45	62	13.4	10.2	414	89.8	10.2
2	4.000	21	4.56	83	18.0	5.6	435	94.4	5.6
3	6.000	11	2.39	94	20.4	3.3	446	96.7	3.3
4	8.000	2	.43	96	20.8	2.8	448	97.2	2.8
5	10.000	2	.43	98	21.3	2.4	450	97.6	2.4
6	12.000	1	.22	99	21.5	2.2	451	97.8	2.2
7	14.000	1	.22	100	21.7	2.0	452	98.0	2.0
8	16.000	1	.22	101	21.9	1.7	453	98.3	1.7
9	20.000	1	.22	102	22.1	1.5	454	98.5	1.5
10	22.000	2	.43	104	22.6	1.1	456	98.9	1.1
11	24.000	3	.65	107	23.2	.4	459	99.6	.4
12	33.000	1	.22	108	23.4	.2	460	99.8	.2
13	40.000	1	.22	109	23.6	.0	461	100.0	.0

B	T	H	N	L	G	OTHER	UNQUAL	ANAL	read	
0	0	0	352	0	0	0	109	461	461	VALUES
.0	.0	.0	76.4	.0	.0	.0	23.6			PERCENT

MIN	MAX	AMEAN	SD	GMEAN	GD	VALUES
2.000	40.00	5.147	6.67	3.430	2.16	109
.250	40.00	1.408	3.84	.464	3.24	461

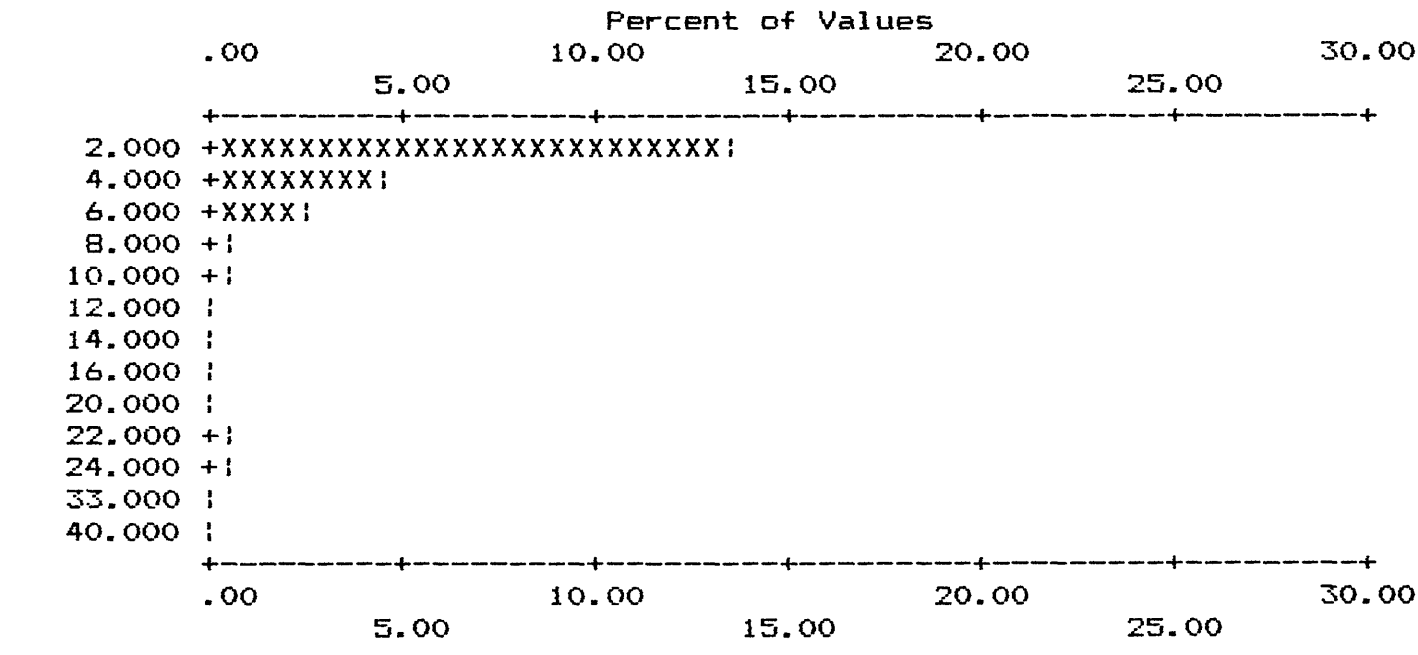

Each increment (each X or ¦ plotted) = .500 %

APPENDIX IV-C. HISTOGRAMS OF STREAM-SEDIMENT SAMPLE DATA, WHITE MTS NRA

COLUMN ID.: AA-ZN-P

	VALUE	NO.	%	CUM.	CUM. %		TOT CUM	TOT CUM %	
1	5.000	2	.43	2	.4	99.6	2	.4	99.6
2	10.000	6	1.30	8	1.7	98.3	8	1.7	98.3
3	15.000	22	4.77	30	6.5	93.5	30	6.5	93.5
4	20.000	44	9.54	74	16.1	83.9	74	16.1	83.9
5	25.000	31	6.72	105	22.8	77.2	105	22.8	77.2
6	30.000	36	7.81	141	30.6	69.4	141	30.6	69.4
7	35.000	24	5.21	165	35.8	64.2	165	35.8	64.2
8	40.000	29	6.29	194	42.1	57.9	194	42.1	57.9
9	45.000	28	6.07	222	48.2	51.8	222	48.2	51.8
10	50.000	29	6.29	251	54.4	45.6	251	54.4	45.6
11	55.000	23	4.99	274	59.4	40.6	274	59.4	40.6
12	60.000	28	6.07	302	65.5	34.5	302	65.5	34.5
13	65.000	15	3.25	317	68.8	31.2	317	68.8	31.2
14	70.000	12	2.60	329	71.4	28.6	329	71.4	28.6
15	75.000	13	2.82	342	74.2	25.8	342	74.2	25.8
16	80.000	13	2.82	355	77.0	23.0	355	77.0	23.0
17	85.000	10	2.17	365	79.2	20.8	365	79.2	20.8
18	90.000	10	2.17	375	81.3	18.7	375	81.3	18.7
19	95.000	5	1.08	380	82.4	17.6	380	82.4	17.6
20	100.000	14	3.04	394	85.5	14.5	394	85.5	14.5
21	110.000	12	2.60	406	88.1	11.9	406	88.1	11.9
22	120.000	9	1.95	415	90.0	10.0	415	90.0	10.0
23	130.000	12	2.60	427	92.6	7.4	427	92.6	7.4
24	140.000	5	1.08	432	93.7	6.3	432	93.7	6.3
25	150.000	2	.43	434	94.1	5.9	434	94.1	5.9
26	160.000	1	.22	435	94.4	5.6	435	94.4	5.6
27	170.000	4	.87	439	95.2	4.8	439	95.2	4.8
28	180.000	2	.43	441	95.7	4.3	441	95.7	4.3
29	190.000	2	.43	443	96.1	3.9	443	96.1	3.9
30	200.000	3	.65	446	96.7	3.3	446	96.7	3.3
31	240.000	2	.43	448	97.2	2.8	448	97.2	2.8
32	260.000	1	.22	449	97.4	2.6	449	97.4	2.6
33	280.000	1	.22	450	97.6	2.4	450	97.6	2.4
34	290.000	1	.22	451	97.8	2.2	451	97.8	2.2
35	300.000	1	.22	452	98.0	2.0	452	98.0	2.0
36	310.000	1	.22	453	98.3	1.7	453	98.3	1.7
37	330.000	1	.22	454	98.5	1.5	454	98.5	1.5
38	390.000	1	.22	455	98.7	1.3	455	98.7	1.3
39	400.000	2	.43	457	99.1	.9	457	99.1	.9
40	420.000	1	.22	458	99.3	.7	458	99.3	.7
41	540.000	1	.22	459	99.6	.4	459	99.6	.4
42	620.000	1	.22	460	99.8	.2	460	99.8	.2
43	1000.000	1	.22	461	100.0	.0	461	100.0	.0

B	T	H	N	L	G	OTHER	UNQUAL	ANAL	read	
0	0	0	0	0	0	0	461	461	461	VALUES
.0	.0	.0	.0	.0	.0	.0	100.0			PERCENT

MIN	MAX	AMEAN	SD	GMEAN	GD	VALUES
5.000	1000.00	68.124	79.56	49.293	2.13	461

APPENDIX IV-C. HISTOGRAMS OF STREAM-SEDIMENT SAMPLE DATA, WHITE MTS NRA

COLUMN ID: AA-ZN-P

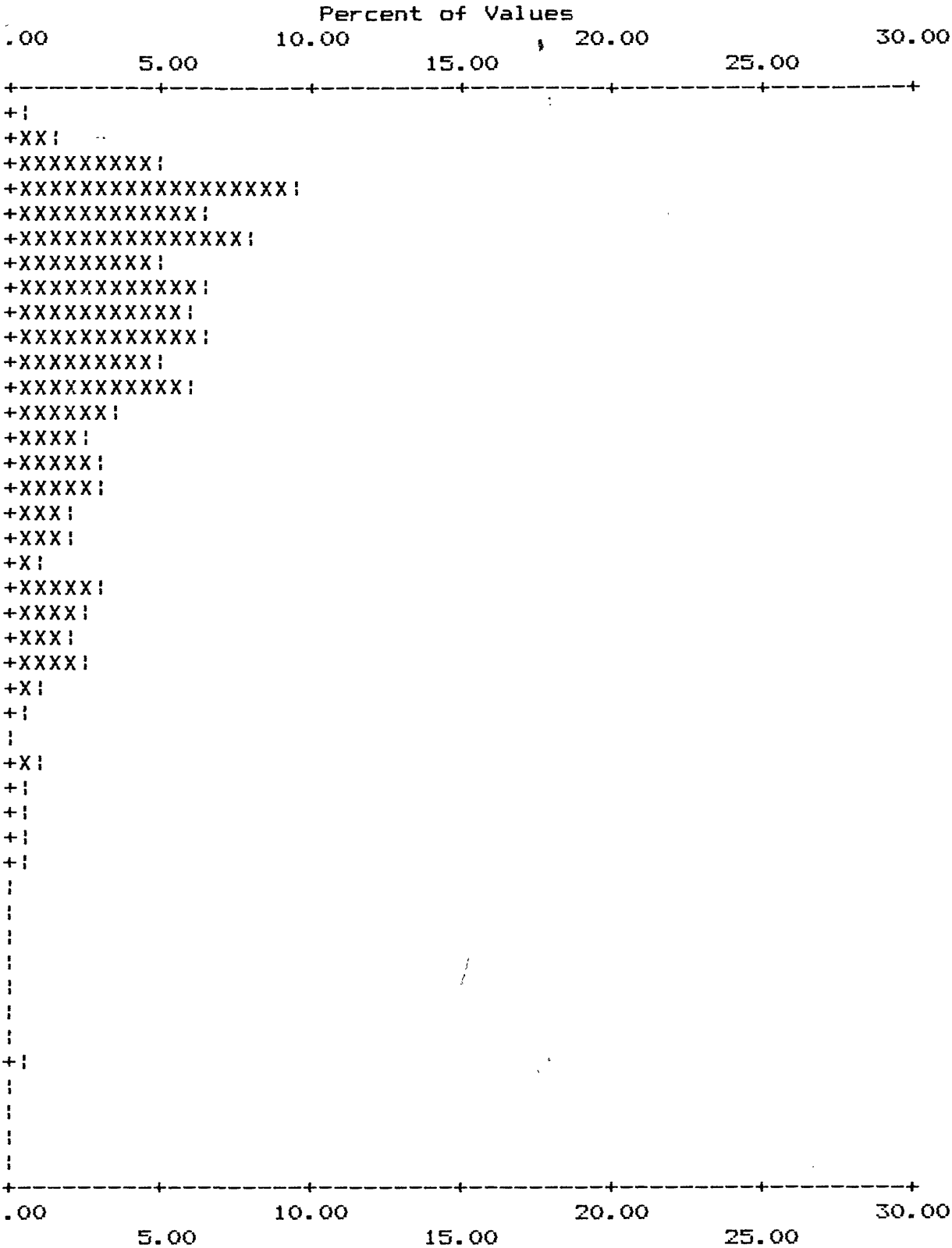

Each increment (each X or ¦ plotted) = .500 %